THE EFFECTS OF EXHAUST GAS RECIRCULATION (EGR) ON THE PERFORMANCE OF DIESEL ENGINE

MAROA, Samwel Semakula, B. Tech (Automotive)

217081370

Supervisor: Prof. Freddie L. Inambao

Dissertation submitted in fulfilment of the requirement for the degree of

Master's in Engineering (M. Sc. Eng.)

(MECHANICAL ENGINEERING)

School of Engineering,

University of KwaZulu-Natal,

Durban South Africa

As the candidate's supervisor, I agree/do not agree to the submission of this dissertation. The supervisor must sign all copies after deleting which is not applicable.

PROF F.N INAMBAO

Name of Supervisor   Signature

MAY 2018

Declaration 1 –Plagiarism

I, **Maroa Samwel Semakula** declare that:

1. The research reported in this thesis, except where otherwise indicated is my original research.

2. This thesis has not been submitted for any degree or examination at any other university.

3. This thesis does not contain other persons' data, pictures, graphs or other information, unless specifically acknowledged as being sourced from other persons.

4. This thesis does not contain other persons' writing, unless specifically acknowledged as being sourced from other researchers. Where other written sources have been quoted, then:

    a) Their words have been re-written but the general information attributed to them has been referenced

    b) Where their exact words have been used, then their writing has been placed in italics and inside quotation marks, and referenced.

5. This thesis does not contain text, graphics or tables copied and pasted from the internet, unless specifically acknowledged, and the source being detailed in the thesis and in the References sections.

Signed.………………………………
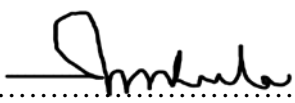
Declaration 2 –Publications

This section presents the articles that form part and/or include the research presented in this thesis.

ISI/DoHET Accredited Journals

Maroa, S., & Inambao, F. (2017). The Effects of Exhaust Gas Recirculation on the Performance and Emission Characteristics of a Diesel Engine–A Critical Review. *International Journal of Applied Engineering Research*, 12(23), 13677-13689. http://www.ripublication.com

Maroa, S., & Inambao, F. (2018). Transportation, Pollution and the Environment. *International Journal of Applied Engineering Research*, 13(6), 3187-3199. http://www.ripublication.com

Maroa, S., & Inambao, F. (2018). The Formation, Effects and Control of Oxides of Nitrogen in Diesel Engines. *International Journal of Applied Engineering Research*, 13(6), 3200-3209. http://www.ripublication.com

Maroa, S., & Inambao, F. (2018). Influence of Exhaust Gas Recirculation and Emission Characteristics of a Diesel Engine Using Pyrolyzed Waste Plastic Biodiesel and Blends. *International Journal of Applied Engineering Research*, 13(10), 8321-8335. http://www.ripublication.com

International and DoHET Accredited Conferences

Maroa, S.S. and Inambao, F. L. (2017). The Effects of EGR on the Performance and Emission Characteristics of a Diesel Engine – A Critical Review Proceedings of the 15th biennial Botswana Institution of Engineers Conference, Gaborone, Botswana: 16th-19th October, 2017: Proceedings Being Processed by Conference Organizers.

DEDICATION

This work is dedicated to my late mother Selina Sibora Marwa.

ACKNOWLEDGEMENTS

ABSTRACT

The aim of this work was to study the effects of EGR on the performance of a diesel engine using waste plastic pyrolysis oil (WPPO) and conventional diesel (CD). WPPO was developed through the pyrolysis extraction method. The blends were made up of WPPO and conventional diesel mixed in the ratios of WPPO10, WPPO20, WPPO30, WPPO40 and WPPO100. The EGR % flow rate chosen was 0 % to 30 % graduated in intervals of 5 %. The lower blend ratios of WPPO10 and WPPO20 showed lower values of brake specific fuel consumption (BSFC) compared to conventional diesel values and the high blend ratio of WPPO100. The brake thermal energy (BTE) showed increased values for lower blend ratios of WPPO10 and WPPO20 of 8.35 % and 8.15 % respectively with application of an EGR % flow rate of 15 % compared to high blend ratios of WPPO30, WPPO40 and WPPO100. The application of EGR % flow rate was observed to cause no significant change in the engine brake power (BP) for all the test fuels used. The application of EGR % flow rate in increasing rates reduced exhaust gas temperature (EGT), with conventional diesel reporting 440 ℃ at 5 % EGR flow rate and 340 ℃ being the lowest at 30 % EGR flow rate. The application of EGR % flow rate reduced the amount of hydrocarbon emissions emitted by the applied test fuels across the board. At EGR flows rate of 5 %, 10 %, 15 %, 20 %, 25 % and 30 %, conventional diesel had 43 ppm, 57 ppm, 70 ppm, 82 ppm and 85 ppm respectively. As the blend ratio increased with increased EGR % flow rate there was an increased rate of NO_X emissions. At 20 % EGR flow rate, blends WPPO10, WPPO2O, WPPO30, WPPO40 and WPPO100 had 591ppm, 645 ppm, 750 ppm, 778 ppm and 851 ppm respectively compared to at the 10 % EGR flow rate where their values were 830 ppm, 971 ppm, 1031 ppm, 1151 ppm and 1116 ppm respectively. There was a significant continuous and marginal increase in the percentage of carbon emissions by volume as the load increased across all the test fuels irrespective of the EGR % flow rate. At 80 % engine load the value for WPPOB100 was 2.0 % up from 1.65 % by volume at part engine load, while the value of conventional diesel was 4.1 % at 80 % engine load compared to 2.95 % by volume at part engine load. The application of EGR % flow rate increased the carbon dioxide emission exponentially by almost doubling the values. At 10 % EGR flow rate the value of conventional diesel was 3.85 % compared to WPPOB100 at 6.25 %, WPPOB10 at 4.75 %, WPPOB20 at 4.25 %, WPPOB30 at 3.95 %, and WPPOB40 at 6.65 %.

TABLE OF CONTENTS

LIST OF TABLES

LIST OF FIGURES

ABBREVIATIONS AND ACRONYMS

AFR   Air Fuel Ratio

ASTM   American Society of Testing Materials

BP   Brake Power

BRICS   Brazil Russia India China and South Africa

BSEC   Brake Specific Energy Consumption

BSFC   Brake Specific Fuel Consumption

BSHC   Brake Specific Heat Capacity

BTE   Brake Thermal Energy

CA   Crank Angle

CI   Compression Ignition

CN   Cetane Number

CNG   Compressed natural gas

CO_2 Carbon Dioxide

COMESA   Common Markets for Eastern and Southern Africa

CBD   Corn Biodiesel

CI   Compression Ignition

CR   Compression Ratio

CSBD   Cotton Seed Biodiesel

CV   Calorific value

DI   Direct Injection

EC   Elemental Carbon

EAC   Eastern African Community

ECOWAS   Economic Community of Western African States

EGR	Exhaust Gas Recirculation
EGT	Exhaust Gas Temperature
EU	European Union
ER	Equivalence Ratio
GCV	Gross Calorific Value
GTL	Gas to Liquid
HD	Heavy Duty
HCCI	Homogeneous Charge Compression Ignition
HP	Horse Power
HRR	Heat Release Rate
HVO	Hydro-Treated Vegetable Oil
IMEP	Indicated Mean Effective Pressure
Irr	Irreversibility Ratio
ISFC	Indicated Specific Fuel Consumption
ITE	Indicated Thermal Efficiency
Kg/kW-h	kilogram per kilowatt hour
Kg/m^3	Kilogram per meter cube
Kj	Kilojoules
kW	kilowatt
L	The Recess Length
LD	Light Duty
LPL	Low Pressure Loop
LSB	Low Swirl Burner
LTC	Low Temperature Combustion

MK	Modulated Kinetics
n	Number of Moles
n_f	Fuel Molar Quantity
nm	Nanometre
NLFS	Normalized Laminar Flame Speed
NO$_X$	Nitrogen Oxides
PBD	Petroleum Based Diesel
PCCI	Pre-Mixed Charge Compression Ignition
PFI	Port Fuel Injection
PPM	Parts Per Million
PHCBD	Preheated Corn Biodiesel
REGR	Reformed Exhaust Gas Recirculation
RPM	Revolutions Per Minute
SADEC	South-African Development Community
SFC	Specific Fuel Consumption
SHR	Specific Heat Ratio
SI	Spark Ignition
SOC	Start of Combustion
SOF	Soluble Organic Fraction
SHC	Specific Heat Capacity
TRAP	Traffic Related Air Pollution
UHC	Unburned Hydrocarbon
ULSD	Ultra Low Sulphur Diesel
VCR	Variable Compression Ratio

VOCs   Volatile Organic Compounds

V_s Flame Speed

WCOME   Waste Cooking Oil Methyl Ester

WPPO   Waste Plastic Pyrolysis Oil

SUBSCRIPTS SYMBOLS

a	Air
amb	Ambient
ax	Axial
bgf	Burnt Gas Fraction
bz	Burnt Zone
c	Compression
cd	Resistance Due to Conduction Heat Transfer
cr	Critical
cv	Resistance Due to The Convectional Heat Transfer
e	Engine
df	Diesel Fuel
dmf	Dual Fuel Mode
eg	Exhaust Gases
exh	Exhaust Manifold
f	Fuel
fd	diesel fuel flow rate
fpo	pyrolysis oil flow rate
fc	Fresh Charge
fr	Fraction of Air Mass
g	force of gravitational acceleration
i	I^{th} Species
j	J^{th} Species
im	Intake Manifold

in	Input / Inside
out	Outside as Output
rad	Radial
ra	Radial Heat Transfer
rf	Flow Rate
s	Stroke
sec	Cross Section/Section
sh	Shell
th	Throttle
v	Kinematic Viscosity of the Air Medium
w	System Wall
x	Exhaust Molar Gas Quantity
y	Inlet Intake Charge Quantity
z	Remainder of the Intake Charge

GREEK SYMBOLS

α	Thermal Diffusivity
λ	Air Excess Ratio
ω	Angular Velocity
γ	Air Fraction Mass
Π	Pressure Ratio
π	PI $\approx$ 3.14
θ	Angle of Emissivity
ρ	Density
φ	Effective Angle of Throttle Opening
β	EGR Gases Temperature Mean Reciprocal
μ	Dynamic Viscosity
η	Efficiency

GENERAL SYMBOLS

A	Area
A_{eff}	Effective Flow Area
A_{th}	Throttle Valve Effective Area
A_{sec}	Cross Sectional Area of Gaseous Exchange
A_{sh}	Area of The Shell of the Cylinder
$\in_C$	Compression Ratio
ε_{egr}	EGR Cooler Efficiency
c	Coefficient of discharge
$COS\varphi_0$	Initial Effective Angle of Opening of the Throttle Valve
$COS\varphi$	Final Effective Angle of Opening
c_i	Empirical Constant
c_p	Specific Heat at Constant Pressure
cr	Critical Pressure
c_v	Specific Heat at Constant Volume
x_{egr}	EGR Rate
η_{vol}	Engine Volumetric Efficiency
d	Diameter
d_{egr}	Diameter of The EGR Valve
d_{out}	Diameter of The Exhaust Manifold
D	Distance
D_p	Particles Diameter
Gr	Grashofs Number

h	Heat Transfer Coefficient
h_{ax}	Axial Heat Transfer Coefficient
h_{cv}	Heat Transfer Coefficient Due to Convection Heat Transfer
h_{rad}	Heat Transfer Coefficient Due to Radial Heat Transfer
h_{egr}	Specific Heat Transfer of The EGR Gases
H	Specific Enthalpy
k	Specific Heat Ratio
k_{amb}	Specific Heat at Constant Pressure and Volume in The System
k	Thermal Conductivity
L	Length
M	Mass
$\dot{m}$	Mass Flow
$\dot{m}_a$	Fresh Air Charge
$\dot{m}_{egr}$	Mass Flow Rate of the EGR % Gas
N	Rotational Speed
Nu	Nusselt Number
P	Pressure
ρ_{egr}	Density of The EGR Gases
Pr	Prandtl Number
Q	Heat Flux / Heat
Q_{ax}	Heat of Axial Direction
Q_{em}	Heat from The Exhaust Manifold
Q_{rad}	Heat of Radial Direction
R	Specific Universal Gas Constant

Ra	Raleigh Number
Re	The Reynolds Number
T	Temperature
T	Torque
T_{amb}	Ambient Temperature
T_e	Temperature of The Engine
T_{eng}	Engine Temperature
T_{em}	Exhaust Manifold Temperature
T_{egr}	Temperatures of The EGR Gases
$T(L)$	Temperature as A Function of Length
T_w	Wall Temperature
T_x	Temperature as A Function of X
T_∞	Temperature of The Exiting Gases
u	Control Signal Input
V	Volume
$v\infty$	Velocity of The Exiting Exhaust Gases
Ψ	Flow Function
μ_{egr}	Dynamic Viscosity
Ω_i	Dimensionless Integral of Order Unity
r	Conductive Heat Transfer Resistance
r_{ax}	Axial Heat Resistance Within the System
u	Control Signal / Input
γ	Fresh Air Fraction Mass
ξ	Stephan-Boltzman Constant

θ Emissivity Angle

υ Velocity

W_{mw} System Flow

w_{egr} The Inlet Intake Manifold System Flow to Engine Cylinders

$\dot{Y}_i^j$ Stoichiometric Coefficient

CHAPTER ONE

INTRODUCTION

1.1 Introduction and Background

The world has witnessed phenomenal growth, particularly in the middle class, of most emerging and developing economies. However, failure of most public transport systems and infrastructure in developing and emerging nations has increased the number of personalized transport vehicles on the road. This development has tended to increase the popularity of diesel propelled vehicles especially in commercial and personal transport. Consequently, there is a high level of demand on conventional sources of fuel energy. Although there have been tremendous achievements in technology and advances in automobile manufacturing and technology, there is still a need to continue with research to reduce the volume of fuel used and pollution emitted. This is necessary to reduce global warming which has seen phenomenal growth in the 21st century. It is imperative, therefore, for automobile and engine manufacturing industries to incorporate new studies related to reduction in emissions and energy wastage from engine exhaust systems and make an effort to improve on and harness exhaust gas recirculation (EGR) system gases [1].

The diesel engine can be defined as a type of heat engine that uses internal combustion processes to convert fuel energy into useful mechanical energy [2]. More efficiency is demanded in most engine management systems of diesel engines as a way of reducing energy losses, particularly those being wasted through the exhaust system which accounts for between 20 % to 25 % of total energy losses. There have been major strides in reduction of this energy waste through re-tapping of the exhaust gases through techniques such as EGR systems. Recycling of waste gate gases improves volumetric efficiency, brake thermal efficiency (BTE), brake specific fuel consumption (BSFC) and reduction of particulate matter (PM) emissions [3].

In order to reduce emissions and particulate matter (PM) effluents from automobile diesel, particularly nitrogen oxide (NO_X), carbon monoxide (CO), and hydrocarbons (HCs), EGR as a technique has gained widespread use due to its efficiency and ease of application. EGR involves the recirculation of a portion of the exhaust gas along with the intake of a fresh air charge into the combustion chamber of the diesel engine for combustion together with the fuel injected in the normal power cycle of the diesel engine. EGR as an emission control system

allows significant reduction in NO_X gases in almost all types of diesel engines, including light duty (LD), medium duty and heavy duty (HD) engine applications. EGR is also suitable for primary engines as low as two stroke such as those used in marine operations and applications.

The use of EGR systems in diesel engines has a primary function of diluting oxygen in the inlet intake fresh air charge, by displacing the combustion products of carbon dioxide (CO_2) and hydrogen dioxide (H_2O). These products are known to be inert and so suppress the combustion process rate, due to their endothermic dissociation. EGR applications have other merits besides increasing efficiency and reduction of emissions [1], including that EGR imparts knock resistance and reduces the need for high load fuel enrichment in closed cycle diesel engines. In spark ignition (SI) engines, EGR systems enable the vaporization of liquid fuels thus enabling improved ignition quality. Cooled EGR reduces the EGR flow rate inlet intake charge temperature leading to reduced peak in-cylinder temperatures [1]. Moreover, EGR systems lead to reduction in lubricating oil consumption, increased fuel injection pressures, increased use of diesel oxidation catalysts, and increased intake manifold boost pressure.

[4] reports that despite the high thermal efficiency in fuels provided by diesel engines, diesel engines have the disadvantage of emitting NOx and PM which are considered to be the main pollutants and toxic gases, contributing to air pollution in major urban centers and the atmosphere in general. Other disadvantages include increased unburned hydrocarbon (UHCs) and soluble organic fractions (SOFs), increased particulate matter (PM), increased condensation in UHC and PM deportation in cooler fouling (i.e. through degraded heat transfer and higher flow resistance). NO_X and PM emissions are currently strictly legislated by environmental protection agencies in almost all countries, making diesel propelled engines and machines more expensive and less appealing. However, EGR systems greatly reduce NO_X emissions of diesel engines making a compelling case for this technology to be incorporated into the design and manufacturing of diesel engines.

[5] emphasizes that since NO_X emission is a product of temperature, especially in-cylinder temperatures above 2000 k, any method that can control instantaneous temperature in the combustion chamber to below 2000 k will ultimately reduce the formation of NO_X. This is the main reason behind the use of EGR as a technique for the reduction of NO_X. In the recent past a number of studies have been conducted on combustion strategies that impact positively on the overall reduction of toxic gas emissions associated with the use of diesel engines, especially NO_X, CO_2, CO, PM, and soot emissions.

There are three general methods of reducing NO_X, CO_2, CO, PM and soot emissions: the alternation of fuel method, the alternation of the combustion process and the after treatment of the exhaust gases [6]. The first two employed widely today because of the low cost of application although these have the disadvantages of higher fuel economy (high BSFC) and low BTE. Azad et al. (2016) propose the combination of low temperature combustion (LTC) and shear stress transport (SST) k-ω model as the best strategy for biodiesel combustion control in compression ignition (CI) engines. The combustion of biodiesel under LTC strategies have been shown to reduce NO_X emission gases by a factor of 2 of mass volume magnitude and soot emissions by a factor of 10 compared to conventional diesel fuel as reported by [7, 8].

Thus, combustion modelling is a vital field due to its role in conserving energy as well as providing in-depth knowledge concerning complex combustion process control strategies. There are three types of LTC modelling widely in use today, namely, homogeneous charge compression ignition (HCCI), pre-mixed charge compression ignition (PCCI), and reactivity controlled compression ignition (RCCI). HCCI is a pioneer in the field of diesel combustion control strategies; it is a change from the conventional combustion process aimed at creating a homogeneous air fuel mixture before ignition in CI engines, which is similar to combustion operation in SI engines. The HCCI uses a two-stage heat release combustion system for diesel fuel. In stage one it has a low temperature kinetic reaction, controlled and dominated by low temperature chemistry. The second stage, which is the main heat release phase, is dominated or controlled by the oxidation of the CO gas [6]. HCCI mixture preparation plays a major role in reducing soot and NO_X emissions. There are two types of charge preparation strategies employed, namely, external mixture formation and in-cylinder direct injection (DI), according to [9]. External mixture formation leads to reduced volumetric efficiency while the in-cylinder DI leads to dilution of the lubricating oil. Various techniques are employed with highly volatile fluids such as gasoline and the alcohols, such as port fuel injection (PFI), wide-open throttle and fumigation. However, for low volatility fuels like diesel, vaporizers are generally deployed. There are a number of researchers who have used this technique and experimented with different types of fuels, for example, [10, 11].

Pre-mixed charge compression ignition (PCCI) is a combustion control strategy which evolved from the HCCI model of combustion due to the limitations that were exhibited by the HCCI model, including noisy combustion and violent uncontrolled combustion. This strategy sought to bring better control over the start of combustion (SOC) phase. PCCI utilizes early premixing of the air fuel mixture followed by a late injection of fuel during the compression stroke, thus

governing how and when the SOC should begin [6]. This makes it possible to utilize very high levels of EGR % flow rates. This factor increases ignition delay duration thereby offering better air-fuel mixing and offering less fuel-rich pockets in the LTC areas, hence the reduction in NO_X emissions and soot emissions [12]. Among the advantages offered by PCCI over HCCI are ignition delay which is achievable through enhancement of charge motion [6] especially for mixtures which are not homogeneous, reduced compression ratio (CR), higher injection pressure and use of very high EGR % flow rate applications. This system allows fuel to be injected into the combustion chamber in three main ways, namely, advanced early pilot injection, PFI, and late direct fuel injection. The first two systems have the disadvantage of increasing HC and CO emissions from the residue fuel on the cylinder walls, which is corrected by use of narrow spray injector nozzles and application of high EGR % flow rate, thus switching the occurring combustion so that it looks similar to conventional combustion especially during low engine loads.

Reactivity controlled compression ignition (RCCI) [13] is a more recent combustion strategy development. It uses multiple fuels with different reactivity rates and properties as a combustion fuel. Fuel is injected at predetermined intervals thus governing the reactivity of the injected fuels in the combustion cylinder for the desired combustion and magnitude. This allows the onset of combustion at different periods and at different rates and intensity. In RCCI the combustion is staged to start from local high reactivity fuel areas to low fuel reactivity areas [14]. The staging of the combustion process leads to significant expansion of the premixed combustion. Hence the high thermal efficiency, low in-cylinder pressure rise rate and low emissions, even when the engine is subjected to high load conditions of up to 16 Mpa of indicated mean effective pressure (IMEP) [15].

Another combustion model worth mentioning is the one reported by [16, 17] i.e., low swirl burner (LSB). It uses premixed flame technology especially for leaner flame stabilization, where its main principle of operation is in propagating turbulent premixed flames. The standing flame front [16] in the LSB is produced through weakening the swirl motion of the premixed mixture thus providing a divergent down stream flow of the premixed mixture which produces a low temperature flame. These conditions make it possible for low levels of NO_X emissions to be achieved.

The use of biodiesel as an alternative fuel because of its physio-chemical fuel properties [6] does not replace diesel. This is due to the difference in the combustion process between the

two fuels, as they too produce toxic gases. Although biodiesels produce toxic gases, this can be mitigated through adoption of good combustion strategies to meet the current demand for leaner and more fuel-efficient engines. This is as demanded from national and global environmental protection agencies. Recently developed biodiesel combustion control strategies have been developed by [18, 19]. However, it should be mentioned here that there is no single and perfect model that can produce a solution to the many combustion emission challenges experienced in modern day diesel internal combustion engines.

Table 1 shows various research groups and their strategies regarding LTC [16].

Table 1.1: LTC research strategies

Acronym	Meaning	Location
ATAC	Active thermo-atmospheric combustion	Nippon Clean Engine Research Institute
TS	Toyota-Soken combustion	Toyota/Soken
CIHC	Compression ignited homogeneous charge	University of Wisconsin Madison
HCCI	Homogeneous charge compression ignition	SwRI
ARC	Active radical combustion	Honda
PREDIC	Pre-mixed diesel combustion	New Ace
HiMICS	Homogeneous intelligent multi-injection system	Hino
UNIBUS	Uniform bulky combustion system	Toyota
MULDIC	Multi stage diesel combustion	New Ace
PCCI	Pre-mixed charge compression ignition	Mitsubishi
MK	Modulated kinetics	Nissan
NADI	Narrow angle direct injection	Institute Francais du Petrole

The importance of EGR in gas emission and control cannot be over-emphasized, as it affects the formation of deposition particles in the diesel engine. The particles formed as a result of

application of EGR % flow rate have far reaching implications on human health and the environment at large. The distribution of particles emitted from diesel engine can be categorized into two major areas: the Nano scale group which is $D_p < 50\ nm$ often referred to as the particle nucleation mode, and the Nano scale group of $50\ nm < D_p < 1000\ nm$ known as the accumulation mode [9]. The former includes the volatile organic compounds (VOCs) and some solid carbon metal compounds while the latter includes carbonaceous soot agglomerates which have a significant effect on the residue particle mass, which can be expressed mathematically in equation form [9] as:

$$M_P = \rho_p \frac{\pi d^3}{6} \qquad\qquad \text{Equation 1}$$

Where M_p is the dependence particle mass, ρ_p is the particle density, d is the particle diameter, π is pi = 3.14.

The finer range particles of PM$_{2.5}$ are more dangerous than the larger range particles PM$_{10}$ [9]. The finer particles are more prevalent in diesel particulate exhaust emissions, especially LD diesel vehicle engines, indicating that there is a correlation between particulate emission size and the cubic capacity of a diesel engine. However, [20] reported lower solid particle emissions from HD diesel engines compared to the emissions from LD diesel engines, a factor they attributed to three main factors: higher EGR rates, rapid combustion in HD diesel engines and higher PM limits of emissions associated with LD diesel engines. Therefore, the authors concluded that emission particles from diesel engines are not directly proportional to engine cubic capacity. [20] further reported that with increase in the use of EGR % flow rate from 0 % to 19 %, the particle diameter increased by 70 %, which can be credited to the thermal effect of EGR % flow rate. This was due to the dilution effect which plays a dominant role in producing most primary emission particles. They concluded that the geometrical size of primary particle diameter formation is affected by the variation of the EGR % flow rate.

1.2 Aims and Objectives

The aim of this dissertation work was to investigate the effects of EGR on diesel engine performance. This work had set three main objectives that were pursued in answering this aim, namely:

1. To investigate the effects of EGR on the performance of a diesel engine.

2. To investigate development of an alternative fuel and assess how it affects diesel engine performance and emissions control under the influence of EGR.

3. To investigate the effects of EGR on performance and emission characteristics of a diesel engine.

1.3 Dissertation Outline

This dissertation work sought to achieve the aims and objectives presented above in nine chapters, as summarized below.

Chapter 1 presents an introduction and background to the study, outlining the need to study exhaust gas recirculation as a technique of for emission control and its effects on performance. This chapter provides a background on the main research question that is linked to the aims and objectives of this study. The layout of this dissertation, its scope of study, research motivation and contribution to the field of science and technology especially renewable energy are outlined.

Chapter 2 is the literature review. This chapter deals with previous work by various authors conducted in the same field of study. Various topics of importance in EGR emission control strategy, development in alternative fuels and recent development in combustion control strategies and their wider implications for diesel engines are comprehensively reviewed and discussed. This review consists of proceedings from conferences, journal articles, published books, online articles and publications and dissertations from masters and thesis from doctoral levels.

Chapter 3 deals with the methodology that was employed in meeting the aim and objectives of this work. Two main approaches are proposed, namely, the numerical and experimental methods. However, in this chapter only the numerical approach is attempted with mathematical models presented to help build a firm foundation for deepening understanding of the aim and objectives of this work. This chapter attempts to link numerical models with the experimental procedure set-up for study.

Chapter 4 is a review publication entitled "The Effects of Exhaust Gas Recirculation on The Performance and Emission Characteristics of a Diesel Engine – A Critical Review". In this chapter various topical issues linked to EGR such as performance, combustion control strategy, emission characteristics of NO_X, CO, CO_2, UHC, PM, and smoke emissions, are discussed.

Chapter 5 is a publication entitled "Transportation, Pollution and the Environment". This chapter discusses the importance of modern day forms of transport and their effects on the environment as a result of vehicular emissions. These emissions result from the combustion characteristics of diesel engines, a primary fuel in the both commercial and personal transport.

Chapter 6 is a publication entitled "The Formation, Effects and Control of Oxides of Nitrogen in Diesel Engines". This chapter covers topical issues on how oxides of nitrogen are formed within diesel engines, the sources of NO_X, types of formation routes and interaction mechanisms with one another and the effects of NO_X emissions on the environment and human public health.

Chapter 7 covers the experimental set-up, the apparatus and the procedure for conducting the experiment. It outlines in detail experimental equipment and specification with percentage error of their measurement and vital modifications for the EGR circuit. In addition, this chapter outlines the procedures experimental material preparation, data collection and the sequence in which the experimental procedure was executed.

Chapter 8 presents the results and discussion as observed and reported from the experimental study work described in Chapter 7. It breaks down the results into comprehensive detailed individual components, through diagrammatic graphic figures. Each result is analyzed and discussed independently, according to the result obtained and conclusions deduced. This chapter provides a systematic sequence of results discussion dealing with performance parameters of BSFC, BTE, BP and EGT with emission components of NO_X, CO, CO_2, UHC and smoke opacity.

Chapter 9 discusses the conclusions and future recommendations from the experimental results obtained in Chapter 8 and discusses the research findings in the light of the research gaps presented in the literature review in Chapter 2.

1.4 Research Motivation

The impact of global warming is growing due to the increasing atmospheric air pollution in our major urban centers and cities. This development is associated with the expansion of urban transport systems, industrial development and the increase in world population (projected to grow by 2 billion people annually) [21]. Environmental degradation caused by pollution threatens food security. There is increasingly stringent emission control legislation being passed in individual countries, emerging economies, the G7, and economic blocks like the

COMESA, EAC, ECOWAS, European Union (EU), SADC, BRICS. These challenges call for research in renewable energy and alternative fuels that can reduce emissions and pollution, allowing time for adjustments and wider applications in the transport sector. The transport sector is a pivotal GDP economic factor in the production chain, without which other equally important sectors of the economy cannot be sustained.

Figure 1 shows the past and predicted future variation of world energy consumption with percentage shares for each source of energy [21].
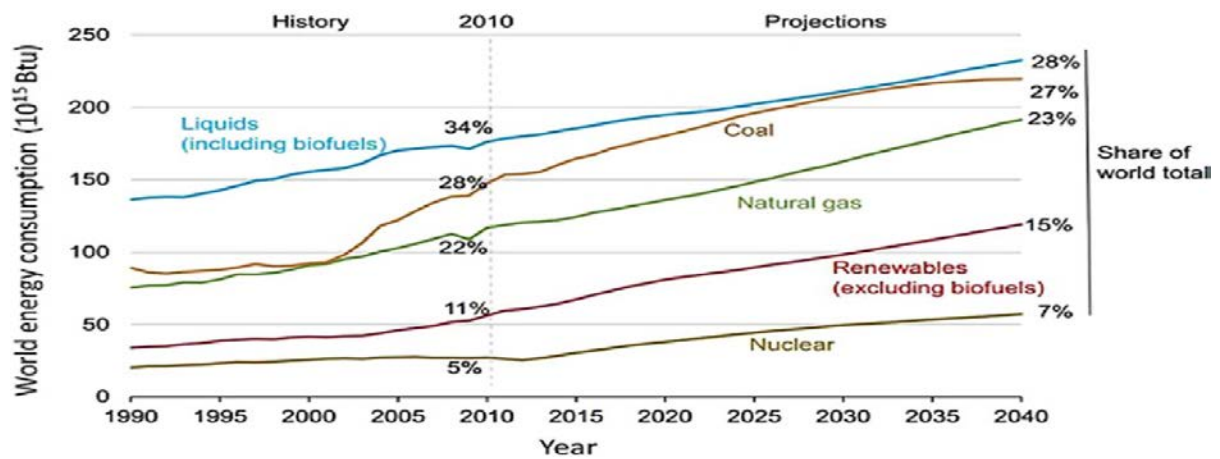
Figure 1.1: Variation of world energy consumption percentage shares for each source of energy [21]

The development of alternative fuels from recycling technology offers a reprieve for the primary sources of energy and of biodiesel alternative fuels some of which rely heavily on food plants and other food sources. Recycling technology mitigates the challenges and disadvantages identified and associated with petroleum-based fossil fuels, which are leading contributors to global warming and atmospheric air pollution. The above factors are a profound motivation for this work and study and have driven my focus, and will continue to do so, with a view to contributing through this work to make our world a better place.

References

[1]   Manieniyan V and S. S, ""Experimental Analysis of Exhaust gas Recirculation on Diesel Engines Operating with Biodiesel," *International journal of Engineering and Technology (IJET),* vol. 3, pp. 129-134, 2013.

[2]   R. Senthilkumar, K. Ramadoss, and R. Manimaran, "Experimental investigation of performance and emission characteristics by different Exhaust gas recirculation methods used in diesel engine," *Global Journal of Research In Engineering,* vol. 13, 2013.

[3]   J. Hussain, K. Palaniradja, N. Alagumurthi, and R. Manimaran, "Effect of exhaust gas recirculation (EGR) on performance and emission characteristics of a three cylinder direct injection compression ignition engine," *Alexandria Engineering Journal,* vol. 51, pp. 241-247, 2012.

[4]   D. Agarwal, S. K. Singh, and A. K. Agarwal, "Effect of Exhaust Gas Recirculation (EGR) on performance, emissions, deposits and durability of a constant speed compression ignition engine," *Applied Energy,* vol. 88, pp. 2900-2907, 2011.

[5]   K. S. Rao, "Effect of EGR on Diesel Engine Performance and Exhaust Emission Running with Cotton Seed Biodiesel," *international journal of mechanical and mechatronic engineering,* vol. 16, pp. 64-69, 2016.

[6]   A. Azad, M. Rasul, M. Khan, S. C. Sharma, and M. Bhuiya, "Recent development of biodiesel combustion strategies and modelling for compression ignition engines," *Renewable and Sustainable Energy Reviews,* vol. 56, pp. 1068-1086, 2016.

[7]   M. Arbab, H. Masjuki, M. Varman, M. Kalam, S. Imtenan, and H. Sajjad, "Fuel properties, engine performance and emission characteristic of common biodiesels as a renewable and sustainable source of fuel," *Renewable and Sustainable Energy Reviews,* vol. 22, pp. 133-147, 2013.

[8]   A. Azad, M. Rasul, M. Khan, A. Omri, M. Bhuiya, and M. Hazrat, "Modelling of renewable energy economy in Australia," *Energy Procedia,* vol. 61, pp. 1902-1906, 2014.

[9]   J. Thangaraja and C. Kannan, "Effect of exhaust gas recirculation on advanced diesel combustion and alternate fuels-A review," *Applied Energy,* vol. 180, pp. 169-184, 2016.

[10]   S. S. Nathan, J. Mallikarjuna, and A. Ramesh, "Effects of charge temperature and exhaust gas re-circulation on combustion and emission characteristics of an acetylene fuelled HCCI engine," *Fuel,* vol. 89, pp. 515-521, 2010.

[11]   M. M. Ibrahim and A. Ramesh, "Experimental investigations on a hydrogen diesel homogeneous charge compression ignition engine with exhaust gas recirculation," *International journal of hydrogen energy,* vol. 38, pp. 10116-10125, 2013.

[12]   M. P. Musculus, P. C. Miles, and L. M. Pickett, "Conceptual models for partially premixed low-temperature diesel combustion," *Progress in Energy and Combustion Science,* vol. 39, pp. 246-283, 2013.

[13]   S. Imtenan, M. Varman, H. Masjuki, M. Kalam, H. Sajjad, M. Arbab*, et al.*, "Impact of low temperature combustion attaining strategies on diesel engine emissions for diesel and biodiesels: a review," *Energy Conversion and Management,* vol. 80, pp. 329-356, 2014.

[14]   D. Splitter, S. Kokjohn, K. Rein, R. Hanson, S. Sanders, and R. D. Reitz, "An optical investigation of ignition processes in fuel reactivity controlled PCCI combustion," *SAE International Journal of Engines,* vol. 3, pp. 142-162, 2010.

[15] K. Pohlkamp and R. D. Reitz, "Reactivity controlled compression ignition (RCCI) in a single-cylinder air-cooled HSDI diesel engine," *SAE Technical Paper* 0148-7191, 2012.

[16] S. I. Pishbin, M. Ghazikhani, and S. M. R. M. Razavi, "Experimental study on the effects of flame regime on the exergy destruction in premixed low swirl combustion," *International Journal of Exergy,* vol. 17, pp. 267-286, 2015.

[17] R. Cheng, D. Littlejohn, W. A. Nazeer, and K. Smith, "Laboratory studies of the flow field characteristics of low-swirl injectors for adaptation to fuel-flexible turbines," *Journal of Engineering for Gas Turbines and Power,* vol. 130, p. 021501, 2008.

[18] L. Coniglio, H. Bennadji, P. A. Glaude, O. Herbinet, and F. Billaud, "Combustion chemical kinetics of biodiesel and related compounds (methyl and ethyl esters): Experiments and modeling–Advances and future refinements," *Progress in Energy and Combustion Science,* vol. 39, pp. 340-382, 2013.

[19] S. J. Klippenstein, V. S. Pande, and D. G. Truhlar, "Chemical kinetics and mechanisms of complex systems: a perspective on recent theoretical advances," *Journal of the American Chemical Society,* vol. 136, pp. 528-546, 2014.

[20] J. Zhu, K. O. Lee, A. Yozgatligil, and M. Y. Choi, "Effects of engine operating conditions on morphology, microstructure, and fractal geometry of light-duty diesel engine particulates," *Proceedings of the Combustion Institute,* vol. 30, pp. 2781-2789, 2005.

[21] A. Hegab, A. La Rocca, and P. Shayler, "Towards keeping diesel fuel supply and demand in balance: Dual-fuelling of diesel engines with natural gas," *Renewable and Sustainable Energy Reviews,* vol. 70, pp. 666-697, 2017.

CHAPTER TWO

LITERATURE REVIEW

2.1 Introduction

There are a number of studies and research publications that have been written on the effects of exhaust gas recirculation (EGR) on diesel engines in relation to their performance and emission characteristics. Emissions is a pivotal factor in internal combustion engines because of the stringent emission control regulations that keep on changing day by day. This review work will look at the development of EGR as a control measure for NO_X emission reduction and how it affects the parameters of diesel engine performance in terms of both the dependent and independent variables. It is imperative for both the old and new emission control techniques to be harnessed, as there is no one solution that can solve the global emission problem associated with diesel internal combustion engines. Since we are dealing with diesel internal combustion engines performance and emission characteristics, this review will look critically at the developments in relation to combustion control strategies. This work will then look at developments in alternative fuel which have been gaining momentum as the reserves of our primary sources of energy become increasingly depleted, and the concerns about pollution increase. Additionally, this review work will examine the impact of EGR on biodiesel fuels whose use is gaining widespread acceptance and is being researched by various groups around the world. This is important as waste to energy solutions are gaining momentum in energy studies and development, to replace earlier biodiesels which were primarily from agricultural food plants. This is intended to address and answer the problem of food security especially in developing countries. Therefore, several works on recycled waste energy have been considered here and reviewed. Finally, this review will look at the global impact of the emissions from diesel propelled automobiles on human health and what the field has been doing to address the problem and the environmental pollution causing it.

2.2 EGR, Combustion and Development in Control Strategies

The future of the diesel engine considering the current context demands modification in combustion strategies coupled with development of high quality fuels not limited to only conventional diesel, to meet increasingly stringent emission control legislation. It would be unfair to this review if modern day combustion strategies were not discussed and reviewed to reveal how this area has been progressing over time, and how these studies have impacted on the performance and emission characteristics of the diesel engine. EGR is considered as one of

the most effective techniques for controlling NO_X and PM emissions, mainly due to the many advantages it offers, which include lower flame temperatures and decrease in oxygen concentration in the combustion mixture of the combustion chamber.

Zheng et al. (2004) reported that the main challenge is to minimize the pollutants by manipulation of the thermodynamic fuel properties and oxygen concentration of the cylinder charge, through limiting and minimizing degradation of power and deficiencies of the diesel engine. [1] says that under conventional operations the diesel engine burns 99.5% of injected fuel, but when operating in LTC environment, this efficiency is decreased to around 95 %, resulting in misfiring brought about by the lower boundaries of LTC and the lack of sufficient fuel for flame propagation. [1] further suggests that to mitigate LTC it is imperative that intake temperatures and intake pressure be controlled as these are reported to reduce LTC NO_X and PM by 24 % and 50 % respectively; when intake boost pressure is increased by 1 bar, it reduces HC and PM by 50 % and 75 % respectively.

The EGR system can be classified into three main categories according to [12].

- Hot EGR, where the circulated exhaust gas is directly delivered into the intake system when hot, resulting in very high inlet intake temperatures.

- Partly Cooled EGR, where the circulated gas temperatures are kept just above the dew point.

- Fully Cooled EGR, where the circulated gas is fully cooled before it is mixed with the intake fresh charge, either using water cooled heat exchangers or intercooling mechanisms.

Figure 2.1 shows the variation of NO_X emissions with oxygen mass fraction in hot and cool EGR modes.
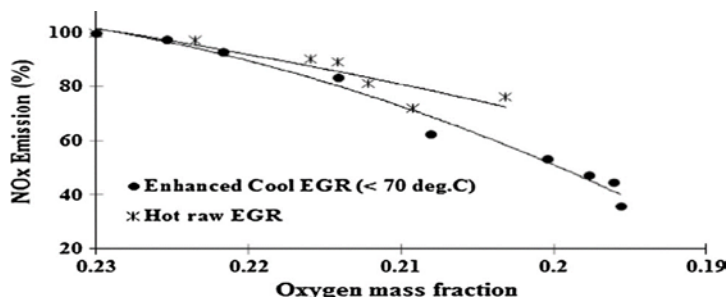
Figure 2.1: Variation of NO$_X$ emissions with oxygen mass fraction in hot and cool EGR modes [2]

Increasing the EGR ratio changes the shape of the heat release rate (HRR) especially during pre-mixed combustion, which greatly suppresses NO_X formation as reported by [3, 4]. When compared to petrol engines, diesel engines almost remain unaffected by the application of a high EGR % flow rate. This is due to the fact that EGR affects the stoichiometric conditions of SI engines by directly reducing the volumetric efficiency i.e. the total number or amount of oxygen that can be combusted with fuel [1].

Due to the increase in the rate of EGR in diesel engines the following effects on performance and combustion are observed [4]:

Dilution Effect

EGR application, as aforementioned, decreases the oxygen concentration in the combustion cylinder, therefore the fuel spray has to travel, diffuse and mix with oxygen to form a balanced stoichiometric mixture suitable for combustion, [3, 5, 6]. The localized regions within the combustion chamber not only contain a stoichiometric mixture or a balanced mixture but also contain other additional gases, namely, CO_2, H_2O and N_2 [4]. These combustion components absorb the heat energy released during combustion, thereby lowering the temperature and consequently affecting the kinetic movement of NO_X elements and thus the formation of NO_X.

Ignition Delay

The presence of diluent elements of CO_2 and H_2O increase ignition delay (combustion retardation) by changing or altering the location of the SOC, shifting it towards the end of the expansion stroke, further reducing the exposure of the combustion mixture to high temperatures and thus forming less NO_X [3, 7].

Chemical Effects

During the high temperature combustion process recirculated CO_2, H_2O and water vapor disassociate, modifying in the process the combustion temperature and the formation of NO_X. Due to the reduction in the flame temperature this leads to decreased NO_X emissions [1, 3].

Thermal Effects

Thermal effects result from the higher heat capacity of CO_2 and H_2O in the EGR gases as compared to the heat specific ratio of the incoming charge i.e. the intake charge which has CO_2 and N_2. This phenomenon is responsible for the overall increase in the heat capacity of the in-cylinder mixture thereby reducing the flame temperatures. [8] conducted various experiments

and detailed research on irreversibility in the combustion process and found out that the chemical reactions and transport phenomena are responsible for irreversibility in the combustion process. This work was achieved by measuring the role of exergy destruction in the combustion process exchange owned by the internal thermal energy exchange. Exergy is defined as energy availability and defined further by [9] as the "maximum possible useful work that can be obtained from energy in a given environment", a discussion derived from the second law of thermodynamics in the analysis and examination of engine performance responses under different operating conditions and parameters. The second law of thermodynamics states that "No heat engine can produce a network output by exchanging heat with a single fixed temperature region" [10] and is expressed in equation form as:

$$Q_{add} \text{ and } Q_{rej} \neq 0 \hspace{3cm} \text{Equation 1}$$

Where Q_{add} is the heat added into the system, Q_{rej} is the heat being ejected by the system.

Another area worthy of mention in connection with this review and the scope of this study, is the EGR ratio which has been expressed by many scholars and researchers in different forms and mathematical equations, for example Equation 2 and 3 [11] and expressed as:

$$EGR \ \% \ = \ \frac{(Co_{2-EGR} - CO_{2-atm})}{(Co_{2-EGR} - CO_2 - atm)} \hspace{2cm} \text{Equation 2}$$

Where CO_2 is the recirculated carbon dioxide fraction, CO_2 is the carbon dioxide in the exhaust system, EGR % is the exhaust gas recirculated mass flow rate percentage.

From Equation 3 [11] define the percentage rate of EGR as "the mass percentage of the recirculated exhaust gas (M_{EGR}) in the total intake mixture (M_{in})." This suggests the use of the recirculated CO_2 fraction by comparing CO_2 concentration in the exhaust (CO_{2-exh}) and CO_2 concentration in the intake manifold of the engine (CO_{2-int}) to determine the EGR flow rate. After defining the EGR % flow rate the authors further found that the use of EGR increases the specific heat capacity (SHC) and decreases oxygen availability. This directly reduces the peak cylinder pressure and leads to the conclusion that decreased combustion temperature affects peak heat release ratios if and when exhaust gas recirculation is applied. Regarding the intake mass flow rate, they observed that an increase of EGR % flow rate reduces the intake mass flow rate as compared to when the EGR % flow rate is zero. This affects the volumetric efficiency as less air is admitted to the engine cylinders. However, as EGR % flow rate increases they observed a decrease in fuel efficiency, which they attributed to the application of the EGR % flow rate.

The second method is derived from the second equation of calculating exhaust gas recirculation proposed by [12], where they represent the percentage of recycled gases by an EGR ratio (the mass ratio of recycled gases as compared to the whole mixture intake into the engine) by comparing it to CO_2 in the fresh air intake which is assumed here to contain negligible amounts of CO_2 and the EGR CO_2 which contains vast amounts of CO_2, as the rate of EGR % flow rate increases. This is captured in Equation 3 from [12]:

$$EGR\ RATIO = \frac{INTAKE\ CO_2\ Concetration}{EXHAUST\ CO_2\ Concentration}$$
Equation 3

The EGR ratio in Equation 3 is calculated or measured from the amounts of CO_2 in the intake charge and the figure is compared to the amount of CO_2 in the exhaust gases. It should be noted that the concentration of the engine intake CO_2 is lower than that from the cylinder charge, but the residue amount is boosted to dilute the fresh charge intake of the engine thereby providing prompt EGR, which normally falls outside the concentration of the intake CO_2 defined above and as shown in the linear Equations 4 and 5 [12] as:

$$x_{O_2} = 0.21\ (1 - x_{CO_2})$$
Equation 4

$$x_{N_2} = 0.79(1 - x_{CO_2})$$
Equation 5

Where x_{O_2} is the exhaust molar concentration of oxygen, x_{N_2} is the exhaust molar concentration of nitrogen, x_{CO_2} is the molar concentration in the exhaust system.

In a simulation experiment of the Equation 4, [12] observed that as the molar concentration of CO_2 increases, the molar concentration of O_2 and N_2 mixtures decrease linearly as in Equation 4. A simulated EGR operation was used to explain the prompt EGR phenomena and the thermodynamic and dilution effect of EGR. However, since EGR affects the equilibrium state of the entire system, it makes feedback control conservation necessary. Therefore, in order to estimate the EGR rate the air intake was measured using a MAF sensor, by making an assumption that the cylinder mass flow rate and that of the EGR % flow rate are to be conserved and therefore assumed to be as in Equation 6:

$$\dot{M}_{EGR} = \dot{M}_{INT} - \dot{M}_{MAF}$$
Equation 6

Where $\dot{M}_{EGR}$ is the mass flow rate of the EGR gases, $\dot{M}_{INT}$ is the inlet intake mass flow, $\dot{M}_{MAF}$ is the mass flow rate as measured by the mass air flow sensor.

But the mass flow rate of the cylinder is dependent on a number of factors such as EGR gases temperatures, engine block temperature, after cooling temperature and boost pressure, which are outside the monitoring capacity of the ECM. General engine operating stabilities are affected by the widespread use of EGR operation through the following key areas as noted by [11]:

- EGR loop differential pressure

- EGR cooler cooling efficiency

- In-cylinder combustion efficiency

- Exhaust temperatures

- Intake temperatures

Although EGR is a vital method in the control of NO_X it is still important to say that it has application limits, which lead to degradation of efficiency of the energy derived from the fuel and the mechanical durability of the diesel engine components. Among the measures [11] recommend is exhaust gas recirculating cooling, because of its proven capacity to increase the intake inlet charge density. This is equivalent to the intercooling boosting of the mass air flow rate of the admitted charge. This was identical to the findings of [13]. In addition to EGR cooling they additionally recommend the adoption of an EGR fuel reforming catalytic rich combustor into the EGR loop to generate gaseous fuels. These gaseous fuels are intended to produce hydrogen gas and carbon monoxide in a controlled amount through the process of diesel reformation. Fuel reforming shares the advantages of homogeneous charge CI engine systems, and can be expressed in equation form to give a mathematical expression as in Equation 7:

$$\lambda \text{ gas} \geq 1.35 \qquad\qquad\qquad\qquad\qquad \text{Equation 7}$$

Where $\lambda\ gas$ is the air fuel ratio, in this case of the gas fuel.

[1] discusses a number of control strategies to be employed in mitigating the effects of emissions, one of which is EGR. The authors point out that the application of EGR alters the normal combustion process in several ways: firstly, by altering the physical properties of the charge mixture; secondly by altering the air fuel ratio (AFR); and thirdly by altering the start of ignition thereby altering the heat release pattern.
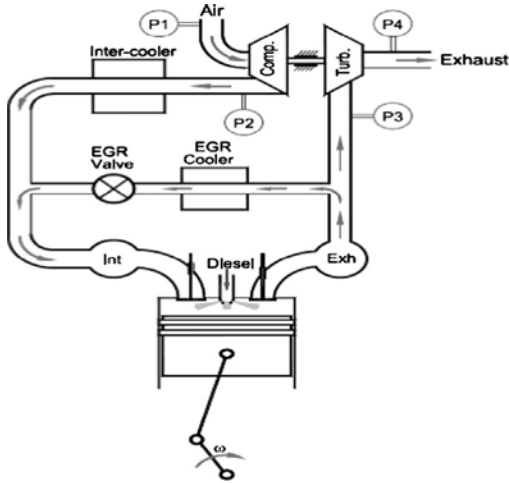
Figure 2.2: EGR loop – high pressure loop (HPL)
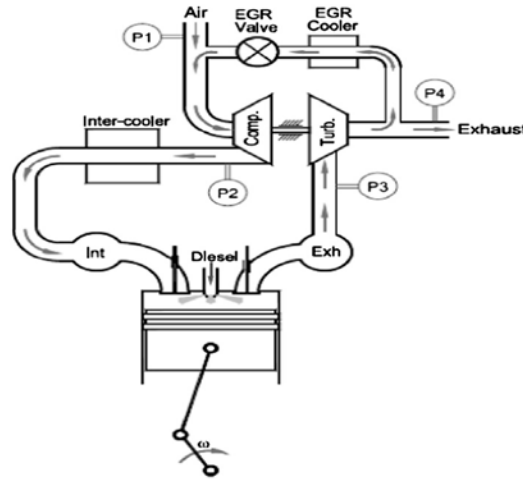
Figure 2.3: EGR loop – low pressure loop (LPL) [14]

From Figure 2.2 above one can see that if the EGR system gases are taken from the exhaust upstream of the turbine directly into the intake manifold where pressure $P_3 - P_2 > 0$, the delivery arrangement pipe is shorter, hence the name short part (HPL) EGR, where the pressure $P_3 > P_2$ where in this case it is the intake pressure. The long part arrangement, known as low pressure loop (LPL) EGR, is when $P_3 - P_2 < 0$ as shown in Figure 2.3. The LPL has the disadvantage of ravaging aluminium made components like the compressor and the plumbing components, while the HPL has the demerit of low boost pressure requiring a turbocharger to be matched as reported by [15]. This allows the turbocharger to increase the boost pressure with the addition of a venturi device as an auxiliary unit [6, 13] to help in expanding the feasible range of boosting without affecting fuel economy (pumping losses increase as boost pressure drops) [16].

While discussing novel combustion strategies it is imperative to mention a very important factor in combustion studies, the factor of the dilution ratio (DR), derived and defined by [6] as in Equation 8 as:

$$DR \% = 100 * \frac{21 - Xo_{2-in}}{21} \qquad \text{Equation 8}$$

Where DR % is the dilution ratio percentage, Xo_{2-in} is the O_2 concentration as measured by the output tools in the inlet manifold, especially for the short part HPL EGR system which is mostly used with commercial diesel engines.

Dilution ratio plays a dominant role in the formation of NO_X emissions especially when LTC modelling is used. [14] add that the EGR effect of dilution, in addition to the aforementioned, plays a very influential role in the reduction of NO_X both in advanced concepts of combustion and conventional concepts of combustion. However, in relation to the emissions of soot and homogeneity of the combustion mixtures, it is ignition delay (combustion retardation) that becomes the dominant factor in advanced combustion control modelling. Among the problems the authors found to be associated with the HCCI include poor cold starting, higher HC/CO emissions, limited operation range, difficulty in combustion phase control, control over auto ignition and preparation of the charge mixture.

The pre-mixed ratio (PR) as a control strategy is normally associated with the PCCI combustion strategy that has been adapted by a number of studies notable among them [17, 18] and defined in Equation 9 as:

$$r_P = \frac{Q_P}{Q_t} \hspace{4cm} \text{Equation 9}$$

Where the r_p is the pre-mixed ratio, Q_P is the ratio of energy of the premixed fuel, Q_t is the total energy

But:

$$Q_P = \frac{M_p}{h_{up}} \hspace{4cm} \text{Equation 10}$$

$$Q_t = M_p h_{up} + M_{dhud} \hspace{3cm} \text{Equation 11}$$

Where M_p is the pre-mixed fuel mass, M_d is the diesel fuel mass, p denotes pre-mixed diesel fuel, h_{up} is the lower heating value of the premixed diesel fuel mass.

[19] in "Fuel Injection and EGR Control Strategy on Smooth Switching Of CI/HCCI Mode in a Diesel Engine" conducted an experiment by varying the cam phase and tapping EGR gases as a heating or vaporizing mechanism of the fuel to harmonize the mixture charge, while using fuel injection to administer HCCI with an electronically controlled fuel injection system. The authors used HCCI combustion modelling to study the effects of a premixed ratio in relation to performance and emission characteristics, when different EGR % flow rates were applied. They observed a 78 % drop in NO_X and lowered smoke and soot emissions of 40 %, when premixed ratios of 80 % and 30 % EGR respectively were applied. An increased pre-mixed ratio led to an increase in IMEP and BSFC, but fared poorly regarding HC and CO emissions.

19

[20] in "Recent Development of Biodiesel Combustion Strategies and Modelling for Compression Ignition Engines" reported recent developments in combustion strategies for biodiesel engines, as biodiesel fuels have the same physio-chemical characteristics often shown and exhibited by conventional fossil fuels save for the combustion characteristics. They concluded that the biodiesel combustion process under LTC combustion strategies reduces NO_X significantly due to reduction in the peak combustion temperature with the application of EGR % flow rate. However, there was increase in PM emission resulting from the unburnt hydrocarbons and the fuel impinged on the cylinder walls. These problems are associated with the difference in the fuel properties of the biodiesel fuel mixture. Other conclusions they reported are that biodiesel fuels had lower BTE and higher fuel consumption, therefore, poor BSFC, besides increasing CO and CO_2 emissions.

[21] in "Control of Combustion Process in an HCCI-DI Combustion Engine Using Dual Injection Strategy with EGR" conducted an experiment using internal and external EGR modes to realize fuel vaporization and in-cylinder temperature reduction of 50 %. EGR from the external mode was used in the compression stroke. The result indicated a significant increase in CO/HC emissions as the mixture seemed to suffer from the effect of almost total incomplete combustion.

[22] in their experimental study "Control of Combustion Process in an HCCI-DI Combustion Engine using Dual Injection Strategy with EGR" compared HCCI and conventional diesel engine performance and emission characteristics. When 30 % EGR flow rate was applied, they noted that the combustion of HCCI produced ULN (ultra-low NO_X) emissions, but produced no meaningful reduction in the emissions of soot and SOF.

[23] in "Combustion Characteristics of Diesel HCCI Engine: An Experimental Investigation using External Mixture Formation Technique" used a twin piston DI diesel engine to conduct a study by means of the modification of one cylinder to use HCCI premixed mixture fuel and the other to operate on conventional diesel. During their study they varied their mixture concentration from $\lambda = 4.96$ (as the lean mixture level) or the misfiring limit and $\lambda = 2.56$ (considered as the rich mixture level) or the knock limit. When a 20 % EGR flow rate was applied the results indicated increased combustion efficiency, especially when the value of $\lambda \leq$ 3.70 with medium range engine loads being maintained. Moreover, when the engine load was increased to high levels it was observed that the values of lambda (λ) recorded at $\lambda \leq$ 3.0 and

produced engine knock and a very rough unpleasant running combustion experience from the experimental engine.

[24] in "Effects of Port Fuel Injection (PFI) of N-Butanol and EGR on Combustion and Emissions of a Direct Injection Diesel Engine" studied the effects of PFI on n-butanol with application of EGR % flow rate and how this influences emission and combustion characteristics in a diesel engine. In their study and experiment, they equipped their engine with independent inlet and outlet systems and varied the EGR % flow rate which they divided into three sections of 0 %, 15 % and 45 % and the premixed fuel of the n-butanol which they divided into four premixed ratios of 0 %, 20 %, 38 % and 47 % by volume.

They observed that as the rate of EGR % flow increased to 45 % there was a significant decrease by 97 % of the total NO_X emissions, although there was an exponential increase in soot emissions and SOFs. However, when they combined the use of the PFI and n-butanol of 47 % while maintaining the EGR % flow rate at 45 %, the emissions of NO_x and those of soot were drastically reduced by 88 % and 17 % respectively, thus achieving the traditional basic fundamental problem of the NO_X versus soot trade-off point.

[25] in their study on "Combustion and Emission Characteristics of a DME (Dimethyl Ether)-Diesel Dual Fuel Premixed Charge Compression Ignition Engine with EGR (Exhaust Gas Recirculation)" studied the effects of external EGR and dimethyl ether (DME) on the premixed ratio and on the performance and emission characteristics of a two cylinder naturally aspirated diesel engine. During their experiment they varied EGR % from 0 % to 27 % while keeping the premixed ratio at between 0 % to 30 %. Their results indicated that an increase in EGR % mass flow rate reduced NO_X emissions significantly, but increased CO_2 and HC emissions considerably. However, a very good result was obtained with higher PR % and higher EGR % flow rates especially in regard to NO_X and smoke emissions.

[26] in "Potential of HCCI Concepts for DI Diesel Engines" investigated late combustion strategies of injection of HCCI combustion using the modulated kinetics type of combustion as comparatively experimented by [27], and observed that reduced NO_X levels could be achieved with the application of a high EGR % flow rate of 40 % although the smoke level emissions increased. Retardation and late injection timing after top dead center (ATDC), the authors reported, led to a decrease in fuel efficiency, thus increasing brake specific fuel consumption (BSFC) with a considerable lineal increase in HC emissions. In order to mitigate this problem, the in-cylinder flow to the mixture gases was strengthened through the

optimization of the geometrical design of the intake port, thus allowing them to achieve their objectives of reducing NO_X using a high EGR flow rate of 40 %.

2.3 The Effect of EGR On the Role of Exergy Destruction

[28] in "Effect of Exhaust Gas Recirculation (EGR) on the Performance Characteristics of a Direct Injection Multi Cylinders Diesel Engine" found that there is a relationship between pre-mixed turbulent combustion with the second law of thermodynamics and lost exergy in irreversibility and entropy generation. The authors employed the low swirl combustion (LSC) technique for flame stabilization. Exergy analysis is defined by [29] as a technique that uses the conservation of mass and the conservation of energy in combination with the second law of thermodynamics for design analysis and improvement of energy and other systems.

In their experimental set-up they used a swirler, which consisted of an outer annular swirled section and a center channel for flow retardation (this is a key component) with an attachment of a perforated plate with 16 vanes that aids the center channel to control the flow rate that is allocated to each plate. Another key component in this design is the LSB swirler recess distance which controls the time of interaction between the swirled and unswirled mixture flows parameters with an effect on flow divergence which affects the performance of the LSB component and its operation (Figures 2.4 and 2.5).
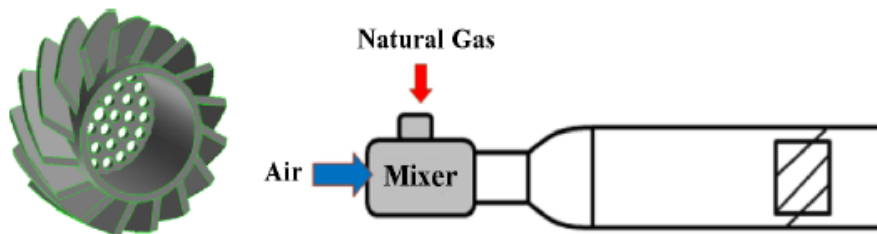
Figure 2.4: The LSB schematic set-up system and the main components
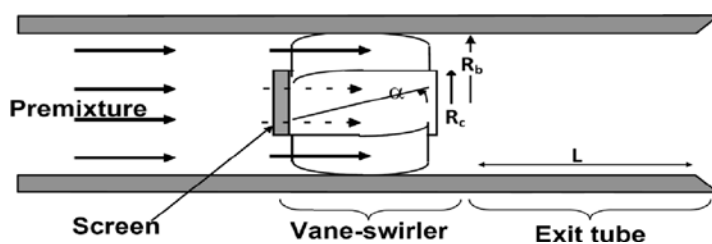
Figure 2.5: The geometrical parameters of the LSB unit as used in the experimental set-up

Figure 2.5 shows the mechanical phenomenon characteristics of geometric, kinematic, and dynamic aspects which affect the swirler combustion performance according to [30]. These factors are as follows: the burner radius(R_b), unswirled core radius (R_c), performance rated plate radius, the vane angle (α), vane numbers, blockage of perforated plate, recess length (L), which are summed up as the geometrical parameters and are considered to be very important.

After the set-up study and experimentation, the following conclusions were reached. The exergy analysis conducted on the LSB running on NG fuel resulted in two distinguished flame regimes, the lifted flame and the attached flame. When the normalized laminar flame speed (V_s) velocity of 10.3 and 17.1 was reached it was observed that a lifted flame type came up, while when the NLFS velocity of 31.9 and 42.9 was reached the flame observed was the attached flame type. Thirdly the exergy of heat transfers between the flame and the combustor walls in the lifted flame type was observed to be greater and more significant compared to the values of the attached flame type, although they observed via the exhaust gases released that the exergy transfer had minimal increment in the attached flame regime when the same was compared to the lifted flame regime.

The value of the irreversibility ratio (Irr) for the diffusion flames was found to be very large, while the irreversibility of the premixed combustion was 35.5 %. However, when the flame regimes were changed the authors reported that the irreversibility decreased as the flames were being altered by a value of 11 %. The Irr was observed to receive significant contribution from the flame regime local temperature gradient, because temperature gradients are stronger when the values of V_s are higher.

Figure 2.6 and Figure 2.7 [28] show the relationship between flame temperature and the combustor, with Figure 2.9 indicating the temperature range of the combustor during the experiment. The lifted flame showed a better heat transfer of 14 % more between the combustor's combustion chamber and the surroundings environment compared to the attached flame.
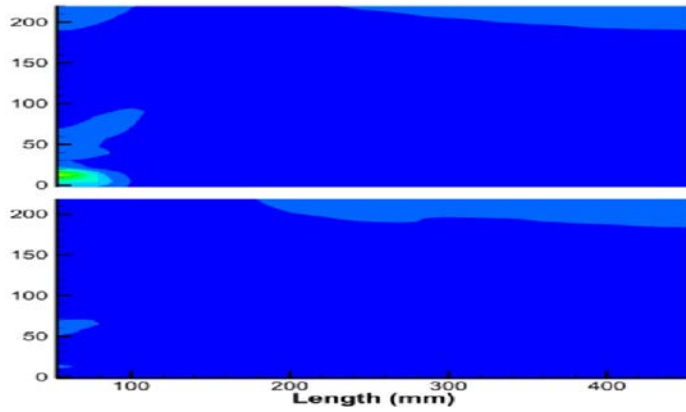
Figure 2.6: Variation of temperature versus flame radius length of lifted and attached flame
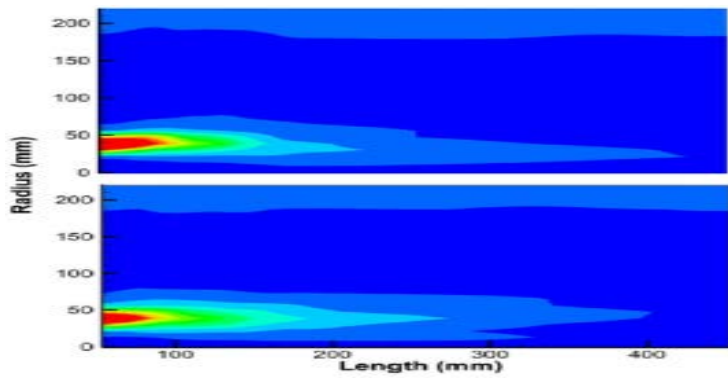
Figure 2.7: Variation of temperature versus flame radius length and flame progression of lifted and attached flame
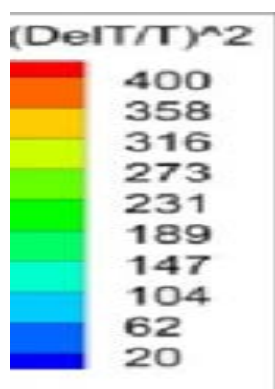
Figure 2.8: Variation of the temperature range for the two types flame progression regimes shown in Figures 2.7 and 2.8.

2.4 The Effects of EGR On Emission and Combustion Characteristics of Biodiesel

In mentioning and discussing the combustion models it is obvious that the development of alternative fuels is of paramount importance. There are several methods that have been proposed for processing alternative fuels also called biodiesels or biofuels, the common methods being transesterification, hydrogenation, pyrolysis (used in plastics) and dilution. The use of alternative fuel for emission control has been increasing, particularly with the use of the EGR control technique to control and reduce NO_X, HC, CO, and soot emissions. A number of authors have carried research in this area and this review will present some of the studies and experimental work conducted and the current direction in research and development.

[31] in "An Experimental Investigation on a DI Diesel Engine using Waste Plastic Oil with Exhaust Gas Recirculation" showed that plastic oil produced the most NO_X emissions but showed reduced NO_X emissions with increasing EGR of 20 % onwards. However, in the smoke, CO and HC levels of emissions there was no noticeable change. The authors concluded that with the application of increasing EGR % flow rate levels, plastic oil can be used as an alternative biodiesel fuel.

[32] in the "Effects of Exhaust Gas Recirculation on the Performance and Emission Characteristics of a Diesel Engine Fueled with Waste Cooking Oil Methyl Ester" used a single cylinder four stroke water cooled DI compression ignition engine, with a dynamometer, coupled to an output shaft. Modifications were carried out to allow the experiment to be carried out. In order to collect data a digital panel was installed, while an exhaust gas analyzer was used to investigate emission characteristics of the various gases in this study, namely, CO, CO_2, HC, NO_X and O_2. The test fuel blends they used were BO = (normal diesel) blended with waste cooking oil methyl ester (WCOME) where B10 = 10 % WCOME + 90 % diesel, B20 % WCOME + 80 % diesel by volume, B30 % WCOME + 70 % diesel by volume. The EGR % mass flow rate ranged from 0 % to 20 % graduated in intervals of 5 %. All the tests were conducted at constant engine speed of 1500 rpm. The following parameters were investigated and their variations: BSFC, BTE, EGT and emission characteristics of NO_X, HC and CO.

During their study they observed that the BTE remained unaffected by the application of EGR % flow rate that was above 15 %, but tended to decrease as the EGR % mass flow rate increased beyond 15 % EGR. This drop is explained from the fact that the availability of oxygen was reduced during combustion with the application of a EGR of 15 %. The brake specific fuel consumption (BSFC) was observed to be independent of the rate of EGR % flow rate,

especially at lower rates of EGR % flow, but it increased as the rate of EGR % flow rate increased above 15 %. This phenomenon is explained by the fact that there was formation of a rich mixture due to the dilution effect in the combustion chamber, this being identical to the findings of [33].

The exhaust gas temperature (EGT) was observed to be lowered if the engine was running on cooled EGR compared to when the engine exhaust gases were not cooled. The cooling of the EGR gases affects the heat specific ratio of the intake air mixture, by causing less oxygen in the combustion chamber. The NO_X emission findings indicate that for all the fuel blends used during the study, the NO_X emissions decreased with the increase in EGR % flow rate. This can be explained by two factors: reduction in the availability of oxygen during combustion, and the lower combustion temperatures (NO_X is temperature dependent for its formation so will decrease as flame temperatures drop). The HC and CO emission showed an increase with the increase of the EGR % flow rate above 15 %, as less oxygen becomes available for combustion, resulting in incomplete combustion and more HC and PM emissions.

[34] in "Experimental Analysis of Exhaust Gas Recirculation on Diesel Engines Operating with Biodiesel" used a four stroke, water cooled engine, single cylinder DI, rated at 5.2 kW power with 1500 rpm rated speed. The experiment was conducted in two phases. The first phase investigated the performance, combustion and emission of the diesel fuel with biodiesel blends of B20 where the EGR application was zero. The second phase of the experiment was conducted using the same equipment and test rig with fuel blend of B20 but under EGR % flow rate application. The range of distribution for EGR % flow rate was 5 %, 10 %, 20 %, while the load was distributed into 20 %, 40 %, 60 % 80 % and 100 %.

The tests and study found that the BSFC for the test fuel without EGR under full engine load was seen to be 0.2779 kg/kW-hr and 0.2794 kg/kW-hr for the biodiesel respectively. The values of the BSFC at full engine load and EGR % flow rates of 5 %, 10 %, 15 % and 20 %, were 0.2853 kg/kW-hr, 0.2796 kg/kW-hr, 0.2832 kg/kW-hr and 0.3050 kg/kW-hr respectively, whereas for higher EGR % flow rate of 20 % the BSFC increased for both diesel and biodiesel. This was attributed to the high calorific values (CVs), high viscosity, high density and boiling point. The BTE for the biodiesel was found to be comparable to that of diesel with or without EGR % flow rate.

The variations between the hydrocarbons and the brake power (BP) results and conclusions indicate that with an increase in EGR % flow rate levels, the HC emissions also increased only

for the biodiesel, attributed to the presence of high oxygen content in most biodiesels, thus compensating for the lack of oxygen to facilitate complete combustion thereby increasing BTE. The values for the NO_X during the study were found to be 736 ppm for diesel fuel running without EGR in a full load environment and 796 ppm for biodiesel at full load without EGR. However, with the application of EGR it was noticed that the levels of NO_X reduced to 157 ppm for diesel and 158 ppm for biodiesel respectively, but a reduction in BTE was established with large increments in smoke density.

Carbon monoxide (CO) in relation to diesel and biodiesel with various levels of EGR % flow rate and load condition was noted to vary from 0.14 % (by volume) for the diesel to 0.18 % (by volume) for the biodiesel all at full engine load conditions. The authors concluded that as the EGR % flow rate increased so did the CO emission increase, caused primarily by the lack of oxygen during the combustion process. The smoke density was generally found to be lower or decreased for biodiesel compared to diesel fuel and this was observed for all engine loads. As the EGR % flow rate increased there was an observed increase in the smoke density. This is explained by the fact that EGR affects the oxygen availability leading to incomplete combustion and the formation of more PM.

The EGT was observed to increase with increase in load, being more noticeable for biodiesel than for diesels at all engine applicable loads and conditions. This increase in temperature during this experiment was attributed to higher oxygen content in all biodiesel fuels particularly those used in the study. This study finding was identical to [35]. The cylinder pressure at full engine loads with EGR at zero was observed to be comparable to biodiesel, arising from the fact that there was a good mixing from the biodiesel mixture under high load, because EGR gases act like heat absorbing agents. Combustion analysis revealed significant HRRs, with or without the application of EGR % flow rate.

[36] in "Effect of EGR on Performance and Emission Characteristics of a Dual Fuel Engine Fueled with CNG and JOME" studied the dual fuel engine mode which has been identified as one of the most promising combustion techniques available today. The experimental set-up used a Kirloskar engine model CAF 8 rated at 5.9 kW/h @1500 rpm. In order for the homogeneous mixture of compressed natural gas (CNG) and air to be introduced into the cylinder, a venture type gas mixture was used. The fuel injection system pressure was not changed but remained at 200 bar and injection timing at 23˚ BTDC. The engine was then coupled to a dynamometer, with other necessary modifications done to enable the engine to be

used during the experiment. In this experiment two different types of fuels were used simultaneously, one as a primary fuel and the other fuel as a pilot fuel. A mixture of the two was then introduced into the combustion chamber during the intake stroke, at different phases. The homogeneous mixture could not ignite automatically due to the high self-ignition temperature, thus requiring injection of the pilot fuel to ignite the homogeneous mixture. This then was a hybrid ignition model of SI and CI engine types.

After testing and evaluation, the BTE was observed to be dependent on the combustion quality produced in the combustion chamber. The BTE for conventional diesel was shown to be relatively higher than the dual fuel, especially in low engine load environment, explained by the high self-ignition temperatures exhibited by the CNG in addition to the its poor flame propagation qualities. There was better utilization of the CNG fuel due to the ignition delay as the engine load was increased, tending the fuel-air mixture towards the richer side, which increased the combustion temperature in the cylinder. At high engine loads the authors reported an improved BTE equaling that normally associated with conventional diesel fuel propelled engines. When EGR % flow rate was employed, the dual fuel showed minimal increment at lower engine loads, but at higher loads with application of EGR % flow rate increasing, the BTE decreased. The application of EGR made the mixture of the dual fuel richer thus leading to poor utilization hence decreased values for the BTE. This outcome was identical to the study of [37, 38].

The brake specific energy consumption (BSEC) or brake specific fuel consumption (BSFC) during the study was found to be higher for conventional diesel fuel compared to the dual fuel at low and intermediate engine loads. This is explained by the relatively poor utilization of the gaseous fuel in the dual fuel mode at low engine loads up to intermediate engine loads. However, as the engine load increased there was better utilization of the high CV of the dual fuel CNG, thus the BSEC increased compared to conventional diesel. The application of EGR showed improved BSEC at low engine loads as reburning of the unburnt hydrocarbons occurred, but as the load was increased the BSEC decreased, explained by the richer mixture and drop in combustion temperatures.

Figure 2.9 shows the variation of UHC with engine load for diesel fuel, CNG and blends of Jatropa oil methyl ester (JOME) operating under EGR [36].
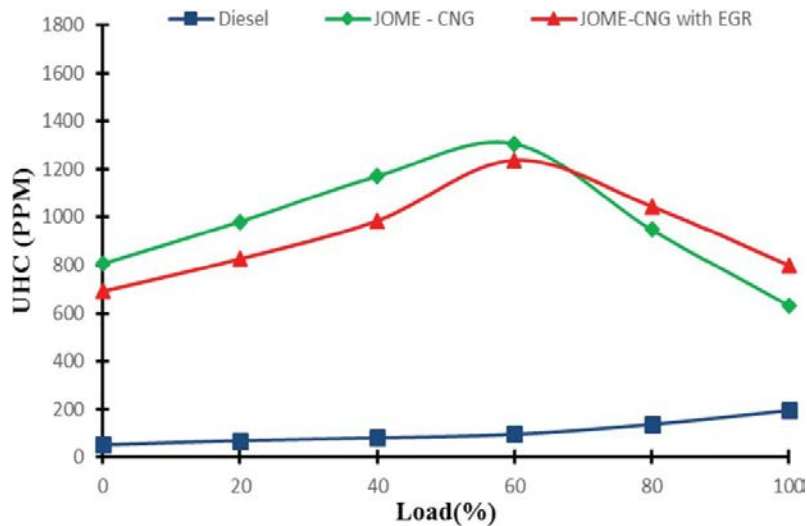
Figure 2.9: UHC vs Load

The emissions of UHC or the un-oxidized particles of fuel showed that at low loads the dual fuel performed poorly in utilization of fuel, but as the load increased, the UHC for the dual fuel was noted to be higher and increasing s compared to conventional diesel fuel for all the remaining load conditions tested. This is explained by the overlapping valves between the exhaust and the inlet valves respectively and the flammability limit of the CNG. The results of this study were identical to those of [39, 40].

UHC emissions are noted to increase with increasing engine load, but at high engine load the dual UHC emission continued to decrease, a phenomenon also identified and observed by [41] as in Figure 2.9. [36] reported that the use of EGR with the dual fuel mode reduced the volume of UHC emissions especially during low and intermediate engine loads. This is explained from the unavailability of O_2 due to the displacement caused by the re-introduction of the exhaust gases back to the combustion cylinder, thus burning the UHC, hence reducing the unburnt hydrocarbon (UHC) emissions. However, higher engine loads mean less availability of O_2 resulting in incomplete combustion and poor oxidation of the induced charge, hence an increase in the UHC emissions for the dual fuel with the application of EGR % flow rate.

The NO_X emissions gases, which depend on combustion temperature and the availability of O_2 for their formation, indicated an increase for conventional diesel fuel compared to the dual fuel at low and intermediate engine loads. This factor is explained by the high in-cylinder temperatures associated with conventional diesel combustion, which is an identical result to the study by [42]. The dual fuel did not show any difference from the conventional diesel fuel

29

results mentioned above. However because biodiesels contain more O_2 content (in this case JOME), there was a considerable increase in NO_X emissions, being an identical outcome to the studies conducted by [43]. The application of the EGR % flow rate with the dual fuel mode was seen to reduce the NO_X, emissions for all the engine load conditions and environment, being identical to the study findings of [38]. The application of EGR % flow rate dilutes the inlet intake mixture, thus increasing its SHC hence reducing in-cylinder temperature, therefore leading to the suppression and reduction of NO_X emissions. However, it should be remembered that increasing the EGR % flow rate reduces NO_X emissions but also decreases BTE.

The CO emissions during the study on the dual fuel showed very poor fuel utilization and incomplete combustion, explained by the low in-cylinder combustion temperature and the limited availability of O_2. Carbon emissions from dual fuel are higher than from conventional diesel fuel for all the engine operating loads except full engine load. The application of EGR % flow rate enhanced complete combustion, hence the decrease in CO emissions at low and intermediate loads. However, at high engine loads the richer mixture reduces the O_2 concentration in the combustion chamber thus reducing CO emissions for the dual fuel mode application. Smoke emissions were observed to increase with increasing engine load for all the operating experimental modes. This was explained by poor utilization of fuel and incomplete combustion during the dual fuel mode operation. The application of EGR increased smoke emissions for all the engine loads that were tested, due to the decreased levels of O_2 in the combustion chamber.

[44] In the "Effects of Varying EGR Rates in the Performance and NO_X Emission of an In-Direct Diesel Injection (IDI) Diesel Engine Fueled With JB100, JB80, JB60, JB40, JB20 And Diesel" used a single cylinder engine, water cooled in direct diesel injection (IDI) diesel engine, connected to an electrical loading system.

After conducting the study, they observed that at 15 % EGR flow rate, blends of JB20 at 25 % EGR rate flow, JB40 at 15 % EGR flow rate, JB60 at 20 % EGR flow rate, JB80 at 40 % EGR flow rate, and JB100 at 5 % EGR flow rate. Their NOX emissions effectively reduced by 10.1 %, 11.94 %, 13.4 %, 15.2 %, 19.8 % and 24.8 % respectively. However, soot emission and PM, CO, and CO_2 increased. The biodiesel blends all showed high levels of NO_X emission explained by the fact that biodiesel blends contain higher amounts of oxygen and can be seen at all full loads in the diesel blends with values of 882 ppm, 848 ppm, 806 ppm, 775 ppm, 737 ppm respectively, whereas for diesel only the value is 643 ppm.

The BTE was observed to be lower for all the JB blends compared to diesel due to the lower CV of the biodiesel but the viscosity index was seen to be very high. During the study diesel and the JB20 blend of fuel showed a better BTE value among all the blends used in the study when 5 % EGR flow rate was applied, while the JB90 blend of fuel showed the maximum reduction of NO_X percentage but with decreased BTE of 1.25 %. The decrease in BTE during this study was attributed to less availability of oxygen in the fresh charge which is an effect from the EGR application, where the addition of exhaust gases resulted in lower flame temperatures and velocity leading to an increase in soot and PM. However, JB60 test fuel with a 20 % EGR flow rate reduced NO_X emissions to 19.81 % with a slight increase in the BTE of 0.77%, attributed to the re-burning of the UHCs entering together with the EGR % flow rate and helping to complete the combustion of the fuel.

[45] in "Performance Analysis of a Single Cylinder Diesel Engine Using Jatropha Oil with EGR" investigated the effects of biodiesel from Jatropha oil on the performance and emissions characteristics of a diesel engine using a single cylinder TV1 Kirloskar model engine, four stroke, water cooled and with a rated power of 3.68 kW at 1500 rpm.

After testing and experimentation the observation was made that the BTE decreased with an increase in EGR flow rate from 5 % to 10 %. The BSFC for all the blends of the Jatropha increased compared to conventional diesel with an EGR flow rate of 5 % to10 %. The B20 blend of Jatropha oil showed the most improved result for BSFC and total fuel consumption. When the blends of B10, B20 and B30 were used without the application of EGR % flow rate, there was an increase in BSFC which was not clearly noticed with EGR flow rate application. Therefore, the authors concluded that CO emissions increased as the rate of EGR is increased, while the NO_X emissions decreased with application of EGR in all the Jatropha blends.

[46] in "Emission Reduction Using Hydro Treated Vegetable Oil (HVO) With Miller Timing and EGR In Diesel Combustion" studied the effects of EGR on hydro-treated vegetable oil (HVO) in reduction of emissions in relation to combustion parameters in a diesel engine. The Miller cycle test included three phases of intake valve closing timing and an advanced (SOC) system, which showed a considerable reduction in the NO_X and the smoke emissions. Their study reported a marked reduction in the emissions of NO_X and smoke, thus concluding that compared to conventional diesel EN590, the hydro treated vegetable oil (HVO) fuel blend can allow the use of higher EGR % flow rates without compromising on PM, UHC and smoke emissions but with an exponential reduction in NO_X emission

2.5 Effects of EGR on Performance, Combustion and Emission Characteristics of Diesel Engines (DI/IDI)

[3] in the "Effect of Exhaust Gas Recirculation (EGR) on the Performance Characteristics of a Direct Injection Multi Cylinders Diesel Engine" used a direct DI, four-cylinder Fiat engine, coupled to a dynamometer and thermocouple with nickel chromium (Ni-Cr) and nickel alumide (Ni-Al) elements, air and fuel flow meters, together with engine speed tachometers. The test fuel was Iraqi conventional diesel CN = 46.8 under varying EGR % flow rates of 5 %,10 %, 20 %, and 30 %. All engine load was maintained at variable speeds of 1250 rpm to 3000 rpm.

EGR % flow rate at increased rates increased the BSFC, while at low engine load ranges it was found to be high compared to when medium engine load ranges were used. This was attributed to the drop in combustion chamber temperature. However, reducing the temperature increased the fuel delay period, thus reducing engine peak pressure resulting in lower engine outputs and increased fuel consumption. [3] observed that at low engine loads diesel engines operate on lean mixture and their volumetric efficiency is very high, but increasing the engine load consumes more fuel in order to meet the load demands as the engine motor speed is increased. However, in increasing the load and engine speed the EGT increases too, while increasing the EGR % flow rate reduces the temperatures, as can be seen in Figure 2.10.
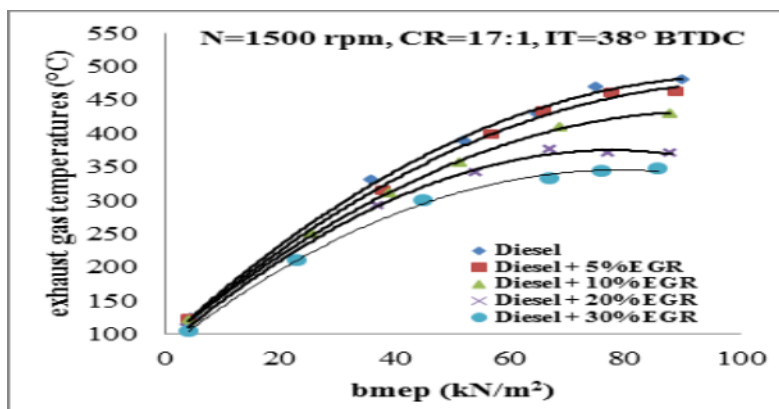
Figure 2.10: Variation of exhaust gas temperature with brake mean effective pressure under different diesel test fuel with application of EGR % rate flow [3]

[47] in "Effects of Compression Ratio and EGR on Performance, Combustion and Emissions of DI Injection Diesel Engine" Studied the effects of cooled EGR on the performance, combustion and emission of a variable compression ignition diesel engine with various compression ratios under different engine loads with varying EGR % flow rates. The output

parameters investigated included indicated specific fuel consumption (ISFC), BTE, HRR and mass fraction of the burnt mixture and the elements composing the gases in the exhaust emissions using a single cylinder DI engine, variable compression, high speed, with rated power of 5 HP at1500 rpm.

During their experimental study the speed was maintained constant using different CRs and it was reported that irrespective of the CR used, the volumetric efficiency of the engine remained the same, while the mechanical efficiency decreased as the engine CR values of 15 and 16 were reached. This factor is explained as being due to the increased loss of friction power. When the CR value was 19 the BTE reached a maximum of 17 %. The increase in CR was observed to decrease the ISFC irrespective of the engine load applied due to two factors, namely, the ignition delay and the long combustion duration period. The HRR at a recirculation of 5 % and a 1/4 engine load condition was noted to occur where crank angle duration was 37 º CA of the total crankshaft angle rotation. The increase in the engine load to 1/2 saw a minimal increase in the combustion duration period from 39 º CA to 42 º CA @ 3/4 engine load and 46 º CA @ full engine load respectively. These increments in the combustion duration time increased the HRR, as there was complete combustion in the combustion chamber.
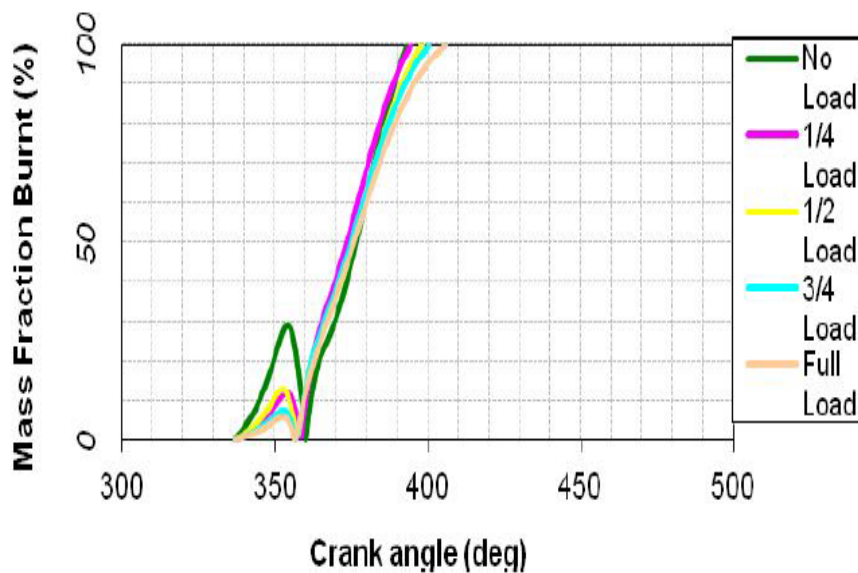
Figure 2.11: Variation of burnt fraction mass with crank angle at different varying engine load conditions [47]

The burned fraction mass in relation to the crank angle was reported to have no combustion at 360 º CA but at 361 º CA, and the whole combustion duration period lasted until the 393 º CA

mark making the duration last for a period of about 32° CA. However, as the engine load was increased they observed an increase in the combustion duration period, thus achieving a burning rate of 70 % of the total mass fraction input in the combustion chamber. This they reported happened within the first 20 ° CA rotation with the remaining balance being burned in the remaining combustion period duration cycle of 32 ° CA as in Figure 2.11.

The emission characteristics of NO_X and smoke opacity in relation to the CR under different engine varying loads showed that an increase in the engine load increased the NO_X emissions as more heat was released as more gases in the combustion chamber pocket disassociated. However, with the application of the EGR % flow rate at increasing mode the NO_X emissions reduced. This is due to low peak temperature and complete combustion of the inlet intake and recirculated EGR gases which are reburned, hence the reduction. At CR 15 % and EGR % flow rate of 10 % there was a reduction of 26.5 % and at full engine load a reduction of 62.5 %. The smoke opacity showed continuous increase as the engine load was increased in all the test levels, a factor the authors linked to the increased amount of fuel injected to the combustion chamber. However, the smoke opacity in all the CR levels tested showed a decrease from a high of 17 % to a low of 4 %.

[48] in their study "Combustion and Emissions of Compression Ignition in a Direct Injection Diesel Engine Fueled with Pentanol" selected from a four-cylinder engine a single cylinder as the test cylinder while maintaining the other three cylinders as experiment control cylinders rated at 4000 rpm. The electronic control module (ECU) was modified to provide flexibility in manipulating injection parameters. The tests were carried out in normal engine operating temperatures of 85 °C. The test fuels used were conventional diesel as the control fuel or the baseline fuel, with three different biodiesel fuels employed and pentanol, as seen in Table 2.1.

Table 2.1: Baseline diesel test fuel and various pentanol blends of test fuels and their properties adapted from [48]

Property	Unit	Diesel	Pentanol	Biodiesel	D70B30	D70P30	D40P30
Viscosity @ 20 ºC	mm/s	41.27	289	7.159	5.03	3.2	3.9
Low heating value	MJ/kg	42.68	35.66	38.29	41.38	40.42	39.09
Oxygen content	%	0	18.15	11.1	3.3	5.5	8.8
Latent heating @ 25 ºC	KJ/kg	270	308	258	-	-	-
Cetane number	-	56.5	20-25	61.7	-	-	-
Density @ 20 ºC	Kg/m^3	830.4	815	871.4	842.7	825.8	838.1
Surface tension @ 20 ºC	10^{-3} Nm^{-1}	27.5	24.7	30.3	28.2	26.2	26.9
Boiling point	ºC	T10-223 T50-266 T90-311	138	T10-323 T50-326 T90-335	T10-230 T50-280 T90-314	T10-135 T50-240 T90-298	T10-135 T50-264 T90-310

The results on the combustion characteristics of the test fuels demonstrated that any addition of pentanol increased atomization and offered easy mixing of the fuel vapor with inlet air intake charge at the same testing conditions, thus leading to higher HRR values during the first stage of the combustion phase process as demonstrated by Figure 2.12. This is defined as the CA interval between the heat release position at CA 5 % and CA 90 % during the main combustion phase process. Thus, with the increase in cylinder temperature after the first stage of the heat release there is a reduction and weakening of the chemical effect ignition delay, while the physical delay due to low viscosity and the high viscosity of the test fuel additive pentanol play

a significant role on the auto ignition of the mixture. Hence, there was no significant difference among the four test fuels based on the ignition delay mentioned above, though each had a different cetane number (CN).
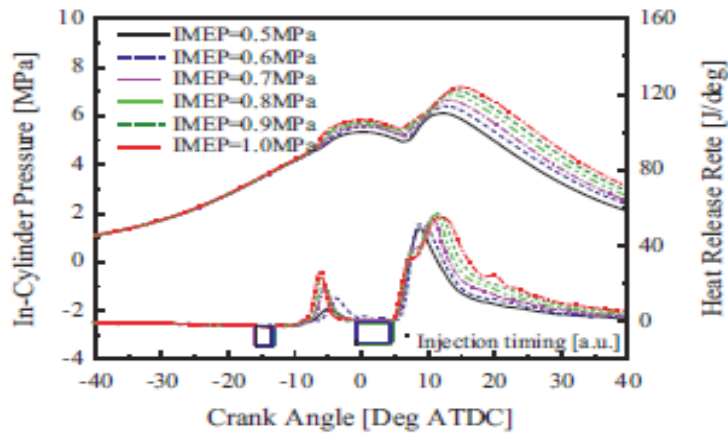
Figure 2.12: Variation of in-cylinder pressure with crank angle change in relation to heat release rate [49]

From Figure 2.12 it is evident that the combustion process phase is shortened with the introduction of pentanol blends as there is marked improvement in the mixing rate of the inlet intake air and fuel blends during the test with smaller values of HRR below CA50 as compared to the conventional diesel and the D70B30 pentanol blend of fuel.

Turning to the performance of the pentanol fuels in terms of emission characteristics, the authors report that when supercharging was applied to the test engine there was considerable reduction in the emissions of NO_X, CO_2, CO, THC and soot emissions for all the test fuels that were used as compared to when the engine was naturally inducted. However, as the load increased there was a minimal increase in the NO_X emissions, but a decrease was observed as the load continued to increase. This is due to the fact that NO_X formation is temperature and equivalence ratio (ER) dependent and does very well in the reduction of NO_X because of its higher latent heat of vaporization (meaning lower combustion temperature). The low CN results in longer ignition delay, hence increase in the burned fraction mass of fuel during premixing with the inlet intake air mass. It should be mentioned here that the only factor that is attributed to the decrease of NO_X in the pentanol based fuels during low engine load conditions is the latent heat of vaporization. The high flame temperatures and high levels of the oxygen content in the pentanol fuels lead to increased NO_X emissions being identical to the study of [50].

The indicated thermal efficiency (ITE) was reported to decrease with an increase in the engine load, explained by the high ER values, longer combustion durations experienced, and the higher fuel efficiency as exhibited by the blended fuels of pentanol. The corrected ISFC showed an increase as the engine load increased, thus providing a reversal of the aforementioned observation for ITE as indicated by Figure 2.13. It should be mentioned here regarding the ISFC, that the D70B30 and conventional diesel fuel produced a result of minimal difference in terms of the values generated in relation to engine loads in all the test conditions shown in Figure 2.14, leading to the conclusion that any addition of an alcohol to any biodiesel does not affect the thermal efficiency.

Figure 2.13 shows the relationship between ISFC and IMEP of the various pentanol fuel blends and the diesel test fuel [49].
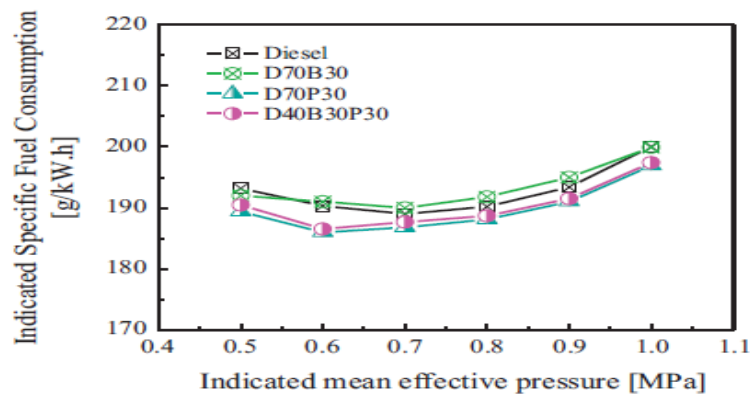
Figure 2.13: ISFC VS IMEP

Figure 2.14 shows the variation of the ITE and IMEP in relation to diesel and pentanol blends [48].
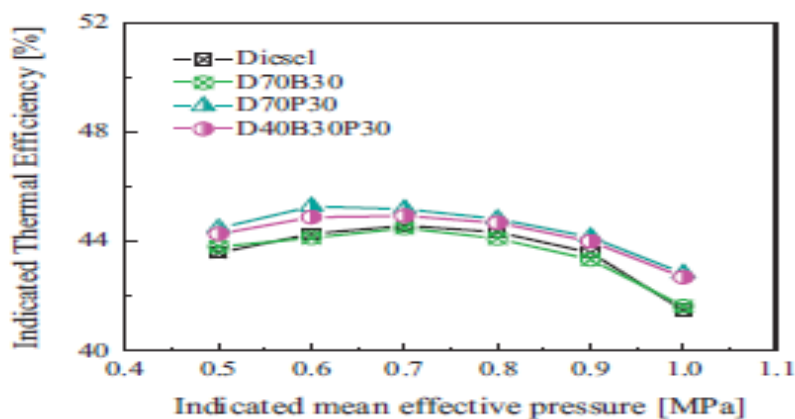
Figure 2.14: ITE VS IMEP

37

The soot emissions show a similar behavior to the NO_X emissions characteristics, although there are some slight variations. As the engine IMEP is increased from 0.5 Mpa to 0.09 Mpa with more fuel being injected into the combustion chamber, the authors report a reduction in the duration of the ignition delay leading to a more diffuse combustion and increase in the soot emissions. This can be attributed to the fact that the ER increases with high engine loads. All the oxygenated blends of pentanol showed decreased and suppressed soot emissions in all the engine operating and testing conditions. This was identical to the study conducted by [51].

On the emissions of HCs, they observed that as the engine load increases, there is a marked reduction in the emissions of HCs in all the test fuels used during the study. This factor is linked to the high in-cylinder temperature as the engine load increased. Other factors which they observed as contributing to the decrease in the HC emissions include low CN and the latent heat of vaporization exhibited in the D70P30 pentanol fuel blend, longer ignition delay, broad lean combustion zones, high oxygen content and the presence of some biodiesels which have high CNs among some of the pentanol fuel blends used in the experiment.

[52] in "Combined Effects of EGR and Varying Inlet Pressure on Performance and Emission of Diesel Engine" investigated the combined effect of EGR and varying inlet intake pressure on the emission and performance of a diesel engine using a single cylinder, DI, water cooled diesel engine with a rated power of 5.0 HP or 3.72 kW at 1500 rpm. Necessary modifications were mounted to allow the experiment, including a manually operated EGR control valve system and asbestos insulation for the exhaust pipe line in order to maintain and reduce heat loss.

After testing and study the authors observed and concluded that increasing the inlet intake air pressure and EGR % flow rate improved overall engine performance, with an increase in the BTE and decreased BSFC. Increasing the intake inlet air pressure and applying varying EGR % flow rates was observed to reduce NO_X emissions due to decreased EGT temperatures.

Figure 2.15 shows the variation of BSFC at varying EGR rates with engine load at 50 % under the influence of intake inlet pressure [52].
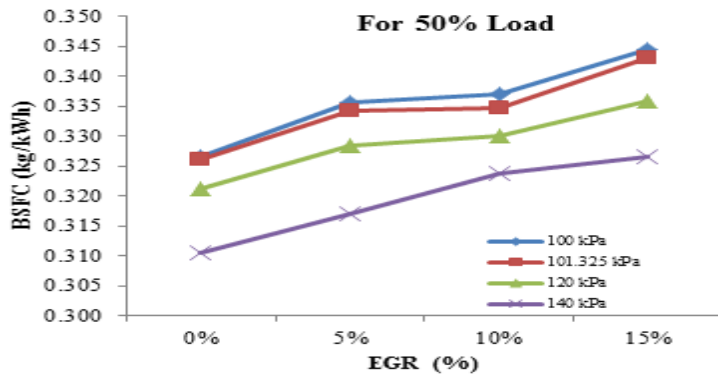
Figure 2.15: BSFC VS EGR % flow rate

The increase in the intake inlet air pressure and the increase in the rate of EGR % flow rate was noticed to decrease the BSFC as the density of air increased and more combustion occurred due to availability of oxygen with the increased inlet air flow as shown in Figure 2.15.

[16] in "Experimental Investigation of Performance and Emission Characteristics by Different Exhaust Gas Recirculation Methods used in Diesel Engine" studied the effects of hot EGR and cold EGR on the performance and emission characteristics of a DI diesel engine. Their test engine was a single cylinder, DI, water cooled CI diesel engine, with a rated capacity power of 6.5 HP or 4.836 kW at 1500 rpm. Various modifications were made to allow study.

Figure 2.16 shows the variation in relationship between SFC and BP with different types of EGR % flow rates with diesel test fuel [16].
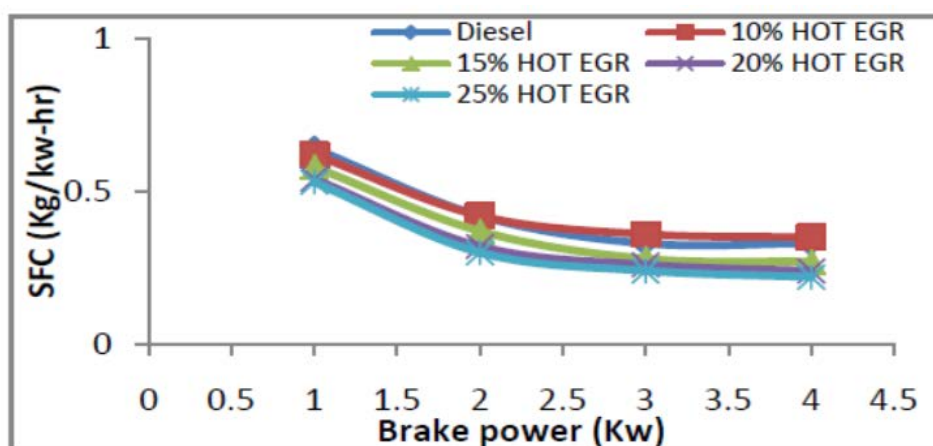
Figure 2.16: Figure 17 SFC VS Brake Power

39

Fig 2.17 shows the variation between the BTE and BP with varying EGR % types and rates with diesel fuel [16].
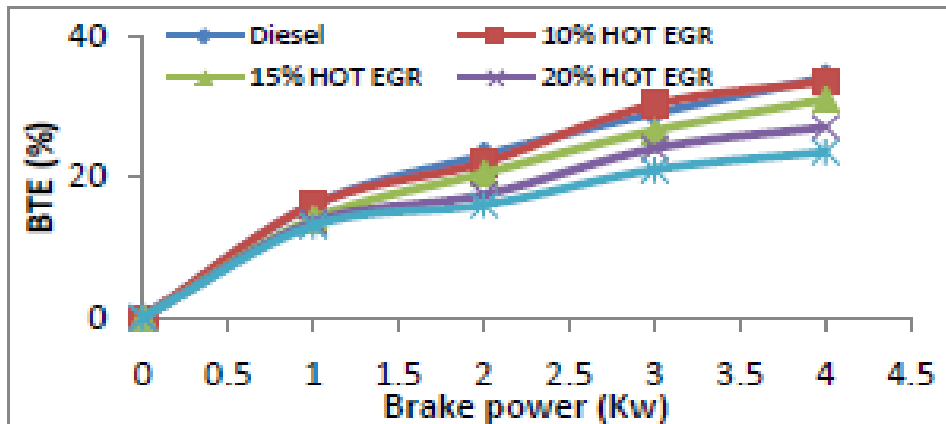
Figure 2.17: Figure 18 BTE VS Brake Power

The tests for performance and emissions were conducted without EGR and with EGR of different flow rates of 10 %, 15 %, 20 % and finally 25 % at 1500 rpm and varying engine loads. The specific fuel consumption (SFC) was noted to be high during all engine loads tested with or without EGR. At 10 % EGR rate flow the BTE equalled the values similar to when there was 0 % application of EGR. However, the indicated thermal efficiency when cold EGR was applied during the experiment showed very good results as compared to when hot EGR was used. The NO_X emissions from cold EGR indicated a significant decrease as compared to the hot EGR gases application. At 10 % cold EGR the emissions of CO_2 were seen to be very high as compared to the hot EGR, increasing at part load but decreasing with higher engine loads as shown in Figures 2.16 and 2.17.

[53] in " Combustion and Emission Characteristics of High N-Butanol and Diesel Engine and EGR Impact" studied the effects of EGR on n-butanol in relation to combustion and emission. The experiment was conducted using a modified four stroke, water cooled engine, six-cylinder research engine with a rated power of 167 kW at 2500 rpm. In order to reduce cylinder interaction one cylinder was isolated and allowed independent intake and exhaust systems, with a common rail injection system controlled electronically by an open circuit control unit.

The tests fuels chosen were conventional diesel as the base fuel, N-butanol as the alternative fuel in mixtures of 0 % and 40 % by volume as blends Bu00 and Bu40 corresponding to the percentages respectively of the blended mixtures. After their study and experimentation, the

40

authors concluded that the Bu40 blend of fuel showed a higher engine cylinder pressure, with longer delays in ignition and higher rates of combustion compared to the blend of fuel of Bu00. However, with the application of EGR flow rate of more than 30 % the cylinder pressure, ignition delay and rate of combustion decreased. There was no significant change in the emission of the HC, CO and the indicated thermal energy until very high EGR % flow rates were applied. However, the Bu40 blend showed change for the named factors in lower EGR % flow rates than other blends that were under consideration. Figure 2.18 shows that the relationship as aforementioned and discussed by [53]. However, as the EGR % flow rate was increased to higher levels the authors noticed a decreased ITE for Bu40 blend of fuel as compared to the Bu00 blend of fuel, but with the application of EGR % flow rate there was a decrease in the emissions of NO_X although with an increase in soot emissions. The authors also reported a significant decrease in NO_X emissions for the Bu40 blend mixture, with minimum increment in soot emissions, besides achieving very good high levels of ITE.

Figure 2.18 shows the variation of the ITE, CO % and HC in relation to the varying EGR % flow rates [53].
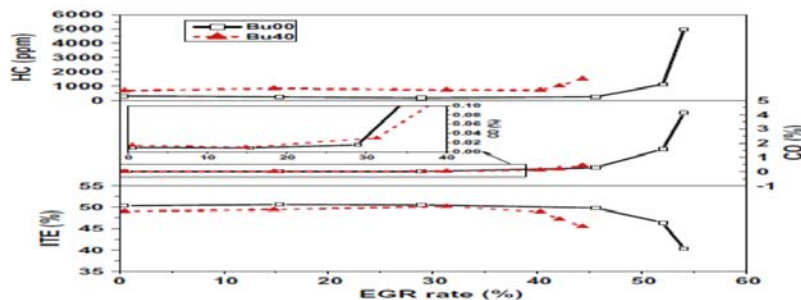
Figure 2.18: ITE %, CO (%) and HC (ppm) VS EGR % flow rate application

The emissions of CO, the authors observed, depended on the production and the oxidation processes. However, the Bu40 was observed to have lower CO formation for the early combustion phase, but for the late phase of combustion process Bu40 showed increased and high levels of CO emissions.

2.6 Effects of EGR On CNG and GTL On Performance Combustion and Emissions

[5] in the study "Performance, Combustion and Emissions a Diesel Engine Operated with Reformed EGR Comparison of Diesel and Gas to Liquid (GTL) Fueling" used a Lister-Pitter TR1 engine, single cylinder, DI, air cooled and naturally aspirated. It was connected to an electric dynamometer with a motor and load cell. The crank shaft position timing was done at

22° CA (BTDC) in all the tests carried out. The EGR % flow rate was managed manually using a gate valve while EGR levels were determined by volume. The rig also included other instruments to do measurements for oil and air inlet/exhaust manifold temperature. The test fuels used for the test were ultra-low sulphur diesel (ULSD) and the ultra-clean GTL which was obtained through a low temperature Fischer-Tropsch (LTFT) process.

The experiment was conducted in the two engine speed modes of 1200 rpm and 1500 rpm and two loads of 25 % (low load) and 50 % (medium load), while the EGR flow rate ratios chosen were classified into standard EGR and reformed exhaust recirculation (REGR) both using ratios of 0 %, 10 %, 20 %, and 30%. The REGR was a simulation based on H_2 and CO in the ratios of 25 % EGR rate flow at H_2 0 % and CO 75 % while in the second scenario 15 % EGR rate flow at H_2 10% and CO 75 %.

The conclusions from this study were as follows: at low engine loads the GTL fuel was found to have high BTE values as compared to the BTE values shown by ULSD, but when REGR was introduced it was observed that GTL had a higher fuel replacement than ULSD, thus showing an improvement in efficiency and reduced emissions. BTE was also found to be load dependent, i.e.at low engine loads efficiency decreased with increasing REGR. However, when the loads were high it was observed the high flame temperatures and velocity of hydrogen gas and the rapid expansion increased the BTE as the REGR was increased.

Regarding HRR, the high octane number of GTL resulted in less pronounced premixed combustion, leading to lower HRR and low in-cylinder pressure, leading to a reduction in NO_X emission where GTL fuels were employed unlike when ULSD fuel was used in the experiment. Whereas the combustion pattern was affected by the REGR, the use of the 30 % REGR brought efficient gas fuel combustibility and an increase in cylinder pressure together with the ROHR. The authors noted that an increase of REGR resulted into a decrease of both NO_X and smoke emissions. However, at higher engine loads, higher REGR resulted in a decrease in smoke emission but compromised the NO_X emissions. Lastly when the combination was used for both REGR and GTL fuel, the results showed a marked improvement in the reduction of emissions. The 30 % REGR when combined with the GTL fuel produced a 60 % decrease in the smoke emission, while the NO_X emission showed a 75 % decrease as compared to when ULSD fuel was used at 0 % REGR and low engine loads.

[38] in "Combustion and Emission Characteristics of a Natural Gas Fueled Diesel Engine with EGR," used a Lister-Petter PH1W single cylinder, naturally aspirated, four stroke, water

cooled, and high speed DI, with a bowl-in-piston combustion design. The engine was modified to suit dual fuel operation with natural gas fuel as the main fuel and diesel as the secondary or pilot fuel. Other modifications were done to enable data acquisition and computation, including EGR % flow piping arrangement, and thermocouples for temperature measurement for the exhaust system.

The results report that the cylinder peak pressure reduced with the application of a dual fuel strategy, as the application of EGR % flow rate increased. The dual fuel exhibited longer ignition delay than conventional diesel fuel with the introduction of EGR % flow rate observed to greatly contribute to increases in ignition delay. The dual fuel strategy suffered significantly from low thermal efficiency compared to conventional diesel fuel at medium range engine loads, but high engine loads demonstrated high values of BTE. However, the application of the EGR % flow rate changed BTE of the dual fuel depending particularly on if the load applied increased, thus showing a general increase in BTE compared to conventional diesel at high engine loads. Therefore, it was concluded and reported that the dual fuel is a factor in reducing NO_X emissions with application of EGR % flow rate in diesel engines.

HC and CO emissions for the dual fuel combination returned more emissions than conventional diesel fuel especially during intermediate load, but with increased load the HC and CO emissions reduced. The application of EGR % flow rate didn't show any significant reduction during the use of dual fuel diesel for HC and CO emission. This is identical to the study and conclusions observed by [54]. However, the values of CO_2 were seen to be lower during the use of dual fuel diesel than during the use of conventional diesel fuel at all engine loads. The use of EGR % flow rate increased CO_2 emissions even though the values continued to remain low compared to conventional diesel fuel.

2.7 Effects of EGR on Temperature and Emissions

[55] in "Effects of Diluent Admissions and Intake Air Temperature in Exhaust Gas Recirculation on the Emissions of an Indirect Injection Dual Fuel Engine Direct Injection" used a Ricardo E 6 modified to accommodate gaseous fuel and normal or conventional diesel use. The engine was single cylinder, four stroke, water cooled, with a maximum rated power of 9 Kw at 3000 rpm. Modifications were done to the engine for the purpose of testing and study.

Following testing and experimentation it was observed that the introduction of CO_2, through the intake manifold resulted in a decrease in NO_X emissions but showed a relative increase in

UHCs. This is a chemical effect that is associated with the use of the EGR application. The authors reported that by continuing to increase the inlet charge temperature there was an increase in UHC emissions, mainly due to a decrease in ignition delay in relation to the rise in the intake charge temperature. By increasing the intake charge temperature, the combustion characteristics were improved due to the decrease in the ignition delay. This improves and increases the BTE and brake horse power parameters, leading to a further decrease in the UHC and CO emissions.

[56] in their study "Effects of EGR on Exhaust Gas Temperature and Exhaust Gas Opacity in Compression Ignition Engine" carried out an experiment study on a two cylinder, DI engine, with a 9.3 kW rated power at 1500 rpm. The engine was air cooled, running on diesel fuel.

The authors found that brake specific fuel consumption was fairly independent of the EGR % flow rate. In other words, increased EGR % didn't show a considerable change of BSFC. Other observations made included that opacity of the exhaust gas increased with the increase in the EGR % flow rate and as such the EGT reduced the combustion temperature with the application of EGR. Since NO_X is a temperature dependent component, reduced combustion chamber temperatures leads to NO_X reduction.

[57] in "Effects of EGR on Diesel Premixed-Burn Equivalence Ratio" investigated the effects of the ER on premixed burn mixture in diesel engine combustion in relation to the application of various rates of EGR % flow rate. PM emissions reduction is related to an increase in ignition delay particularly if the delay exceeds injection duration and good fuel mixing, and if cooled EGR is used. This allows more mixing time for the air-fuel before ignition decreasing the ER of the igniting fuel, thus preventing soot formation where the $\phi < 2$.

[58] in their study on "Combined Effect of EGR and Inlet Air Pre-Heating on Engine Performance in Diesel Engines" used a four stroke diesel engine S195, single engine, with a maximum speed of 2000 rpm, DI, water cooled and naturally aspirated for their study. The fuel used for this study was conventional diesel with a density of 0.80 g/cc at 25 ° C. Other modifications to suit the experiment were done to provide measurement readings, particularly the preheating mechanism for inlet intake air – to maximize the heat loss the inlet intake air passage was insulated by plaster.

The authors found that the emissions of NO_X from the test engine increased as the engine speed increased in both the phases of the experiment. i.e. when the inlet intake air preheating was applied without EGR application and vice versa. They attributed this to the decrease in the

duration of ignition delay and combustion chamber premixing time of the inlet intake charge. In addition, they observed that the application of EGR reduced the in-cylinder combustion peak temperature due to the higher CO_2 heat specific ratio. This result is identical to other results in other studies, particularly those where the EGR % was limited to between 20 % to 25 % by [59]. In terms of the relationship between the effects of EGR on inlet intake air preheating and NO_X emissions, the authors observed that on increasing the inlet intake air temperature the emissions of NO_X and CO decreased. This factor was linked to the ignition delay and premixed combustion mixture, two factors whose time is shortened by the introduction of EGR % flow rate. There are other identical studies consistent with this study by [60].

On the relationship between the effects of the adiabatic flame temperature on the emissions of NO_X, particularly when conventional diesel fuel is applied, the authors observed that as the ER increased (hitting a maximum ratio of 0.9), the adiabatic flame temperature also increased. However, the ER begins to decrease as it hits this maximum value. The application of the inlet intake air charge preheating at a controlled temperature of 55 ° C and without application of EGR % flow rate, lowered CO emissions to almost a minimum, explained by the fact that inlet intake air preheating provides CO oxidation. However, when EGR flow rate of 25 % was applied the CO emissions increased significantly. This concurs with the findings of a study conducted by [54], where it was concluded that the application of EGR doesn't have similar effects on the different species of emission characteristics.

The BTE was found to be affected by the inlet intake air preheating in combination with the application of 25 % EGR flow rate, but at varying engine speeds and constant load the authors found that the BTE was higher for the preheated inlet intake air as compared to when preheating was not applied. This was seen to be due to higher amounts of heat energy that was being transferred from the exhaust gas to the inlet intake air. This allowed for better burning of the fuel in the combustion chamber, therefore minimizing the overall heat loss by the system. In addition, they observed that the BTE increased with the increase in engine speed both at low and intermediate speeds, but at higher speeds they noted a decrease in the BTE, a factor which they attributed to shorter mixing time of the air fuel which is normally associated with higher engine speeds.

[54] in "The Influence of Exhaust Gas Recirculation on Combustion and Emissions of N-Heptane and Natural Gas Fueled Homogeneous Charge Compression Ignition (HCCI)" conducted a study at the University of Alberta fuel and combustion emission research facility.

They used a Waukesha CFR single cylinder research engine, water cooled, coupled to a dynamometer. The speed was maintained at 800 rpm at wide throttle. A temperature controlled air preheating system was installed using a 2.4 kW heater motor, also included were two port fuel injectors controlled electronically via an alternative fuel system (AFS) sparrow module. The EGR rate was manually controlled, the fuels used for this experiment were n-heptane and natural gas either as blends or used individually.

During their study the authors observed that the recycled gases from the exhaust contained tri-atomic molecules of H_2O and CO_2. This species increases the SHC of the combustion mixture and reduces the overall specific heat ratio leading to the mixture acting like a thermal heat absorbing sink, thereby decreasing the after-compression temperature. The other observation they made with regard to EGR % flow rate application was the reduction in peak in-cylinder charge temperature due to delayed auto ignition of the combustion charge. Applying EGR % flow rate affected the peak in-cylinder pressure by reducing auto ignition. This is explained by the fact that the recycled exhaust gases in the form of EGR act as a thermal sink as mentioned earlier, thus reducing the charge temperature during combustion. The pressure rise during the combustion becomes reduced which becomes a means of avoiding engine knock.

Heat transfer was noticed to decrease with the application of EGR, since the heat transfer coefficient is proportional to pressure and inversely proportional to temperature. Therefore, the heat transfer coefficient did not vary much with the application of EGR, since by increasing EGR % flow rate both the pressure and temperature decreased. The gross HRR was seen to be affected by the application of EGR flow rate because recycled exhaust gases substitute part of the fresh air intake charge, thus affecting the in-cylinder ER and the combustion process in general. However, considering that EGR rate application can cause delay in SOC this prolongs the burning and exposes the elements of combustion to more time for combustion, hence increasing the IMEP limit and operating range.

The effects of EGR on combustion timing was demonstrated to increase the specific heat ratio of the combustion elements as the cylinder inlet charge temperature decreased, thus delaying the ignition. This occurrence introduces retardation of SOC and increases the combustion duration. Defined as the indicated work output per unit of engine swept volume, the IMEP was seen to be less affected by the application of the EGR % flow rate which is identical with other studies done in this area by [61]. Regarding ISFC, the authors found out that the retardation of SOC (ignition delay) reduced ISFC, whereas when the EGR flow rate was applied it produced

the opposite effect i.e. it increased the ISFC. This factor can be explained by the fact that introduction of EGR% flow rate removed the availability of oxygen thus causing incomplete combustion in the combustion process thereby decreasing efficiency.

The formation of NO_X was limited due to the low charge temperature and that of the air mass flow rate. This is explained from two factors; firstly, applying EGR % rate flow depresses peak in-cylinder temperature thus reducing NO_X emission formation and, secondly, the application of EGR % flow rate depresses the availability of O_2 concentration in the combustion chamber due to EGR flow rate dilution effect. However, the increase of EGR rate was noticed to increase HC and CO emissions, as the EGR flow rate continued to increase, which can be explained by the unavailability of O_2 and the reduced inlet intake charge temperature which results into incomplete combustion due to poor mixing and oxidation of the combustion mixture.

[35] in the "Effects of EGR on Performance and Emission Characteristics of a Diesel Piloted Biogas Engine" used a single cylinder engine four stroke engine, water cooled, naturally aspirated constant speed CI engine. The engine was coupled to a hydraulic dynamometer for load application. Modifications were made to the engine to enable it to run on dual fuel with conventional diesel as a pilot fuel and biogas as the main fuel.

After conducting tests and the experiment they came out with the following findings on BSFC. Through the variation of EGR flow rates and engine load from 0 % to 100 %, the BSFC was found to decrease as the rate of EGR % flow was increased obtaining a maximum value when the EGR flow rate was at 20 %. The decrease in the BSFC with the application of the EGR % rate flow was due to an increase in the inlet intake charge temperature, thus increasing the rate of fuel consumption. Regarding BP, they reported that the application of the EGR didn't produce any significant effect on the total output power of the engine (with an application rate of 30 % EGR rate flow), while the BTE increased with the increase in the engine load for all operating conditions. However, it should be mentioned that the BTE showed some insignificant increase before the EGR rate flow passed the 20 % mark, attributed to the reburning of the hydrocarbons entering the combustion chamber together with EGR and the increase of inlet intake charge temperature as a result of EGR % rate flow application, which causes an increase in the rate of combustion. This finding is identical to the findings of [62].

Regarding EGT, they concluded that the EGT increases with engine load for all the operating conditions, which they attributed to the increase in input energy at high engine loads, as fuel consumption increases to accommodate high load and speed. Another observation they made

47

during this study was that EGT temperature reduced with the increase of EGR % flow rate, which they attributed to the unavailability of O_2 when EGR % flow rate is applied leading to lowered combustion temperatures. This is identical to other studies conducted by [63].

The CO emissions variations in relation to the increase in EGR % flow rate was noted to increase with an increase in EGR % flow rate but was seen to significantly reduce as the EGR % flow rate and engine load increased to 75 % and 100 %. This factor is explained by the lack of O_2 during combustion due to the dilution effect of EGR % flow rate. On the other hand, HC emissions are noticed to increase in all the engine load conditions as the EGR % flow rate is increased, explained by the fact that the induced charge (intake air + EGR rate) have a higher CO_2 content when compared to fresh charge of inlet intake air only. However, the increased load across the entire engine load shows a decrease in HC emissions particularly when the dual fuel is employed for operation. This study findings are identical to the findings of [64]. Finally, on carbon emissions and how they interacted with the EGR % flow rate, the authors noted an increase of CO emissions with an increase in engine load, while when an EGR flow rate of 10 % to 30 % was applied, there was a minimal decrease associated with the substitution of fresh charge with the elements of the exhaust gas which decreased the CO_2 emissions.

Figure 2.19 shows the variation of CO_2 with varying engine load operating under the influence of different EGR flow rates [35].
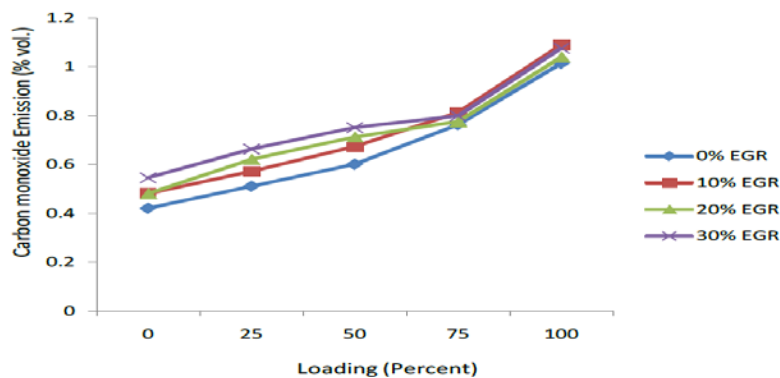
Figure 2.19: Carbon Dioxide Vs Load

[65] in "Effect of biodiesel–butanol fuel blends on emissions and performance characteristics of a diesel engine" investigated the effects of a butanol-biodiesel blend on emissions and performance of a diesel engine, single cylinder, naturally aspirated, indirect injection and water

48

cooled, using standard diesel (D100) and neat biodiesel B100 at four loads. The blend ratios were 5 %, 10 % and 20 % as B95Bu5, B90Bu10, B80Bu20 respectively.

After testing and evaluation they reported that, compared to diesel, butanol blends showed lower EGT and lower NO_X emissions. However, CO and UHC showed increased tendencies especially for higher blend ratios as compared to lower blend ratios of 5 % and 10 %. The butanol blend of B80Bu20 produced the highest emissions values for CO and UHC but lower NO_X emission values as compared to diesel fuel.

Figure 2.20 shows the variation of EGT with different fuels of diesel and the blends of butanol under varying engine load [65].
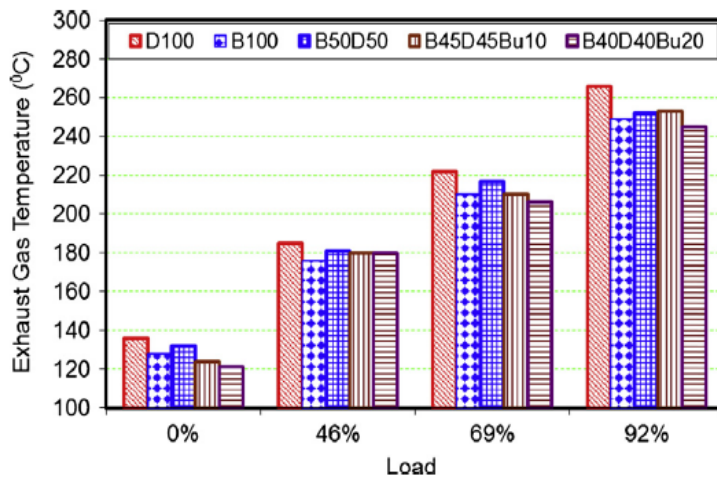
Figure 2.20: EGT VS Load

Regarding EGT, the authors reported diesel fuel to have the highest EGT temperatures of all the test fuels used due to its high CV and high CN. The blends of butanol reported lower values for EGT as they have a lower CN and lower energy density factors which accounts for the difference between the two fuels. The high oxygen content of the butanol blends decreases the overall energy content in the blended fuels hence the lower EGT temperature and combustion as illustrated in Figure 2.20.

[63] in the "Effect of Exhaust Gas Recirculation (EGR) Temperature for Various EGR Rates on Heavy Duty DI Diesel Engine Performance and Emissions" conducted a study using a heavy-duty DI diesel engine, single cylinder engine, with high compression peak pressure. To improve the BSFC, advanced timing was employed. The EGR for test study was constantly cooled and maintained throughout the experiment. The test engine condition was maintained

at full load with variations of engine speed. The theoretical study was on a 3D multi zone model modified to suit the experimental set up under study, to include the effects of EGR % rate flow and temperature and for calculation analysis. The boost pressure and injection pressure were kept constant at 280 BAR and 140 °C for the EGR gas.

The study found a reduction in cylinder pressure during combustion and expansion of the mixture in the combustion chamber. The SHC increased due to the presence of exhaust gas recirculation which reduces the availability of O_2 thereby affecting the combustion process rate and the disassociation of CO_2 and H_2O, which further reduces the peak cylinder pressure values as EGR % flow rate increases. During part engine load different results were be obtained, as the availability of O_2 was higher compared to when the engine was at full load. As the EGR inlet intake temperature increases with EGR % flow rate, it leads to a delay in SOC which leads to increased peak cylinder pressure as EGR % flow rate increases. These findings are identical to [35, 63, 66].

The BTE result indicated a negative effect of the EGR % flow rate on the BTE, especially at low engine speeds and full load; increase in EGR % flow rate showed a significant lineal decrease in BTE of 5.5 % at 15 % EGR% flow. The authors found that the theoretical and measured values of NO_X and soot at engine full load and varying EGR % flow rate showed that as the rate of EGR flow increased NO_X emissions reduced lineally but soot emissions increased exponentially [63], the effects becoming more apparent and critical at low engine speeds.

2.8 Effects of EGR On Performance, Combustion and Emissions on Biodiesel Fuels

In recent years there has been a strong interest in the alcohols which contain long carbon chains such as butanol. The butanol molecular structure contains 4 carbons and good physical and thermodynamic properties. The higher alcohols have a greater potential to overcome the problem of the low energy density associated with alcohols from the lower segment of the molecular structure, thus reducing soot and CO emissions compared to the NO_X emissions emitted by the conventional diesel fuel.

[67] in "Study of a Diesel Engine Performance with Exhaust Gas Recirculation (EGR) System Fueled with Palm Biodiesel" investigated the effects of EGR on the parameters of SFC, EGT, and the emissions of NO_X, CO, CO_2 and UHC in experimental and simulated study situations. The study was conducted using a four-cylinder diesel engine with modified EGR application,

naturally aspirated, air cooled, and with a maximum power of 64.9 kW at 4500 rpm using palm biodiesel and mineral diesel.

Figure 2.21 shows the variation of EGT with different blends of diesel and palm biodiesel [67].
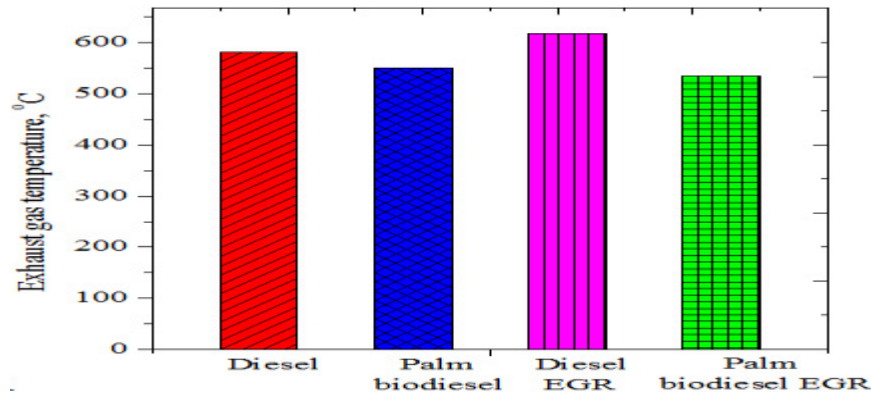
Figure 2.21: EGT VS diesel and palm biodiesel with and without EGR flow rate application

The application of EGR % flow rate mode on the palm biodiesel and mineral diesel fuels during the study led to a noted decrease in the EGT by 2.8 % when palm biodiesel was used as compared to 1.6 % decrease when mineral diesel was used. These findings are similar and identical to [68] and lead to the conclusion that most biodiesel fuels produce lower EGT temperature values at varied engine speeds and constant engine loads as illustrated in Figure 2.21. This conclusion is attributed to the fact that the exhaust gases mix with the inlet intake fresh charge which dilutes the methyl ester rich oxygen content in the combustion mixture, thereby improving combustion quality and completion.

Figure 2.22 shows the variation of BSFC and different test fuels of palm biodiesel with application of EGR [67].
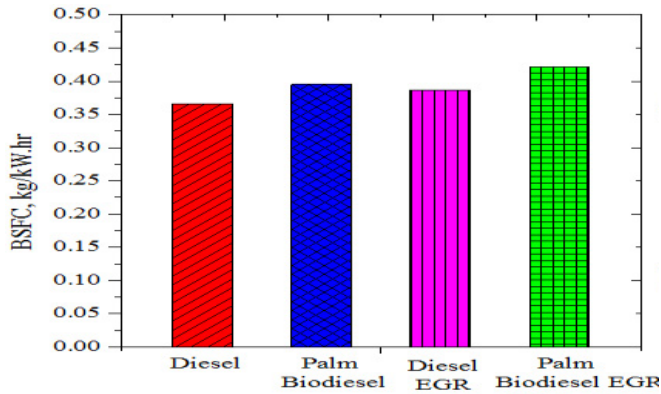
Figure 2.22: BSFC vs different test fuels with and without application of EGR

The effect of EGR on the performance and combustion characteristics of the biodiesel palm biodiesel and mineral diesel under normal modes, at full load condition, was that palm biodiesel produced higher values of BSFC, as illustrated in Figure 2.22. This increase in BSFC was attributed to the drop in the efficiency of the engine and the lower HRR values associated with the palm biodiesel, in addition to the unavailability of O_2 in the inlet intake air mass flow with the application of EGR % flow rate, which mixes the inlet intake air with the EGR gases. In general, the authors concluded that the combustion of biodiesel in diesel engines contributes lower COUHC, PM and smoke emission while conversely emitting higher NO_X. The study further shows that palm biodiesel increases the EGT by 5.6 % above the exhaust temperature values that are produced when mineral diesel is used. This is attributed to the presence of high oxygen content in the palm biodiesel test fuel leading to a higher combustion efficiency and higher in-cylinder temperature. This result is identical to the findings of [69].

Although the results obtained showed that palm biodiesel produced 4.7 % higher NO_X emissions compared to the mineral diesel with EGR % flow rate application, it should be noted that low NO_X emission of 5.4 % was achieved when mineral diesel was used compared to 22 % by volume when palm biodiesel fuel was used. This is explained by the fact that an increase in total heat capacity (specific heat capacity) of the exhaust gases and a reduction in in-cylinder peak temperature tends to reduce NO_X emissions. These findings are identical to the findings of [38] as shown Figures 2.23 and 2.24.

Figure 2.23 shows the variation of the rate of pressure release (ROPR) in relation to the engine crank angle (CA) position at varying cylinder pressures [38].
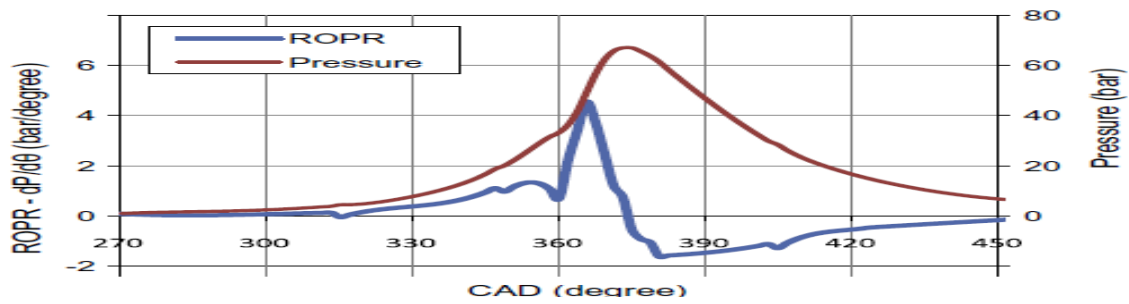
Figure 2.23: ROPR VS Crank Angle

Figure 2.24 shows the variation of ER with full engine load under the influence of EGR, with diesel fuel and compressed natural gas (CNG) [38].
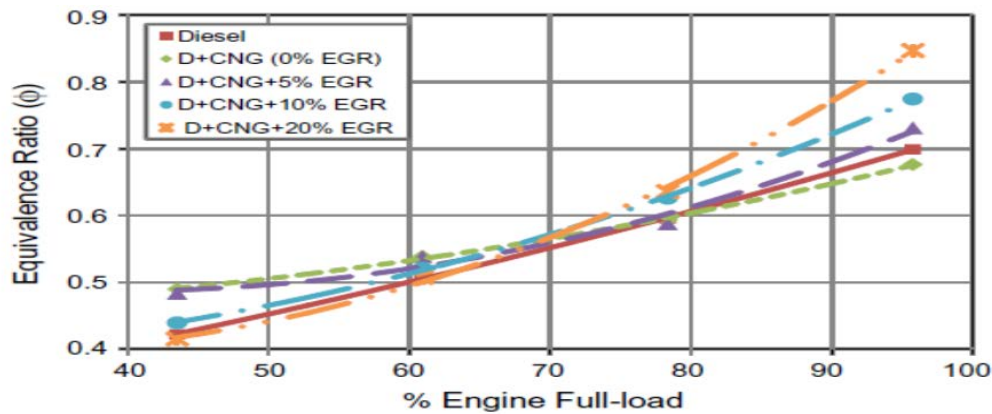
Figure 2.24: Equivalence ratio VS Engine Full Load (diesel fuel and compressed natural gas)

[33] in the "Effects of EGR (Exhaust Gas Recirculation) on the Performance and Emission of a CI Compression Ignition Engine Fueled with a Blend" used a single cylinder engine, four stroke water, compression ignition engine, with the test fuel being methanol at a concentration of 99 %. The test set up consisted of a test engine, a hydraulic dynamometer, fuel flow meters and incorporated various pieces of measuring equipment.

In their findings, the BTE increased as the load increased. Using 10 % methanol diesel blend they found increased the BTE by up to 12.85 %, as compared to 20 % blend of methanol which improved the BTE by 26.23 % at 10 % EGR flow rate. (BSFC was reduced in 10 % and 90 % methanol and diesel blend, while the 20 % and 80 % had an increase of 4.28 % only on the BSFC. On the effects of emissions of CO, they found that the 10 % and 90 % methanol diesel

blend had a 30 % reduction in the emissions of CO, while with the methanol diesel blend of 20 % and 80 %, the reduction was 40 %. The HC in the exhaust system reduced by 13.04 % in the 10 % and 90 % methanol diesel blend and by 17.39 % with the 20 % and 80 % methanol diesel blend. The NO_X reduced by 3.33 % in the 20 % and 80 % methanol diesel blend, and by 5.55 % with the 10 % and 90 % methanol diesel blend. The exhaust temperature gas reduction was observed to reduce by 4°C with 10 % EGR flow rate as compared to 6°C 20 % EGR flow rate was applied.

[70] in the "Effect of EGR on Diesel Engine Performance and Exhaust Emission Running with Cotton Seed Biodiesel" used a single engine four stroke, water cooled engine with cotton seed biodiesel (CSBD) and PBD (petroleum based diesel) blends as test fuels, where 0 % PBD was CSBD10, 20 % PBD was CSBD20 and 30 % PBD was CSBD30. The EGR % flow rate was limited to between 0 % to 20 % graduated in steps of 5 %. The engine speed was kept constant at 1500 rpm. The set up was to examine the following parameters in relation to the effects of EGR % flow rate; BSFC, BTE, EGT and the emission characteristics of NO_X, HC and CO.

The results indicate that the BSFC was slightly independent at lower EGR rates, but increased as the rate of EGR flow rate increased to 15 %. This was explained by the fact that less oxygen produces a rich mixture formation in the combustion chamber, hence more and increased fuel consumption. The BTE remained equally unaffected when low EGR rates and full engine loads were applied. However, BTE decreased with increase in EGR flow rate above 15 % in the combustion chamber, due to the displacement and replacement of fresh air charge by the EGT gases. The EGT partly operated with cooled EGR % flow rate was observed to lower the EGT as compared to EGT at normal engine operating condition without partially cooled EGR. This means that EGT decreased with increased EGR % flow rate, informed by two factors, namely, unavailability of oxygen and the high specific heat ratio of the intake air mixture which included exhaust mixture.

On emission characteristics the authors noticed a significant decrease in NO_X for all the test fuels used due to reduction in O_2 and decrease in flame temperature within the combustion chamber. The hydrocarbon emissions showed an increase with the application of EGR % flow rate for all the test fuels used, especially when the EGR flow rate was above 15 %. This is explained by the incomplete combustion occasioned by the unavailability of O_2 resulting in poor oxidation of the combustion mixture causing incomplete combustion. The CO emissions

were noted to increase with increase in EGR % flow rate for all the fuels used during the experimental study, mainly due the aforementioned O_2 phenomenon.

[71] in "Performance Characteristics of a Diesel Engine Operated on Biodiesel with Exhaust Gas Recirculation" studied the effects of EGR on the performance of a diesel engine using biodiesel. The diesel engine was a naturally aspirated single cylinder 4 stroke, water cooled, DI engine with rated power of 3.7 kW at 1500 rpm. After evaluation and testing the authors concluded that the BSFC increased for the pure biodiesel fuel, but decreased for biodiesel blends B10 and B20 compared to conventional diesel, a factor they attributed to the high viscosity index of biodiesels. With the application of EGR % flow rate they noticed an increase in the emissions of HC and CO but with reduced values for the biodiesel and the pure biodiesel blended fuels.

The NO_X emissions were observed to decrease with application of increased rate of EGR % flow. The authors noticed that biodiesel fuel with a combination of EGR % flow rate produced NO_X reduction without increase in the fuel penalty. The smoke opacity with application of EGR % flow rate was observed to increase soot and PM emissions. This is explained by the reduction of EGT by dilution which causes less oxidation thus lowering the combustion temperatures. In their final observation they noted that the EGR % flow rates of 10 % to 15 % were the best rates relative to the traditional trade-off between NO_X, HC and the fuel penalty.

[72] in their study of "Exhaust Gas Recirculation for Advanced Diesel Combustion Cycles" used a four-cylinder Ford common rail diesel engine coupled to an eddy current dynamometer. The engine was operated in two modes; single cylinder mode (3 cylinder to 1 cylinder) where 3 cylinders were operated in a conventional mode and the number 1 cylinder was marked for research with independent control of the parameters of intake pressure, exhaust back pressure and fuel injection. The second mode involved all the four cylinders with the engine running using a turbo charger, air fuel and EGR with no major system alterations.

The authors proposed two methods widely used presently to measure and quantify the amount of EGR % flow rate; the mass-based approach method and the gas concentration approach method as illustrated in Figure 2.25. The gas-based method uses the carbon dioxide (CO_2) gas concentration in the intake side by volume to make determination of the EGR % flow rate fraction. Thus, for this method there are two equations that can be used to define the EGR % flow rate fraction in terms of the gases of CO_2 and O_2. The Equations 12 and 13 [72] showing the two variations as:

$$r_{EGR} \approx \frac{[CO_2]int - [CO_2]amb}{[CO_2]exh - [CO_2]amb} \approx \frac{[CO_2]int}{[CO_2]exh} \qquad \text{Equation 12}$$

$$r_{EGR} = \frac{[O_2]air - [O_2]exh}{[O_2] \ air - [O_2]exh} \qquad \text{Equation 13}$$

Where r_{EGR} is the EGR % flow rate, $[CO_2]int$ is the carbon dioxide gas in the intake manifold, $[CO_2]exh$ is the carbon dioxide gas in the exhaust manifold side, $[CO_2]amb$ is the carbon dioxide gas in the ambient or atmosphere, $[O_2]air$ is the oxygen amount in the intake charge, $[O_2]exh$ is the oxygen in the exhaust manifold.

Figure 2.25 illustrates the second method which is mass-fraction-based model in a mathematical diagram representation with symbols.
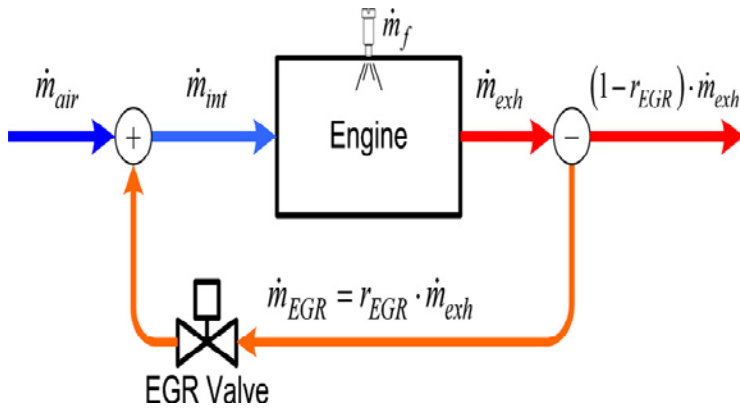
Figure 2.25: EGR schematic for the mass fraction method of calculating the EGR % flow rate in a system [72]

After testing the models and how they interacted with the EGR % flow rate application the following results and conclusions were reached. The impact of intake and in-cylinder charge composition was characterized by in-cylinder excess air ratio for the recycled O_2 with the EGR as a function of the EGR displacement. The effects of EGR on intake pressure and engine load showed that dilution of the intake charge with application of EGR could correctly be predicted through the intake oxygen concentration as compared to the EGR fraction as it was shown to lack additional information to show the effectiveness of the EGR % flow rate application [73].

During low engine loads and low EGR it was noticed that the effectiveness of EGR decreased as EGR gases displaced small amounts of fresh air in the intake system due to the fact that the EGR gases contained O_2 and N_2 elements and vice versa. In other words, increasing the intake reduced the intake charge dilution for the same EGR ratio, while increase in EGR % flow rate (intake dilution) produced a leaner AFR with increased premixed combustion, which caused

reduced soot emissions, and improved the engine combustion efficiency. It should be emphasized here that O_2 in the EGR is both a function of the engine load and EGR ratio. This is identical to the study findings of [74].

[68] in the "Effects of Exhaust Gas Recirculation (EGR) on the Performance of a Constant Speed Diesel Engine Fueled with Pentanol Blends" investigated the effects of EGR on diesel engine performance and emissions using four pentanol blends of 10%, 20 %, 30 % and 45 %with EGR flow rates of 10%, 20 % and 30%. They set out to reduce high NO_X emissions prevalent during high engine loads. Their results reported that increasing EGR % flow rates reduced NO_X emissions by almost 41 % at intermediate engine loads. The full load results indicate a drop in the increase of the NO_X emissions to 33.7 % as in Figures 27.

Smoke emissions increased for all the blends of pentanol with application of EGR past the 20 % flow rate point, leading to a conclusion that reduction of NO_X and UHC emissions can be achieved using pentanol blends especially with moderated EGR % flow rate of 20 % to 30 %. This point had the lowest emission values for CO and UHC respectively.

Figure 2.26 shows variations of NO_X at full engine load with application of EGR % flow rate with different pentanol blends and diesel fuel [68].
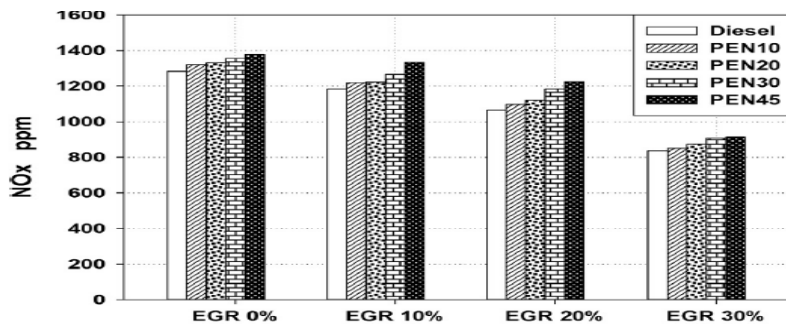
Figure 2.26: NO_X VS EGR % with different blends of pentanol and diesel

Figure 2.27 shows the variation of BTE under the influence of EGR % flow rate with different blends of pentanol and diesel fuel [68].
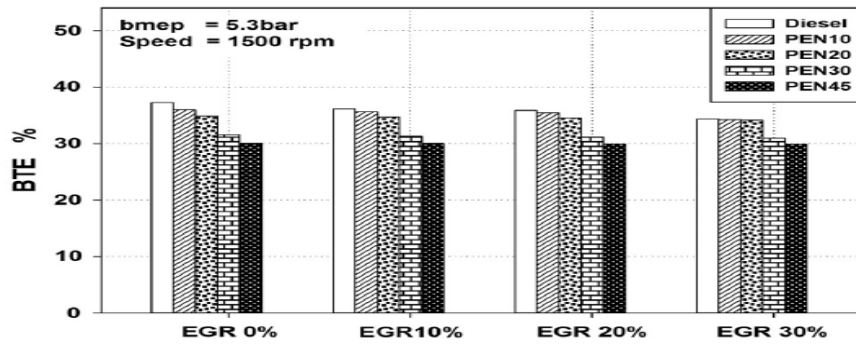
Figure 2.27: BTE VS EGR % flow rates

On performance they reported that the BTE and BSFC decreased with increased EGR % flow rate. The blend PEN45 showed the most decrease in the BTE OF 7.2 % compared to diesel fuel as can be seen in Figure 2.27.

[75] in "Characteristics of a DI-CI Engine Fueled with Preheated Corn Biodiesel" investigated the characteristics of a DI-CI that was made to run on preheated corn biodiesel fuel (PHCBD). The following engine parameters were measured and investigated: BSFC, IMEP, BTE, BSEC, combustion characteristics of cylinder pressure, HRR, EGT and emission characteristics of hydrocarbons, CO, NO_X, and HC The study used a DI-CI Kirloskar engine, single cylinder naturally aspirated, water cooled and with a constant speed of 1500 rpm.

There were three types of test fuels used during this experiment, petroleum diesel (PD), corn biodiesel (CBD), and the preheated corn biodiesel (PHCBD). The engine load was varied in four major steps of 25 %, 50 %, 75 % and 100 %. After the tests and experimentation, the authors came up with the following observations and conclusions: The BTE of PD, CBD, and PHCBD was found to increase as the power output increased for all the test fuels available during the experiment and for all engine load conditions recording 38.1 %, 33.8 % and 36.1 % respectively as illustrated in Figure 2.27.

Figure 2.28 shows the variation of BTE with BP at different loads and with test fuels of PD, CBD and PHCBD [75].
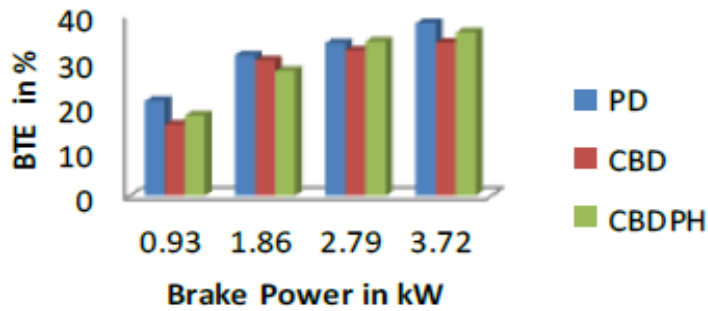
Figure 2.28: Figure 29 BTE VS Brake Power

The BSFC for the PHCBD is observed to be lower, but when compared to the other test fuel PDs both CBD and PHCBD consumed more fuel to produce the same amount of power per unit mass of the BP as the two biodiesels have a lower CV. However, at power output of 2.79 kW the BSFC of the PD test fuel was equal to the BSFC of the CBDPH test fuel. This was due to improved fuel spray characteristics experienced with preheating. On the other hand, the BSEC which is defined as the amount of fuel energy required to produce a unit of BP output for test fuel PHCBD had a lower BSEC than that of the CBD in all the engine loads. However, it should be observed that the BSEC of the test fuel PH CBD was equal to brake specific energy consumption of PD due to the high rate of evaporation and good fuel atomization as a result of pre-heating of the PHCBD test fuel.

The IMEP which indicates the available pressure of combustion product in the cylinder was observed to increase with increase in power output for all the test fuels applied. The IMEP of PHCBD was higher than PD and CBD for all the power output, while the peak cylinder pressure for the PHCBD was seen to be higher than both PD and CBD with highest peak pressure recorded at 66.6 % when the power output was 2.79 kW. The EGT for the CBD and PHCBD test fuels was lower compared to the PD test fuel, although CBD and PHCBD test fuels recorded very close temperature variant values. The lower EGT of test fuel PHCBD and CBD can be linked to the fuels having lower heating values.

During combustion with the piston nearing TDC and the crank angle cycles of 360 º CA to 440 º CA, the PD and CBD showed almost identical pressure curves, while the PHCBD test fuel showed a sloping and gentle pressure curve. Regarding HRR, the authors observed that it was negative at the SOC for all the test fuels, but it rapidly expanded at late combustion stages. The PHCBD was seen to have the lowest HRR at the SOC than the CBD and PD test fuels but continued to increase as the combustion progressed.

The rate of mass fraction burnt in relation to the crank angle position at 2.79 kW for all the test fuels indicated to initiate at the 351 º CA position and complete the combustion cycle at the 398 º CA position. It should be mentioned here that even though there are different burning rates for all the test fuels, the duration of the combustion was the same for all the test fuels. PHCBD test fuel had the lowest burning rate but experienced rapid combustion after the 370 º CA mark as in Figure 30.

Figure 2.29 shows the variation of HRR in relation to the crank angle (CA) with the engine load after top dead center (TDC) position, for various test fuels [75].
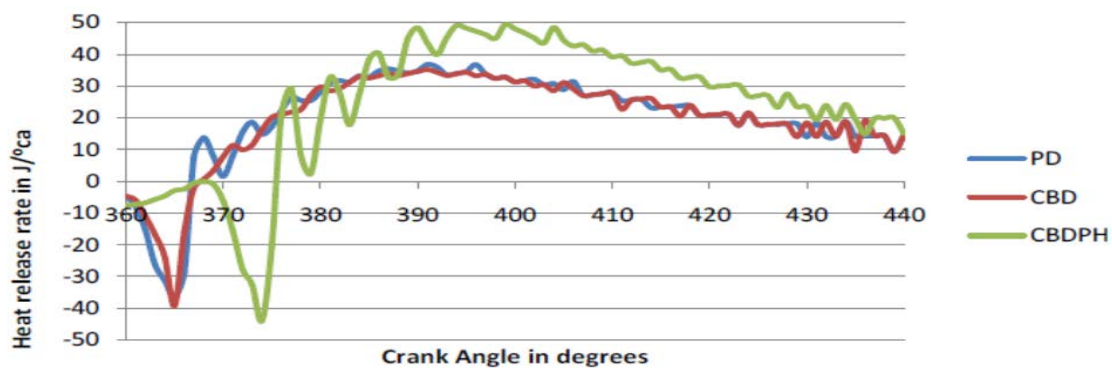
Figure 2.29: HRR VS Crank Angle

The exhaust emissions of HC, CO, and NO_X showed that CO emissions increased with increase in the power output load for all the test fuels used, due to the increase in the fuel consumption and knock resistance with increase in engine load. The CBD test fuel showed less CO emissions compared to the PD test fuel and these emissions reduced further with the use of the PHCBD test fuel due to reduced viscosity and density in addition to increased rate of evaporation.

The HC emissions of corn biodiesel showed that without preheating it had the lowest emissions of HC, compared to PD test fuel, due to the high content of O_2 in most biodiesel fuels. However, as the engine load increased the emissions of HC increased. The NO_X emissions for PHCBD, PD and CBD test fuels in relation to engine load showed an increase for CBD, but there was reduced emission for PHCBD test fuels compared to when there was no preheating. It is important to note here that PHCBD showed almost similar values for NO_X as the PD test fuel values.

2.9 The Effects of EGR On Particle Formation and Oil Degradation

Though EGR has been adopted as the most effective technique in emission control in diesel engines, it also has the disadvantage of in-cylinder soot formation due to the poor oxidation; it produces smoke particles with the diameter of most particles being between 0.1 μm to 0.8 μm compared to the lubricant boundary layer thickness of 0.001 μm to 0.005 μm. The increase in soot deposition is solely blamed on the wear of engine parts, namely, cylinder liners, piston rings, valve train and the bearing inserts both main and con bearing [76]. This is influenced by the additive degradation of the lubricating oil, as the chemical composition is altered due to the accumulation of the soot in the oil. The main wear mechanisms associated with soot presence in the engine lubricating oil are abrasion adhesion and scuffing which are known to damage surfaces mechanically as reported by [77].

[77] in "The Role of Soot Particles in the Tribological Behavior of Engine Lubricating Oils," studied the tribological behavior of soot particles in the lubricating oil. The study mainly focused on the two types of lubricants CDSAE15W-40 as test pilot oil and 150SN as the base oil to conduct their experiment. Using carbon black, they simulated soot particles normally contained in the oil, while the engine wear was measured by a four ball tribometer. After the tests and results they concluded that the anti-wear and anti-friction properties of CDSAE15W-40 were better than the base oil 150SN, a factor they attributed to the presence of carbon black as a dispersant and additive.

Due to the intensification of the formation of particles as a result of application of EGR % flow rate in an engine, control aspects during transient operation need to be addressed for the proper implementation of LPL EGR % flow rate. The resistance to wear and frictional properties of base oil 150SN could be improved if an additive or dispersant was added. For the CDSAE15W-40 formulated lubricant, the friction coefficient decreased to a contamination level of 4 wt. %. This phenomenon was ascribed to uniform dispersion of carbon black that occurred in the test oil used during the study and experiment. The principal tribological mechanism of the simulated engine soot was attributed to the absorption and agglomerate effects of the tested lubricants. The wear resistance and frictional properties of the 150SN base oil with 2.4 wt. % carbon black contents were improved by the addition of the T154 dispersant.

Table 2.2 shows the comparison between the mean oil film thickness (h_{min}) and the mean carbon black diameter.

Table 2.2: Comparison between the mean oil film thickness (h_{min}) and the mean carbon black diameter [77]

Property	Oil 150SN		Oil CD SAE 15W-40	
Temperature ⁰C	40	100	40	100
Kinematic viscosity (cSt)	32	4.80	110.60	15.02
Mean oil film thickness (nm)	48.48	13.38	107.10	28.10
Minimum oil film thickness (nm)	30.42	8.26	68.35	17.58
Minimum soot diameter (nm)	40	40	40	40

[78] in "Characteristics of Diesel Engine Soot that Lead to Excessive Oil Thickening" studied diesel engine soot characteristics which lead to oil thickening. Based on examination and analysis of the morphology of used oil from HDD operating with different levels of EGR, the authors concluded that severe oil thickening is directly linked to soot agglomeration seen in HDD oils due to the ineffectiveness of the oil dispersant to retard the growth of soot particles in engine lubrication oil.

In "Impact of Exhaust Gas Recirculation (EGR) on Soot Reactivity from a Diesel Engine Operating at High Load", [79] studied soot reactivity from a diesel engine operating at high engine load of over 75 % (336 Nm) under the influence of 0 %, 10 %, and 30 % EGR flow rates. Following testing and analysis they reported increased combustion duration of 39.8 % as the EGR flow rate increased from 0 % to 30%. The authors continued to report that there was a corresponding change in the oxidative reactivity, soot particle nanostructure and carbonaceous components, as the EGR flow rate increased, as can be seen in Figure 2.30. This they attributed to deterioration of engine performance as the EGR % flow rate was applied at high load with oxygen concentration decreased thus lowering the in-cylinder temperature. Finally, the authors reported soot with high soot-elemental carbon (EC) content, high ordered graphitic structure and low carbon fraction in relation to the soot particle samples analyzed from high EGR % flow rates. They attributed this to longer combustion duration and a decrease in the AFR.

Figure 2.30 shows the variation of specific emission and mass fraction with exhaust gas recirculation.
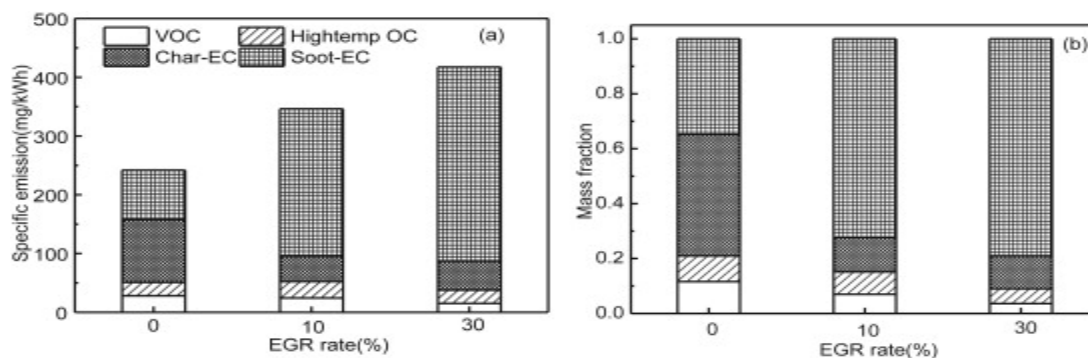
Figure 2.30: Effects of EGR on (a)specific emissions and (b) mass fractions of carbonaceous components [79]

2.10 Effects of Emission Gases on Public Health

The modern day mass transport systems which include road, rail, water and air produce a lot of air pollution both in the developed countries and the developing nations, with major health implications. This is more apparent in highly congested major metropolitan urban centers and cities. The pollutants of health concern can be classified into the several source areas of production such as TRAP (traffic related air pollution), particulate matter (PM), VOCs, and EC [80].

In major urban cities and centers tail pipe emission account for approximately 30 % of the total PM emissions production by mass. This is in addition to the PM emissions emanating from suspended road dust, wear from tires, and brake pad dust [80]. However, it should be mentioned that the side effects of TRAP are diverse and numerous despite the human body's ability to cleanse itself, with most of the inhaled TRAP PM never being able to move out of the respiratory system completely. The most vulnerable elements of the population are the elderly, infants, pregnant women and those that have already been struggling with chronic respiratory system diseases. Table 2.3 is a summary of the various sources of and types of pollution and their effects on human health and the environment.

Table 2.3: The main sources of pollution, types of pollutants, the environmental and health effects of these pollutants [80]

MAIN SOURCE	TYPE OF POLLUTANT	ENVIROMENTAL EFFECTS	HEALTH EFFECTS
Industry	Sulphur dioxide (SO_2)	Causes acid rain, which pollutes all water sources, and corrodes housing settlements.	Direct cause of cardiovascular complications
Automobiles and industry	Nitrogen oxide (NO_X)	Over fertilization and eutrophication due to excess nitrogen	Health complications arising from cardio-vascular diseases
Industry and Auto-mobiles	Particulate matter (PM)	Smog leading to poor visibility	Penetration of lungs and bloodstream
Automobiles	Carbon-monoxide (CO)	Increases greenhouse gases and global warming	Headaches and Fatigue
Automobile and industrial processes application	Volatile organic compounds (VOCs	Smog causing poor air quality	Skin and eye irritation, carcinogenic, nausea and headaches
Use of fossil fuels in transport application processes	Lead (Pb)	Leading cause of death in animal and marine life	Damages to the human nervous system if it accumulates in the blood-stream
Chemical reactions of NO_X and VOCs	Ozone	Smog, increased food insecurity due to poor harvests and affects the forest cover due to prolonged drought	Leading cause of respiratory diseases

[81] in "Human Health Risk Assessment of Air Emissions from Development of Unconventional Natural Gas Resources" report that the process of mining natural gases results in direct and fugitive air emissions that are a complex mixture of pollutants from natural gas resources as well as from diesel engines tanks which produce water due to condensation.

Multiple studies that have been conducted reveal that inhalation of toxic gases from petroleum hydrocarbons like conventional diesel used in heavy duty and LD engines indicates an increased risk of cardiovascular diseases [82], eye irritation, headaches, asthma symptoms, acute childhood leukemia, acute myelogenous leukemia, and multiple myeloma [81]. It should be mentioned here that toxicity information on some of the toxic gases emitted by diesel engines is still limited according to the studies that have been done so far. Although tremendous progress has been made in reducing air pollution and thus improvement in public health, there is still a need for isolation of the individual pollutants species and source categorization to increase specific understanding of the effects produced on human health, making it possible to adapt control actions to be developed for different sources and better prioritization of mitigating measures.

The problem of air pollution is becoming a serious global concern and as such more emphasis has to be put on the role of the transport sector in impacting the health of the general public, considering the negative environmental, social and economic impact arising from the existing transport sector planning and execution of policies. There seems to be a bias towards the short-term public health indicators like accidents and noise exposures, while ignoring the long-term effects like pollution from diesel car emissions because their impact on public health is easily noticeable or complained about [83, 84].

Additional work proposed by Bhalla et al. (2015) and Lelieveld et al. (2015) is the need to integrate the emerging understanding of health effects into improved model simulations and assessments of human health outcomes allowing better emission mitigation and quantification of the health benefits and challenges. Therefore, collaboration between transport and urban planning is needed [85] in order to make improvements, structurally and globally between modern transport and human health issues. The recent scandal involving Volkswagen motors in relation to emission cheating in their diesel operated vehicles sold in the world market has brought to the attention of the public the impact of pollution on public health from the private and the commercial transport sectors and how commercial interests can override public health issues.

Though diesel engines have low carbon emissions and improved fuel efficiency, it has been proved that they are a primary cause of major health concerns due to their emission of NO_X and PM compared to other fuels in use today.

In "What We Breathe Impacts Our Health: Improving Understanding of the Link Between Air Pollution and Health", [86] state that air pollution contributes to the premature death of millions of people annually with increasing air quality problems in developed and developing nations. The call for closer cooperation between air pollution scientists and engineers especially concerning understanding of the chemical and physical properties of air pollution mixtures and their long-term implications. The past 15 years has seen the growth of ambient air pollution increasing exponentially, and so the array of acute and chronic health effects associated with it. The global burden of disease (GBD) study report ranked exposure to ambient fine PM ($PM_{2.5}$) as the seventh largest factor contributing to global mortality of 2.9 million to 3.3 million people in 2013 alone [87], of which 184 000 deaths annually are directly linked to the impact of air pollution alone [84]. Using more sophisticated source modelling, [83] estimated that about 1/5 of all the premature deaths in UK, USA and Germany occur due to ambient $PM_{2.5}$ and ozone (O_3) emissions. This accounts for 5 % globally for the figure of 2.9 million to 3.3 million people whose death is associated with outdoor air pollution. Therefore, there needs to be a serious reduction in global emissions from the transport sector, in order to prevent increases in health effects and the GBD arising from atmospheric air pollution.

[86] propose a multi-faceted and multi-disciplinary approach between the various fields of health sciences, toxicology, epidemiology, exposure science, clinical medicine and engineering and the physical science fields of atmospheric science, physics and chemistry. However, there has been a lot of progress made in the categorization of air pollution in recent years due to the widespread use of the satellite imaging technology. Among the advances are the aerosol mass spectrometer and the proton transfer reaction mass spectrometer [88], as well as the introduction of novel methods of analysis method in the study of aerosol components with adverse health effects utilizing mobile and wearable monitoring devices, thus making monitoring of human exposure in new locations possible and easy. This facilitates simulation modelling of the transportation modes and mechanical formation of the main pollutants locally, regionally and globally.

References

[1]   B. Haber and J. Wang, "A Robust Control Approach on Diesel Engines with Dual-Loop Exhaust Gas Recirculation Systems," Ohio State University, 2010.

[2]   M. Zheng, D. K. Irick, and J. Hodgson, "Stabilizing excessive EGR with an oxidation catalyst on a modern diesel engine," *ASME ICE,* vol. 38, 2002.

[3]   K. I. Abaas, "Effect of Exhaust Gas Recirculation (EGR) on the Performance Characteristics of a Direct Injection Multi Cylinders Diesel Engine," *Tikrit Journal of Engineering Science (TJES),* vol. 23, pp. 32-39, 2016.

[4]   M. Ghazikhani, M. E. Feyz, and A. Joharchi, "Experimental investigation of the exhaust gas recirculation effects on irreversibility and brake specific fuel consumption of indirect injection diesel engines," *Applied Thermal Engineering,* vol. 30, pp. 1711-1718, 2010.

[5]   A. Abu-Jrai, J. Rodríguez-Fernández, A. Tsolakis, A. Megaritis, K. Theinnoi, R. Cracknell*, et al.*, "Performance, combustion and emissions of a diesel engine operated with reformed EGR. Comparison of diesel and GTL fuelling," *Fuel,* vol. 88, pp. 1031-1041, 2009.

[6]   A. Maiboom, X. Tauzia, and J.-F. Hétet, "Experimental study of various effects of exhaust gas recirculation (EGR) on combustion and emissions of an automotive direct injection diesel engine," *Energy,* vol. 33, pp. 22-34, 2008.

[7]   G. Avolio, C. Beatrice, N. Del Giacomo, C. Guido, M. na Migliaccio, and V. Fraioli, "Effects of highly cooled egr on modern diesel engine performance at low temperature combustion condition," SAE Technical Paper 0148-7191, 2007.

[8]   S. Som and A. Datta, "Thermodynamic irreversibilities and exergy balance in combustion processes," *Progress in energy and combustion science,* vol. 34, pp. 351-376, 2008.

[9]   W. K, *Advanced thermodynamics for engineers*. NEW YORK USA: McGRAW-HILL, 1995.

[10]   K. C. Rolle, *Thermodynamics and heat power*, 6 ed. Upper Saddle River, NJ: Pearson/Prentice Hall, 2005.

[11]   D. De Serio, A. de Oliveira, and J. R. Sodré, "Effects of EGR rate on performance and emissions of a diesel power generator fueled by B7," *Journal of the Brazilian Society of Mechanical Sciences and Engineering,* pp. 1-9, 2017.

[12]   M. Zheng, G. T. Reader, and J. G. Hawley, "Diesel engine exhaust gas recirculation—a review on advanced and novel concepts," *Energy conversion and management,* vol. 45, pp. 883-900, 2004.

[13]   G. Zamboni, S. Moggia, and M. Capobianco, "Effects of a Dual-Loop Exhaust Gas Recirculation System and Variable Nozzle Turbine Control on the Operating Parameters of an Automotive Diesel Engine," *Energies,* vol. 10, p. 47, 2017.

[14]   J. Thangaraja and C. Kannan, "Effect of exhaust gas recirculation on advanced diesel combustion and alternate fuels-A review," *Applied Energy,* vol. 180, pp. 169-184, 2016.

[15]   L. Cornolti, A. Onorati, T. Cerri, G. Montenegro, and F. Piscaglia, "1D simulation of a turbocharged Diesel engine with comparison of short and long EGR route solutions," *Applied energy,* vol. 111, pp. 1-15, 2013.

[16]   R. Senthilkumar, K. Ramadoss, and R. Manimaran, "Experimental investigation of performance and emission characteristics by different Exhaust gas recirculation methods used in diesel engine," *Global Journal of Research In Engineering,* vol. 13, 2013.

[17]   K. Bhaskar, G. Nagarajan, and S. Sampath, "The performance and emission characteristics of fish oil methyl esters (fome) and diesel blends in a partially premixed charge compression ignition engine," *International journal of green energy,* vol. 11, pp. 389-403, 2014.

[18]   K. Bhaskar, G. Nagarajan, and S. Sampath, "The effects of premixed ratios on the performance and emission of PPCCI combustion in a single cylinder diesel engine," *International journal of green energy,* vol. 10, pp. 1-11, 2013.

[19]   M. Xu, Y. Gui, and K.-y. Deng, "Fuel injection and EGR control strategy on smooth switching of CI/HCCI mode in a diesel engine," *Journal of the Energy Institute,* vol. 88, pp. 157-168, 2015.

[20]   A. Azad, M. Rasul, M. Khan, S. C. Sharma, and M. Bhuiya, "Recent development of biodiesel combustion strategies and modelling for compression ignition engines," *Renewable and Sustainable Energy Reviews,* vol. 56, pp. 1068-1086, 2016.

[21]   P. Das, P. Subbarao, and J. Subrahmanyam, "Control of combustion process in an HCCI-DI combustion engine using dual injection strategy with EGR," *Fuel,* vol. 159, pp. 580-589, 2015.

[22]   M. T. Garcia, F. J. J.-E. Aguilar, and T. S. Lencero, "Experimental study of the performances of a modified diesel engine operating in homogeneous charge compression ignition (HCCI) combustion mode versus the original diesel combustion mode," *Energy,* vol. 34, pp. 159-171, 2009.

[23]   A. P. Singh and A. K. Agarwal, "Combustion characteristics of diesel HCCI engine: an experimental investigation using external mixture formation technique," *Applied Energy,* vol. 99, pp. 116-125, 2012.

[24]   Z. Chen, J. Liu, Z. Wu, and C. Lee, "Effects of port fuel injection (PFI) of n-butanol and EGR on combustion and emissions of a direct injection diesel engine," *Energy conversion and management,* vol. 76, pp. 725-731, 2013.

[25]   Y. Zhao, Y. Wang, D. Li, X. Lei, and S. Liu, "Combustion and emission characteristics of a DME (dimethyl ether)-diesel dual fuel premixed charge compression ignition engine with EGR (exhaust gas recirculation)," *Energy,* vol. 72, pp. 608-617, 2014.

[26]   A. Wimmer, H. Eichlseder, M. Klell, and G. Figer, "Potential of HCCI concepts for DI diesel engines," *International journal of vehicle design,* vol. 41, pp. 32-48, 2006.

[27]   Y. Lee and K. Y. Huh, "Analysis of different modes of low temperature combustion by ultra-high EGR and modulated kinetics in a heavy duty diesel engine," *Applied Thermal Engineering,* vol. 70, pp. 776-787, 2014.

[28]   S. I. Pishbin, M. Ghazikhani, and S. M. R. M. Razavi, "Experimental study on the effects of flame regime on the exergy destruction in premixed low swirl combustion," *International Journal of Exergy,* vol. 17, pp. 267-286, 2015.

[29]   M. Granovskii, I. Dincer, and M. A. Rosen, "Exergy and industrial ecology: an application to an integrated energy system," *International Journal of Exergy,* vol. 5, pp. 52-63, 2008.

[30]   G. E. Ballachey and M. R. Johnson, "Prediction of blowoff in a fully controllable low-swirl burner burning alternative fuels: Effects of burner geometry, swirl, and fuel composition," *Proceedings of the Combustion Institute,* vol. 34, pp. 3193-3201, 2013.

[31]   M. Mani, G. Nagarajan, and S. Sampath, "An experimental investigation on a DI diesel engine using waste plastic oil with exhaust gas recirculation," *Fuel,* vol. 89, pp. 1826-1832, 2010.

[32]   Rao KS, Mutyalu KB, and R. A, "effects of exhaust gas recirculation on the performance and emission characteristics of a diesel engine fueled with waste cooking oil methyl ester," *ARPN Journal oF Engineering and Applied Sciences,* vol. 10, pp. 4799-4804, 11 JUNE 2015.

[33] H. B. Charola, P. B. Makwana, and R. D. Makwana, "Effect of EGR (Exhaust gas recirculation) on performance and emission of CI (Compression ignition) engine fuelled with blend," *International Journal on Advances in Engineering Technology and Science,* vol. 3, pp. 1-5, 2016.

[34] Manieniyan V and S. S, ""Experimental Analysis of Exhaust gas Recirculation on Diesel Engines Operating with Biodiesel," *International journal of Engineering and Technology (IJET),* vol. 3, pp. 129-134, 2013.

[35] M. Hawi, R. Kiplimo, and H. Ndiritu, "Effect of exhaust gas recirculation on performance and emission characteristics of a diesel-piloted biogas engine," *Smart Grid and Renewable Energy,* vol. 6, p. 49, 2015.

[36] P. Kumar and N. Kumar, "Effect of EGR on performance and emission characteristics of a dual fuel engine fuelled with CNG and JOME," *Biofuels,* vol. 7, pp. 743-751, 2016.

[37] R. Papagiannakis, "Study of air inlet preheating and EGR impacts for improving the operation of compression ignition engine running under dual fuel mode," *Energy conversion and management,* vol. 68, pp. 40-53, 2013.

[38] M. Abdelaal and A. Hegab, "Combustion and emission characteristics of a natural gas-fueled diesel engine with EGR," *Energy conversion and management,* vol. 64, pp. 301-312, 2012.

[39] B. Ashok, S. D. Ashok, and C. R. Kumar, "LPG diesel dual fuel engine–A critical review," *Alexandria Engineering Journal,* vol. 54, pp. 105-126, 2015.

[40] K. Ryu, "Effects of pilot injection pressure on the combustion and emissions characteristics in a diesel engine using biodiesel–CNG dual fuel," *Energy conversion and management,* vol. 76, pp. 506-516, 2013.

[41] L. Tarabet, K. Loubar, M. Lounici, K. Khiari, T. Belmrabet, and M. Tazerout, "Experimental investigation of DI diesel engine operating with eucalyptus biodiesel/natural gas under dual fuel mode," *Fuel,* vol. 133, pp. 129-138, 2014.

[42] M. S. Lounici, K. Loubar, L. Tarabet, M. Balistrou, D.-C. Niculescu, and M. Tazerout, "Towards improvement of natural gas-diesel dual fuel mode: An experimental investigation on performance and exhaust emissions," *Energy,* vol. 64, pp. 200-211, 2014.

[43] S. Palash, M. Kalam, H. Masjuki, B. Masum, I. R. Fattah, and M. Mofijur, "Impacts of biodiesel combustion on NO x emissions and their reduction approaches," *Renewable and Sustainable Energy Reviews,* vol. 23, pp. 473-490, 2013.

[44] P. S. Kumar, F. Antony, and P. Sahoo, "The Performance and NOx Emissions of a IDI diesel Engine at Distinct EGR Rates Fuelled with JB100, JB80, JB60, JB40, JB20 & Diesel," *International Journal of Engineering Science and Technology,* vol. 5, p. 519, 2013.

[45] R. Selvan and D. K. Maniysundar, "Performance and Emission Analysis of single cylinder Diesel Engine using Jatropha oil with EGR," *International Journal of Science, Engineering and Technology Research (IJSETR),* vol. 3, pp. 14-18, 2014.

[46] K. Lehto, A. Elonheimo, K. Hakkinen, T. Sarjovaara, and M. Larmi, "Emission reduction using hydrotreated vegetable oil (HVO) with Miller timing and EGR in diesel combustion," *SAE International Journal of Fuels and Lubricants,* vol. 5, pp. 218-224, 2011.

[47] N. R. Kumar, Y. Sekhar, and S. Adinarayana, "Effects of compression ratio and EGR on performance, combustion and emissions of DI injection diesel engine," *International Journal of Applied Science and Engineering,* vol. 11, pp. 41-49, 2013.

[48] L. Li, J. Wang, Z. Wang, and H. Liu, "Combustion and emissions of compression ignition in a direct injection diesel engine fueled with pentanol," *Energy,* vol. 80, pp. 575-581, 2015.

[49]   L. Li, J. Wang, Z. Wang, and J. Xiao, "Combustion and emission characteristics of diesel engine fueled with diesel/biodiesel/pentanol fuel blends," *Fuel,* vol. 156, pp. 211-218, 2015.

[50]   L. Wei, C. Cheung, and Z. Huang, "Effect of n-pentanol addition on the combustion, performance and emission characteristics of a direct-injection diesel engine," *Energy,* vol. 70, pp. 172-180, 2014.

[51]   X. Wang, C. Cheung, Y. Di, and Z. Huang, "Diesel engine gaseous and particle emissions fueled with diesel–oxygenate blends," *Fuel,* vol. 94, pp. 317-323, 2012.

[52]   H. Dangar and G. P. Rathod, "Combine effect of exhaust gas recirculation (EGR) and varying inlet air pressure on performance and emission of diesel engine," *IOSR Journal of Mechanical and Civil Engineering (IOSR-JMCE),* vol. 6, pp. 26-33, 2013.

[53]   Z. Chen, Z. Wu, J. Liu, and C. Lee, "Combustion and emissions characteristics of high n-butanol/diesel ratio blend in a heavy-duty diesel engine and EGR impact," *Energy conversion and management,* vol. 78, pp. 787-795, 2014.

[54]   M. Fathi, R. K. Saray, and M. D. Checkel, "The influence of Exhaust Gas Recirculation (EGR) on combustion and emissions of n-heptane/natural gas fueled Homogeneous Charge Compression Ignition (HCCI) engines," *Applied Energy,* vol. 88, pp. 4719-4724, 2011.

[55]   G. Abd-Alla, H. Soliman, O. Badr, and M. Abd-Rabbo, "Effects of diluent admissions and intake air temperature in exhaust gas recirculation on the emissions of an indirect injection dual fuel engine," *Energy Conversion and Management,* vol. 42, pp. 1033-1045, 2001.

[56]   A. K. Agrawal, S. K. Singh, S. Sinha, and M. K. Shukla, "Effect of EGR on the exhaust gas temperature and exhaust opacity in compression ignition engines," *Sadhana,* vol. 29, pp. 275-284, 2004.

[57]   C. A. Idicheria and L. M. Pickett, "Effect of EGR on diesel premixed-burn equivalence ratio," *Proceedings of the Combustion Institute,* vol. 31, pp. 2931-2938, 2007.

[58]   M. Shahadat, M. Nabi, M. Akhter, and M. Tushar, "Combined Effect of EGR and Inlet Air Preheating on Engine Performance in Diesel Engine," *International Energy Journal,* vol. 9, 2008.

[59]   T. Jacobs, D. N. Assanis, and Z. Filipi, "The impact of exhaust gas recirculation on performance and emissions of a heavy-duty diesel engine," SAE Technical paper 0148-7191, 2003.

[60]   K. Ishiki, S. Oshida, M. Takiguchi, and M. Urabe, "A study of abnormal wear in power cylinder of diesel engine with EGR-wear mechanism of soot contaminated in lubricating oil," SAE Technical Paper 0148-7191, 2000.

[61]   M. Y. Au, J. W. Girard, R. Dibble, D. Flowers, S. M. Aceves, J. Martinez-Frias, *et al.*, "1.9-liter four-cylinder HCCI engine operation with exhaust gas recirculation," SAE Technical Paper 0148-7191, 2001.

[62]   K. Venkateswarlu, B. S. R. Murthy, and V. V. Subbarao, "The Effect of Exhaust Gas Recirculation and Di-Tertiary Butyl Peroxide on Diesel-Biodiesel Blends for Performance and Emission Studies," *International Journal of Advanced Science and Technology,* vol. 54, pp. 49-60, 2013.

[63]   D. Hountalas, G. Mavropoulos, and K. Binder, "Effect of exhaust gas recirculation (EGR) temperature for various EGR rates on heavy duty DI diesel engine performance and emissions," *Energy,* vol. 33, pp. 272-283, 2008.

[64]   S. K. Mahla, L. M. Das, and M. K. G. Babu, "Effect of EGR on performance and emission characteristics of natural gas fueled diesel engine." Jordan Journal of Mechanical and Industrial Engineering 4.4 (2010)." in *Jordan Journal of Mechanical and Industrial Engineering* 2010, pp. 523-530.

[65] N. Yilmaz, F. M. Vigil, K. Benalil, S. M. Davis, and A. Calva, "Effect of biodiesel–butanol fuel blends on emissions and performance characteristics of a diesel engine," *Fuel,* vol. 135, pp. 46-50, 2014.

[66] N. Ladommatos, S. M. Abdelhalim, H. Zhao, and Z. Hu, "The effects on diesel combustion and emissions of reducing inlet charge mass due to thermal throttling with hot EGR," SAE Technical Paper 0148-7191, 1998.

[67] M. H. M. Yasin, R. Mamat, A. F. Yusop, D. M. N. D. Idris, T. Yusaf, M. Rasul*, et al.*, "Study of a diesel engine performance with exhaust gas recirculation (EGR) system fuelled with palm biodiesel," *Energy Procedia,* vol. 110, pp. 26-31, 2017.

[68] S. Saravanan, "Effect of exhaust gas recirculation (EGR) on performance and emissions of a constant speed DI diesel engine fueled with pentanol/diesel blends," *Fuel,* vol. 160, pp. 217-226, 2015.

[69] I. A. Badruddin, A. Badarudin, N. Banapurmath, N. S. Ahmed, G. Quadir, A. A. Al-Rashed*, et al.*, "Effects of engine variables and heat transfer on the performance of biodiesel fueled IC engines," *Renewable and Sustainable Energy Reviews,* vol. 44, pp. 682-691, 2015.

[70] K. S. Rao, "Effect of EGR on Diesel Engine Performance and Exhaust Emission Running with Cotton Seed Biodiesel," *international journal of mechanical and mechatronic engineering,* vol. 16, pp. 64-69, 2016.

[71] D. Jagadish, P. R. Kumar, and K. Madhu Murthy, "Performance characteristics of a diesel engine operated on biodiesel with exhaust gas recirculation," *International Journal of Advanced Engineering Technolog,* vol. 2, pp. 202-208, 2011.

[72] U. Asad and M. Zheng, "Exhaust gas recirculation for advanced diesel combustion cycles," *Applied Energy,* vol. 123, pp. 242-252, 2014.

[73] U. Asad, P. Divekar, M. Zheng, and J. Tjong, "Low temperature combustion strategies for compression ignition engines: operability limits and challenges," SAE Technical Paper 0148-7191, 2013.

[74] Y. Aoyagi, H. Osada, M. Misawa, Y. Goto, and H. Ishii, "Advanced diesel combustion using of wide range, high boosted and cooled EGR system by single cylinder engine," SAE Technical Paper 0148-7191, 2006.

[75] K. S. Rao, S. Narendra, and P. Rao, "Characteristics of a DI-CI Engine Fueled with Preheated Corn Biodiesel," *International Journal of Mechanical Engineering,* vol. 40, pp. 350-361, 2012.

[76] S. Peng, X. Yun, L. Xiao, Y. He, F. Linjun, and L. Ping, "The Role of Diesel Soot in the Tribological Behavior of 150SN Base Oil," *China Petroleum Processing & Petrochemical Technology,* vol. 19, pp. 89-95, 2017.

[77] E. Hu, X. Hu, T. Liu, L. Fang, K. D. Dearn, and H. Xu, "The role of soot particles in the tribological behavior of engine lubricating oils," *Wear,* vol. 304, pp. 152-161, 2013.

[78] C. Esangbedo, A. L. Boehman, and J. M. Perez, "Characteristics of diesel engine soot that lead to excessive oil thickening," *Tribology International,* vol. 47, pp. 194-203, 2012.

[79] X. Li, Z. Xu, C. Guan, and Z. Huang, "Impact of exhaust gas recirculation (EGR) on soot reactivity from a diesel engine operating at high load," *Applied Thermal Engineering,* vol. 68, pp. 100-106, 2014.

[80] K.-H. Kim, P. Kumar, J. E. Szulejko, A. A. Adelodun, M. F. Junaid, M. Uchimiya*, et al.*, "Toward a better understanding of the impact of mass transit air pollutants on human health," *Chemosphere,* 2017.

[81] L. M. McKenzie, R. Z. Witter, L. S. Newman, and J. L. Adgate, "Human health risk assessment of air emissions from development of unconventional natural gas resources," *Science of the Total Environment,* vol. 424, pp. 79-87, 2012.

[82]   R. D. Brook, S. Rajagopalan, C. A. Pope, J. R. Brook, A. Bhatnagar, A. V. Diez-Roux, *et al.*, "Particulate matter air pollution and cardiovascular disease," *Circulation,* vol. 121, pp. 2331-2378, 2010.

[83]   J. Lelieveld, J. Evans, M. Fnais, D. Giannadaki, and A. Pozzer, "The contribution of outdoor air pollution sources to premature mortality on a global scale," *Nature,* vol. 525, pp. 367-371, 2015.

[84]   K. Bhalla, M. Shotten, A. Cohen, M. Brauer, S. Shahraz, R. Burnett, *et al.*, *Transport for health: the global burden of disease from motorized road transport*, 2014.

[85]   M. J. Nieuwenhuijsen, H. Khreis, E. Verlinghieri, and D. Rojas-Rueda, "Transport and health: a marriage of convenience or an absolute necessity," *Environment international,* vol. 88, pp. 150-152, 2016.

[86]   J. J. West, A. Cohen, F. Dentener, B. Brunekreef, T. Zhu, B. Armstrong, *et al.*, "What we breathe impacts our health: improving understanding of the link between air pollution and health," ed: ACS Publications, 2016.

[87]   J. S. Apte, J. D. Marshall, A. J. Cohen, and M. Brauer, "Addressing global mortality from ambient PM2. 5," *Environmental science & technology,* vol. 49, pp. 8057-8066, 2015.

[88]   J. de Gouw and C. Warneke, "Measurements of volatile organic compounds in the earth's atmosphere using proton-transfer-reaction mass spectrometry," *Mass Spectrometry Reviews,* vol. 26, pp. 223-257, 2007.

<center>**CHAPTER THREE**</center>

<center>**METHODOLOGY**</center>

3.1 Introduction

This work used two methodological approaches in answering the main research aim and objectives of this study work. The first approach was numerical with the development of equations in modelling that could objectively help in providing the answers to the aim and objectives. The second approach was experimental work, which enable the harmonization of the experimental work and the numerical theoretical equation work. The two approaches and their findings will be presented and discussed in the Chapters 8 and 9 of this work.

This work utilized numerical equations to help in the calculation and data collection processes of this work especially in relation to the parameters of performance, namely: BTE, BSFC, BP, and EGT, and emission characteristics of NO_X, CO, CO_2, UHC and smoke opacity which are all closely interlinked with one another.

3.2 Numerical Equations Model

The main control equations used in the numerical equation modelling in this work were taken from [1-5]. The first equations deal mostly with the first law of thermodynamics and its wider applications in the equations of rate of change of mass in an open system across the system boundaries. The first law of thermodynamics states that energy can neither be created or destroyed but can be adapted into other forms of energy [6]. There are three types of systems applied in the thermodynamics of internal combustion engines, namely, the open system, the closed system, and the isolated system. For the purpose of this work the open system was utilized and defined according to [7], that it is a system whose boundaries allow for mass transfer, heat transfer and work.

3.3 Definitions of Numerical Equations

3.3.1 First Law and Conservation of Mass

The first equation relates to the conservation of mass clearly following the definition of the first law as aforementioned, and expressed mathematically as:

$$\frac{dm}{dt} = \sum_j \dot{m}_j \qquad\qquad\qquad \text{Equation 1}$$

<center>73</center>

Where dm/dt is the rate of change of the mass within an open system, $\sum_j \dot{m}_j$ is the sum or net flux of mass flow rate of the jth species.

3.3.2 The Second Law and Conservation of Species

The second equation tracks and looks at the combustion products and the processes within the combustion chamber based on the conserved mass balance of the individual species within the combustion process and after combustion, referred to as the *conservation of species* and expressed as:

$$\dot{Y}_j = \sum_j \left(\frac{\dot{m}_j}{m}\right)\left(\dot{Y}_i^j - \dot{Y}_i^{cyl}\right) + \frac{\Omega_i W_{mw}}{\rho} \qquad \text{Equation 2}$$

Where Ω_i is the dimensionless integral of order unity dependent on the force interaction during collision of the ith species, $\dot{Y}_i^j$ is the stoichiometric coefficient on the product side, ρ is the density of air, $\dot{m}_j$ is the mass flow rate of the jth species, $\dot{Y}_i^{cyl}$ is the stoichiometric coefficient on the reactant side, W_{mw} is the system flow representation, m is the total mass within the control cylinder.

3.3.3 The Conservation of Energy

The third equation concerns the *conservation of energy* in an open system, in a thermodynamic internal combustion engine, where the mass transferred in and out of the system can be given as a statement in the form of Equations 3 and 4 as:

$$\dot{m}_{in} = \dot{m}_{out} = \Delta\dot{m}_{system} \qquad \text{Equation 3}$$

$$d\frac{(mu)}{dt} = -p\frac{dv}{dt} + \frac{dQ_{ht}}{dt} + \sum_j \dot{m}_j h_j \qquad \text{Equation 4}$$

Where $d\frac{(mu)}{dt}$ is the internal energy, $-p\frac{dv}{dt}$ is the work done by piston displacement, $\frac{dQ_{ht}}{dt}$ is the heat transfer within the system, $\sum_j \dot{m}_j h_j$ is the enthalpy flux of the system, $\dot{m}_{in}$ is the mass flow in the inlet intake, $\dot{m}_{out}$ is the mass of exhaust outlet gases, $\Delta\dot{m}_{system}$ is the change in the mass flow rate in the system.

In the following equations some assumptions have been made concerning the opening and the closing times for the exhaust and inlet valves in order for the operational equations that are used during the simulation of this work to be simplified, for the cylinder equations concerning conservation of energy in the cylinder volume. The assumptions made are that the pressure remains constant and uniform during compression stroke and remain so as the charge in the

cylinder moves to the expansion stage. Secondly that the gases in this open thermodynamic system will be and continue to be ideal gases. The third assumption is that during propagation of the combustion flame in the combustion cylinder the burned and unburned gas regions are separated and there is no heat exchange between the burned and the unburned areas referred to as combustion zones.

The following parameters of engine performance were calculated based on the above assumptions: BSFC, BTE, BP, EGT and the emission parameters of NO_X, CO_2, CO, UHC and smoke emissions, which were analyzed through measurements by a five channel gas analyzer machine and the data collected relayed to a data logging interface machine.

3.3.4 Air/Fuel Ratio

The of air/fuel ratio (with symbol λ) is given in the following equation and defined as:

$$\lambda = \frac{(A/F)}{(A/F)_S} = \frac{(m_a/m_f)}{(m_a/(m_f)_S}$$
Equation 5

Where λ is the lambda symbol for the air/fuel ratio, A/F is the air fuel ratio, $(A/F)_S$ is air fuel ratio under the stoichiometric conditions, m_a is the inlet air intake mass flow rate, m_f is the inlet intake fuel flow rate.

3.3.5 Brake Thermal Efficiency (BTE)

This can be defined as the BP of a heated engine as a function of the thermal input from the fuel used to propel that engine, by converting the heat from fuel into useful mechanical energy. This is achieved by comparing the output of the engine system to the input of the engine system i.e. BP as the output dividing it against fuel power as the input as in Equation 6 to obtain BTE as:

$$\eta_{bte} = \frac{\dot{W}_{bp}}{\dot{m}_f \times CV}$$
Equation 6

Where η_{bte} is the BTE, $\dot{W}_{bp}$ is the engine BP, $\dot{m}_f$ is the conventional diesel fuel flow rate to the engine, CV is the calorific value of the test fuel.

However, for dual fuel operating mode, the following equation is used to calculate the BTE as follows:

$$\eta_{bte} = \frac{\dot{W}_{bp}}{\dot{m}_{fd} + CV_{df} + \dot{m}_{fpo} + CV_{fpo}}$$
Equation 7

Where η_{bte} is the BTE, $\dot{W}_{bp}$ is the engine BP, $\dot{m}_{fd}$ is the rate of conventional diesel fuel flow into the engine, CV_{df} is the calorific value of the conventional diesel fuel, $\dot{m}_{fpo}$ is the WPPO fuel rate flow into the engine, CV_{fpo} is the calorific value of WPPO fuel.

In order to establish the amount of diesel that is substituted with the use of WPPO fuel blend, a diesel substitution calculation is commuted and attempted as in Equation 8 as:

$$DS = \frac{D_{df} - D_{dmf}}{D_d} \times 100 \qquad \text{Equation 8}$$

Where DS is the diesel substitution in percentage form, D_{df} is the conventional diesel fuel consumption by the experimental engine in single fuel mode in kg/h, D_{dmf} is the diesel fuel consumption in dual fuel mode.

3.3.6 Brake Power (BP)

The BP is given by the following equation considering that the probability of the air fuel mixture in the combustion chamber was fully burnt as it is assumed to contain the necessary amount of air to allow to it burn completely the fuel available and to produce the BP, is calculated as a product of the engine torque (T) and the angular rotational speed (ω) of the engine crankshaft in Equation 9 as:

$$P_b = T * \omega \qquad \text{Equation 9}$$

Where P_b is the BP theoretically, T is the engine torque, ω is the angular engine rotational speed as measured from the crankshaft.

3.3.7 Brake Specific Fuel Consumption (BSFC)

BSFC is a measure of the amount of fuel that an engine often uses or utilizes to produce a unit of power measured in kilowatt hour (kW), and is defined in Equation 10 as:

$$BSFC = \frac{\dot{m}_f}{P_b} \qquad \text{Equation 10}$$

Where BSFC is the brake specific fuel consumption, $\dot{m}_f$ is the intake fuel flow rate, P_b is the BP.

3.3.8 The Volumetric Efficiency (VE)

The volumetric efficiency (VE) with symbol (η), is a measure of how efficiently an engine can move the products of the air fuel mixture in and outside the engine cylinder, in other words,

it's the actual ratio of the quantity or amount of fuel and air that enter the engine cylinder during the intake stroke in relation to the actual holding capacity of engine cylinder and as such the volumetric efficiency is not a volume ratio but a mass ratio [8], especially in static engine conditions and defined in Equation 11 as:

$$\eta_V = \frac{n m_a}{\rho_a V_C N} \qquad \text{Equation 11}$$

Where η_V is the cylinder volumetric efficiency, N is the engine speed, V_C is the displaced volume by the piston depending on the number of cylinders, ρ_a is the air density, m_a is the inlet intake air flow rate, n is the number of revolutions of the crankshaft per cycle.

3.4 The EGR Valve Model Equations

Though EGR as a technology reuses the engine exhaust system gas products in the combustion process to reduce the amount of O_2 in the inlet intake manifold, to suppress NO_X, there is a limitation on the amount of exhaust gases that can be recirculated without compromising AFR levels and thus depriving the engine of the necessary O_2 causing damage and failure.

There are two types of EGR quantification systems that are in use today and which have been adopted by various studies to conduct EGR flow rates for various works as presented in the literature reviewed in Chapter 2. The first utilizes the gases in the combustion product and hence the name of *gas method*. The second one utilizes the mass of the combustion products hence the name *mass method* and shares the same definition as the *molar method*. There are two assumptions made in order for *molar method* to be the same as the *mass method* of quantifying the EGR flow rate. These assumptions are: *i)* $M_y = M_f$ and *ii)* $n_f < y$, where the M_y is the molecular mass of the inlet intake charge, M_f is the molecular mass of the fuel, n_f is the fuel molar quantity, and y is the inlet intake molar gas quantity.

During the model development of the EGR only the gaseous components of the combustion mixtures are taken into consideration [2] for purposes of simplification of the combustion equations. This is despite the fact that the EGR applications include all the components that are found in the exhaust manifold system. The combustion components considered are N_2, O_2, CO_2, and H_2O, while from the exhaust the components are N_2, O_2, CO_2 and H_2O vapor, while the inlet intake side contains N_2 and O_2. The equations for the EGR valve model are taken from [2, 9] as in Figure 3.1.
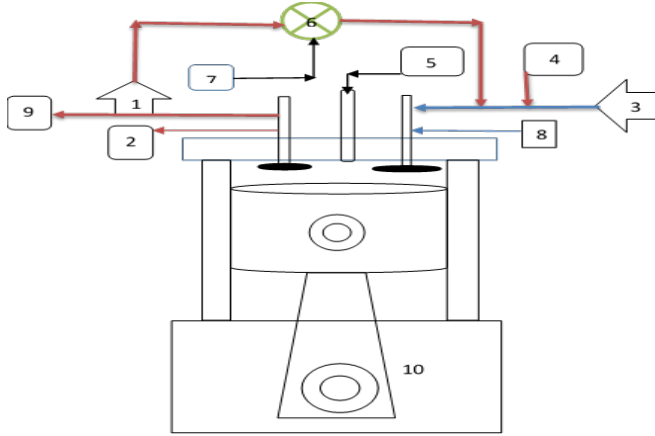
Figure 3.1: The EGR schematic loop nomenclature

Figure 3.1 illustrates the EGR schematic loop definitions and nomenclature as follows: 1. is the *direction of EGR gases*, 2. is the x subscript representing the exhaust molar gas quantity, 3. is the direction of inlet gases fresh charge, 4. is the z subscript representing remainder of the intake charge, 5. is n_f which is the fuel molar quantity, 6. is the EGR valve, 7. is the R_x molar gas ratio, 8. is the subscript y representing the inlet intake molar gas quantity, 9. is the direction of the exhaust gases exit, 10. is the engine unit.

$$y = n_{O_2} + n_{N_2} + n_{CO_2} + n_{H_2O} \qquad \text{Equation 12}$$

$$x = e_{O_2} + e_{N_2} + e_{CO_2} + e_{H_2O} \qquad \text{Equation 13}$$

Where n_i and e_i are the component species of the ith of the number of moles of the molecular components of (O_2, N_2, CO_2, and H_2O) of the test engine combustion products respectively, leading to the conservation of mass equation of the combustion process as:

$$yM_y + n_f M_f = xM_y \qquad \text{Equation 14}$$

Where y is the inlet intake molar gas quantity, x is the exhaust molar gas quantity, M_y is the molecular mass of the inlet intake charge, M_f is the molecular mass of the cycle fuel, n_f is the cycle fuel molar quantity.

Since the molecular masses are assumed to be equal for the inlet and the combustion process products, for the chemical balance of the atomic components of O, N, C, and H the equations for the exhaust molar quantities take the form:

$$e_{O_2} = n_{O_2} + \left(\frac{\gamma}{2} - \alpha - \frac{\beta}{4}\right) n_f \qquad \text{Equation 15}$$

$$e_{N_2} = e_{N_2} \qquad \text{Equation 16}$$

$$e_{CO_2} = n_{CO_2} + \alpha n_f \qquad \text{Equation 17}$$

$$e_{H_2O} = n_{H_2O} + \frac{\gamma}{2} n_f \qquad \text{Equation 18}$$

Where e_{O_2} is the exhaust engine oxygen molar quantity, e_{N_2} is the exhaust molar quantity of nitrogen, e_{CO_2} is the exhaust molar quantity of carbon dioxide, e_{H_2O} is the exhaust molar quantity of water vapor, n_f is the cycle fuel molar quantity, γ is the fresh air fraction mass, α is the thermal diffusivity of the cooling medium of the exhaust gases in the exhaust manifold, n is the number of moles from fresh inlet intake charge.

Manipulating and combining Equations 15, 16, 17 and 18, the exhaust molar gas quantity can be expressed as:

$$x = y + \left(\frac{\beta}{4} + \frac{\gamma}{2}\right)n_f \qquad \text{Equation 19}$$

Where x is the subscript for exhaust molar quantity, y is the inlet intake molar gas quantity, β is the reciprocal of the temperature mean of the EGR gases, n_f is the cycle fuel molar quantity, γ is the fresh air fraction mass.

Using the definition of the molar EGR ratio which is given by the Equation 20 as:

$$R = \frac{r}{x} \qquad \text{Equation 20}$$

Where R is the EGR molar ratio, x is the exhaust molar gas quantity, r is the total moles of the exhaust gas recirculated and considering the steady state produced in each engine cycle, in order to express the in cylinder charge in terms of the volumetric combination of the air fresh and EGR and the remainder of the inlet intake charge denoted as subscript z, the equation thus becomes as follows:

$$y = z + R_x \qquad \text{Equation 21}$$

Where y is the inlet intake molar gas quantity, z is the remainder of the inlet intake air charge, R_x is the total EGR molar ratio quantity of the moles of exhaust gases recirculated per engine cycle done.

The value of R as the universal gas constant can be calculated as follows by manipulating and combining Equations 19 and 21 and obtaining:

$$R = \frac{y-z}{y+\left(\frac{\gamma}{2}+\frac{\beta}{4}\right)n_f}$$
Equation 22

Where R is the universal gas constant, y is the inlet intake molar gas quantity, z is the remainder of the inlet intake air charge, n_f is the cycle fuel molar quantity, γ is the fresh air fraction mass, β is the reciprocal of the temperature of the EGR gases mean.

The y component as a subscript for the inlet intake molar gas quantity can also be derived from the engine speed-density relationship based on the conditions of the intake manifold and the in cylinder volumetric efficiency in Equation 23 as:

$$y = \eta_V \frac{p_{im}V_s}{\check{R}T_{im}}$$
Equation 23

Where p_{im} is intake manifold pressure, T_{im} is intake manifold temperature, R is the EGR molar gas constant, η_V is the cylinder volumetric efficiency, y is the subscript of the intake molar gas quantity and V_s is the piston swept volume.

It's imperative to mention here that in Equation 22, the EGR ratio has been defined as a function of the inlet intake manifold with existing measurable engine conditions including the fuel quantity delivered by the injection system and the fuel type used. Consequently, Equation 21 can be manipulated in combination with other equations notably Equations 15, 16, 17 and 18, so that the volumetric concentration individual gas components in the combustion zones can be derived and defined. Hence the volumetric concentration for O₂ becomes as follows:

$$[O_2]_{int} = \frac{[O_2]_{fr}cz + R\left(\frac{\gamma}{2}-\alpha-\frac{\beta}{4}\right)nf}{y(1-R)}$$
Equation 24

$$[O_2]_{exh} = \frac{[O_2]_{int}y +\left(\frac{\gamma}{2}-\alpha-\frac{\beta}{4}\right)nf}{y +\left(\frac{\gamma}{2}+\frac{\beta}{4}\right)nf}$$
Equation 25

Where $[O_2]_{int}$ is the volumetric oxygen concentration at the inlet intake manifold, $[O_2]_{exh}$ is the volumetric oxygen concentration in the exhaust manifold, y is the inlet intake molar gas quantity, γ is the fresh air fraction mass, n_f is the cycle fuel molar quantity, z is the remainder of the inlet intake air charge, $[O_2]_{fr}cz$ is the volumetric concentration of fresh inlet oxygen in the combustion zone, β is the reciprocal of the temperature of the EGR gases mean, α is the thermal diffusivity of the cooling medium of the exhaust gases in the exhaust manifold.

Since the EGR ratio influences the air excess ratio λ, it can be coupled with the EGR ratio and the engine in-cylinder availability of O₂ especially in lean burn engines which diesel engines

are normally associated. Practically, λ is simply an indicator of the amount of oxygen present that can allow complete combustion relative to the fuel delivered by the system. Thus, as seen from Equation 24, the expression can be shown as:

$$\lambda_{cyl} = \frac{y[O_2]_{int}}{\left(\alpha + \frac{\beta}{4} - \frac{\gamma}{2}\right) n_f} \qquad \text{Equation 26}$$

Where λ_{cyl} is the engine in cylinder air excess ratio, $y[O_2]_{int}$ is the inlet intake volumetric oxygen concentration molar gas quantity, β is the mean reciprocal of the temperature of the EGR gases, α is the thermal diffusivity, n_f is the cycle fuel molar quantity, γ is the fresh air fraction mass.

3.4.1 Modelling the EGR Valve Using the Orifice Equation

The EGR valve is modelled as a function of the upstream pressure and downstream pressure of the EGR valve [10] by adopting the standard orifice flow equations as:

$$W_{egr} = CA_{eff} \frac{p_i}{\sqrt{RT_i}} \Psi\left(\frac{p_j}{p_i}\right) \ if \ p_{j<} \ p_i \qquad \text{Equation 27}$$

$$W_{egr} = 0 \ if \ p_1 = p_2 \qquad \text{Equation 28}$$

$$W_{egr} = CA_{eff} \frac{p_j}{\sqrt{RT_i}} \Psi\left(\frac{p_i}{p_j}\right) \ if \ p_j > p_i \qquad \text{Equation 29}$$

Where the i is the subscript of the upstream flow condition of the EGR cooler exit (upstream EGR cooler exit), j is the subscript of the downstream conditions exhibited by the inlet intake manifold (downstream = intake manifold), C is the discharge coefficient of the engine valve opening, A_{eff} is the effective flow area as a function the EGR valve relative to its position, Ψ is the pressure ratio factor and p is the pressure of the system and γ is the ratio of specific heat of the exhaust gas produced by the system or the engine, W_{egr} is the system flow of gases from the inlet intake manifold side to the engine cylinders available, with subscript k which in this case has been substituted with subscript egr denoting EGR flow for all equations shown above, T is the temperature of the upstream gases.

The following equations are adopted from the work of [10, 11] and give the relationship between the system and the pressure ratio correction factor and help in determining modelling the boundary conditions that will be available for the system, for the mass flow through the standard orifices. For the mass flow through an isothermal orifice assuming no losses during

acceleration of the fluid flowing through the system (in this case the air), and assuming that the entire potential energy is completely converted into thermal energy, the equation becomes:

$$\dot{m} = CA \frac{p_{in}}{\sqrt{RT_{in}}} \psi \qquad \text{Equation 30}$$

Where $\dot{m}$ is the mass flow rate, C is the discharge coefficient, A is the effective area of flow, P_{in} is the pressure of the intake air, R is the specific universal gas constant, T_{in} is the temperature of the upstream.

But if we define the P_{in} and P_{out} then this relationship becomes the ratio of pressure upstream and the ratio of pressure downstream through the restriction represented by the sign symbol Π as the pressure ratio and is given in Equation 31 as:

$$\Pi = \frac{p_{out}}{p_{in}} \qquad \text{Equation 31}$$

Where Π is the pressure ratio, P_{out} is the pressure of the ambient (atmospheric), P_{in} is the pressure in the system.

But the flow function with symbol ψ is given by the following equations with two critical existing modelling conditions and thus becomes:

$$\psi = \sqrt{k[\frac{2}{k+1}]^{\frac{k+1}{k-1}}} \; if \; p_{out} \; < p_{cr} \; (\text{condition } i) \qquad \text{Equation 32}$$

$$\psi = \Pi^{\frac{1}{k}} \sqrt{\frac{2k}{k-1}[1 - \Pi^{\frac{k-1}{k}}]} \; if \; p_{out} \geq p_{cr} \; (\text{condition } ii) \qquad \text{Equation 33}$$

$$p_{cr} = p_{in} [\frac{2}{k+1}]^{\frac{k}{k-1}} \qquad \text{Equation 34}$$

Where P_{cr} is the critical pressure, P_{in} is the pressure in the upstream of the system, P_{out} is the pressure of the downstream of the system, Π is the pressure ratio, k is the thermal conductivity.

However, in order to prevent the flow function with symbol (ψ) from developing some kind of infinite gradient when the resultant value of the pressure ratio is approaching one or equaling one (Π=1), the flow function is corrected using Equations 35 and 36 with pre-existing conditions as:

$$\psi = \frac{1}{\sqrt{2}} \; if \; p_{out} \; < \frac{1}{2} p_{in} \qquad \text{Equation 35}$$

$$\psi = \sqrt{2\Pi [1 - \Pi} \; if \; p_{out} \; \geq \frac{1}{2} p_{in} \qquad \text{Equation 36}$$

Where P_{in} is the pressure upstream, p_{out} is the pressure downstream, T_{in} is the temperature upstream, A is the flow area, R is the specific gas constant, ψ is the flow function, $\dot{m}$ is the mass flow measured in kg/s, p_{cr} is critical pressure that is achieved in the most narrowed section of the orifice device, k is the cp / cv (where c_p and c_v are the specific heat at constant pressure and volume in the system), Π is the pressure ratio of the engine produced by the valves.

Thus, the flow ψ function is defined and calculated with two main existing assumption conditions as follows:

$$\psi\left(\frac{p_i}{p_j}\right) = \{\sqrt{\gamma}(\frac{2}{\gamma+1})^{\frac{(\gamma+1)}{2(\gamma-1)}} \; if \; \frac{p_i}{p_j} \le (\frac{2}{\gamma+1})^{\gamma/(\gamma-1)} \quad\quad\text{Equation 37}$$

$$\psi\left(\frac{p_i}{p_j}\right) = \sqrt{\frac{2\gamma}{\gamma-1}(\frac{p_i}{p_j})^{\frac{2}{\gamma}} - (\frac{p_i}{p_j})^{(\gamma+1)/\gamma}} \;) \; if \; \frac{p_i}{p_j} > (\frac{2}{\gamma+1})^{\gamma/(\gamma-1)} \quad\quad\text{Equation 38}$$

Where ψ is the flow function, P_i is the pressure of the ith of the upstream pressure, P_j is the pressure of the jth of downstream pressure, γ is the ratio of specific heats of the exhaust gas produced by the system or the engine.

3.4.2 The Throttle Valve Equation

Through the study of diesel engines, we learn that they are normally operated with fully opened throttle so as to allow high flow of EGR, through the use of a throttle actuator valve which allows certain operating conditions to generate a pressure drop in the intake manifold. For this reason, modelled equations take mostly the format of the mass flow equation through the orifice. However, because the throttle is never completely closed in diesel engines but leaves an aperture opening φ_0 as a bypass during operational running, the mass flow therefore through the throttle can be determined by using Equation 39 as:

$$\dot{M}_{th} = \; C_{th}A_{th}\frac{P_{ic}}{\sqrt{RT_{ic}}}\psi_{th} \quad\quad\text{Equation 39}$$

Where $\dot{M}_{th}$ is the mass flow through the throttle, A_{th} is the throttle valve effective area, C_{th} is the discharge coefficient of the throttle valve where ($C_{th} = 1$ (assumed) and ($0 \le u_{th} \le 1$), P_{im} is the intake manifold pressure, T_{int} is the inlet intake air temperature, ψ is the flow function through the throttle, R is the specific gas constant.

Thus, the throttle effective angle of the opening of the inlet intake throttle valve is given by the following equation as:

$$\varphi = u_{th}\left(\frac{\pi}{2} - \varphi_0\right) + \varphi_0 \qquad \text{Equation 40}$$

Where π is pi 3.14, φ is the effective angle of opening of the throttle, φ_0 is the initial throttle angle of opening, u_{th} is the controlled scale variable of the throttle valve.

But because the inlet intake throttle valve area varies as a function of the scaled control variable as per the second condition in equation 39 where $0 \le u_{th} \le 1$, the effective area of the throttle valve is thus calculated as:

$$A_{th} = \frac{\pi d^2{}_{th}}{4}\left[1 - \frac{cos\varphi}{cos\varphi_0}\right] \qquad \text{Equation 41}$$

Where A_{th} is the throttle valve effective area, π is pi 3.14, d is the diameter of the throttle valve, $COS\varphi$ is the final effective opening angle of the throttle valve, $COS\varphi_0$ is the initial effective angle of opening of the throttle valve.

3.4.3 Fresh Air Fraction

The fresh air fraction mass explains the amount of excess air associated with diesel engine operation. The diesel exhaust gases have and contain an amount of fresh air charge $\dot{m}_a$ which mathematically is defined as:

$$\gamma = \frac{\dot{m}_a}{\dot{m}_f} \qquad \text{Equation 42}$$

Where $\dot{m}_a$ is the fresh air charge, γ is the fresh air fraction mass, $\dot{m}_f$ is the intake fuel flow rate.

This equation thus forms part of the essential quantities for the calculation to define and determine the specific heat when c_p and c_v are constant in terms of pressure and volume respectively, and when they are to be expressed as a function of the air fraction especially in the inlet intake and exhaust manifolds as γ_{im} and γ_{em} respectively and calculated thus from the work of [11] as:

$$C._{,em} = \gamma_{em}\left(c._{,a} - C._{,eg}\right) + CC._{,eg} \qquad \text{Equation 43}$$

Where $C._{,eg} = (\lambda = 1)$ is the specific heat of the exhaust gases, $C._{,a}$ is the fresh air mass fraction, $C._{,im}$ is the specific heat of the inlet intake manifold gases.

While for the inlet intake manifold the equation then becomes:

$$C_{,im} = \gamma_{im}(C_{,a} - C_{,em}) + C_{,em} \qquad \text{Equation 44}$$

Where $C_{,im}$ is the specific heat of the inlet intake manifold gases, $C_{,a}$ is the fresh air mass fraction, γ_{im} is the fresh air fraction mass if the intake manifold.

However, for the purposes of this experiment and the experimental set-up, the EGR % mass flow rate was calculated using the Equation 45 as:

$$(EGR\ \%)_{rf} = \frac{\dot{m}_{EGR}}{\dot{m}_i} \times 100 \qquad \text{Equation 45}$$

But

$$\dot{m}_i = \dot{m}_a + \dot{m}_f + \dot{m}_{EGR} \qquad \text{Equation 46}$$

Where $EGR\ \%_{rf}$ is the percentage mass flow rate of the exhaust gases, $\dot{m}_i$ is the mass of the inlet intake air, $\dot{m}_a$ is the mass of the ambient air, $\dot{m}_f$ is the mass of the injected fuel into the engine, $\dot{m}_{EGR}$ is the mass of the exhaust recirculated gas into the engine.

3.5 The EGR Cooler and The Exchange of Heat in the Exhaust Manifold

The EGR cooler can be modelled following the heat exchangers and thus assumed to be having a constant wall temperature T_w as suggested by the works and equations of [11, 12].
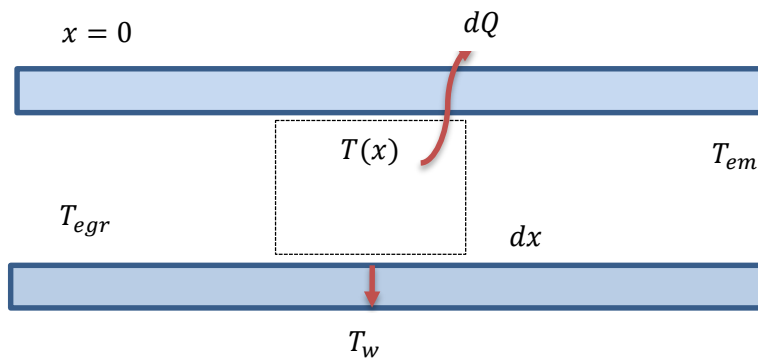
Figure 3.2: The EGR cooler heat balance definitions and nomenclature

Figure 3.2 shows the EGR cooler heat balance definitions and nomenclature, where T_w is the wall temperature, T_{em} is the exhaust manifold temperature, T_{egr} is the temperatures of the EGR gases, L is the length of the EGR cooler, T_x is the temperature as a function of x in the cooler.

Looking at Figure 3.2 and utilizing a small control volume and assuming that the heat transfer h and the specific heat c_p at constant pressure is independent of the temperature T and the function x, the heat flow into the cooler wall can be defined as:

$$-\frac{dQ}{dt} = \pi d * dx * h[T(x) - T_w] \qquad \text{Equation 47}$$

Where $-\frac{dQ}{dt}$ is the rate of change of internal energy, π is pi 3.14, d is the diameter of the pipes making up the EGR cooler, h is the heat transfer, dx is the rate of change of x, $T(x)$ is the temperature as a function of x, T_w is the wall temperature.

But the change of internal energy of the EGR % mass flow rate is defined by Equation 48 as follows:

$$\frac{dQ}{dt} = dT \times \dot{m}_{egr} \times c_p \qquad \text{Equation 48}$$

Where dQ/dt is the change in internal energy of the EGR % mass flow rate, d is the diameter of the pipes making the EGR cooler, T is the temperature, $\dot{m}_{egr}$ is the mass flow rate of the EGR % gas, c_p is the specific heat at constant pressure.

In order to get the differential equation for the gas temperature Equations 47 and 48 are combined to become Equation 49 as:

$$\frac{dT}{dx} = \frac{\pi dh}{\dot{m}_{egr}c_p}(T(x) - T_w) \qquad \text{Equation 49}$$

Where dT/dx is the rate of change in temperature, π is pi 3.14, h is the heat transfer, d is the diameter of the pipes making the EGR cooler, $\dot{m}_{egr}$ is the mass flow rate of the EGR % gas, c_p is the specific heat at constant pressure. $T(x)$ is the temperature as a function of x, T_w is the wall temperature.

But at the point where $x = L$ the temperature at the outlet of the EGR cooler corresponds to the solution of Equation 48. Therefore, the equation for T_{egr} is defined and expressed as a function of the length L as:

$$T(L) = T_{egr} = T_w + (T_{em} - T_w)e - \frac{\pi dh}{\dot{m}_{egr}c_p} \qquad \text{Equation 50}$$

Where $T(L)$ is the temperature as a function of length, T_{egr} is the EGR gas temperature, T_w is the wall temperature, T_{em} is the exhaust manifold temperature, e is the engine unit and its components, π is pi 3.14, d is the diameter of the pipes making the EGR cooler, h is the heat

transfer, $\dot{m}_{egr}$ is the mass flow rate of the EGR % gas, c_p is the specific heat at constant pressure.

When $\mathcal{E}_{egr}$ is defined as the EGR cooler efficiency and as a function of the EGR % mass flow rate it is expressed as:

$$\mathcal{E}_{egr} = 1 - e - \frac{\pi dL \times h_{egr}}{c_p \times \dot{m}_{egr}}$$
Equation 51

Where $\mathcal{E}_{egr}$ is the EGR cooler efficiency, e is the engine unit and components of internal recirculated EGR, h_{egr} is the specific heat transfer of the EGR gases, d is the diameter of the pipes making up the EGR cooler, c_p is the specific heat at constant pressure, $\dot{m}_{egr}$ is the mass flow rate of the EGR % gas, π is pi 3.14, L is the total length of the EGR cooler.

But since the engine cooling medium used in this case is water, approximating T_e as wall temperature using Equation 49 becomes as follows:

$$T_{egr} = T_{em} - \mathcal{E}_{egr}(T_{em} - T_e)$$
Equation 52

Where T_{egr} is the EGR gas temperature, T_{em} is the exhaust manifold temperature, $\mathcal{E}_{egr}$ is the EGR cooler efficiency, T_e is the engine unit temperature.

However, since in this case the heat transfer is still unknown for the internal convection between the heat transferring and exchanging fluids and the wall of the EGR cooler, we have to identify it by using the *Nusselt number* (Nu), it should be mentioned here that the heat transfer can be calculated by two methods using the *Prandtl number* and *Nusselt number*. The *Nusselt number* is preferred due to its values remaining almost constant for all gases as expressed in Equations 53 and 54 as two definitions:

$$Nu = \frac{h_{egr}L}{k}$$
Equation 53

$$Nu = C_0 \times Re^{c_i}$$
Equation 54

Where c_i is the empirical constant, k is the thermal conductivity of the exhaust gases, L is the total length of the EGR cooler, h_{egr} is the specific heat transfer of the EGR gases, Re is the Reynold's number, Nu is the Nusselt number.

But for circular pipes which the exhaust manifold and the calorimeter can be classified as one the Reynolds number is defined and expressed in Equation 55 as:

$$Re = \frac{\rho_{egr}v\infty d_{egr}}{\mu_{egr}} = \frac{\dot{m}_{egr}d_{egr}}{\mu_{egr}A_{egr}} = \frac{4\dot{m}_{egr}}{\pi d_{egr}\mu_{egr}}$$ Equation 55

Where μ_{egr} is the dynamic viscosity, ρ_{egr} is the density of the EGR gases, $v\infty$ is the velocity of the exiting exhaust gases and A_{egr} is the effective flow area of the EGR cooler, $\dot{m}_{egr}$ is the mass flow rate of the EGR % gas, π is pi 3.14, d_{egr} is the diameter of the EGR valve, Re is the Reynold's number. If we combine Equations 54 and 55 we can now easily define the total heat coefficient of the EGR gases as:

$$h_{egr} = \frac{k_{egr}}{L_{egr}}Nu = \frac{k_{egr}c_0}{L_{egr}}\left(\frac{4\dot{m}_{egr}}{\pi d_{egr}\mu_{egr}}\right)^{c_i} = \alpha \times \dot{m}_{egr}\beta$$ Equation 56

Where h_{egr} is the coefficient of the EGR gases, k_{egr} is the thermal conductivity of the EGR gases, L_{egr} is the total distance of travel across the cooler of the EGR gases, Nu is the $Nusselt$ number, C_0/C^i are empirical constants, d_{egr} is the diameter of the EGR valve, μ_{egr} is the dynamic viscosity of the EGR gases, $\dot{m}_{egr}$ is the EGR mass flow rate, α is the thermal diffusivity, β is the reciprocal of the temperature of the EGR gases mean.

3.5.1 The Axial Heat Transfers in the Exhaust Manifold
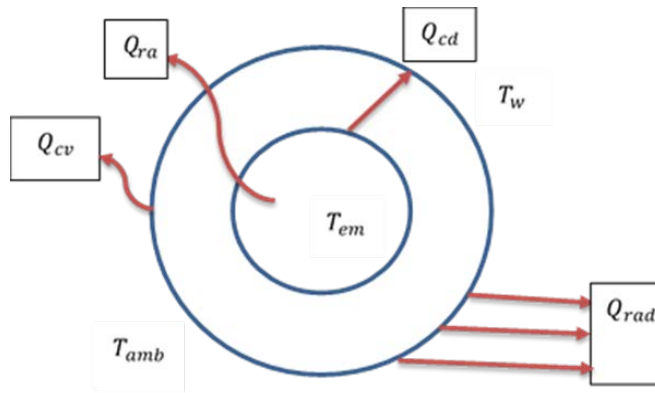
Figure 3.3: Axial and radial components of the heat transfer model of the exhaust pipe and its nomenclature

Figure 3.3 shows the axial and radial components of the heat transfer model of the exhaust pipe. The exchange of the burnt gases between the engine cylinders' outlet and exhaust manifold is affected by mostly three types of heat factors i.e. heat along the exhaust pipe which occurs through conduction, the loss of heat from the pipe to the ambient environment through radiation and etc., and finally the loss of energy due to dissipation of radiation and convection. The nomenclature shown on Figure 3.3 indicates that the system is modelled in static mode where it is assumed that the inside wall of the pipe seems to operate with almost the same

values of temperature as the exhausting gases (this assumes there is no loss through internal structural convection). This is expressed in equation form as:

$$Q_{em} = Q_{ax} + Q_{ra}$$ Equation 57

Where Q_{ax} is the heat of axial direction relative to the engine, Q_{ra} is the heat of radial direction flowing out relative to the ambient and Q_{em} is the heat from the exhaust manifold.

But Q, which here is the heat flux from the exhaust manifold with temperature component T_1 to the heat sink, which in this case is the cooling system coolant with temperature T_2 across a surface area A, is expressed and defined as:

$$Q = Ah(T_1 - T_2)$$ Equation 58

Where Q is the heat flux from the exhaust manifold, A is the area, h is the heat transfer, T_1 is the temperature of the heat sink, T_2 is the temperature of the cooling medium.

However the heat normally in axial flow direction from the exhaust manifold wall relative to the engine block is in this case assumed to have the same temperature as that of the engine exhaust manifold, where the T_{em} is the main source of the heat with the engine cooling system acting as the heat sink, thus defining the heat flux as:

$$Q_{ax} = A_{sec}h_{ax}(T_{em} - T_e)$$ Equation 59

Where A_{sec} is the cross sectional area through which the gaseous exchange occurs in the axial direction and does correspond to the number of cylinder contained by the model engine, Q_{ax} is the axial heat transfer, h_{ax} is the axial heat transfer coefficient, T_e is the temperature of the engine and T_{em} is the exhaust manifold temperature.

From Equation 57 we can deduce a very important factor which is resistance to the flow of the gases along the exhaust manifold. The thermal resistance here consists of the conductive resistance r, which is the reciprocal of or inversely proportional to h (the heat transfer coefficient) and defined in two Equations 60 and 61 as:

$$r = \frac{1}{h}$$ Equation 60

Where r is the resistance to flow along the exhaust manifold, h is the heat transfer along the exhaust manifold.

But it can also be expressed as:

$$Q_{ax} = \frac{1}{h_{ax}}$$
<div align="right">Equation 61</div>

Where Q_{ax} is the axial heat transfer, h_{ax} is the axial heat transfer coefficient.
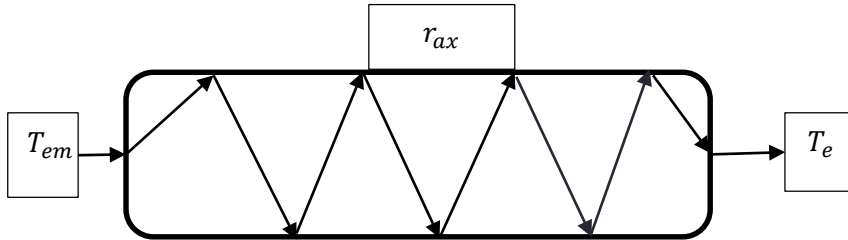
Figure 3.4: Axial heat resistance model for the exhaust pipe with its nomenclature

Figure 3.4 is showing the axial heat resistance model for the exhaust pipe with its nomenclature. T_{em} is the temperature of the exhaust manifold, r_{ax} is axial heat resistance within the system, T_{eng} is the temperature from the engine itself.

However, it should be noted at this point that the coefficient of heat transfer has so many methods of derivation from many geometric calculation and models, but this equation expression was chosen as it is a more direct expression of coefficient heat transfer and is expressed in Equation 62 as:

$$h_{ax} = \frac{1}{L/ncyl}$$
<div align="right">Equation 62</div>

Where $L/ncyl$ is the overall length of the exhaust pipe equally divided to the number of cylinder the engine contains, h_{ax} is the axial heat transfer coefficient.

3.5.2 The Radial Heat Exchange in the Exhaust Manifold
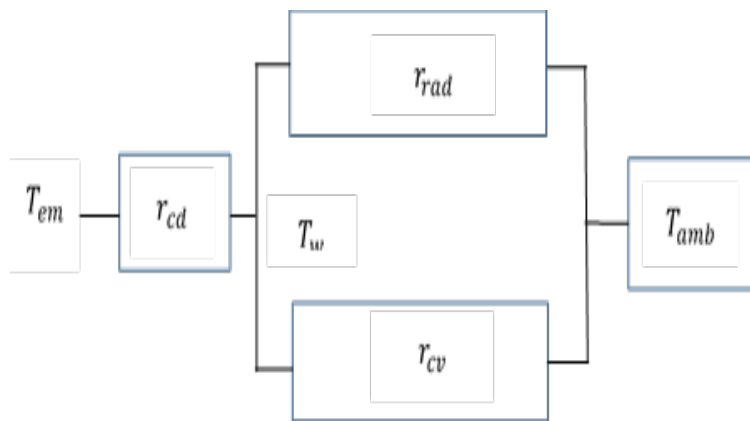
Figure 3.5: Modelled radial heat resistance of the exhaust pipe

Figure 3.5 shows the modelled radial heat resistance of the exhaust pipe, where all the thermal resistance is modelled and calculated like an electrical system in which the circuits are arranged in a series and parallel configurations. However, it is important to mention that the internal structural convection heat transfer has been neglected, thus the total overall thermal radial resistance as expressed in Equation 63 does not include internal structural convection heat transfer and is expressed as:

$$r_{ra} = r_{cd} + (\frac{1}{r_{cv}} + \frac{1}{r_{rad}})^{-1}$$

Equation 63

Where r_{ra} is the resistance due to the radial heat transfer, r_{cd} is the resistance due to conduction heat transfer, r_{cv} is the resistance due to the convectional heat transfer, r_{rad} is the resistance due to the radial heat transfer.

3.5.3 The Calculation of Coefficients of Heat Transfer

The coefficient of heat transfer can be calculated using different methods and formulas, namely, the radial conduction method, the free convection method which utilizes the Raleigh number (Ra), the Grashofs number (Gr) and the already mentioned Prandtl number (Pr), as per [11, 13].

The Raleigh number is expressed in the following equation:

$$Ra = Gr \times Pr = \frac{g\beta(T - T_\infty)d^3}{v^2} \times \frac{v}{\alpha}$$

Equation 64

Where the Ra is the Raleigh number, α is the thermal diffusivisity through the cooling medium, v is the kinematic viscosity of the air medium, g is the force of gravitational acceleration acting on the cooling medium, β is the reciprocal of the temperature mean between the source (in this case the exhaust manifold) and the heat sink (cooling medium air). Gr is the Grashofs number, Pr is the Prandtl number.

Thus:

$$\beta = \frac{2}{T+T_\infty}$$
<div align="right">Equation 65</div>

Where β is the reciprocal of the temperature mean between the source (in this case the exhaust manifold) and the heat sink (cooling medium air), T_∞ is the temperature of the exiting gases.

But for the exhaust manifold $T = T_{em} T_\infty = T_{amb}$ and $d = d_{out}$ and the coefficient of heat transfer therefore is calculated using the Nusselt number in its definition as:

$$h_{cv} = Nu \times \frac{k_a}{d_{out}}$$
<div align="right">Equation 66</div>

Where h_{cv} is the heat transfer coefficient due to the convection heat transfer, Nu is the Nusselt number, k_{amb} = the cp / cv (where c_p and c_v are the specific heat at constant pressure and volume in the system of the ambient air), d_{out} is the diameter of the exhaust manifold.

However, the Nusselt number as defined here can also be described and determined by just following the empirical formula which defines it as:

$$Nu = (0.6 + \frac{0.387 Ra^{\frac{1}{6}}}{[1+(\frac{0.559}{Pr})^{\frac{9}{16}}]^{\frac{8}{27}}})^2$$
<div align="right">Equation 67</div>

But looking at the energy of radiation exhibited in this process and heat transfer processes, the heat of radiation transfer then can be defined as:

$$Q = A_{sh} \theta \xi (T - T_\infty)^4$$
<div align="right">Equation 68</div>

Where $\xi = 5.6704 * 10^{-8}$ is the Stefan-Boltzman constant, A_{sh} is the area of the shell of the cylinder, θ is the measure of the emissivity angle relative to the black surface, 0.6 is the angle of emissivity for the exhaust manifold, $T = T_{em}$ is exhaust manifold temperature and $T_\infty = T_{amb}$ is the ambient temperature.

However, if we substitute into the power in the bracket in Equation 68 by using the products of exhaust manifold, where $T = T_{em}$ and $T_\infty = T_{amb}$, the radiation and heat transfer equation becomes:

$$Q_{rad} = A_{sh}\theta\xi(T_{em}^2 + T_{amb}^2)(T_{em} + T_{amb})(T_{em} - T_{amb})$$ Equation 69

Where A_{sh} is the area of the shell of the cylinder, T_{em} is the exhaust manifold temperature, T_{amb} is the ambient temperature, Q_{rad} is the heat flux due to the radial heat transfer, ξ is the Stefan-Boltzman constant, θ is the measure of the emissivity angle relative to the black surface.

This equation thus makes it possible for the coefficient of heat of radiation transfer process to be calculated as in Equation 70 as:

$$h_{rad} = \theta\xi(T_{em}^2 + T_{amb}^2)(T_{em} + T_{amb})$$ Equation 70

Where h_{rad} is the heat transfer coefficient due to radial heat transfer, θ is the measure of the emissivity angle relative to the black surface, T_{em} is the exhaust manifold temperature, T_{amb} is the ambient temperature, ξ is the Stefan-Boltzman constant.

References

[1]   G. Paul, A. Datta, and B. K. Mandal, "An experimental and numerical investigation of the performance, combustion and emission characteristics of a diesel engine fueled with jatropha biodiesel," *Energy Procedia,* vol. 54, pp. 455-467, 2014.
[2]   P. Divekar, Q. Tan, X. Chen, and M. Zheng, "Characterization of Exhaust Gas Recirculation for Diesel Low Temperature Combustion," *IFAC-PapersOnLine,* vol. 48, pp. 45-51, 2015.
[3]   M. Hamdan and R. H. Khalil, "Simulation of compression engine powered by Biofuels," *Energy Conversion and Management,* vol. 51, pp. 1714-1718, 2010.
[4]   M. Hawi, R. Kiplimo, and H. Ndiritu, "Effect of exhaust gas recirculation on performance and emission characteristics of a diesel-piloted biogas engine," *Smart Grid and Renewable Energy,* vol. 6, p. 49, 2015.
[5]   J. B. Heywood, "Internal combustion engine fundamentals," 2012.
[6]   S. R. Turns, *An introduction to combustion* vol. 287: McGraw-hill Education India,Private limited,New Delhi, 2012.
[7]   K. C. Rolle, *Thermodynamics and heat power*, 6 ed. Upper Saddle River, NJ: Pearson/Prentice Hall, 2005.
[8]   C. R. Ferguson and A. T. Kirkpatrick, *Internal combustion engines: applied thermosciences*: John Wiley & Sons, 2015.
[9]   L. Guzzella and C. Onder, *Introduction to modeling and control of internal combustion engine systems*: Springer Science & Business Media, 2009.
[10]   L. Kocher, E. Koeberlein, K. Stricker, D. Van Alstine, B. Biller, and G. M. Shaver, "Control-oriented modeling of diesel engine gas exchange," in *American Control Conference (ACC), 2011*, 2011, pp. 1555-1560.

[11] E. Alfieri, "Emissions-controlled diesel engine," 2009.

[12] T. L. Bergman and F. P. Incropera, *Fundamentals of heat and mass transfer*: John Wiley & Sons, 2011.

[13] M. F. Modest and D. C. Haworth, *Radiative Heat Transfer in Turbulent Combustion Systems: Theory and Applications*: Springer, 2016.

CHAPTER FOUR

THE EFFECTS OF EXHAUST GAS RECIRCULATION ON THE PERFORMANCE AND EMISSION CHARACTERISTICS OF A DIESEL ENGINE – A CRITICAL REVIEW

Journal article

The Effects of Exhaust Gas Recirculation on the Performance and Emission Characteristics of a Diesel Engine – A Critical Review

Maroa Semakula[1] and Prof Freddie Inambao[2]

University of KwaZulu-Natal, Durban South-Africa.

Orcid: 0000-0001-9922-5434

Abstract

Exhaust gas recirculation (EGR) is one of the most widely used methods of controlling emissions, particularly nitrogen oxide (NO_X), CO, CO_2, HC (hydrocarbons) and particulate matter (PM). EGR is a system where portions of the exhaust gases are re-introduced back into the combustion chamber via the intake manifold. The systems that are affected by the application of EGR are: brake specific fuel consumption (BSFC), lubricating system, diesel engine combustion characteristics, the brake thermal efficiency (BTE), the combustion characteristics of DI diesel engines, engine speed, CO_2 and HC emissions, the performance characteristics of turbocharged diesel engine, fuels, temperature, on EGR rates on the diesel engine performance and emission, the durability of engine components, and cooled EGR and the challenges of cooled EGR.

Keywords: EGR, BSFC, Carbon dioxide, PM, direct injection, brake thermal efficiency.

INTRODUCTION

The exhaust gas recirculation (EGR) technique is gaining widespread use as one of the most efficient methods or techniques for reducing emissions and particulate matter (PM) effluents from diesel automobiles, particularly nitrogen dioxide (NO_X), carbon monoxide (CO), and hydrocarbons (HC). This involves the circulation of part of the exhaust gas along with the intake fresh air charge, into the combustion chamber of the diesel engine for combustion together with the fuel injected in the normal power cycle of the diesel engine. EGR is an emission control system which allows significant reduction in NO_X gases in almost all types of diesel engines including Light Duty, Medium Duty and Heavy Duty engine use or applications, and primary engines as low as two stroke as used in marine operations and applications.

The use of EGR systems in diesel engines is not limited to increasing efficiency and reduction of emissions only [1], but also includes imparting knock resistance and reduction in the need for high load fuel enrichment in diesel engines. However, in spark ignition (SI) engines EGR systems also aide in or help in the vaporization of liquid fuels, though it is an enabler for closed cycle diesel engines in particularly improving ignition quality and reduction of high load fuel enrichment in diesel engines. Other benefits of EGR, particularly cooled EGR, is that it enables more EGR flow and cooler intake charge temperatures, thus reducing peak in-cylinder temperatures which improves ignition quality in diesel engines; reduction in lubricating oil consumption; increase in fuel injection pressures; increase in use of diesel oxidation catalysts; and increased intake manifold boost pressure. Currently, more efficiency is being demanded in the management systems of diesel engines as a way of reducing energy losses, particularly those being wasted through the exhaust system which typically wastes between 20% to 25% of all energy released. Thus, there has been tremendous development of ways or methods to continually reduce this energy wasted through re-tapping of the exhaust gases by utilizing EGR systems, for example, in scavenging for pre-heating purposes. This recycling of waste gate gases improves fuel efficiency economy, volumetric efficiency, brake thermal efficiency, brake specific fuel consumption, and reduces emissions and PM [2].

The phenomenal growth of the middle class of most emerging and developing countries, and the failure of most public transport systems and infrastructure in developing and emerging nations, has tended to increase the number of personalized transport vehicles on the road, with diesel propelled vehicles gaining popularity including in day to day commercial activities. This growth has produced many studies looking into ways of reducing energy spending through harnessing of systems gases and redirecting and harvesting the available energy within the gases which would have otherwise have been lost. This reduces demands on the primary sources of energy experienced in the world today. Although there have been tremendous achievements in technological advances in automobile manufacture and technology, there is a need for us to continue to reduce the amount of energy use and emissions, thereby reducing pollution in our primary and atmospheric environment. These studies and technological changes can initiate a reduction in global warming, which has seen a phenomenal growth in 21st century. It is imperative, therefore, for automobile and engine manufacturing industries to incorporate these new studies regarding reduction in emissions and energy wastage from engine exhaust systems and undertake deliberate measures to improve on and harness EGR system gases [1].

Agarwal, Singh and Agarwal [3] state that despite the high fuel efficiency provided by diesel engines, they have the

disadvantage of emitting nitrogen NOx and PM which is considered as the main pollutants and main toxic gases emitted to the atmosphere and as significant contributors to air pollution in major urban centres and modern-day cities. Other challenges or disadvantages include: more HCs and soluble organic fractions (SOF), PM, more condensation HC and PM deportation in cooler fouling (i.e. degraded heat transfer and higher flow resistance). These emissions are currently legislated by stringent environmental protection agencies in most countries, making diesel propelled engines and machines more expensive and less appealing. However, with the introduction of the EGR system, NOx emissions of diesel engines are greatly reduced making it increasingly compelling to incorporate such a system in the design and manufacture of diesel engines.

THE REVIEW

A number of studies have been published regarding the effects of (EGR on the performance and emission characteristics of diesel engines. Several of these have been considered and are reviewed here to highlight the developments in this area of study.

Abaas [4] in his study "Effect of Exhaust Gas Recirculation (EGR) on the Performance Characteristics of a Direct Injection Multi Cylinders Diesel Engine," used a direct injection (DI), four-cylinder FIAT engine, coupled to a dynamometer and thermocouple with Ni-Cr and Ni-Al elements, air and fuel flow meters, together with engine speed tachometers. Fuel used during the test was Iraqi conventional diesel CN = 46.8 under varying EGR rates of 5%, 10%, 20%, and 30%. Engine speed was maintained at constant for all loads and variable speeds of 1250 rpm to 3000 rpm at constant engine load were used.

Abaas [4] noted that increasing the EGR percentage or mass flow rate increased the brake specific fuel consumption (BSFC). Other findings on the BSFC were that at low engine load ranges the BSFC was found to be high as compared to when medium engine load ranges were used. The researcher attributed this to the drop in combustion chamber temperature. However, with reducing temperature the researcher observed increased fuel delay period, thus reducing engine peak pressure resulting in lower engine output and a greater increase in the fuel consumed. Therefore, according to this study, the brake thermal efficiency reduces with an increase in EGR % mass flow rate application.

Other findings from Abaas [4] include the effect of reduction in oxygen availability during combustion, which is the factor explaining the relative incomplete combustion and the increase in particulate matter (PM), but credited with the reduction of NO_X emissions. On volumetric efficiency, Abaas [4] argues that at low engine loads, since diesels operate on lean mixture, the volumetric efficiency was observed to be very high, but increasing the engine load. He observed that the engine consumed more fuel in order to meet the load demands as the

engine motor speed is increased. However, in increasing the load and engine speed he noted that the exhaust gas temperature increased, whereas increasing the EGR% mass flow rate reduced the temperatures (Figure 1).
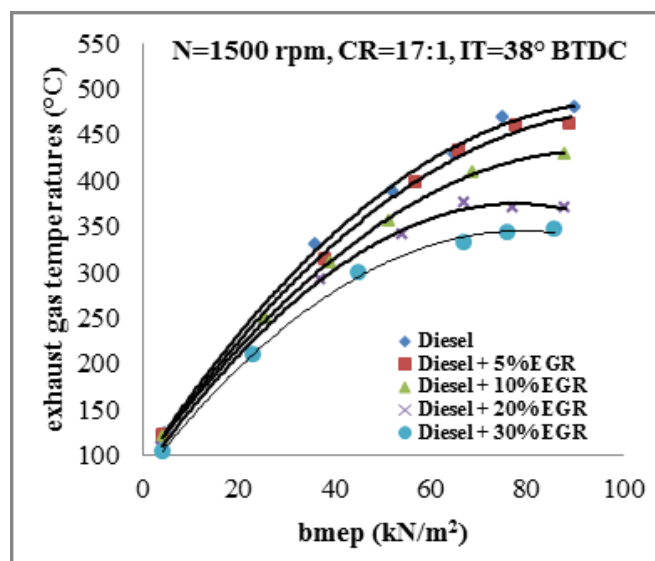
Figure 1: Abaas (2016)

Figure 1 Showing the relationship between the EGT and BSFC and application of EGR.

The increase in temperature is explained by the fact that more load and speed need more fuel to be burned; by increasing the load the work of dilution, as already explained, increases as more combustion reactants are exposed to the low temperature environment. Thus, increasing EGR% mass flow rate reduced exhaust gas temperature (EGT) by 1.41%, 15.64%, 16.08% and 26.38% for EGR% mass flow rate of 5%, 10%, 20% and 30% respectively (Abaas, 2016). On the brake power (BP), Abaas [4] noted an increase as the engine speed increases. However, by increasing the percentage of the EGR mass flow rate, the brake power reduced 1.12%, 3.26%, 5.42%, and 16.79% when compared to EGR% mass flow rates of 5%, 10%, 20% and 30%, which indicate true effects of dilution in the combustion chamber and on the performance of a diesel engine.

Charola, Makwana and Makwana [5] in their study "Effects of EGR (Exhaust Gas Recirculation) on the Performance and Emission of a CI Compression Ignition Engine Fueled with a Blend" used a single cylinder, four stroke, water compression ignition engine, with the test fuel being methanol (industrial chemical) with purity or concentration level of 99%. The test set up consisted of a test engine, a hydraulic dynamometer, fuel and flow meters, and incorporated various measuring equipment and relevant modifications for test study.

In their findings, the BTE (brake thermal efficiency) increased as the load increased. Using 10% methanol diesel blend they found that it increased the BTE by up to 12.85% and a 20% blend of methanol and diesel improved the BTE by 26.23% on the level of 10% EGR, while in BSFC (brake specific fuel

consumption) they observed a reduction of 3.57% in the BSFC in a 10%/90% methanol and diesel blend, and an increase of 4.28% when the 20%/80% was used [4]. On how the methanol diesel blend affects emissions of CO, they found that with the 10%/90% methanol diesel blend there was a 30% reduction in the emissions of CO, while with the 20%/80%, methanol diesel blend there was a reduction of 40% during the experiment study period. Regarding the HC in the exhaust system, it was observed that there was a reduction of 13.04% in the 10%/90% methanol diesel blend and a reduction of 17.39% with the 20%/80% methanol diesel blend. The NO_X emission showed a reduction of 5.55% with the 10%/90% methanol diesel blend, and 3.33% in the 20%/80% methanol diesel blend [4]. The exhaust temperature gas reduction was observed to reduce or drop by 4°C, when the 10% EGR mass flow rate was used, compared to 6°C when the EGR% mass flow rate was applied.

Rao, Mutyalu and Ramakrishna [6] in "Effects of Exhaust Gas Recirculation on The Performance and Emission Characteristics of a Diesel Engine Fueled with Waste Cooking Oil Methyl Ester", used a single cylinder, four stroke, water cooled direct injection, compression ignition engine, with a dynamometer coupled to an output shaft. Modifications were carried to allow the experiment to be carried out. In order to collect data a digital panel was installed, while an exhaust gas analyzer was used to investigate emission characteristics of the various gases in this study: CO, CO_2, HC, NO_X and O_2. Finally, the fuel they used was BO (Normal diesel), B10 (10%WCOME+90%) diesel by volume, B20 (20%WCOME+80%) diesel by volume, B30 (30%WCOME+70%) diesel by volume. The EGR % mass flow rate ranged from 0% to 20% graduated in intervals of 5%. During this experiment all the tests were conducted at constant 1500 rpm, in order to study the effects of EGR on the emission and engine performance characteristics when waste cooking oil is used together with diesel blends. The parameters investigated and their variations were: BSFC, BTE, EGT and emission characteristics of NO_X, HC and CO.

During their study they observed that the BTE remained unaffected by the application of an EGR% mass flow rate that is above 15%, but tended to decrease as the EGR% mass flow rate was increased beyond 15% EGR. This drop is explained by the fact that the availability of oxygen is reduced during combustion with the application of EGR of 15%. Regarding the BSFC it was observed to be independent of the rate of EGR% mass flow rate, particularly at lower rates of EGR% mass flow rate, but it increased as the rate of EGR% mass flow rate increased above 15%. This phenomenon is explained by the fact that there is formation of a rich mixture due to the dilution effect in the combustion chamber. This was identical to the findings of Charola et al. [5].

The effects of EGT that were observed if the engine was run on cooled EGR were that the in-cylinder temperatures were lowered, as compared to when the engine exhaust gases were run without being cooled. The cooling of the EGR gases affects the heat specific ratio of the intake air mixture by causing less oxygen in the combustion chamber. The NO_X emission findings indicate that for all the fuel blends used during the study, the NO_X emissions decreased with the increase in EGR% mass flow rate. This is explained by two factors: reduction in the availability of oxygen during combustion and the lower combustion temperatures. But since NO_X is temperature dependent for its formation to take place, this explains its decrease as flame temperatures drop. The HC and CO emission showed an increase with the increase of the EGR% mass flow rate above the 15% EGR rate level, as less oxygen becomes available for combustion, resulting in incomplete combustion and more HC and PM.

Kumar, Antony and Sahoo [7] In the "Effects of Varying EGR Rates in The Performance and NO_X Emission of an IDI Diesel Engine Fueled with JB100, JB80, JB60, JB40, JB20 and Diesel" used a single cylinder engine, water cooled IDI diesel engine, connected to an electrical loading system. The fuel line was connected to the fuel tank. NO_X, CO, CO_2 and HC were measured using an AVL gas analyzer, while the air intake mass flow rate was measured by a circle edge orifice plate. After conducting the study, they observed that at an EGR of 15% of the mass flow rate, using the blends of JB20% at 25% EGR mass flow rate, JB40% at 15% EGR mass flow rate, JB60% at 20% EGR mass flow rate, JB80% at 40% EGR mass flow rate and JB100 at 5%EGR mass flow rate [8], the NO_X emissions were seen to be reduced by 10.10%, 11.94%, 13.4%, 15.2%, 19.8% and 24.8% respectively. Soot emission, PM, CO, and CO_2 increased.

The NO_X emissions were observed in all the biodiesel blends at high levels, explained by the fact that biodiesel blends contain higher amounts of oxygen content; this trend is most visible at all full loads. Among the diesel blends the following values were found 882 ppm, 848 ppm, 806 ppm, 775 ppm, 737 ppm respectively, whereas for diesel only the value was 643 ppm [7]. The BTE was observed to be lower for all the JB blends compared to diesel due to the lower calorific value of the biodiesel but the viscosity index was seen to be very high. During the study, diesel and the JB20 blend of fuel showed a better maximum BTE value among all the blends used in the study with 5% EGR mass flow rate and the JB90 blend of fuel showing a maximum reduction of NO_X reduction percentage but with a decreased BTE of 1.25%. The decrease in BTE during this study was attributed to the reduced availability of oxygen in the fresh charge which is an effect from the EGR application, where the exhaust gases result in lower flame temperatures and velocity, leading to an increase in soot and PM. However, in the JB60 test fuel and 20% EGR mass flow rate, the NO_X emissions reduced to 19.81% with only a slight increase in the BTE of 0.77, attributed to the reburning of the unburned hydro-carbons together with the EGR% mass flow rate so helping to complete the combustion of the fuel. It is important to note that during the study the exhaust gas temperature for all the study fuels (biodiesel and the blends)

was found to be lower than when conventional diesel alone was used.

Manieniyan and Sivaprakasam [1] in their study "Experimental Analysis of Exhaust Gas Recirculation on Diesel Engines Operating with Biodiesel" used a four stroke, water cooled, single cylinder direct injection DI engine, rated at 5.2 kW power with a 1500 rpm as the rated speed. The experiment was conducted in two phases. Phase 1 investigated the performance, combustion and emission of diesel fuel and biodiesel blends of B20 where the EGR application was 0 (zero) or not applied. Phase 2 of the experiment used the same equipment and test rig and fuel i.e. B20, but with the EGR application employed. The range of distribution for EGR% mass flow was 5%, 10%, and 20%, while the load distribution was 20%, 40%, 60%, 80% and 100%. The emission gases were measured using a gas analyzer and the density of the smoke was measured using a smoke meter. Finally, the exhaust gas temperatures were measured using a thermocouple. Other combustion parameters like cylinder pressure, heat release and cycle to cycle variations were measured using a combustion analyzer.

The tests and study found that the BSFC for the test fuel without EGR under engine full load was seen to be 0.2779 kg/KW-hr and 0.2794 kg/kW-hr for biodiesel. The value of the BSFC and the engine at full load and EGR% mass flow rate at 5%, 10%, 15% and 20%, were 0.2853 kg/kW-hr, 0.2796 kg/kW-hr, 0.2832 kg/kW-hr and 0.3050 kg/kW-hr respectively, whereas for the higher EGR% mass flow rate of 20% the BSFC increased for both diesel and biodiesel. This was attributed to the high calorific values, higher viscosity density and boiling point.

The BTE was found to be comparable for diesel and biodiesel with or without EGR. At full load the BTE returned a figure of 29.006% for a test with EGR and 29.4933% without EGR application in full load. At 20% EGR BTE was reduced by 1.5% in diesel and biodiesel and more exhaust gases were produced, predominantly due to the dilution effect of EGR resulting in a drop in efficiency.

The variations between the hydrocarbons and the brake power results and conclusions indicate that with an increase in EGR mass flow rate levels, the HC emissions also increased only for the biodiesel, attributed to the presence of high oxygen content in most biodiesels, thus compensating for the lack of oxygen to facilitate complete combustion thus the increase in BTE. The values for the NO_X during the study were found to be 736 ppm for diesel fuel running without EGR in full load environment and 796 ppm for the biodiesel at full load without EGR. However, with the application of EGR it was noticed that the levels of NO_X reduced to 157 ppm for diesel and 158 ppm for the biodiesel respectively, but a reduction in BTE was established with large increments in smoke density.

Carbon monoxide (CO) in relation to diesel and biodiesel with various levels of EGR% mass flow rate and load condition was noted to vary from 0.14% (by volume) for the diesel and 0.18%

(by volume) for the biodiesel all under full engine load conditions. Thus, they concluded that as the EGR % mass flow rate increases so do the CO emissions, caused primarily by the lack of oxygen and poor mixing during the combustion process.

The smoke density was generally found to be lower or decreased for biodiesel as compared to diesel fuel and this was observed for all engine loads. As the EGR % mass flow rate is increased there is an observed increase in the smoke density. This is explained by the fact that EGR affects the oxygen availability leading to incomplete combustion and the formation of (PM.

The EGT was observed to increase with the increase in the load, especially noticeable for biodiesel compared to diesels at all engine applicable loads and conditions during the study. This increase in temperature was attributed to higher oxygen content in all biodiesel fuels particularly those used in the study. This study finding was identical to Hawi, Kiplimo and Ndiritu [9].

The cylinder pressure at full engine loads and EGR% at 0 (zero) was observed to be comparable to biodiesel, arising from the fact that there was a good mixing from the biodiesel mixture under high load, because EGR gases act like heat absorbing agents due to the presence of CO_2 and H_2O caused by disassociation in the chemical effects of EGR application. Thus the combustion analysis showing or revealing significant heat release rates, with or without the application of EGR% mass flow rate.

Abu-Jrai et al. [10] in their study "Performance, Combustion and Emissions a Diesel Engine Operated with Reformed EGR Comparison of Diesel and Gas to Liquid (GTL) Fueling," used a Lister-Pitter TR1 engine, single cylinder, direct injection, air cooled, and naturally aspirated. It was connected to an electric dynamometer with a motor and load cell. The crank shaft position timing was set at 22° CA (BTDC) in all the tests. The EGR% mass flow rate was set manually using a gate valve while EGR levels were determined by volume. The rig also included other instruments to do measurements for oil and air inlet/exhaust manifold temperature respectively.

Data was acquired using software for measurement of: peak cylinder pressure, IMEP (indicated mean effective pressure), COV (percentage coefficient variation) of IMEP, average values of COV of peak cylinder pressures, ROHR (rate of heat release). The AVL gas analyzer was used in the measurement of NO_X, CO and CO_2 gases. The test fuels used for the test were ULSD (ultra-low sulphur diesel) and the ultra-clean GTL (gas to liquid) which was obtained through a LTFT (low temperature Fischer-Trosph) process, which is a synthetic fuel.

The experiment was conducted at two engine speeds of 1200 rpm and 1500 rpm and two loads only tested at 25% load and 50% (medium load), while the EGR ratios chosen were classified into two; standard EGR and REGR (reformed exhaust recirculation) both using ratios of 0%, 10%, 20%, and 30%. The REGR was a simulation based on H_2 gas and CO gas

in the ratios of 25% = H$_2$(gas) - 0% CO(gas)-75%EGR while in the second scenario 15% = H$_2$(gas)-10%CO(gas)-75% EGR.

The conclusions from this study were as follows: at low engine loads the GTL fuel was found to bring or return high BTE values as compared to the BTE efficiency values the ULSD returned, but when REGR was introduced it was observed that GTL had a higher fuel replacement than ULSD, thus showing an improvement in efficiency and reduced emissions. BTE was also found to be load dependent, i.e. at low engine loads efficiency decreased with increasing REGR [10]. However, when the loads were high it was observed that the high flame temperatures and velocity of hydrogen gas and the rapid expansion increased the BTE as the REGR was increased.

On rate of heat release, the high octane number of GTL resulted in less pronounced premixed combustion, leading to lower heat release rate and in-cylinder pressure, leading to reduction in NO$_X$ emission where GTL fuels were employed, unlike when ULSD fuel was used in the experiment. Whereas the combustion pattern was affected by the REGR, the use of the 30% REGR brought efficient gas fuel combustibility and an increase in-cylinder pressure together with the ROHR [10]. At low engine loads the authors noted that an increase of REGR resulted in a decrease of both NO$_X$ and smoke emissions. However, at higher engine loads higher REGR resulted in a decrease in smoke emission but compromised NO$_X$ emission.

Lastly, when the combination was used of both REGR and GTL fuel, the results showed a marked improvement in the reduction of emissions The 30% REGR when combined with the GTL fuel produced a 60% decrease in smoke emission, while the NO$_X$ emission showed a 75% decrease as compared to when ULSD fuel was used at 0% REGR and low engine loads [10].

Shahadat, Nabi, Akhter and Tushar [11] in their study on "Combined Effect of EGR and Inlet Air Pre-Heating on Engine Performance in Diesel Engines" used a four stroke diesel engine S195, single engine, with a maximum speed of 2000 rpm, direct injection, water cooled and naturally aspirated. The fuel used for this study was conventional diesel, with a density of 0.80g/cc@25°C. Other modifications to suit the experiment were made to provide measurement readings, particularly the preheating mechanism for inlet intake air. To maximize the heat loss, the inlet intake air passage was insulated by plaster.

The overall heat transfer between the two exchange mediums (the inlet intake air and the exhaust gas) was calculated using the equation from [12]. The experiment was conducted in two phases or two parts; Phase 1 was conducted without the inlet air preheating and without EGR% mass flow rate application, while Phase 2 involved preheating the inlet intake air charge and EGR% application. The gas emission measurements were made using a gas analyzer to obtain values for comparative analysis.

After running the experiment, the following results and conclusions were observed. The emission of NO$_X$ from the test engine increased as the engine speed increased in both the phases of the experiment. i.e. when the inlet intake air preheating was applied without EGR application and vice versa, a factor they attributed to the decrease in the duration of ignition delay and combustion chamber premixing time of the inlet intake charge. In addition, they observed that the application of EGR reduced the in-cylinder combustion peak temperature due to the higher CO$_2$ heat specific ratio. This result is identical to results in other studies, particularly those where the EGR% rate application was limited to between 20% to 25%, this being identical to the study done by [13].

However, on the relation between the effects of EGR on inlet intake air preheating and NO$_X$ emissions, they observed that with an increasing in the inlet intake air temperature, the emissions of NO$_X$ and CO indicated a decrease. This factor was linked to the ignition delay and premixed combustion mixture, two factors whose time is shortened by the introduction of EGR. There are other identical studies whose findings are consistent with this study [14].

Lastly, the authors wanted to show the relationship between the effects of adiabatic flame temperature on the emission of NO$_X$ particularly when conventional diesel fuel is applied or used. When conventional diesel was used the authors observed that as the equivalence ratio increased (hitting a maximum ratio of 0.9), the adiabatic flame temperature also increased. However, the equivalence ratio began to decrease as it hit the maximum value, though at this point the NO$_X$ emission continued to increase and vice versa.

Regarding CO emissions, the application of inlet intake air charge preheating at a controlled temperature of 55°C and without application of EGR% brought about a lowering of CO emissions to almost a minimum as explained by the fact that inlet intake air preheating provides CO oxidation. However, when the EGR mass flow rate of 25% was applied it was observed that the CO emissions increased greatly. This concurs with the findings of a study conducted by Fathi, Saray and Checkel [15], where it was concluded that the application of EGR does not have similar effects on the different species of emission characteristics.

The BTE during this study was found to be affected by the inlet intake air preheating in combination with the application of 25% EGR mass flow rate but at varying engine speeds and constant load. The authors found that the BTE was higher for the preheated inlet intake air than when compared to when preheating is not applied. This was seen to be due to higher amounts of heat energy that were being transferred from the exhaust gas to the inlet intake air, thus providing better burning of the fuel in the combustion chamber, hence minimizing the overall heat loss by the system. In addition, they also observed that the BTE increased with the increase in engine speed both at low and intermediate speeds, but at higher speeds they noted a decrease in the BTE, a factor which they attributed to shorter mixing time of the air fuel that is normally associated with higher engine speeds leading to poor or low fuel efficiency.

Abdelaal and Hegab [16] in "Combustion and Emission Characteristics of a Natural Gas Fueled Diesel Engine with EGR," used a Ricardo E-6 engine modified to accommodate gaseous fuel and normal or conventional diesel use. The engine was single cylinder, indirect injection, four stroke, water cooled, with a maximum rated power of 9 kW, and a maximum rated speed of 3000 rpm. Modifications were made to testing and gathering of data. Following testing and experimentation it was observed that the introduction of CO_2, through the intake manifold resulted in a decrease in NO_X emissions, but showed a relative increase in unburned hydrocarbons.

The disassociation of CO_2 and its introduction into the intake charge is attributed to the reduction in NO_X. This is a chemical effect that is associated with the use of the EGR application. Another observation the authors' made was that by continuing to increase the inlet charge temperature there was an increase in the unburned hydrocarbons emissions mainly due to a decrease in ignition delay in relation to the rise in the intake charge temperature. Increasing the intake charge temperature resulted in improved combustion characteristics due mainly to the drop in the ignition delay, thus improving and increasing the BTE and BHP (brake horse power) power parameters and a decreasing the unburned HC emissions and carbon monoxide (CO). It is imperative to note at this point that the increase in intake charge temperature during this experiment resulted in an increase in the NO_X emission i.e. dual fuels reduce NO_X emissions during low engine loads only. The admission of diluents was shown to produce poor combustion characteristics if they were increased, thereby causing reduction in the NO_X due to the lowering of the cyclic cycle temperature and the oxygen concentration due to the dilution of the intake charge by introduction of the EGR gases.

Fathi et al. [15] in "The Influence of Exhaust Gas Recirculation on Combustion and Emissions of N-Heptane and Natural Gas Fuelled Homogeneous Charge Compression Ignition (HCCI)," conducted a study at the University of Alberta fuel and combustion emission research facility. They used a Waukesha CFR single cylinder research engine, water cooled, coupled to a dynamometer. The speed was maintained at 800 rpm at wide throttle. A temperature controlled air preheating system was installed using a 2.4 kW heater motor. Also included were two port fuel injectors controlled electronically via an AFS sparrow module. The EGR rate was manually controlled. The fuels used for this experiment were n-heptane and natural gas either as blends or used individually.

During their study the authors observed that the recycled gases from the exhaust contained tri-atomic molecules of H_2O and CO_2 species which increase the specific heat capacity of the combustion mixture and reduce the overall specific heat ratio. This makes the mixture act like a thermal heat absorbing sink, thereby decreasing the after-compression temperature. The other observation they made with EGR application is a reduction in peak in-cylinder charge temperature due to delayed auto ignition of the combustion charge.

Applying EGR they noticed affected the peak in-cylinder pressure by reducing it. This is explained by the fact that the recycled exhaust gases in the form of EGR act as a thermal sink as earlier mentioned above, thus reducing the charge temperature during combustion. The pressure rise during the combustion becomes reduced which is a means of avoiding engine knock.

Heat transfer was noticed to decrease with the application of EGR, since the heat transfer coefficient is proportional to pressure and inversely proportional to temperature [15]. Therefore, the heat transfer coefficient did not vary much with the application of EGR, since by increasing EGR% mass flow rate both the pressure and temperature decreased.

The gross heat release rate (HRR) was seen to be affected by the application of EGR flow rate because recycled exhaust gases replace or substitute part of the fresh air intake charge, thus affecting the in-cylinder equivalence ratio and the combustion process at large. EGR rate application can cause delay in SOC (start of combustion) hence prolonging the burning or exposing the elements of combustion to more time to combust, which in return leads to increase in the IMEP limit and the operating range of the EGR rate.

The effects of EGR on combustion timing demonstrated that since EGR increases specific heat ratio of the combustion elements, the in-cylinder inlet charge temperature decreases thus delaying ignition as mentioned in the discussion above, thereby introducing retardation of SOC and increasing the combustion duration. Defined as the indicated work output per unit of engine swept volume, the IMEP was seen to be less affected by the application of the EGR rate which is identical with other studies conducted in this area [17].

Regarding the indicated specific fuel consumption (ISFC) the authors found that the retardation of the start of combustion (SOC) reduced ISFC, whereas when the EGR rate was applied it produced the opposite effect i.e. increased the ISFC. This is explained by the fact that introduction of EGR rate removed the availability of oxygen thus causing incomplete combustion in the combustion process thereby decreasing efficiency.

The formation of NO_X emissions as observed during this study with EGR application, was due to the nature of the combustion in homogeneous charge compression ignition (HCCI) engines which show a fast combustion. The formation of NO_X is limited due to the low charge temperature of the air mass flow rate. This is explained by two factors: applying EGR rate flow depresses peak in-cylinder temperature thus reducing NO_X emissions formation, and secondly the application of EGR rate depresses the availability of O_2 concentration in the combustion chamber due to the EGR rate dilution effect. However, an increase of EGR rate was noticed to increase HC and CO emissions as the EGR rate continued to increase. The explanation provided by the authors was the unavailability of O_2 and reduced inlet intake charge temperature which resulted in incomplete combustion due to poor mixing.

Hawi et al. [9] in the "Effects of EGR on Performance and Emission Characteristics of a Diesel Piloted Biogas Engine" used a single cylinder, four stroke engine, water cooled, naturally aspirated constant speed CI engine, coupled to a hydraulic dynamometer for load application. Modifications were made to the engine to enable it to run on dual fuel with conventional diesel as a pilot fuel and biogas as the main fuel. A gas analyzer was used, with a digital portable laser tachometer for engine speed. Thermocouples were used to do temperature readings.

After conducting tests and the experiment they came out with the following findings on BSFC. Through the variation of EGR rates from 0% to 100% of engine load, the BSFC was found to decrease as the rate of EGR% rate was increased, obtaining a maximum value when the EGR rate was 20%. The decrease in the BSFC with the application of the EGR rate was due to an increase in the inlet intake charge temperature, thus increasing the rate of fuel consumption.

On the brake power (BP) they observed that the application of the EGR did not produce any significant effect on the total output power of the engine with the application rate of 30% EGR, while the BTE was observed to increase with the increase in the engine load for all operating conditions. However, it should be mentioned that the BTE showed some insignificant increase before the EGR rate passed the 20% mark, attributed to the returning of the hydrocarbons entering the combustion chamber for re-combustion together with EGR, and the increase of inlet intake charge temperature as a result of EGR rate application, which causes an increase in the rate of combustion. This is identical to the findings of Venkateswarlu, Murthy and Subbarao [18].

Regarding EGT, the authors concluded that it increases with engine load for all the operating conditions, which they attributed to the increase in input energy at high engine loads, as fuel consumption increases to accommodate high load and speed. Another observation they made during this study was that EGT temperature reduced with the increase of EGR% rate flow, which they attributed to the unavailability of O_2 when EGR is applied, leading to lowered combustion temperatures. This is identical to other studies conducted [19].

CO emissions variations in relation to the increase in EGR% rate was noted as increasing with the increase in the percentage of EGR, but was seen to significantly reduce as the EGR and engine load increased to 75% and 100%. This factor is explained by the lack of O_2 during combustion due to the dilution effect of EGR. On the other hand, HC emissions are noticed to increase in all the engine loads conditions as the EGR rate is increased, explained by the fact that the induced charge (intake air + EGR rate) has a higher CO_2 content when compared to fresh air only. However, the increased load across the entire engine load shows a decrease in HC emissions particularly when the dual fuel is employed for operation. This study finding was identical to those of Mahla, Das and Babu, [20].

Finally, on the CO emission and how they interacted with the EGR rate, the authors noted an increase of the CO emissions with an increase in the engine load. However, when a n EGR% rate of 10% to 30% was applied, there was a minimal decrease associated with the substitution of fresh charge with the elements of the exhaust gas which decreased the CO_2 emissions.

Hountalas, Mavropoulos and Binder [19] in the "Effect of Exhaust Gas Recirculation (EGR) Temperature for Various EGR Rates on Heavy Duty DI Diesel Engine Performance and Emissions." conducted their study using a heavy duty DI diesel, single cylinder engine, with high compression peak pressure. To improve the BSFC advanced timing was employed, while for NO_X emissions control the EGR was constantly cooled throughout the experiment. The test engine condition was maintained at full load with variations of engine speed employed, with the theoretical study on 3D multi zone model modified to suit the experimental set up under study to include the effects of EGR% and temperature and for calculation analysis. The boost pressure and injection pressure were kept constant at 280 BAR and 140°C for the EGR gas.

Figure 2 shows the comparison between the calculated and experimental cylinder pressure for EGR% rates at 1130 rpm, 100% load and -9 ATDC injection timing [19].
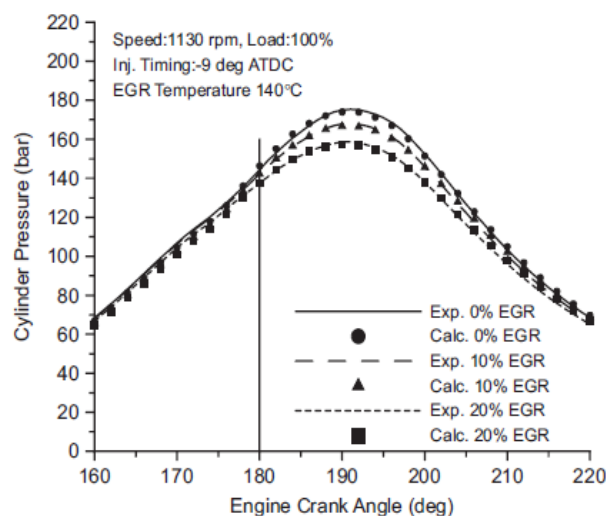
Figure 2: Showing the calculated and experimental cylinder pressure in relation to different EGR% rates.

Source: Hountalas, Mavropoulos and Binder [19]

As can be seen from Figure 2, simulated and theoretical measured values results show similarities and coincidences for the values of the EGR rate examined [19]. The study indicates a reduction in-cylinder pressure during combustion and expansion of the mixture in the combustion chamber. This increase in the SHC as occasioned by the presence of exhaust gas recirculation reduced the availability of O_2 thereby affecting the combustion process rate and the disassociation of

CO_2 and H_2O, further reducing the peak cylinder pressure values as EGR% rate mass flow increased. During part engine load different results were obtained, as the availability of O_2 was higher compared to when the engine was operated at full load. As the EGR inlet intake temperature increases with the EGR% rate mass flow this leads to delay in SOC leading to increased peak cylinder pressure as EGR % rate mass flow is increasing. These results are identical to those of [9], [19], [21].

The results indicated a negative effect of the EGR% rate mass flow on the BTE, especially at low engine speeds and full load, where an increase in EGR% rate mass flow showed a significant lineal decrease in BTE % of 5.5% @ 15% EGR. In relation to emissions of NO_X and soot emissions, the study found that the theoretical and measured values of NO_X and soot at full engine load and varying EGR% rates showed that as the rate of EGR mass flow increases it reduces the NO_X emissions linearly but increases the soot emissions significantly and exponentially [19], with the effects becoming more critical at low engine speeds.

The effects of EGR rate flow temperature on the engine performance and emission was investigated by Moiz [22]. The tests done for each case were 5% EGR, 10% EGR, and 15% EGR and the temperatures examined were from 90°C to 240°C calibrated in steps of 50°C. However, it is imperative to note here that this temperature range is a representative range value because the cooling media is the engine coolant. As the test results show it is evident that the increase in EGR% rate of mass flow at constant boost pressure led to a decrease in the intake air mass flow rate sucked or induced per cycle, leading to a drop in the AFR (volumetric efficiency). This type of result should be expected especially when the EGR gas temperatures are increased with the increase in EGR%, thus forming a lineal relationship between the AFR and EGR gas temperature. In all the examined test cases the authors observed that any increase on the EGR% rate mass flow temperature resulted in a decrease in AFR, but was more pronounced during low engine speeds i.e. at full loads thermal throttling becomes significant and increases with increase in EGR% rate mass flow gas temperature [19].

The effects of high EGR% gas temperature on the peak combustion pressure was noted by the authors as a reduction on the peak combustion pressure, which was noted to be significant at very high EGR% rates where one should note that the AFR was minimum. However, it should be emphasized that the use of the high EGR% rate gas temperature reduces O_2 availability thereby reducing the combustion rate or SOC. It is also important to remember or mention that the effect on ignition delay or retardation is negligible due to the high boost pressure and high charge temperature.

Yasin et al. [23] in their "Study of a Diesel Engine Performance with Exhaust Gas Recirculation (EGR) System Fuelled with Palm Biodiesel" intended to study the effects of EGR on the parameters of SFC, EGT, and the emissions of NO_X, CO, CO_2 and UHC both in experimental and simulated study situations.

The study was conducted using a four-cylinder diesel engine with modified EGR application, naturally aspirated, air cooled, and with a maximum power of 64.9 kW @ 4500 rpm. The engine was coupled to an eddy current ECB dynamometer that was controlled by a Dynaelec load controller.

The result on the effect of EGR on the performance and combustion characteristics of the palm biodiesel and mineral diesel under normal modes, EGR application and at full load condition, was observed. The test fuel, which in this case was palm biodiesel, produced higher values of BSFC when the exhaust gas temperature was low compared to when the EGT gas temperature was high. This increase in BSFC was attributed to the power loss or drop in the efficiency of the engine and the lower heat release rate values that are associated with palm biodiesel, in addition to the unavailability of O_2 in the inlet intake air mass flow with the application of EGR [23], which mixes the inlet intake air with the EGR gases. The study further showed palm biodiesel increased the exhaust gas temperatures by 5.6% above the exhaust temperature values that were produced when mineral diesel was used [23]. This is attributed to the presence of greater O2 content in the palm biodiesel leading to a high combustion efficiency and high in-cylinder temperature, being identical to the findings of Badruddin et al. [24]. The experimental engine set up test rig is shown in Figure 3.
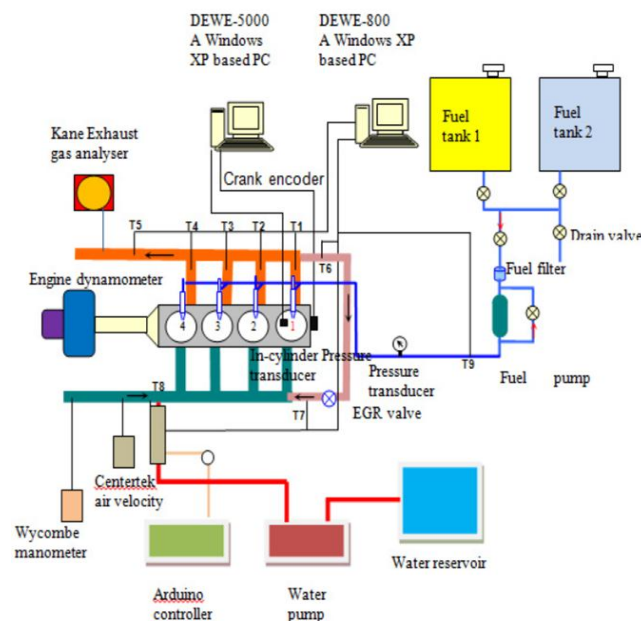
Figure 3: Showing the experimental set-up rig.

Source: Yasin et al. [23]

The application of EGR% mass flow rate mode on the palm biodiesel and mineral diesel fuels during the study lead to a noted decrease in the exhaust gas temperatures of 2.8% when palm biodiesel was used and a 1.6% decrease when mineral diesel was used [23]. This finding is similar to Saravanan [25] and therefore confirms that most biodiesel fuels produce lower

EGT temperature values at varied engine speeds and constant engine loads.This conclusion is attributed to the fact that the exhaust gases as mentioned earlier mix with the inlet intake fresh charge which dilutes the methyl ester rich oxygen content in the combustion, thereby improving combustion completion.

The palm biodiesel and mineral diesel emission characteristics compared to normal modes under EGR application and full engine load conditions at constant speed of 2500 rpm showed an increase in NO_X emissions, a factor that is linked to the increase in the in-cylinder temperature and the presence of more O_2 content within the natural chemical composition of the palm biodiesel fuel used during the study. The palm biodiesel thus seemed to contribute to an increase in the emissions of NO_X compared to the mineral diesel, because of the factor already mentioned regarding the oxygen content which causes high oxidation of the combustion mixture which leads to highly flammable rapid combustion thus increasing the exhaust gas temperatures.

Although the results obtained showed that palm biodiesel produced 4.7% higher NO_X emissions compared to the mineral diesel with EGR mass flow rate under normal engine conditions and loads, it should be noted that low NO_X emission of 5.4% was achieved when mineral diesel was used as compared to 22% when palm biodiesel was used. This is explained by the fact that an increase in total heat capacity (specific heat capacity) of the exhaust gases and reduction in in-cylinder peak temperature tends to reduce the NO_X emissions [23], these results being identical to the findings of Abdelaal and Hegab [16].

The carbon emissions for the test fuels used with application of EGR showed a decrease in carbon emissions for the palm biodiesel compared to mineral diesel. This is explained by the complete burning of the mixture as the palm biodiesel contains more O_2 content compared to mineral diesel, which provides the oxidation of CO to CO_2 which is an inert gas [23]. However, from the result obtained it is evident that there is an increase in CO emission of 9.7% when palm biodiesel was employed compared to a 2.45% increase using mineral diesel especially with the application of EGR, at full engine load i.e. both the fuels showed an affinity to produce CO emissions when EGR is applied under all engine operating conditions and load.

Rao [26] in the "Effect of EGR on Diesel Engine Performance and Exhaust Emission Running with Cotton Seed Biodiesel." used a single engine, four stroke, water cooled engine with cotton seed biodiesel (CSBD) and PBD (petroleum based diesel) blends as test fuels, where 0% PBD = CSBD10, 20%PBD = CSBD20 and 30%PBD = CSBD30. The EGR% rate of mass flow was limited to 0% to 20% in steps of 5%. The engine speed was kept constant at 1500 rpm. The set up was to examine the following parameters in relation to the effects of EGR: BSFC, BTE, EGT and the emission characteristics of NO_X, HC and CO. The engine was modified to allow experimental work to be done and for data to be obtained from the digital control panel. The gases were measured using an Indus gas analyzer. All tests were conducted under full engine load conditions and speed. The result from this study indicate that the BSFC is shown to be slightly independent at lower EGR rates, but increases as the EGR% rates increase to 15%. This can be explained from the fact that less oxygen means a rich mixture formation in the combustion chamber.

The results showed that BTE remains equally unaffected when low EGR rates and full engine loads were applied. However, BTE decreased with an increase in EGR above 15% in the combustion chamber, due to the displacement and replacement of the fresh air charge by the EGT gases. The EGT partly operated with cooled EGR% mass flow rate was observed to lower the exhaust gas temperatures compared to EGT at normal engine operating conditions without EGR. i.e. EGT decreased with an increase in EGR rate. This is informed by two factors, namely, unavailability of oxygen and the high specific heat ratio of the intake air mixture [26]. It is imperative to note here that a decrease in exhaust gas temperature is noticed irrespective of the continuous increase in EGR% rate even above the value of 15% EGR.

Regarding emission characteristics, the authors noticed a significant decrease in NO_X for all the test fuels used due to a reduction in O_2 and a decrease in flame temperature within the combustion chamber [26]. The hydrocarbon emissions showed an increase with the application of EGR% rate for all the test fuels used, especially when the EGR% was above 15%. This is explained by the incomplete combustion occasioned by the unavailability of O_2 resulting in poor oxidation of the combustion mixture causing incomplete combustion. The CO emissions were noted to increase with increase in EGR% rate for all the fuels used during the experimental study, mainly due to the aforementioned O_2 phenomenon.

Asad and Zheng [27] in their study of "Exhaust Gas Recirculation for Advanced Diesel Combustion Cycles" Used a four-cylinder Ford common rail diesel engine coupled to an eddy current dynamometer. The engine was operated in two modes. The first mode was a single cylinder mode (3 cyl to 1 cyl) where the 3 cylinders are operated in a conventional mode, with the #1 cylinder designated for research with independent controls of the parameters of intake pressure, exhaust back pressure and fuel injection. The second mode involved all the four cylinders with the engine running using a turbo charger, air fuel and EGR with no major system alterations. The exhaust gas analyzer was used to measure NO_X, THC, CO, CO_2 and O_2 concentration, while the intake CO_2 and O_2 were measured in the intake manifold using a different intake analyzer. The soot concentration was measured using an AVL smoke meter, while all the cylinder pressure data was processed with a 0.1° angle resolution using a pressure transducer mounted on cylinder #1 and connected to a data acquisition system.

After testing the models and how they interacted with the EGR% application, the following results and conclusions were reached. The impact of intake and in-cylinder charge composition was characterized with in-cylinder excess air ratio

for the recycled O_2 with the EGR as a function of the EGR displacement [27]. The effects of EGR on intake pressure and engine load showed that the dilution of the intake charge with application of EGR could correctly be predicted through the intake oxygen concentration as compared to EGR fraction, as it was shown to lack additional information to show the effectiveness of the EGR ratio in relation to displacement [28]. It is imperative to note at this point about the EGR% ratio: there are two methods which Asad and Zheng, [27] propose in this study which are presently widely used to measure and quantify the value of EGR rate, the gas concentration based method and the mass based method. So far there has not been a standard method of defining EGR rate. The two equations for defining the EGR% rate flow as proposed by [27] are:

$$r_{EGR} \approx \frac{[CO_2]int - [CO_2]amb}{[CO_2]exh - [CO_2]amb} \approx \frac{[CO_2]int}{[CO_2]exh} \qquad \text{equation 1}$$

$$r_{EGR} = \frac{\dot{m}_{EGR}}{\dot{m}_{air} + \dot{m}_f + \dot{m}_{EGR}} \qquad \text{equation 2}$$

But since the fuel flow measurement is less than the mass air flow [27], equation 2 is modified to define the EGR ratio rate as shown in equation 3:

$$r_{EGR} = \frac{\dot{m}_{EGR}}{\dot{m}_{int}} = 1 - \frac{\dot{m}_{air}}{\dot{m}_{int}} \qquad \text{equation 3}$$

where $rEGR$ is the EGR fraction mass rate of the recirculated gases, $\dot{m}_{EGR}$ is the flow rate of the mass of EGR gas, $\dot{m}_{air}$ is the gas flow rate of intake air mass, $\dot{m}_f$ is the flow rate of the injected fuel mass, $[CO_2]amb$ is the carbon dioxide gas in the ambient air, $[CO_2]int$ is the carbon dioxide gas in the inlet intake air, $CO_2]exh$ is the carbon dioxide gas in the exhaust system.

During low engine loads and low EGR it was noticed that the effectiveness of EGR decreased as EGR gases displaced small amounts of fresh air in the intake system due to the fact that EGR gases contain O_2 and N_2 elements and vice versa i.e. increasing the intake reduced the intake charge dilution for the same EGR ratio [27], while increase in EGR (intake dilution) produced a leaner air fuel ratio with increased premixed combustion, which caused reduced soot emission, which is identical to the findings of Aoyagi, Osada, Misawa, Goto, & Ishii [29] and improved on combustion efficiency [28]. It should be emphasized here that O_2 in the EGR is both a function of the engine load and EGR ratio.

In mentioning and discussing the combustion models, it should suffice to say that the development of alternative fuels becomes of paramount importance. There are several methods that have been proposed for processing the alternative fuels otherwise called biodiesels, the commonly used ones being transesterification, hydrogenation, pyrolysis (used in plastics) and dilution. The use of alternative fuel for emission control has been increasing, particularly with the use of the EGR control technique to control and reduce NO_X, HC, CO and soot emissions. A number of authors have carried out research in

this area and this review will present some of these studies and their current position in so far as this area is concerned.

Mani, Nagarajan and Sampath [30] in "An Experimental Investigation on a DI Diesel Engine Using Waste Plastic Oil with Exhaust Gas Recirculation" showed that plastic oil produced the most NO_X emissions but showed reduced NO_X emissions with increasing EGR of 20% onwards. There was no noticeable change in the smoke, CO and HC levels of emissions, thus reaching a conclusion that with the application of EGR% rate levels plastic oil can be used as an alternative to biodiesel fuel.

Xu, Gui and Deng [31] in "Fuel injection and EGR control strategy on smooth switching of CI/HCCI mode in a diesel engine" conducted an experiment by variation of the cam phase and tapped EGR gases as a heating or vaporizing mechanism of the fuel and to harmonize the mixture charge, while using the fuel injection to administer HCCI in an electronically controlled fuel injector. They used HCCI combustion modelling to study the effects of a premixed ratio in relation to performance and emission characteristics, when different EGR % rates are applied. They observed a 78% drop in NO_X and lowered smoke and soot emissions of 40%, when premixed ratio of 80% and 30% EGR respectively were applied. Increased PR lead to increase in IMEP and BSFC, but fared poorly on the HC and CO emissions.

Haber and Wang [32] in "A Robust Control Approach on Diesel Engines with Dual-Loop Exhaust Gas Recirculation Systems," discuss a number of control strategies to be employed in mitigating the effects of EGR and emission. One of the methods suggested is EGR. The authors point out that the application of EGR alters or affects the normal combustion process in several ways. Firstly, it alters the physical properties of the charge mixture; secondly it alters the air fuel ratio (A/F); and thirdly it alters the start of ignition and finally alters the heat release pattern [32]. Other effects they noted as responsible for NO_X reduction were the dilution effect, the chemical effect, and the thermal effect. They also noted that the application of EGR resulted in modification of both the composition and physical conditions of the inlet charge (by modification of composition they mean addition of CO_2 and H_2O, and by modification of physical conditions they mean temperature density) [32]. By replacing the intake air charge using EGR they observed that it decreases the air fuel ratio leading to a shortened delay in ignition. Other effects they noted in their study is that reduced oxygen availability due to the admission of EGR also explains the phenomenon of delayed ignition, which they observed to be due to increased mixing time between the amount of injected fuel and fresh oxygen [32]. In conclusion they argue that as a control strategy EGR cannot be used alone because of the increased soot emissions, fuel penalties, degradation of the combustion quality, increased piston cylinder wearing, deteriorating efficiency, operational instability, and higher EGR temperature accounting for low fuel efficiency [32].

Lehto, Elonheimo, Hakkinen, Sarjovaara and Larmi [33] in their study "Emission Reduction using Hydro Treated Vegetable Oil (HVO) with Miller Timing and EGR in Diesel Combustion." noted a marked reduction in the emissions of NO_X and smoke compared to conventional diesel. EN590, a HVO fuel blend, can allow the use of higher EGR% rates without compromising the PM, HC and smoke emissions but with exponential reduction in the NO_X emissions.

Chen, Liu, Wu and Lee [34] in "Effects of Port Fuel Injection (PFI) Of N-Butanol and EGR On Combustion and Emissions of a Direct Injection Diesel Engine," studied the effects of PFI on n-butanol and application of EGR and how they influence emission and combustion characteristics in a diesel engine. In their study the engine was equipped with independent inlet and outlet systems. The researchers varied the EGR% rate which they divided into three sections 0%, 15% and 45%, and the premixed fuel of the n-butanol was divided into four premixed ratios of 0%, 20%, 38% and 47% by volume.

They observed and noted that as the rate of EGR% increased to 45% there was a significant decrease of 97% of the NO_X emissions though there was an exponential increase in the soot emissions and the SOFs. However, when they combined the use of the PFI and the n-butanol of 47% while maintaining the EGR% rate at 45%, the emissions of NO_x and those of soot were drastically reduced by 88% and 17% respectively, thereby addressing the traditional basic fundamental problem of the NO_X – soot trade-off.

Zhao, Wang, Li, Lei and Liu [35] in their study on "Combustion and Emission Characteristics of a DME (Dimethyl Ether)-Diesel Dual Fuel Premixed Charge Compression Ignition Engine with EGR (Exhaust Gas Recirculation)" studied the effects of external EGR and di-methyl ether (DME) on the premixed ratio on the performance and emission characteristics of a two cylinder naturally aspirated diesel engine. They varied EGR% from 0% to 27% while they kept the premixed ratio at between 0% and 30%.

Their results indicated that an increase in EGR% mass flow reduced NO_X emissions, but increased CO_2 and HC emissions considerably. However, a very good result was obtained with higher PR% and higher EGR% rate especially in NO_X and smoke emissions.

Singh and Agarwal [8] in "Combustion Characteristics of Diesel HCCI Engine: An Experimental Investigation Using External Mixture Formation Technique," used a twin piston DI diesel engine to conduct a study by the modification of one cylinder to use HCCI premixed fuel and the other one using conventional diesel. During the study they varied their mixture concentration from $\lambda = 4.96$ (as the lean mixture level) or the misfiring limit and $\lambda = 2.56$ (considered as the rich mixture level) or the knock limit. The EGR applied was at the rate 20%. The results observed indicated an increased combustion efficiency, when the value of $\lambda \leq 3.70$ which is medium range engine loads, but when the engine load was increased to high levels it was observed that the values of λ was recorded was $\lambda \leq 3.0$ thereby producing knock and a very rough combustion experience.

CONCLUSION

It can be safely concluded that the use of the EGR as a technique for controlling emissions of NO_X, CO, CO_2, HC and SOF in conjunction with other techniques discussed in this review when implemented will adequately address the underlying issues of the effects of EGR on diesel engine performance parameters and reduction in emissions as was seen during the studies that were reviewed here.

However, more needs to be done to bridge the gap and disconnect between research and industry. For example, EGR cooling is not widely used in stationery engine systems and in marine applications and in industrial production where carbon emissions are more pronounced, but is relegated and left to industry handlers and policy makers to decide, something they might not be able to do.

EGR cooling will allow us to retain the benefits of low NO_X emissions but without compromising engine efficiency. EGR cooling is necessary as it reduces soot and soluble organic fraction (SOF) emissions, for example when used with other techniques like VGT technology, which proposes to recirculate all exhaust gases together with the intake mixture thus increasing the mixture heat capacity but leading to lowered combustion temperature and consequently lower NO_X emissions; due to O_2 concentration levels being maintained, oxidation of the soot emissions becomes insignificant.

During the review it was observed and noted, based on the studies that have been done, that the preheating of the inlet air reduced CO emissions by the introduction of EGR into the system, though it is observed that CO emissions increased linearly as the rate of EGR% was being increased; which raises the question of how the two systems can be harmonized to achieve low carbon emissions without compromising engine performance and emission control systems. From the combustion control strategies discussed, the question arises regarding what implementation strategies can be employed to improve combustion characteristics of the various fuels available, particularly the biodiesel fuels that have been developed, especially their chemical and physical properties, which sometimes lack proper testing and analysis facilities. Biodiesel is still a grey area in terms of industrial commercial development and industry regulators who impose stringent control on its use

ACKNOWLEDGEMENTS

REFERENCES

[1] Manieniyan V, and Sivaprakasam, S., 2013, "Experimental Analysis of Exhaust gas Recirculation on Diesel Engines Operating with Biodiesel," International Journal of Engineering and Technology (IJET), 3(2), pp. 129-134.

[2] Hussain, J., Palaniradja, K., Alagumurthi, N., and Manimaran, R., 2012, "Effect of Exhaust Gas Recirculation (EGR) on Performance and Emission Characteristics of a Three Cylinder Direct Injection Compression Ignition Engine," Alexandria Engineering Journal, 51(4), pp. 241-247.

[3] Agarwal, D., Singh, S. K., and Agarwal, A. K., 2011, "Effect of Exhaust Gas Recirculation (EGR) on Performance, Emissions, Deposits and Durability of a Constant Speed Compression Ignition Engine," Applied Energy, 88(8), pp. 2900-2907.

[4] Abaas, K. I., 2016, "Effect of Exhaust Gas Recirculation (EGR) on the Performance Characteristics of a Direct Injection Multi Cylinders Diesel Engine," Tikrit Journal of Engineering Science (TJES), 23(1), pp. 32-39.

[5] Charola, H. B., Makwana, P. B., and Makwana, R. D., 2016, "Effect of EGR (Exhaust Gas Recirculation) on Performance and Emission Of CI (Compression Ignition) Engine Fuelled with Blend," International Journal on Advances in Engineering Technology and Science, 3(2), pp. 1-5.

[6] Rao K. S., Mutyalu, K. B., and Ramakrishna, A., 2015, Effects of Exhaust Gas Recirculation on the Performance and Emission Characteristics of a Diesel Engine Fueled with Waste Cooking Oil Methyl Ester," ARPN Journal oF Engineering and Applied Sciences, 10(11), pp. 4799-4804.

[7] Kumar, P. S., Antony, F., and Sahoo, P., 2013, "The Performance and NOx Emissions of a IDI Diesel Engine at Distinct EGR Rates Fuelled with JB100, JB80, JB60, JB40, JB20 & Diesel," International Journal of Engineering Science and Technology, 5(3), p. 519.

[8] Singh, A. P., & Agarwal, A. K., 2012, "Combustion Characteristics of Diesel HCCI Engine: An Experimental Investigation Using External Mixture Formation Technique," Applied Energy, 99, pp. 116-125.

[9] Hawi, M., Kiplimo, R., and Ndiritu, H., 2015. "Effect of Exhaust Gas Recirculation on Performance and Emission Characteristics of a Diesel-Piloted Biogas Engine," Smart Grid and Renewable Energy, 6(04), p. 49.

[10] Abu-Jrai, A., Rodríguez-Fernández, J., Tsolakis, A., Megaritis, A., Theinnoi, K., Cracknell, R., and Clark, R., 2009, "Performance, Combustion and Emissions of a Diesel Engine Operated with Reformed EGR. Comparison of Diesel and GTL Fuelling," Fuel, 88(6), pp. 1031-1041.

[11] Shahadat, M., Nabi, M., Akhter, M., and Tushar, M., 2008, "Combined Effect of EGR and Inlet Air Preheating on Engine Performance in Diesel Engine," International Energy Journal, 9(2).

[12] Holman, J., 2002, Heat Transfer, 9th edition, McGraw-Hill, New York.

[13] Jacobs, T., Assanis, D. N., and Filipi, Z. 2003, "The Impact of Exhaust Gas Recirculation on Performance and Emissions of a Heavy-Duty Diesel Engine," SAE Technical Paper 2003-01-1068, https://doi.org/10.4271/2003-01-1068.

[14] Ishiki, K., Oshida, S., Takiguchi, M., and Urabe, M. 2000, "A Study of Abnormal Wear in Power Cylinder of Diesel Engine with EGR-Wear Mechanism of Soot Contaminated in Lubricating Oil," SAE Technical Paper 2000-01-0925, https://doi.org/10.4271/2000-01-0925.

[15] Fathi, M., Saray, R. K., and Checkel, M. D., 2011, "The Influence of Exhaust Gas Recirculation (EGR) on Combustion and Emissions of n-Heptane/Natural Gas Fueled Homogeneous Charge Compression Ignition (HCCI) engines," Applied Energy, 88(12), pp. 4719-4724.

[16] Abdelaal, M., and Hegab, A., 2012, "Combustion and Emission Characteristics of a Natural Gas-Fueled Diesel Engine with EGR," Energy Conversion and Management, 64, pp. 301-312.

[17] Au, M. Y., Girard, J. W., Dibble, R., Flowers, D., Aceves, S. M., Martinez-Frias, J., . . . Maas, U., 2001, "1.9-liter four-cylinder HCCI engine operation with exhaust gas recirculation," SAE Technical Paper 2001-01-1894, https://doi.org/10.4271/2001-01-1894.

[18] Venkateswarlu, K., Murthy, B. S. R., and Subbarao, V. V., 2013, "The Effect of Exhaust Gas Recirculation and Di-Tertiary Butyl Peroxide on Diesel-Biodiesel Blends for Performance and Emission Studies," International Journal of Advanced Science and Technology, 54, pp. 49-60.

[19] Hountalas, D., Mavropoulos, G., and Binder, K., 2008, "Effect of Exhaust Gas Recirculation (EGR) Temperature for Various EGR Rates on Heavy Duty DI Diesel Engine Performance and Emissions," Energy, 33(2), pp. 272-283.

[20] Mahla, S. K., L. M. Das, and Babu, M. K. G., 2010, "Effect of EGR on performance and emission characteristics of natural gas fueled diesel engine," Jordan Journal of Mechanical and Industrial Engineering 4.4 (2010). Paper presented at the Jordan Journal of Mechanical and Industrial Engineering.

[21] Ladommatos, N., Abdelhalim, S. M., Zhao, H., and Hu, Z., 1998, "The effects on diesel combustion and emissions of reducing inlet charge mass due to thermal throttling with hot EGR," SAE Technical Paper 980185, https://doi.org/10.4271/980185.

[22] Moiz, A. A., 2016, "Low Temperature Split Injection Spray Combustion: Ignition, Flame Stabilization and Soot Formation Characteristics in Diesel Engine Conditions," PhD thesis, Michigan Technological University, Houghton, Michigan.

[23] Yasin, M. H. M., Mamat, R., Yusop, A. F., Idris, D. M. N. D., Yusaf, T., Rasul, M., and Najafi, G., 2017, "Study of a diesel engine performance with exhaust gas recirculation (EGR) system fuelled with palm biodiesel," Energy Procedia, 110, pp. 26-31.

[24] Badruddin, I. A., Badarudin, A., Banapurmath, N., Ahmed, N. S., Quadir, G., Al-Rashed, A. A., . . . Kamangar, S., 2015, "Effects of Engine Variables And Heat Transfer on the Performance of Biodiesel Fueled IC Engines," Renewable and Sustainable Energy Reviews, 44, pp. 682-691.

[25] Saravanan, S., 2015, "Effect of Exhaust Gas Recirculation (EGR) on Performance and Emissions of a Constant Speed DI Diesel Engine Fueled with Pentanol/Diesel Blends," Fuel, 160, pp. 217-226.

[26] Rao, K. S., 2016, "Effect of EGR on Diesel Engine Performance and Exhaust Emission Running with Cotton Seed Biodiesel," International Journal of Mechanical and Mechatronic Engineering, 16(02), pp. 64-69.

[27] Asad, U., and Zheng, M., 2014, "Exhaust Gas Recirculation for Advanced Diesel Combustion Cycles," Applied Energy, 123, pp. 242-252.

[28] Asad, U., Divekar, P., Zheng, M., and Tjong, J., 2013, "Low Temperature Combustion Strategies for Compression Ignition Engines: Operability Limits and Challenges," SAE Technical Paper 2013-01-0283, https://doi.org/10.4271/2013-01-0283.

[29] Aoyagi, Y., Osada, H., Misawa, M., Goto, Y., and Ishii, H., 2006, "Advanced diesel combustion using of wide range, high boosted and cooled EGR system by single cylinder engine," SAE Technical Paper 2006-01-0077, https://doi.org/10.4271/2006-01-0077.

[30] Mani, M., Nagarajan, G., and Sampath, S, 2010, "An Experimental Investigation on a DI Diesel Engine Using Waste Plastic Oil with Exhaust Gas Recirculation," Fuel, 89(8), pp. 1826-1832.

[31] Xu, M., Gui, Y., and Deng, K.-Y., 2015, Fuel Injection And EGR Control Strategy on Smooth Switching Of CI/HCCI Mode in a Diesel Engine," Journal of the Energy Institute, 88(2), pp. 157-168.

[32] Haber, B., and Wang, J., 2010, "A Robust Control Approach on Diesel Engines with Dual-Loop Exhaust Gas Recirculation Systems," MSc dissertation, Ohio State University, Columbus, Ohio.

[33] Lehto, K., Elonheimo, A., Hakkinen, K., Sarjovaara, T., and Larmi, M., 2011, "Emission Reduction Using Hydrotreated Vegetable Oil (HVO) with Miller Timing and EGR in Diesel Combustion," SAE International Journal of Fuels and Lubricants, 5(2011-01-1955), pp. 218-224.

[34] Chen, Z., Liu, J., Wu, Z., and Lee, C., 2013, Energy Conversion and Management, 7, pp. 725-731.

[35] Zhao, Y., Wang, Y., Li, D., Lei, X., and Liu, S., 2014, "Combustion and Emission Characteristics of a DME (Dimethyl Ether)-Diesel Dual Fuel 5remixed Charge Compression Ignition Engine with EGR (Exhaust Gas Recirculation)," Energy, 72, pp. 608-617.

CHAPTER FIVE

TRANSPORTATION, POLLUTION AND THE ENVIRONMENT

Journal article

Maroa, S., & Inambao, F. (2017). The Effects of Exhaust Gas Recirculation on the Performance and Emission Characteristics of a Diesel Engine–A Critical Review. *International Journal of Applied Engineering Research*, 12(23), 13677-13689. http://www.ripublication.com

Transportation, Pollution and the Environment

Maroa Semakula[1]and Prof Freddie Inambao[2]

[1,2]*University of Kwazulu-Natal Durban South-Africa.*

Abstract

The importance of modern day transport systems and the transportation industry in the world economy cannot be over emphasized. However, it is now widely recognized that air pollution and environmental degradation are directly linked to the rapid growth of automobile, air, rail, and sea modes of transport. These transportation services and their allied industries are key contributors to every nation's gross domestic product. This work will endeavour to highlight the general areas of concern with regard to pollution and environmental degradation as a consequence of this rapid growth and expansion, with a focus on diesel emissions. These areas are (1) Pollution in highly populated urban areas (cities) with their high rate of personal or private transport rather than public transport systems; (2) The effects of modern day transport systems on the depletion of the ozone layer, which is responsible for climatic changes; and (3) The legislative and effective control systems required to meet the current environmental demands, which this work will endeavour to critically present and analyse.

Keywords; Environmental Degradation, Transport Industry, Urban Pollution, Modes of Transport.

Nomenclature and Abbreviations

$\dot{m}_{EGR}$	Mass Flow Rate of Egr Gases
$\dot{m}_{air}$	Mass Flow Rate of Air
$\dot{m}_{exh}$	Mass Flow Rate from The Exhaust
$\dot{m}_f$	Mass of Fuel Injected
$\dot{m}_{int}$	Mass Flow Rate from The Intake Side
r_{EGR}	Percentage of Recirculated Egr Gases
CeO_2	Cerium Oxide
CO	Carbon Monoxide
CO_2	Carbon Dioxide
DOC	Diesel Oxidation Catalyst
DPF	Diesel Particulate Filter
EC	Elemental Carbon
EPA	Environmental Protection Agency
GBD	Global Burden of Disease
HC	Hydrocarbon Emissions
IEA	International Energy Agency
IF	Inorganic Fraction
IPCC	Intergovernmental Panel on Climate Change
NAC	NOX Absorber Catalyst
LNT	Low NO_X Trap
NASA	National Aeronautical and Space Administration
NH3	Ammonia
NNH	NNH Route of NO_X Formation
NOAA	National Oceanic and Atmospheric Administration
NOX	Agglomerates of Oxides of Nitrogen
NSR	NOX Storage Catalyst
OECD	Organisation for Economic Cooperation and Development
PAGASA	National State Weather Bureau of Philippine
PCV	Positive Crankcase Ventilation
Pd	Palladium
PM	Particulate Matter
PM_{10}	Particulate Matter of Size 10nm
$PM_{2.5}$	Particulate Matter of Size 2.5nm
Pt	Platinum
Rh	Rhodium
SAWS	South-African Weather Services
SCR	Selective Catalytic Reduction
SI	Spark Ignition
SO_3	Sulphur Trioxide
SOF	Soluble Organic Fraction
TDC	Top Dead Centre
VOCs	Volatile Organic Compounds
WHO	World Health Organization
ZrO_2	Zirconium Oxide
λ	The Air Excess Factor Symbol Lambda

INTRODUCTION

The word 'pollution' has a wide variety of contextual meanings and applications, but in the context of this work it means the damage caused by human activity to the environment and ecological systems. Considering all sources of the environmental pollution and categories of pollution emitted and excluding land use for the purpose of agriculture, the transport industry in the world is responsible for about one third of all environmental emissions of volatile organic compounds (VOCs) released into the atmosphere and the environment, including two thirds of the carbon-monoxide (CO). The VOCs, which are hydrocarbon based, are a direct result of combustion, particularly inefficient combustion emitted from vehicle tail pipes as exhaust gases when they burn fuel to produce propulsion power. Some hydrocarbons are known carcinogens. Among the greenhouse gases, CO_2 is the main culprit of global warming and has reached 34 billion tonnes per year with an increase of 3 % in 2011 alone [1] and is projected to rise to 41 billion tonnes by the year 2020 [2].

Human activities, especially the use of and burning of fossil fuels, enhance the greenhouse gas effect by increasing their concentration levels in the atmosphere. The major gases emitted through human activity are CO_2, methane, oxides of nitrogen (NO_X), fluorinated gases (hydrofluorocarbons, perfluorocarbons and sulphur hexafluoride) [3].

There are several methods of VOC emissions control in the modern day automobile, through the use of high pressure fuel injection systems, catalytic converters and positive crankcase ventilation systems (PCV). However, 20 % of all uncontrolled vehicular emissions are as a result of crankcase blow-by and evaporating oil. The particulate VOC pollutants, which result from incomplete combustion and evaporating lubricating oil, have an emission rate of 0.6 g/bkWh to 2.2 g/bkWh for light duty diesel automotive propelled engines, whereas the large ones have 0.5 g/bkWh to 1.5 g/bkWh [4, 5].

The global threat caused by human activities to the environment is the second most serious issue after war facing the world today. This is due to the rise in global warming levels above the pre-industrial levels by over 0.94 °C, acidifying of the oceans, and 3.2 cm of sea level rise per decade. Extreme heat waves, global temperature rise and drought have affected food chains across the globe [6, 7] Unless these activities are legislated for, curbed and controlled, it is expected that globally the negative effects of climatic change will cause a warming of 4 ^{0} C and a sea level rise of 0.5 m to 1.0 m as early as 2060 [8].

The transport industry which is a major contributor to the global economy is also a major cause of environmental pollution and climate change, especially due to the emission from motor vehicles which accounts for 22 % of all the global CO_2 emissions [9]. Air pollution in developing countries and emerging economies accounts for tens of thousands of deaths, with the World Health Organization estimating an annual death toll from air pollution alone to be around 2.4 million people using 2009 estimates and projections [10]. Thus, environmental protection, air pollution control and climatic change management have become issues of global concern, with many agencies such as the Environmental Protection Agency (EPA) of the United States of America, the Organisation for Economic

Cooperation and Development (OECD), the Intergovernmental Panel on Climate Change (IPCC), the European Environment Agency (EEA) and the International Energy Agency (IEA) being constituted and empowered to act in this regard. To this end these agencies have recommended legal measures and control systems, as well as supporting relevant technological research and development in research to improve the pollutions standards of the transport service industry.

The reason this study focuses on diesel propelled engines is because they have the highest proportion of usage globally as compared to gasoline propelled engines, given their numerous merits such as low-operational cost, energy efficiency, reliability, and durability. These merits have made diesel propelled engines the top choice of business leaders in the transport industry as power sources for commercial transportation in trucks, buses, trains, ships and for power generation. Their environmental impact is caused by the exhaust gases released via the tail pipe which contain very high amounts of particulate matter (PM) and NO_X emissions and other pollutants. These pollutants are responsible for severe environmental degradation of air quality causing smog, acid rain and disturbance to the ozone balance. They also cause major health problems, especially diseases related to the respiratory system, and cancer [11].

DIESEL ENGINE STATUS ON EMISSIONS IN THE TRANSPORT SECTOR

From Tables 1 and 2 and presented below it can be seen that transport contributes the largest amounts of NO_X, PM, CO, SO_3 and HC emissions annually, globally. The PM percentage referred to in Tables 1 and 2 does not include dust from the road, rubber particulates from tyres, the photochemical smog particles arising from brake pads and asbestos brake linings used in braking systems of automobiles passenger and commercial vehicles. In addition, there is noise pollution which is predominantly attributed to heavy duty diesel vehicles especially around major urban centres and cities (from highways, ports and stations) and air transport.

Table 1. Atmospheric pollutants and their sources in percentage form

SOURCE	NO_X %	PM %	CO %	SO_3 %	HC %
INDUSTRY	22	44	4	32	26
POWER GENERATION	32	21	0	48	0
SPACE HEATING	5	14	3	12	3
REFUSE BURNING	0	7	1	4	6
TRANSPORT	42	14	92	4	65

Table 2 showing emissions of air pollutants by source in the United States in 2011[12]

Table 2.
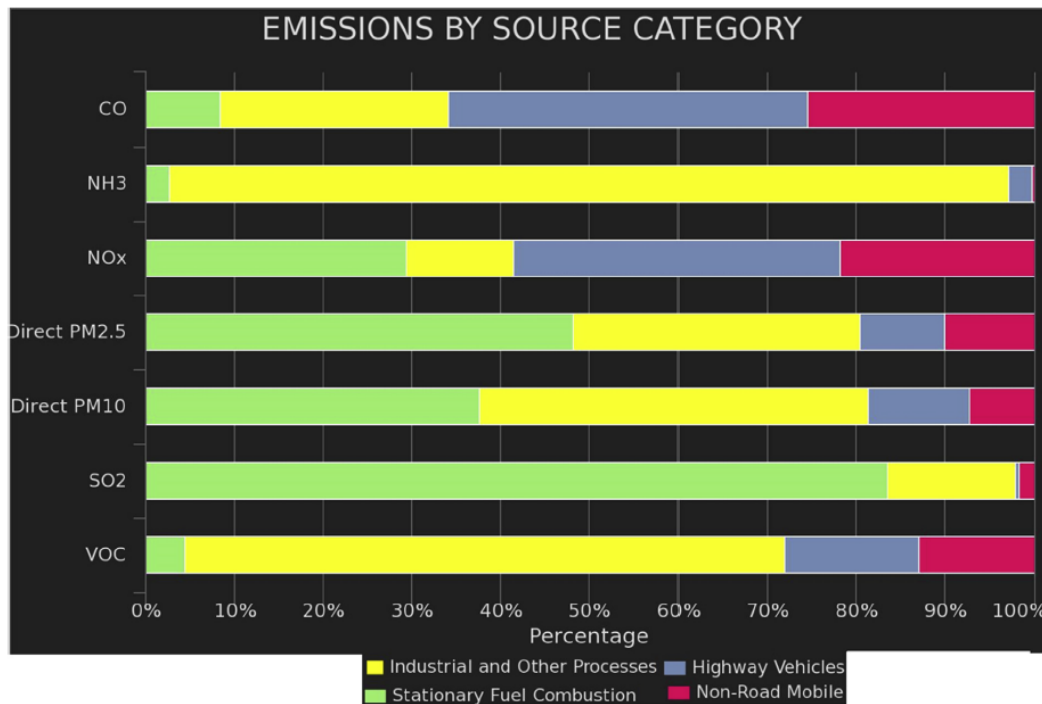
Figure 1 shows the compositions of hydrocarbon pollutant of diesel exhaust gas as analysed at the tail pipe exit [2]. Molecular nitrogen, which is an agent of NO_X emissions, is the largest percentage at approximately 67 %.
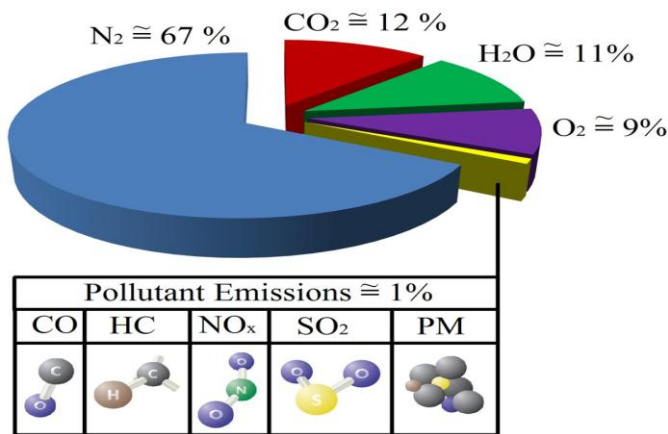
Figure 1. The compositions of hydrocarbon pollutants of diesel exhaust gas as analysed at the tail pipe exit [2].

THE FORMATION OF DIESEL ENGINE POLLUTANTS, AND THEIR EFFECTS

Unburned Hydrocarbons (UHC)

Unburned Hydrocarbon (UHC) emissions are an indication of the quality of combustion within an internal combustion engine, arising from vaporized unburnt fuel and partially burned fuel by-products exiting the combustion chamber and being released to the atmosphere via the exhaust manifold. UHC emissions are inherently independent of the air-fuel ratio of a working engine, as they do not depend on the engine alone but also on other factors outside the engine itself. Such emissions can also be created, for example, if there is a malfunction of other systems or an operational malfunction of other systems, particularly the input data systems in modern injection and engine management systems.

There are two features of a fuel injection systems in spark ignition engines (SI) which cause or can bring about HC emissions, namely, secondary injection and high nozzle sac volumes. However, when it comes to compression ignition engines, which this work is dealing, the hydrocarbon emissions are caused due to insufficient temperature near most cylinder walls of the compression ignition engines. Diesel propelled engines emit low hydrocarbons principally at light loads; the lean air fuel mixture which is the main source of light load emissions is caused by low speed flames which disallow completion of combustion during the normal cycle of the power stroke and secondly due to lack of the actual combustion thus leading to high emissions of hydrocarbons.

There are three main factors that may affect the type of hydrocarbons emitted, namely, engine adjustments, design and fuel type. Engine operating environment can also affect the content of hydrocarbons, where temperatures are 400 ^{0} C to 600 ^{0} C in the combustion cylinder and when oxygen is still available, hydrocarbons will continue to react in the exhaust. Therefore, this will lower emissions exiting the tail-pipe as compared to the engine cylinder prior to it, stated in terms of their CH_4 equivalent content [13, 14]. Emission consists of thousands of chemical species of alkanes, alkenes and aromatics.

Hydrocarbon emissions are not limited to the vehicle exhaust system only but also occur in the vehicle fuel system, from vapors during fuel distribution and dispensing (15 % to 25 %) and the engine crank-case itself (20 % to 30 %). However, the largest culprit of all vehicular hydrocarbon emissions is the exhaust tail pipe which accounts for 50 % to 60 % of all hydrocarbon emissions [15, 16].

Oxides of Nitrogen (NOx) Emissions

As shown and indicated in the literature discussed above, the transport industry (particularly the road component) is the principal and primary source of nitrogen oxide (NO) emission and its oxidized products nitrogen dioxide (NO_2). NO and NO_2 constitute 85 % to 95 %, while NO and N_2 are lumped together as NO_X. There are fundamental differences between the two gases; NO is colourless and odourless, while its counterpart NO_2 is a reddish brown gas with a pungent smell and odour [17]. These two gases are considered to be extremely toxic, especially NO_2 which is five times more toxic than NO, which is a threat to human health as it affects the respiratory system causing irritation and poor resistance to even simple respiratory infections like the common cold and influenza [2].

The temperature dependence of oxides of nitrogen is due to the equilibrium concentration of NO_X compounds of oxygen and nitrogen when they are mixed in a very high flame temperature adiabatically with temperatures of 2000 K to 3000 K [18]. There are basically four types of mechanisms through which the nitrogen oxide emissions are formed and constituted in the combustion chamber and within the automobile combustion chamber, namely: The Zeldovich mechanism, the prompt mechanism, through engine fuel mechanism, and the NNH mechanism [19]. The Zeldovich mechanism is represented in Equation 1, 2 and 3 with Equation 2 as the reaction rate determining step equation [20].

$$O_2 \leftrightarrow 2O \qquad \text{Equation 1}$$

$$N_2 + O \leftrightarrow NO + N \qquad \text{Equation 2}$$

$$N + O_2 \leftrightarrow NO + O \qquad \text{Equation 3}$$
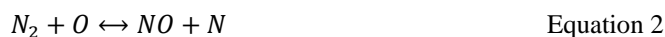
The prompt mechanism, otherwise known as the Fenimore mechanism [21] (named after the man who discovered it), involves reactions of the fragmented hydrocarbons with molecular nitrogen under weak temperature dependency, thus accounting for a relatively smaller portion of the hydrocarbon emissions. Equations 4, 5 and 6 show the occurrence of prompt NO_X [22].

$$O + N_2 + M \rightarrow N_2O + M \qquad \text{Equation 4}$$

$$H + N_2O \leftrightarrow NO + NH \qquad \text{Equation 5}$$

$$O + N2O \leftrightarrow NO + NO \qquad \text{Equation 6}$$

As mentioned earlier, the oxides of nitrogen form an important constituent of photochemical smog besides the greenhouse gas effects, thus contributing in many ways to the depletion of the ozone, causing acid rain, air pollution and a general decrease in the air quality in modern urban metropolises and cities in the world today.

Table 3. Transport patterns and their contribution to overall emissions in selected cities
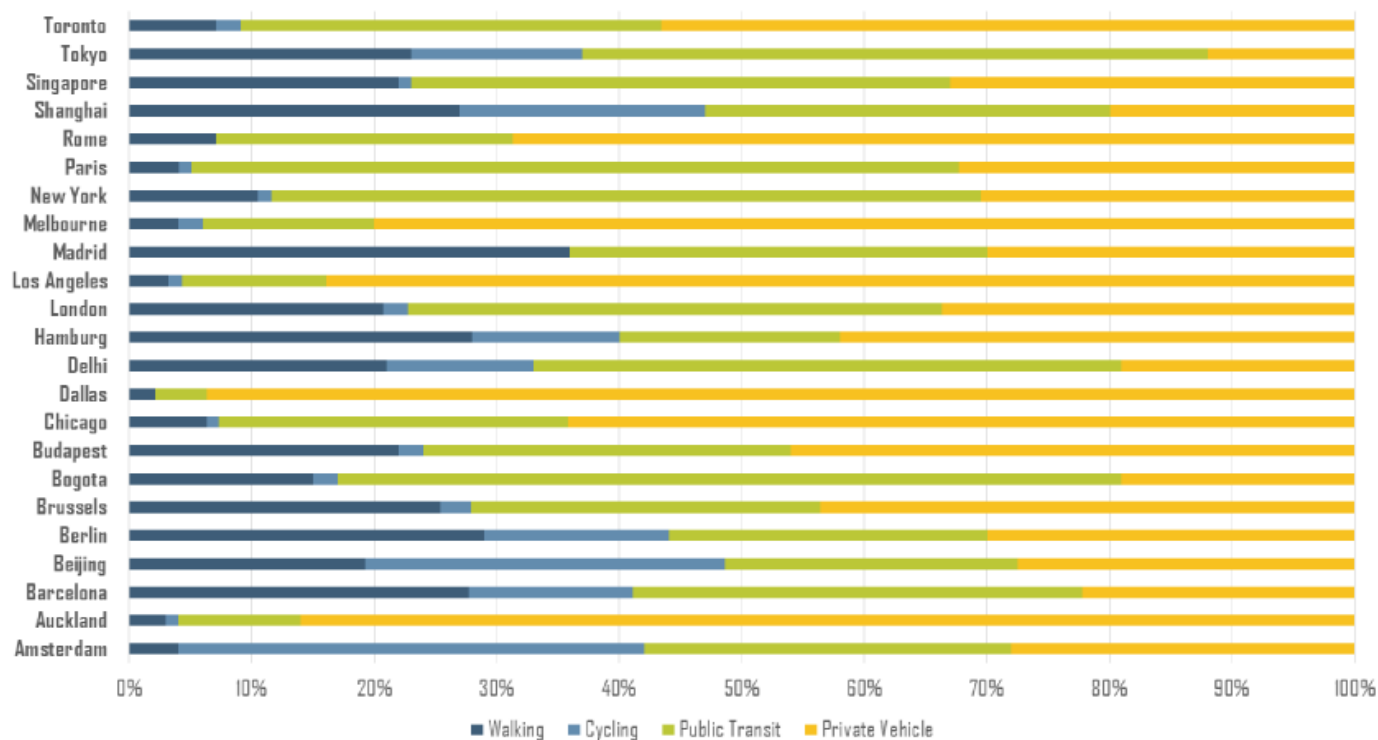
Table 3 shows transport patterns in 23 sampled cities in various regions and the contribution of individual modes of transport to the overall emission percentages in these cities. The leading percentages of pollution by source as seen in Table3 is caused by public transport and private public transport vehicles, with Dallas in USA as the leading city in terms of private public transport pollution, and Tokyo in Japan is the leading city in in terms of public transport pollution.

The amount of NO_X produced during emission from the engine is a function of three factors, namely: the amount of time taken or the combustion duration, the level of concentration of oxygen, and, because NO_X is temperature dependent, the maximum existing temperature in the combustion cylinder. Most of the NO_X emitted is formed in the early combustion phase process with the engine piston nearing the end of compression or top dead centre (TDC) at which period the combustion process propagated flame temperature is at maximum or at peak levels. The amount of NO_X increases three-fold for every 100 ^{0} C increase in the cylinder combustion temperature [16].

Particulate Matter (PM) Emissions

PM emissions can be defined as the agglomerations of small particles resulting from the combustion process due to partly burned lubrication oil, ash content of the fuel used by the engine, sulphates from the engine cylinder wall lubrication oil, and water from condensation and the combustion process. For example, in an experimental study of a heavy duty diesel engine, the researchers classified and characterized the emissions as 41 % as carbon, 7 % as unburned fuel, 25 % as unburned oil, 14 % as sulphates and water, and 13 % as ash and other component emissions [23]. In an earlier study conducted by Agarwal (2007)[24] it was observed that PM emissions consisted of $\cong$ 31 % elemental carbon, $\cong$ 14 % sulphates and moisture, $\cong$ 7 % unburnt fuel, and $\cong$ 40 % unburnt lubricating oil, with the remaining percentages being metals and a variety of other substances.

Diesel PM are particles usually in the region of 15 $nm\ to$ 40 nm measured by diameter, though almost 85 % to 90 % of all PM emissions are less than 1 μm in measured diameter. PM emissions can be divided into three forms or main components: soluble organic fraction (SOF), soot, and the inorganic fraction (IF) of which 50 % is emitted as soot in the form of black smoke in exhaust tail-pipes. SOF is made up of absorbed or condensed hydrocarbons that are embedded within the soot emissions in very fine particles derived partly, as already mentioned, from lubrication oil, unburned fuel and compounds of the combustion process from the combustion chamber (Table 4). These emissions are more pronounced when starting and during idling when the exhaust temperatures are low [25].

Table 4. The components of SOF emissions and their total fraction percentages [4].

Fraction	Components of fraction	Percentages of total fraction
Acidic	Aromatic or aliphatic Acidic functional groups Phenolic and carboxylic acids	3-15
Basic	Aromatic or aliphatic Acidic functional group Amines	< 1-2
Paraffin	Aliphatic, normal and branched Numerous isomers From unburned fuel and /or lubricant	34-65
Aromatic	From unburned fuel, partial combustion, recombination of combustion, from lubricants, Single ring compounds Polynuclear aromatics	3-4
Oxygenated	Polar functional groups but not acidic or basic Aldehydes, ketones, or alccohols Aromatic phenols and quinones	7-15
Transitional	Aromatic or aliphatic Carbonyl functional groups Ketones, aldehydes, esters, ethers	1-6
Insoluble	High molecular weight organic species Hydroxyl and carbonyl groups Inorganic compounds Glass fibre from filters	6-25

The size distribution of particles exhausted from diesel engines generally has two peaks: the nucleation mode which includes all volatile hydrocarbons that are below 50 μm, and the accumulation mode which is made up of soot and particles that are above 50 μm [26, 14]. PM emissions formation is controlled by a number of factors such as the combustion process, fuel quality (sulphur and ash content in the fuel), the power stroke or the expansion process of the fuel, the engine lubrication quality, the fuel consumption per engine cycle and the exhaust gas cooling [27].

PM emissions impact negatively on human health as well as the environment. For example, in 2010 alone the global burden of diseases (GBD) index attributed 3.2 million deaths to ambient pollution [28] where $PM_{2.5}$ emissions were the main

contributor, thus highlighting the seriousness of air pollution from the transport industry.

Figure 2 shows the cause specific global mortality attributable to ambient $PM_{2.5}$ emissions.
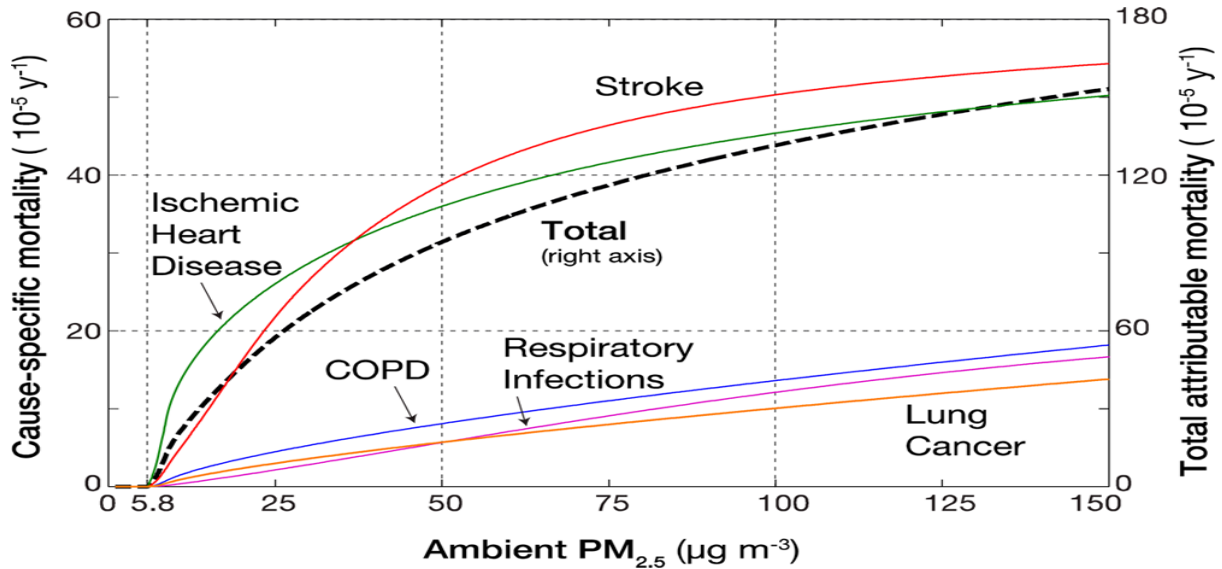
Figure 2 shows global and regional distributions of deaths as a function of ambient $PM_{2.5}$ concentration.
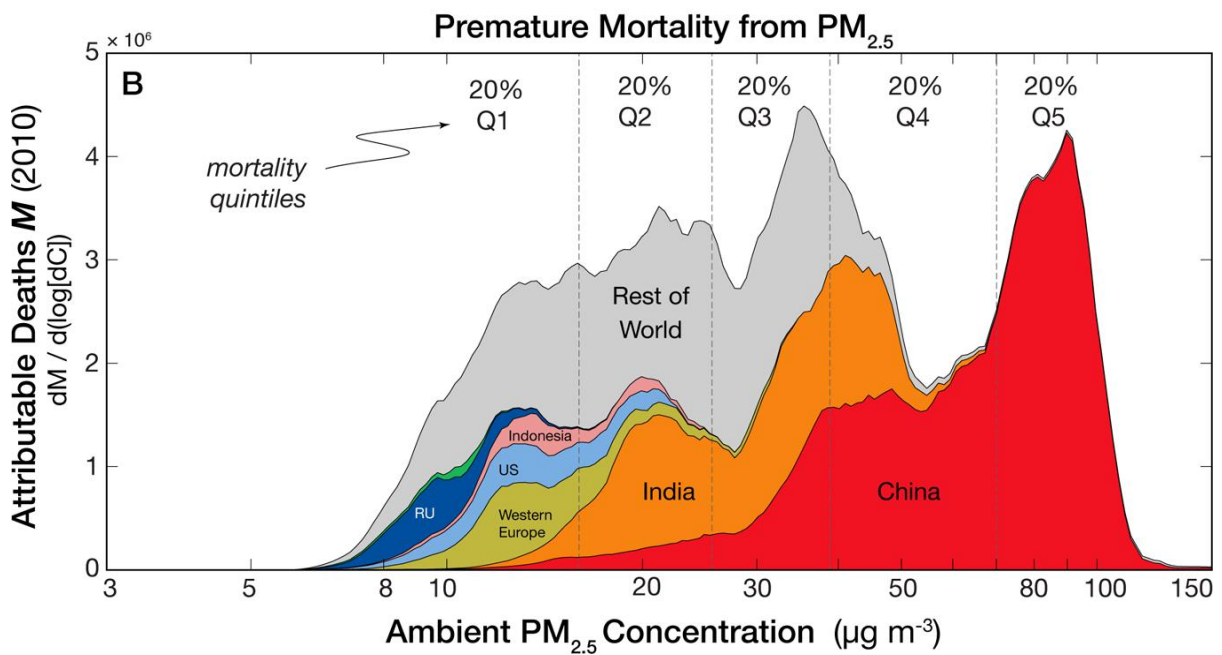
Figure 3. Global and regional distribution of deaths as a function of ambient $PM_{2.5}$ in different countries in quantile percentages.

Carbon Monoxide Emissions

Carbon monoxide emissions result from the incomplete combustion of hydrocarbon fuels as a result of failure of oxidation during the combustion process in a diesel engine, particularly where excess air factor λ satisfies the condition λ < 1 for SI engines and thus the mixture is classified as a rich mixture, which occurs especially during start-ups and sudden acceleration where rich mixtures are a conditional requirement. CO is defined as a colourless, tasteless and odourless toxic gas produced primarily due to the incomplete combustion of the carbon containing fuels. The United States of America is the single largest producer of this pollutant gas and a leading producer of pollution from anthropogenic sources – anthropogenic sources being the major contributor of this gas, as seen from Figure 4.
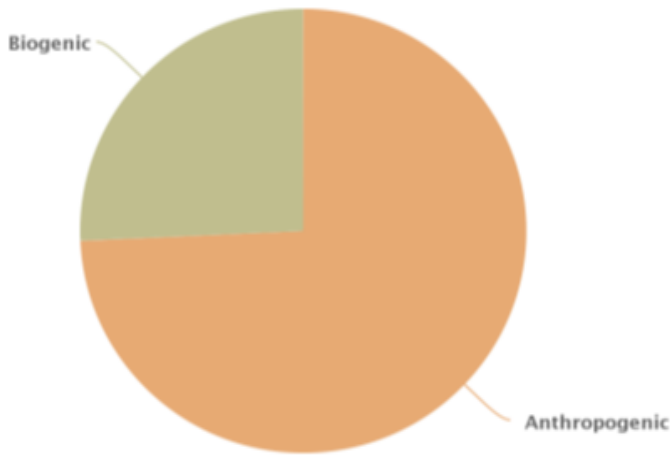
Figure 4. carbon monoxide (CO) emissions by anthropogenic and biogenic sources in the USA [29].

The measured average CO concentration for fuel rich mixtures is very close to equilibrium in burned gas especially during the expansion process. However, for lean fuel mixtures of which diesel engines form a large segment, measured CO emissions are higher than most prediction models of any kind. One possible explanation for this is that from a practical point of view, CO oxidation mechanisms are determined by the fuel air equivalence ratio. This phenomenon in the rich mixture areas and lack of availability of enough oxygen makes the reactant concentration fail to convert fully during combustion, thus exhausting a smaller portion through the tail-pipe due to the kinetic effects. CO emissions tend to form and accumulate in areas of heavy concentrated traffic, parking garages, and under building overheads and overhangs. Among the human health effects of CO emissions due to exposure are headaches, dizziness and in extreme cases of exposure, death.
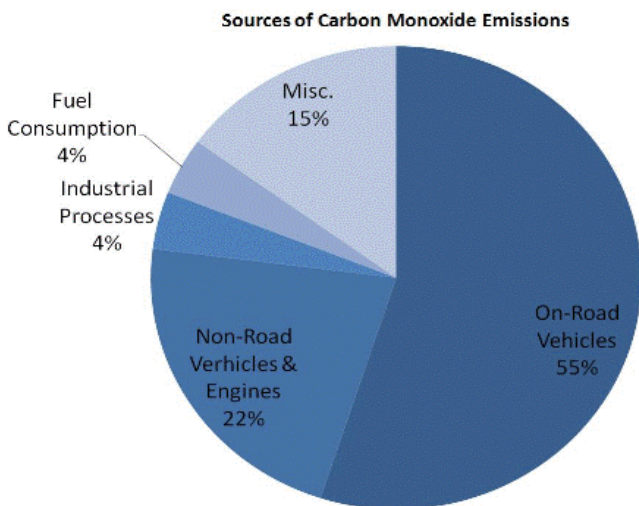
Figure 5 is a pie chart showing how anthropogenic sources contribute to carbon monoxide emissions with the largest share of 55 % being contributed by the transportation industry whose core players are heavy and light duty vehicles on the road [30].

Effects of Traffic Pollutants on the Natural Environment

The demand for energy supply associated with economic growth and development causes emissions which deplete the ozone layer. The ozone layer raises particular concern for ecology since it leads to sun radiation exposure to ultra-violet rays in the $200\,\mu m$ to $300\,\mu m$ range which is toxic to unicellular organisms and most surface cells of animals and [31].

Pollution from automobiles is one of the leading causes of global warming, as cars (light duty and heavy duty) release greenhouse gases and carbon dioxide into the atmosphere through their exhaust systems. These types of gases tend to trap heat in the atmospheric environment thus causing a global rise in temperatures. Because of the combustion of increasing volumes of fossil fuels, global temperatures have risen by 0.5 ^{0} C to 1 ^{0} C since the pre-industrial age. The global rise in temperature or global warming affects the natural environment by causing higher sea levels, damaging farming activities which have a bearing on food security, damaging wild life, and destroying natural habitats and landscapes

Effect of Greenhouse Gases and Global Warming

Since the first recorded temperatures in 1860, earth temperatures have risen by over 1 ^{0} C, and 2017 was one of the hottest years after 2016 in human history. The first six months of 2017 recorded an average surface temperature of 1.1^0 C above the 1950 to 1980 averages [32].
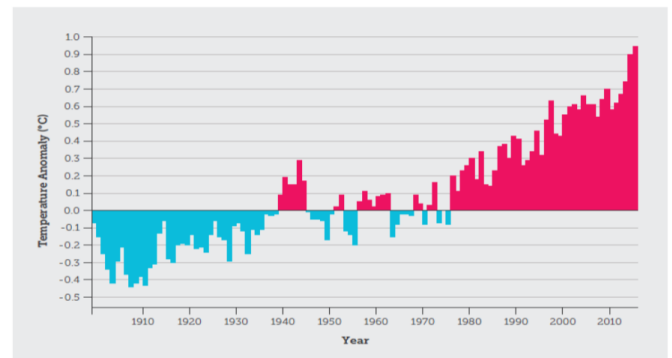
Figure 6. Annual global temperature anomalies from 1901 to 2016 relative to the global annual average temperature for the 20th century (1901-2000) [32].

Figure 6 shows the way in which the annual global temperature has consistently been above the global average for the 20th century, climbing steeply since 2010. Data is from the US National Oceanic and Atmospheric Administration (NOAA) as cited in [32].

Coming closer home to South Africa, the Western Cape province has experienced unprecedented drought and severe unpredictable weather patterns for the last three years. South Africa had intense 2016 January heatwaves in about 62 locations nationally with recorded temperatures reaching up to 46 ^{0} C in Tosca in North West province according to the South African Weather Services (SAWS) [33] 2016. Botswana

recorded and broke a national record of 72 years for its maximum temperature in Maun at 44^0 C.

Alaska in the United States of America had its warmest month in February 2016 breaking a 96-year national record predating the 20th century average with increment levels of 6.9 ^{0} C according to the NOAA, with California and Australia recording unending wild fires due to excessive drought and heat, leading to massive loss of life and property besides the economic loss suffered by individuals and the state [32].

The Effects of Traffic Pollution On Agriculture and Food Security

As a result of the climatic changes that have been enumerated and discussed in previous sections, there has been a shift in the meteorological equator leading to changed forecast trends and scenarios of desert expansion, drought and change in weather patterns across the globe [34]. The following are examples of scenarios that have already started happening:

- Reduction of rainfall, turning some areas like California into deserts, with similar changes being experienced in the Cape provinces in South Africa, where the water conditions are worsening. Punjab in India and other areas are facing intense heat waves with the countryside experiencing droughts of untold proportions.

- There has been an increase in the intensity of severe weather conditions, where the severity of typhoons has been increasing in places like Philippines with 2016 alone accounting for more than 20 tropical cyclones according to PAGASA, the national state weather bureau of Philippines. In 2013 35 000 to 39 000 people lost their lives and damage of more than 40 billion USD was caused by extreme weather conditions, according to the national disaster risk reduction management council of Philippines [35, 36].

- Expansion of the African desert beyond Africa, to Spain Greece and Italy, besides the sub-Saharan countries known as the Sahel countries, which are currently experiencing severe drought and food insecurity.

AUTOMOBILE POLLUTION CONTROL MEASURES

The world is now pre-occupied by environmental protection and the dangers of human activities that degrade the environment. From the United Nations to organizations in regional blocks and individual countries, everyone is embarking on saving and preventing extensive damage to the environment and human health as a result of emissions of pollutants.

Due to the effects of diesel engine emissions on human health and the environment, government agencies in charge of human health and the environmental development have put forward requirements and permissible standards to curb vehicular emissions. In Europe the European Environmental Agency (EEA) has been in operation since 1993 with recommendations and standards of Euro I to Euro IV, as shown in Table 5.

Table 5. EURO standards for heavy duty vehicles according to Delphi 2016 to 2017 as per Walker (2016) [37] and [2].

	CO (g/kWh)	HC (g/kWh)	NOₓ (g/kWh)	PM (g/kWh)
Euro I	4.5	1.1	8.0	0.61
Euro II	4	1.1	7.0	0.15
Euro III	2.1	0.66	5.0	0.13
Euro IV	1.5	0.46	3.5	0.02
Euro V	1.5	0.46	2.0	0.02
Euro VI	1.5	0.13	0.4	0.01

From Table 5 it can clearly can be seen that the standards have become more stringent, thus obliging the vehicle manufacturers and industry service providers to work harder towards reducing emissions from public, private, and commercial vehicles. For almost two and a half decades now (from 1993 to 2017) studies have been carried out on engine modifications and electronic control systems for fuel injection have been introduced, along with tremendous improvement on fuel properties and development. Among the techniques investigated to cut down emissions in combination with other techniques are: the use of exhaust gas recirculation (EGR), lean NO_X trap (LNT), diesel oxidation catalyst (DOC), diesel particulate filter (DPF) and the selective catalytic reduction (SCR) technique [38]. However, these developments have failed to attain sufficient reduction of pollutant emissions to the required regulatory standards as prescribed by the controlling environmental protection agencies.

Exhaust Gas Recirculation

Exhaust gas recirculation is a system which allows the recirculation of the exhaust gases back into the combustion chamber for mixing and reburning with the fresh charge [39] (Figure 7). This technology, though able to reduce NO_X, leads to other problems such as an increase in HC and CO emissions due to the lowered combustion temperature besides affecting overall engine efficiency. While it is accepted that universally there is no standard definition of EGR to be able to quantify the amount of EGR recirculated, there are two methods that are widely accepted and are commonly used to define EGR: the mass based method and the gas concentration method [40].
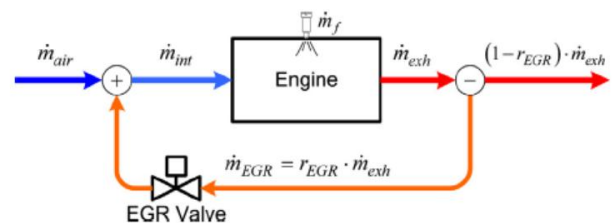
Figure 7. Schematic representation of an EGR system and some of its nomenclature and control design for the EGR valve.

Both of these methods can be demonstrated from the diagram shown in Figure 7 and can also be expressed mathematically as follows in Equations 7 and 8 [41].

$$r_{EGR} = \frac{\dot{m}_{EGR}}{\dot{m}_{air} + \dot{m}_f + \dot{m}_{EGR}}$$ Equation 7

$$r_{EGR} \approx \frac{[CO_2]_{int} - [CO_2]_{amb}}{[CO_2]_{exh} - [CO_2]_{amb}} \approx \frac{[CO_2]_{int}}{[CO_2]_{exh}}$$ Equation 8

Where the $\dot{m}_{EGR}$ is the mass flow rate of the gas recirculated, $\dot{m}_{air}$ is the mass flow rate of fresh air, $\dot{m}_f$ is the mass flow rate of the injected fuel and r_{EGR} is the mass fraction of the recirculated exhaust gases.

Low NOX Trap (LNT)

The low NO_X trap (LNT) system is has two other names by which it is also known: NO_X storage reduction (NSR) and NO_X absorber catalyst (NAC). The LNT has three main components, namely, the oxidation catalyst made of platinum (Pt), the NO_X storage ambience made up of barium (Ba) together with other oxides, and a reduction catalyst made up of Rhodium (Rh). A platinum catalyst is preferred due to its ability to reduce NO_X emissions even at very low temperatures while still offering stability in the presence of sulphur and water moisture. However, this technology cannot offer all the solutions to vehicular emissions as a stand-alone technology.
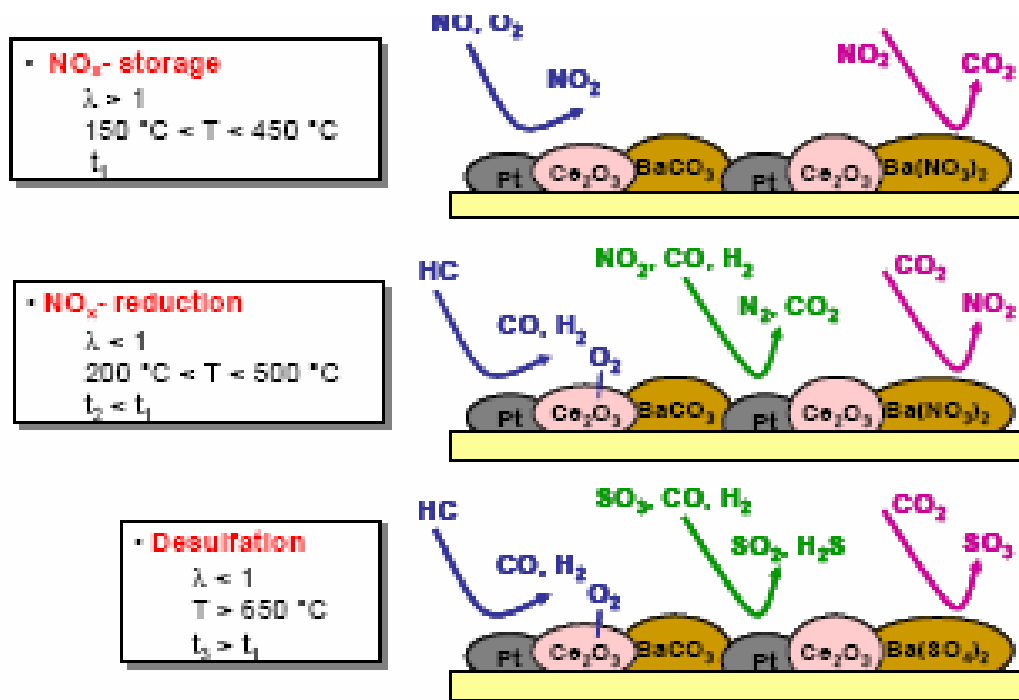
Figure 7. The low NO_X trap (LNT) has three operating modes of operation: NOx storage during lean engine operation, NOx reduction during rich operation phases, low NO_X trap (LNT) desulfurization under rich conditions and high temperatures [42].

Selective Catalyst Reduction

The most recent developments have seen the introduction of the SCR technology especially for heavy duty vehicles [43]. It has already been in use with light duty vehicles. For example, Audi motors and Volkswagen motors have widely adopted these technologies for most of their passenger vehicles. SCR works by utilizing ammonia as a reductant to minimize NO_X emissions in the exhaust gases emitted releasing N_2 and H_2O. There are two processes that an SCR catalyst system undergoes namely hydrolysis and thermolysis. Equation 9 for the hydrolysis process and Equation 10 for the thermolysis process summarizes the two processes [2] and [22].

$$HNCO + H_2O \rightarrow NH_3 + CO_2$$ Equation 9

$$(NH_2)_2CO \rightarrow NH_3 + HNCO$$ Equation 10
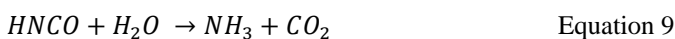
After the hydrolysis and thermolysis process, the following are the chemical reactions which take place in the SCR catalyst as indicated by Equations 11, 12 and 13 [22] and [4].

$$4NO + 4NH_3 + O_2 \rightarrow 4N_2 + 6H_2O$$ Equation 11

$$2NO + 2NO_2 + 4NH_3 \rightarrow 4N_2 + 6H_2O$$ Equation 12

$$6NO_2 + 8NH_3 \rightarrow 7N_2 + 12H_2O$$ Equation 13
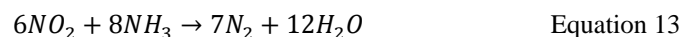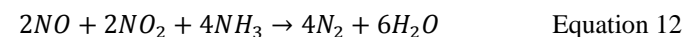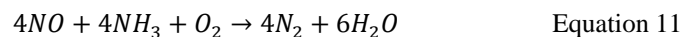
Figure 8 shows a schematic diagram of a car exhaust gas emissions control system comprising an oxidation catalyst, wall-flow particulate filter, and flow-through SCR catalyst. Key components include a urea solution tank (heated in cold weather), dosing spray module and static mixer, temperature and NO_X sensors (Robert Bosch GmbH) [44].
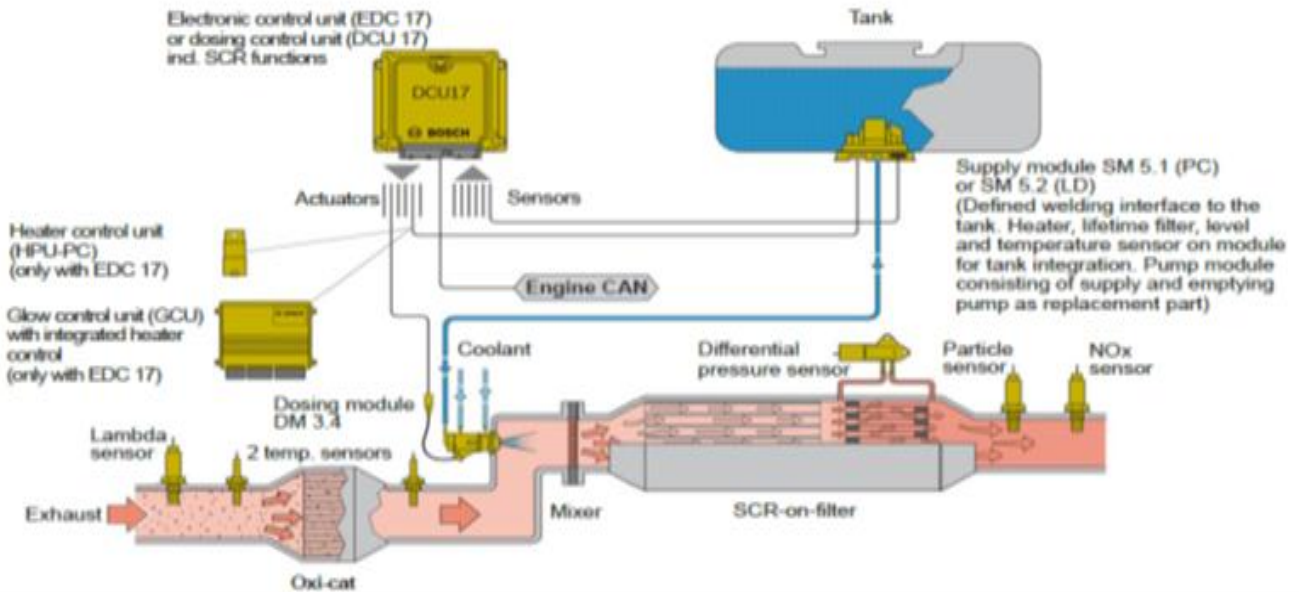
Figure 8. Schematic diagram of the SCR NO$_X$ control system as used in a standard production vehicle [44].

Diesel Particulate Filters (DPF)

DPF have been applied in automotive manufacturing production units since the year 2000 and are primarily used to remove PM emissions from the exhaust gases through physical filtration. Most of the DPFs are made in a honey comb structure of silicone carbide or cordierite ($2MgO - 2Al_2O_2 - 5SiO_2$) with both ends of the monolith structure blocked so that particulate matter is forced through the porous substrate walls thus acting as a mechanical filtering system. The walls of the DPF filter are made in such a way that they enable exhaust gases to pass through the walls with little resistance while maintaining the capability to collect PM emissions particle species as shown on Figure 9.
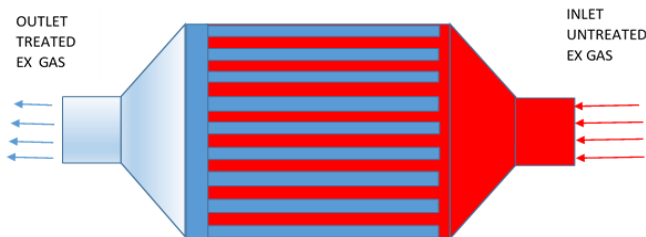
Figure 9. Schematic of the working mechanism of a diesel particulate filter (DPF) filter. With DPF, care must be taken to avoid excessive saturation of the filter as this builds up back pressure which is harmful for engine operation and durability, increases fuel consumption, increases engine stress levels and premature failure of the filter and engine [45].

The Diesel Oxidation Catalyst (DOC)

The main purpose of a diesel oxidation catalyst (DOC) is the oxidation of the CO and HC emissions by the reduction of the PM through oxidation of the hydrocarbons absorbed into the carbon particles. The DOC is made up of a metal or a ceramic structure with an oxide mixture (wash coat) composed of aluminum oxide (Al_2O_3), cerium oxide (CeO_2), zirconium oxide (ZrO_2) and an active catalytic metal such as platinum (Pt), palladium (Pd) and rhodium (Rh) [46].
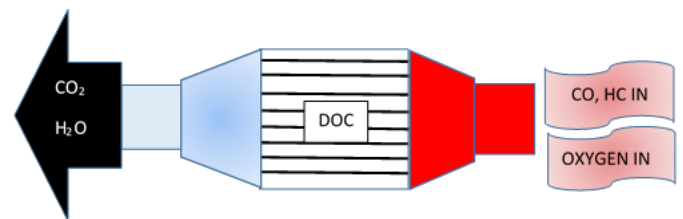
Figure 10 shows a schematic diagram of a DOC and its operation in reducing emissions through the process of oxidation.

There are six factors which influence the choice of DOCs, namely conversion efficiency, temperature stability, light-off temperature, tolerance to poisoning, the cost of manufacturing, and parametrical factors. Parametrical factors include channel density measured in channels per square inch, the individual channel wall thickness, the cross-sectional area, and the length of the channels (external dimensions) [47].

The DOCs are the preffered choice for most emission control systems for heavy duty and light duty vehicles in Europe, the USA and Japan, with the DOCs that contain platinum and palladium being the most popular among manufacturers and consumers alike in the world market. However, DOCs cause a reaction with sulphur oxide and sulphur tri-oxide thus generating sulphates and sulphuric acid which shortens the life of such control systems and causes several environmental and human health issues.

CONCLUSION

From the current work and as discussed in the literature, the road transport industry accounts for the major part of atmospheric and environmental pollution through emission of harmful compounds and elements. It has been shown that pollution from the transport industry has serious health effects and a negative impact on the natural environment.

Technological development has evolved in order to reduce and mitigate these effects. There are a number of technologies that have been implemented to reduce harmful pollutant emissions, with the after treatment systems offering the greatest potential to considerably reduce pollution from diesel propelled vehicles and other sources of emissions. Therefore, more research funds should be directed towards improving their efficiencies and working systems. At the same time, more needs to be done regarding the change of behavior and attitudes, where instead of putting commercial and economic interests first, human and environmental interests should take precedence.

From the control strategies discussed from literature, the ammonia SCR system looks set to become the natural choice for the control and reduction of NO_X emissions for light and heavy duty vehicles. There is a wide variety of materials that are catalytically active with ammonia and are established commercially with very good selectivity and longevity and with thermal durability in relation to N_2O formation.

More stringent measures, legislation and penalties for companies and organizations or even countries should be encouraged, for example emission cheating companies like Volkswagen should be put out of business. Although it would look harsh it would to serve as a lesson to other companies flouting emission regulations and standards. Due to the fact that diesel fuel is the major emission generating fuel in diesel engines, besides the control systems to control emissions the use of alternative fuels should be encouraged and developed through allocation of more funds towards reducing over dependency on diesel fuel. In addition, new combustion control strategies and schemes need to be developed, and these require further study and research and development to realize their full potential. The issue of fuel recovery where waste will be turned into green energy thus reducing fossil fuel must be further investigated.

ACKNOWLEDGEMENTS

REFERENCES

[1]   Olivier, J. G., Peters, J. A. and Janssens-Maenhout, G., 2012, "Trends in Global CO2 Emissions 2012 Report," The Hague: PBL Netherlands Environmental Assessment Agency.

[2]   Reşitoğlu, İ. A., Altinişik, K. and Keskin, A., 2015, "The Pollutant Emissions from Diesel-Engine Vehicles and Exhaust Aftertreatment Systems," Clean Technologies and Environmental Policy, 17(1), pp. 15-27.

[3]   Venkateswarlu, K., Murthy, B. S. R. and Subbarao, V. V., 2013, "The Effect of Exhaust Gas Recirculation and Di-Tertiary Butyl Peroxide on Diesel-Biodiesel Blends for Performance and Emission Studies," International Journal of Advanced Science and Technology, 54, pp. 49-60.

[4]   Heywood, J. B., 2012, Internal Combustion Engine Fundamentals, (Vol. 930), Mcgraw-Hill, New York.

[5]   Stone, R., 2012, Introduction to Internal Combustion Engines, Palgrave Macmillan, Basingstoke.

[6]   Levitus, S., Antonov, J. I., Boyer, T. P., Baranova, O. K., Garcia, H. E., Locarnini, R. A., . . . Yarosh, E. S., 2012, "World Ocean Heat Content and Thermosteric Sea Level Change (0-2000 m), 1955-2010," Geophysical Research Letters, 39(10).

[7]   Meyssignac, B. and Cazenave, A., 2012, "Sea level: a Review of Present-Day and Recent-Past Changes and Variability," Journal of Geodynamics, 58, pp. 96-109.

[8]   Huddleston, N., 2012, "Climate Change: Evidence, Impacts and Choices," PDF Booklet, Washington, DC: The National Academies Press.

[9]   International Energy Agency, 2012, "CO2 Emissions from Fuel Combustion 2012," Paris, International Energy Agency.

[10]   World Health Organization, 2009, "Global Health Risks: Mortality and Burden of Disease Attributable to Selected Major Risks," Geneva, World Health Organization.

[11]   Xia, M., Viera-Hutchins, L., Garcia-Lloret, M., Rivas, M. N., Wise, P., McGhee, S. A., . . . Chatila, T. A., 2015, "Vehicular Exhaust Particles Promote Allergic Airway Inflammation Through an Aryl Hydrocarbon Receptor-Notch Signaling Cascade," Journal of Allergy and Clinical Immunology, 136(2), pp. 441-453.

[12]   IEA, C. (2012). emissions from Fuel Combustion. International Energy Agency. [13] Yamada, H., Misawa, K., Suzuki, D., Tanaka, K., Matsumoto, J., Fujii, M. and Tanaka, K., 2011, "Detailed Analysis of Diesel Vehicle Exhaust Emissions: Nitrogen Oxides, Hydrocarbons and Particulate Size Distributions," Proceedings of the Combustion Institute, 33(2) pp. 2895-2902.

[14]   Shirneshan, A., 2013, "HC, CO, CO2 and NOx Emission Evaluation of a Diesel Engine Fueled with Waste Frying Oil Methyl Ester," Procedia-Social and Behavioral Sciences, 75, pp. 292-297.

[15] Dhariwal, H., 1997, "Control of Blowby Emissions and Lubricating Oil Consumption in IC Engines," Energy Conversion and Management, 38(10), pp. 1267-1274.

[16] Lee, T., Park, J., Kwon, S., Lee, J. and Kim, J., 2013, "Variability in Operation-Based NOx Emission Factors with Different Test Routes, and its Effects on the Real-Driving Emissions of Light Diesel Vehicles," Science of The Total Environment, 461, pp. 377-385.

[17] Hoekman, S. K. and Robbins, C., 2012, "Review of the Effects of Biodiesel on NOx Emissions," Fuel Processing Technology, 96, pp. 237-249.

[18] Rao, K. S., 2016, "Effect of EGR on Diesel Engine Performance and Exhaust Emission Running with Cotton Seed Biodiesel," International Journal of Mechanical and Mechatronic Engineering, 16(02), pp. 64-69.

[19] Bowman, C. T. 1992, "Control of Combustion-Generated Nitrogen Oxide Emissions: Technology Driven by Regulation," Paper presented at the Twenty Fourth Symposium (International) on Combustion, The Combustion Institute, Pittsburgh.

[20] Paul, G., Datta, A. and Mandal, B. K., 2014, "An Experimental and Numerical Investigation of the Performance, Combustion and Emission Characteristics of a Diesel Engine Fueled with Jatropha Biodiesel," Energy Procedia, 54, pp. 455-467.

[21] Fenimore, C., 1971, "Formation of Nitric Oxide in Premixed Hydrocarbon Flames," Paper presented at the Thirteenth Symposium (International) on Combustion, The Combustion Institute, Pittsburgh.

[22] Turns, S. R., 1996, An Introduction to Combustion (Vol. 287), McGraw-Hill, New York.

[23] Wang, Y., Liu, H. and Lee, C.-F. F., 2016, "Particulate Matter Emission Characteristics of Diesel Engines with Biodiesel or Biodiesel Blending: A Review," Renewable and Sustainable Energy Reviews, 64, pp. 569-581.

[24] Agarwal, A. K., 2007, "Biofuels (Alcohols and Biodiesel) Applications as Fuels for Internal Combustion Engines," Progress in Energy and Combustion Science, 33(3), pp. 233-271.

[25] Tighe, C., Twigg, M., Hayhurst, A. and Dennis, J., 2012, "The Kinetics of Oxidation of Diesel Soots by NO 2," Combustion and Flame, 159(1), pp. 77-90.

[26] Kittelson, D. and Kraft, M., 2014, "Particle Formation and Models in Internal Combustion Engines," Preprint No. 142.

[27] Barrios, C. C., Domínguez-Sáez, A., Martín, C. and Álvarez, P., 2014, "Effects of animal Fat Based Biodiesel on a TDI Diesel Engine Performance, Combustion Characteristics and Particle Number and Size Distribution Emissions," Fuel, 117, pp. 618-623.

[28] Apte, J. S., Marshall, J. D., Cohen, A. J. and Brauer, M., 2015, "Addressing Global Mortality from Ambient PM2.5," Environmental Science & Technology, 49(13), pp. 8057-8066.

[29] Environmental Protection Agency (USA)., 2011, Inventory of US Greenhouse Gas Emissions and Sinks: 1990-2009, Washington, Environmental Protection Agency.

[30] Pisupati, S. 2017. Products of combustion. EGEE 102: Energy Conservation and Environmental Protection. https://www.e-education.psu.edu/egee102/node/1951

[31] Masters, G. M. and Ela, W., 2008, Introduction to Environmental Engineering and Science (Vol. 3), Prentice Hall, Englewood Cliffs, NJ.

[32] Climate Council. 2016, Global Heat Record Broken Again. Potts Point, Australia: Climate Council.

[33] South African Weather Services (SAWS) http://www.weathersa.co.za/about-us/2015-09-10-13-04-27

[34] Grainger, A., 2013, The Threatening Desert: Controlling Desertification, Routledge, Abingdon, United Kingdom.

[35] Lapinig, V. T. and Bolante, J. M. M., 2017, "Typhoon Analysis. Intensity, Damage and Casualty Relationship in Fractal Context," Northwestern Mindanao State College of Science and Technology Research Journal, 3(1).

[36] Lao, M. E. J., 2016, "The Philippines in 2015: Slowly, on the Straight and Narrow," Southeast Asian Affairs, 2016(1), pp. 265-280.

[37] Walker, A., 2016, "Future Challenges and Incoming Solutions in Emission Control for Heavy Duty Diesel Vehicles," Topics in Catalysis, 59(8-9), pp. 695-707.

[38] Twigg, M. V., 2015, "Urea-SCR Technology for deNOx After Treatment of Diesel Exhaust," Johnson Matthey Technology Review, 59(3), pp. 221-232.

[39] Thangaraja, J. and Kannan, C., 2016, "Effect of Exhaust Gas Recirculation on Advanced Diesel Combustion and Alternate Fuels – A Review," Applied Energy, 180, pp. 169-184.

[40] Semakula, M. and Inambao, F., 2017, "The Effects of Exhaust Gas Recirculation on the Performance and Emission Characteristics of a Diesel Engine – A Critical Review," International Journal of Applied Engineering Research, 12(23), pp. 13677-13689.

[41] Asad, U. and Zheng, M., 2014, "Exhaust Gas Recirculation for Advanced Diesel Combustion Cycles," Applied Energy, 123, pp. 242-252.

[42] Schnitzler, J., 2006, Particulate Matter and NOx Exhaust Aftertreatment Systems, FEV Motorentechnik GmbH, Aachen, Germany.

[43]   Yun, B. K. and Kim, M. Y., 2013, "Modeling the Selective Catalytic Reduction of NO x by Ammonia over a Vanadia-based Catalyst from Heavy Duty Diesel Exhaust Gases," Applied Thermal Engineering, 50(1), pp. 152-158.

[44]   Nova, I. and Tronconi, E., 2014, Urea-SCR technology for deNOx Aftertreatment of Diesel Exhausts, Springer, New York.

[45]   Zhang, Y., Lou, D., Tan, P., Hu, Z. and Feng, Q., 2017, "Experimental Study on Particulate Emission Characteristics of an Urban Bus Equipped with CCRT After-Treatment System Fuelled with Biodiesel Blend," SAE Technical Paper 2017-01-0933, 2017, https://doi.org/10.4271/2017-01-0933.

[46]   Azama, A., Alia, S. and Iqbala, A. 2016, "134. Emissions from Diesel Engine and Exhaust After Treatment Technologies," 4th International Conference on Energy, Environment and Sustainable Development 2016 (EESD 2016)

[47]   Guardiola, C., Pla, B., Piqueras, P., Mora, J. and Lefebvre, D., 2017, "Model-Based Passive and Active Diagnostics Strategies for Diesel Oxidation Catalysts" Applied Thermal Engineering, 110, pp. 962-971.

CHAPTER SIX

THE FORMATION, EFFECTS AND CONTROL OF OXIDES OF NITROGEN IN DIESEL ENGINEs

Journal article

Maroa, S., & Inambao, F. (2018). The Formation, Effects and Control of Oxides of Nitrogen in Diesel Engines. *International Journal of Applied Engineering Research*, 13(6), 3200-3209. http://www.ripublication.com

The Formation, Effects and Control of Oxides of Nitrogen in Diesel Engines

Maroa Semakula[1] and Prof Freddie Inambao[2]

[1,2]*University of Kwazulu-Natal Durban South-Africa.*

Abstract

The transport service industry is a heavy user of diesel propelled engines as prime movers of goods and services. The diesel propelled engine is praised due to its high fuel efficiency, reliability and durability. However, the nitrogen emissions as a result of diesel fuel combustion characteristics raise major concerns for the manufacturing industry, environmentalists and health care researchers. The manner in which diesel engines combust their fuel is the main cause of the nitrogen oxide emission proportion. Although there are other sources of nitrogen oxide emission, this work will cover the sources of nitrogen oxides and their formation within the diesel engine, their routes of formation, identify the mechanisms under which the formations occur, identify their types and interactions, look at the various effects of the oxides of nitrogen on human health and the overall damage to the natural environment, and look critically at control systems.

Keywords: Nitrogen Oxides, Human Health, Formation Mechanisms, Durability.

NOMENCLATURE AND ABBREVIATIONS

A/F	Air-Fuel Ratio
ATDC	After Top Dead Centre
B	Cylinder Bore
BTDC	Before Bottom Dead Centre
CA	Crank Angle
CI	Compression Ignition
CN	Carbon of Nitrogen
CO	Carbon Oxide
DICI	Direct Injection Compression Ignition
DOC	Diesel Oxidation Catalyst
DPF	Diesel Particulate Filter
EGR	Exhaust Gas Recirculation
F/A	Fuel-Air Ratio
HCCI	Homogeneous Charge Compression Ignition
HCN	Hydrogen Cyanide
HPL	High Pressure Loop EGR
IDICI	Indirect Injection Compression Ignition
L	Length or Piston Stroke
LPL	Low Pressure Loop EGR
M	Organic Residue
NG	Natural Gas
NO	Nitrogen Oxide
NO_X	Oxides of Nitrogen Excluding Nitrogen Trioxide Up
OH	Water or Hydroxide Radical
P	Pressure
PCCI	Pre-Mixed Charge Compression Ignition
PM	Particulate Matter
r_c	Compression Ratio
RCCI	Reactivity Charge Compression Ignition
SCR	Selective Catalytic Reduction
SI	Spark Ignition
SO_2	Sulphur Dioxide
SOI	Start of Injection
UV	Ultra-Violet Rays
V_c	Clearance Volume
V_d	Swept or Displaced Volume
λ	The Air Excess Factor Symbol Lambda

INTRODUCTION

The modern-day diesel engine, also known as the compression ignition engine, offers high fuel efficiency, low engine noise, reliability and durability during its life and service. However, diesel engines produce more oxides of nitrogen emissions than their counterparts, spark ignition (SI) engines. This collection of oxides of nitrogen emissions are collectively referred to as NO_X. Along with particulate matter emissions (PM), these

emissions have become major environmental and health concerns and have also become important themes in global discussions and forums.

Due to the ever increasingly stringent regulations on emissions by environmental protection agencies and governments, there has been development and improvement in design to accommodate and conform with the growing list of emission standards, especially developments in diesel fuel improvement [1] and [2]. Among the fuels for the 21st century being proposed as an alternative to diesel fuel is natural gas (NG), which is highly promising and attractive according to Abdelaal and Hegab (2012) [3]. The advantages of NG include availability, lower price, and reduction in CO emissions due the low carbon to hydrogen ratio. Further, because of its high octane number, NG has a high auto-ignition temperature characteristic which eliminates compression ignition (CI) engine knock such as it occurs during high compression ratios due to the low octane number of diesel fuel. Above all, it is eco-friendly with clean combustion compared to conventional diesel fuel engines. NO_X emissions are approximately 50% to 80% less, with zero smoke and PM emissions – something that is very hard to achieve in basic diesel propelled engines [3].

Besides the use of alternative fuels as a method of reducing NO_X emissions, the use of other control strategies and measures besides fuels has become equally important in mitigating the effects and impact of NO_X emissions. One of the techniques that has gained widespread use, although not as a standalone technology, is exhaust gas recirculation (EGR). This technique has been found to be an effective tool in reducing the emissions of NO_X [4, 5].

Although the combustion of biodiesels and its blends is different from conventional diesel and fossil fuel in compression ignition engines due to their physio-chemical fuel properties, they do also cause emission of NO_X, PM, CO and HC [6]. There has been a tremendous development in combustion technologies for biodiesel fuel combustion in diesel compression ignition engines, to accommodate the developments witnessed in the growth and expansion in alternative fuels, especially the biodiesels. Among the strategies that have been developed are: homogeneous charge controlled ignition (HCCI), pre-mixed charge controlled ignition (PCCI) and reactive charge controlled ignition (RCCI). These strategies have been extensively studied and found to significantly reduce NO_X and other emissions [7].

SOURCES OF OXIDES OF NITROGEN AND FORMATION

There are five mechanisms of NO_X formation in a diesel engine combustion process:

- Fenimore CN and HCN pathways.
- N_2O intermediate route or the Zeldovich mechanism.
- Due to super equilibrium concentrations of O and OH.
- Radicals in the extended Zeldovich mechanism reactions.
- The NNH route.

Prompt NOx or The Fenimore Mechanism

Prompt NO_X, also known as Fenimore mechanism (named after the person who discovered it [8], accounts for the smallest contribution to the quantity of NO_X. It is usually formed at the flame front especially in rich fuel-air ratio areas due to unavailability of oxygen, from the radicals of CH through their oxidation when they react with molecular nitrogen (N_2), leading to the formation of cyanhydric acid (HCN) and nitrogen oxide (NO) at the termination of the reactions. The general scheme of prompt NO_X causes hydrocarbon radicals to react with molecular nitrogen to form amines or cyano compounds which are then transferred and converted to intermediate compounds thus forming NO as can be shown in equation 1 and equation 2 below and expressed as:

$$CH + N_2 \leftrightarrow HCN + N \qquad \text{Equation 1}$$

$$C + N_2 \leftrightarrow CN + N \qquad \text{Equation 2}$$

Where equation 2 forms the primary path and becomes the rate limiting step in the reaction chain of the entire mechanism. However, it is vital to mention here that in the diesel engine combustion process, NO_X is generated through the Fenimore mechanism or prompt NO_X and the thermal mechanism or Zeldovich mechanism only. The conversion of hydrogen cyanide (HCN) to form NO takes the following path as expressed in the following equations as:

$$HCN + O \leftrightarrow NCO + H \qquad \text{Equation 3}$$

$$NCO + H \leftrightarrow NH + CO \qquad \text{Equation 4}$$

$$NH + H \leftrightarrow N + H_2 \qquad \text{Equation 5}$$

$$N + OH \leftrightarrow NO + H \qquad \text{Equation 6}$$

2.2 The Thermal NO_x (Zeldovich Mechanism)

The Zeldovich mechanism which takes the intermediate route is an important mechanism in lean fuels $\Phi < 0.8$ operating under low temperature conditions as can be seen in the three equations below with M as the organic residue [9] as:

$$O + N_2 + M \rightarrow N_2O + M \qquad \text{Equation 7}$$

$$H + N_2O \leftrightarrow NO + NH \qquad \text{Equation 8}$$

$$O + N_2 \leftrightarrow NO + NO \qquad \text{Equation 9}$$

The Zeldovich scheme mechanism consists of three main reaction chains as shown in the following equations and are coupled to fuel combustion chemistry through O_2, O and OH species [10] as follows:

$$O + N_2 \leftrightarrow NO + N \qquad \text{Equation 10}$$

$$N + O_2 \leftrightarrow NO + O \qquad \text{Equation 11}$$

$$N + OH \rightarrow NO + H \qquad \text{Equation 12}$$

The thermal NO_X formation of oxides of nitrogen depend on the following factors for their formation and propagation:

- Temperature especially in the reaction zone. Other than the disassociation process in the equation 2 of

oxygen, the reaction chain is inherently a temperature function as concluded by the studies conducted by Dangar and Rathod (2013) [11].

- The equivalence ratio or the air-fuel ratio in the reaction zone as it influences the atomic oxygen concentration within a combustion mixture. It has been observed that the NO_X emissions decrease with a decrease in the air-fuel ratio [12].

- The amount of time or duration of the reacting gases, also called retention time, spent in the reaction zone at maximum temperature determine the amount of NO_X formed. The shorter the time the smaller the quantity of NO_X and vice versa.

The NNH Mechanism

This is a recently discovered reaction pathway [13], with two major reaction mechanisms which has been shown to be important especially in the combustion of hydrogen [14, 15] and hydrocarbon fuels which have large carbon to hydrogen ratios [16]. The following two equations illustrate this route as follows:

$$N_2 + H \rightarrow NNH \qquad \text{Equation 13}$$

$$NNH + O \rightarrow NO + NH \qquad \text{Equation 14}$$

The Fuel NOx

Fuel NO_X can be defined as the reaction of fuel bound nitrogen from the compounds of N-H or N-C leading to the formation of ammonia (NH_3) and cyanhydric acid (HCN), which, when disassociated during the chain reaction, form NO. For lean fuel-air ratio mixtures almost two thirds of fuel bound nitrogen becomes converted to NO with the rest being converted to molecular nitrogen N_2 [17]. However, for rich mixtures (that is fuel-air ratios that have high fuel-to-air ratios), less NO is formed but more ammonia and cyanhydric acid (HCN) is produced, which, when released to the atmosphere, form NO through decomposition [18]. It is imperative to mention here that the NO formed from this mechanism and route cannot be optimized and controlled through combustion. The various forms of nitrogen bound fuel from different fuel sources are shown in Table 1.

Table 1: Forms of nitrogen bound fuel from different fuel sources [19]

FUEL TYPE	PERCENTAGE OF FUEL BOUND NITROGEN (WEIGHT%, DRY, ASH FREE BASIS)
COAL	0.5-2.0
BIOMASS (WOOD)	< 0.5
PEAT	1.5-2.5
FUEL OIL	0.0
NATURAL GAS	0.0
DERIVED GASES	0.1-1.0 (>>1 chemical sources)

Due to the fact that hydrocarbon fuel contains organic bonded nitrogen (organic nitrogenous compounds) some of the in-oxidized nitrogen will eventually be oxidized to be NO_X. The percentage amount of nitrogen going through this process depends on the nature of the combustion process. This is compounded by the fact that light distillate fuels contain 0.06 % by volume of organic hydrogen, while the heavy distillates contain 1.5 % or above. Thus, it can clearly be seen that depending on the amount of or percentage of nitrogen converted into fuel, NO_X can contain large portions of and percentages of total NO_X emissions [20].

The oxidation of the nitrogenous compounds is known to be less temperature dependent; thus, oxidation can even occur at low temperatures as the air excess ratio increases. However, during combustion a portion of the nitrogen fuel is changed to NO_X especially in fuel rich areas of combustion where thermally formed NO_X can be reduced to molecular nitrogen [21] as demonstrated by Figure 1 with the reactions taking the following forms:

$$NH_2 + \frac{1}{2}O \rightarrow NO + H_2 \qquad \text{Equation 15}$$

$$NH_3 \rightarrow \frac{1}{2}N_2 + 1\frac{1}{2}H_2 \qquad \text{Equation 16}$$

$$NO + CO \rightarrow \frac{1}{2}N_2 + CO_2 \qquad \text{Equation 17}$$

$$HCN + 2NO \rightarrow 1\frac{1}{2}N_2 + CO_2 + \frac{1}{2}H_2 \qquad \text{Equation 18}$$
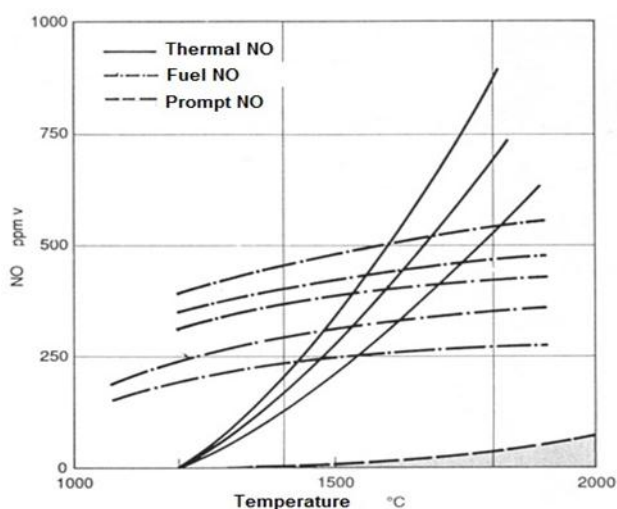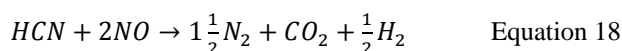
Figure 1: The relationship between temperature and NO_X formation, the air excess factor also known as the oxygen excess factor, and the parameters of thermal NO_X formation, fuel NO_X and prompt NO_X [22]

From Figure 1 we can see the relationship between combustion and the NO_X formation path. The figure shows a positive correlation between fuel and prompt NO_X with temperature that is almost linear with the amount or quantity of thermal NO_X increasing disproportionately with increasing combustion temperature. In addition, the figure shows that those areas where there is a rich fuel-air ratio naturally have reduced oxygen availability, thus making insufficient oxygen available

to react with the molecular nitrogen (N_2) in the combustion mixture, leading to reduced fuel conversion and thermal NO_X.
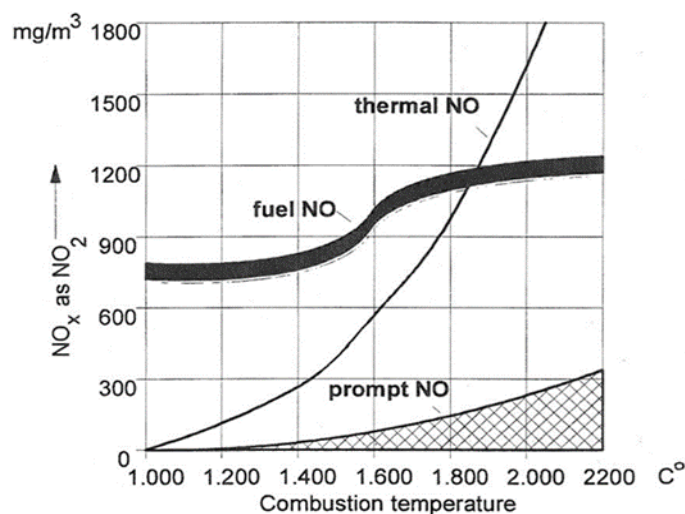
Figure 2: The relationship between the various types of NO_X formation under the influence of varying combustion temperature ranges

Figure 2 shows the relationship between the various types of NO_X formation under the influence of varying combustion temperature ranges where thermal NO_X, prompt NO_X and fuel NO_X set in, and the quantity of NO_X emissions produced under varying temperatures. A conversion mechanism of NO_X from fuel bound nitrogen shows the following trends and characteristics as can be seen in Figure 2 above as suggested by [23]:

- Conversion of fuel based nitrogen to NO_X is practically complete for fuel lean flames operating on low nitrogen concentrations of $< 0.5\%$ by weight ratio.
- Conversion increases slowly with increase in flame temperatures as indicated by all routes and mechanisms of NO_X formation in preceding sections and Figure 2.
- The composition of the nitrogen bearing compounds do not have any effect on the nitrogen bound fuel conversion rate percentage.

It is imperative to mention here that according to Figure 1, the temperature range at which fuel NO_X sets in is relatively higher than the prompt NO_X, but it is less than the thermal NO_X formation temperatures which kick in at temperatures exceedingly 1800 ^{0}C. Table 1 shows that fuels with a high nitrogen content have a natural inclination to produce more NO_X emissions than those with a low nitrogen content. However, it is important to note that in diesel propelled engines NO_X formation from nitrogen fuel is strongly controlled and overlapped by thermal NO_X formation, therefore there is no guarantee that low nitrogen fuel content would not cause high production of NO_X emissions.

THE EFFECTS OF OXIDES OF NITROGEN

The oxides of nitrogen are recognised now as causing negative effects for human health and the natural environment. The harmful effects of oxides of nitrogen pollution do not necessarily take effect immediately after exposure, but after prolonged exposure. In the environment, oxides of nitrogen pollutants are known to cause destruction of the ozone layer, acid rain, poor visibility due to smog, poor air quality, and they contribute to the rise in earth surface temperatures leading to global warming, All these effects cause serious environmental degradation and poor human health, thereby increasing the rate of natural disasters and the global health burden, requiring billions of dollars for repair and reconstruction of the destroyed environment and of health.

Global Warming

Among the fundamental effects of oxides of nitrogen emission is global warming, although these are not the only emissions that contribute to global warming of the earth's surface. The stratosphere ozone layer is destroyed by oxides of nitrogen emissions therefore increased high energy ultra-violet rays (UV) warm up the earth's surface due to the decreased reflective capacity of the lower atmospheric layers.

The increase in earth's surface temperature has serious repercussions, shifting the climatic zones and thus shifting habitable regions of the earth leading to increase of the deserts and increasing the unpredictability of the weather patterns. For example, flooding and an increase in the intensity of typhoons have been witnessed in recent times or example in the USA (hurricane Katrina) and in the Philippines (typhoon Haiyan), leaving behind massive destruction of infrastructure, life and economies of the hit areas [24].

Smog and Visibility

Smog is a combination of smoke and fog and represents cloud formation from photochemical reactions of the sun with the hydrocarbons and oxides of nitrogen emission effluents from automobiles and stationary engines. Besides automobiles, smog can also be derived from other sources like coal emissions, industrial emissions, frost, agricultural fires and natural causes. Smog irritates eyes and the throat, and causes impairment to the lungs decreasing capacity, emphysema, bronchitis, asthma, inflammation of the breathing passages, shortness of breath, damages plants and crops, and destroys rubber products by cracking them through deterioration. One of the major impacts of smog has been poor visibility in cities such as Beijing (China), New Delhi (India), and London (United Kingdom) amongst others. Poor visibility is caused by nitrogen oxide absorbing the full visible spectrum of the light energy, thus leading to poor visibility even in the absence of particulate matter (PM) that would cause physical absorption of light.

The Ozone

The tremendous increase in the urbanization has seen an increase in energy consumption putting millions of cars on the road [25, 24]. As a consequence, many cities are feeling pressure from severe air pollution and air quality. The oxides of nitrogen are key to the formation of ozone and aerosols ($PM_{2.5}$) in the atmosphere which have a negative effect on air quality, acid deposition and the balance of atmospheric radiation [24].

The consequence of the anthropogenic pollutants like NO_X in decreasing the thermal layering of the stratosphere and increase of earth's surface temperatures cannot be over-emphasized. Animals, plants and humans are known to be sensitive to UV-B and UV-C rays of radiation which are richer in radiation energy. Exposure to a concentration level of 2500 $\mu m/m^3$ of NO_X for one-hour decreases a human being's lung volume and maximum breathing thus impairing breathing and can lead to death, while exposure to ozone causes pulmonary haemorrhage with symptoms such as a dry throat, severe headache, disorientation and altered breathing patterns.

Toxicity

Nitrogen dioxide is a very toxic gas which irritates the entire pulmonary system. Though little is known by what mechanism it causes toxicity, high concentrations have been known to cause pulmonary oedema which is an abnormal accumulation of fluid in the pulmonary tissues [26]. In humans, oxides of nitrogen interact with vitamin B12 leading to selective inhibition of methione synthase, with long exposure leading to megaloblastic bone marrow depression and other neurological diseases [27].

Acid Rain

The accumulation of oxides of nitrogen in the atmosphere increases acid deposition which tends to decrease ecosystem stability. Acid rain is caused by a chemical reaction which starts first with sulphur dioxide compounds reacting with oxides of nitrogen that have been released to the stratosphere [28]. Sulphur dioxide and oxides of nitrogen react and dissolve in water and can be transported by wind. Once they mix and react in the presence of moisture they form more pollutants with the result being acid rain [29]. Human activities, which release various chemicals into the air, are the main cause of acid.

The major contributors and sources of sulphur dioxide (SO_2) and oxides of nitrogen (NO_X) are:

- Burning fossil fuels to generate power and electricity, producing two thirds of the sulphur dioxide and a quarter of oxides of nitrogen in the atmosphere.
- Heavy duty equipment and vehicles.
- From manufacturing industries, oil refineries and other industrial manufacturing processes.

There are two forms of acid deposition mechanisms – wet deposition and dry deposition. The former is where sulphuric acid and nitric acid in the atmosphere fall to the ground in the form of rain, snow, fog or hail, and the latter is when acidic particles and gases deposit on surfaces of water bodies, on vegetation and buildings in the absence of moisture but quickly react during atmospheric transportation to form particles that can harm human health. The dry mechanism largely depends on the amount of rainfall an area receives to cause maximum effect.

FACTORS OF NO_X EMISSIONS AND CONTROL

NO_X or oxides of nitrogen emissions control is the most difficult problem engineers and environmentalists have been grappling with since the discovery of the automobile, since most control methods tend to present additional problems in their own right. Most control systems will either increase fuel consumption or introduce new forms of emissions. However it is important to note that NO_X emissions can only be obtained by carefully considering air-fuel ratios, combustion and exhaust temperatures, design features that will reduce quench zones, fuel injection timing, fuel injection rate, compression ratios, catalytic reductants and convertors, exhaust gas recirculation systems, and advanced combustion control strategies. No single method can handle the issue of NO_X emissions efficiently, but by combining two or more of these methods, the objective of reducing NO_X emissions can be achieved. The following sections will endeavour to discuss some of the methods that have been developed to mitigate the emissions of NO_X and show that through a multiple approach this objective is achievable.

Injection Timing

Injection timing is one of the most influential factors in control of oxides of nitrogen emissions, especially in lean burn diesel engines, also known as direct injection compression ignition (DICI) engines, or their variant, indirect injection compression ignition (IDICI) engines. By retarding ignition or injection timing, significant reduction of oxides of nitrogen emissions can be achieved [30, 31] and as shown in Figure 3.

It is observed from Figure 3 that advancing the injection timing or the SOI causes an increase in NO_X emissions for all the test fuels covered by the study under multiple injection schemes. This can be explained by the fact that ignition and combustion then occur much earlier leading to early peak pressure as the piston approaches top dead centre (TDC), thus causing a rapid increase in combustion temperatures which promotes NO_X via the thermal mechanism also known as the Zeldovich mechanism.
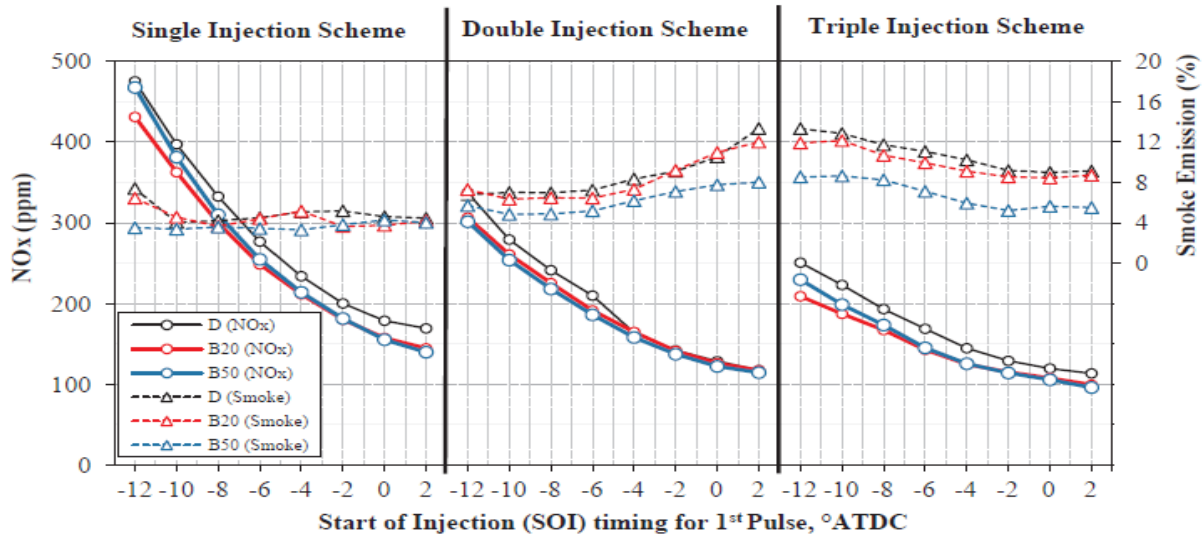
Figure 3: Effects and influence of start of injection (SOI) timings and injection timing strategies on NO$_X$ and smoke emission reduction for various diesel fuel blends compared to conventional diesel [31].

Injection Rate

The rate of injection determines the level and quantity of emissions of oxides of nitrogen. This is due to an increase in the mixing time or ignition delay during the injection period which gives a very hot flame when combustion occurs, thus a greater quantity of NO$_X$ emission are released to the environment [32]. Research conducted so far points to the successful reduction in the NO$_X$ emissions by use of this strategy [33, 34].
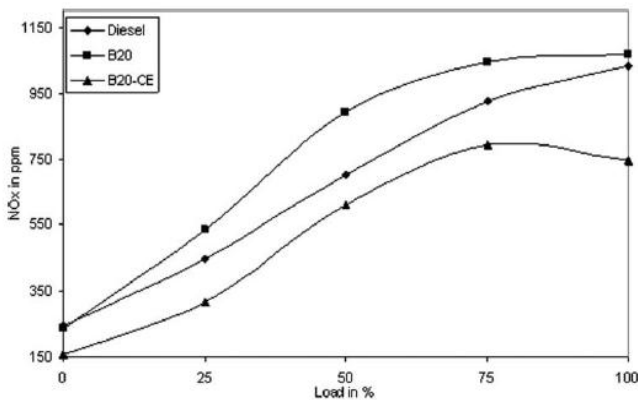
Figure 4: NO$_X$ emissions at different engine loads of 25%, 50%, 75% and 100%, with application of EGR of 15% and injection pressure rate of 240 bar, with two diesel blends of B20, B20-CE and conventional diesel at normal operating conditions.

Considering the effects of oxides of nitrogen on the environment, it is important to note from Figure 4 above that diesel engines working to move goods and services normally operate at injection timings slightly retarded from the best fuel economy timing. Indirect injection (IDICI) engines have a lower NO$_X$ emission level due to the fact that their retarding is greater than direct injection (DICI) engines with common values for BTDC being 2^0 and as late as 5^0 ATDC without an effect on fuel economy. Continued retardation is observed to continue reducing NO$_X$ emissions but creates more hydrocarbon emissions and particulate matter (PM) emissions.

The NO$_X$ emissions in Figure 4 were observed to significantly reduce with the combined effect of EGR, injection pressure and injection timing, with reduced injection rate showing an increase in the NO$_X$ emissions as compared to high injection pressure [35].

The Air-Fuel Ratio

Any change to the air-fuel ratio mixture affects the combustion temperature which in turn affects the formation of NO$_X$ because it is a temperature dependent function as aforementioned. Therefore, an increase in air-fuel ratio achieved by decreasing the air amount in the mixture increases the amount of oxides of nitrogen. At higher fuel-air ratios the additional fuel has a tendency to cool the intake charge mixture temperatures, resulting in a drop in local peak temperatures within the combustion area, which decreases the NO$_X$ concentrated emissions. However, IDICIs behave differently due to the presence of a pre-chamber unit where the pre-chamber tends to operate in rich fuel situations and conditions, thus producing less NO$_X$ emissions [36, 37].

In diesel engines both air mass flow rate $\dot{m}_a$ and the fuel mass flow rate $\dot{m}_f$ are measured parameters, with most modern diesel engines running on an air-fuel ratio of lambda λ between 1.65 to 1.10, with the lowest fuel consumption occurring at $\lambda = 1.65$. This ratio of the flow rate is vital when defining engine operating conditions [18] as shown in these two equations:

$$A/F = \frac{\dot{m}_a}{\dot{m}_f} \text{ (air/fuel)} \qquad\qquad \text{Equation 19}$$

$F/A = \dfrac{\dot{m}_f}{\dot{m}_a}$ (fuel/air)   Equation 20

The Compression Ratio

The compression ratio is defined as the ratio of the volume of the cylinder and of the combustion chamber of the cylinder head when the cylinder piston is at bottom dead centre (BDC) to the volume of the cylinder and of the combustion chamber of the cylinder head when the cylinder piston is at top dead centre (TDC), as shown on Figure 5 below.
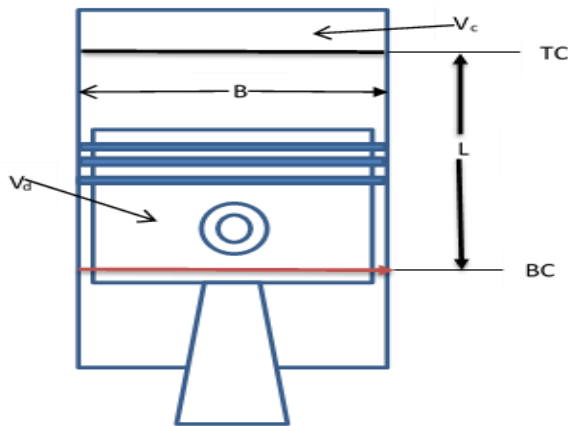
Figure 5: Schematic diagram of an engine theoretical cylinder and the cylinder head showing the definition of the compression ratio. Where TC is top dead centre, BC is bottom dead centre, V_c is clearance volume, B is the cylinder bore, L is the stroke and V_d is the swept or the displaced volume.

The compression ratio (r_c) thus can be expressed in equation form as:

$r_c = \dfrac{V_d + V_c}{V_c}$ Equation 2
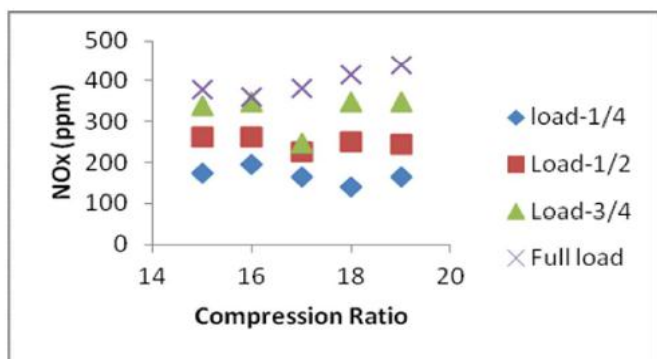
Figure 6: Effects of the compression ratio on NO_X formation, at different engine loads

The increase in the compression ratio in Figure 6 shows that the combustion duration also decreases by almost 2^0CA to 3^0CA, due to the decrease in ignition delay which is a crucial factor of compression ratio in compression ignition engines [38].

Increasing the compression ratio increases the power created by the higher thermal efficiency that accrues due to the increase in the compression ratio. However, it is noticed that a continued increase in the compression ratio increases NO_X emissions by increasing the cycle temperatures [39].

4.5 The Catalysts

As a means of reducing NO_X emissions in automobiles (both heavy and light duty) and stationary engines, several kinds of catalytic converters have been developed to reduce the NO_X emissions in the presence of oxygen within the normal operating conditions of diesel engines, achieving some very positive results especially when used in tandem with other NO_X control systems or in combination with themselves. Currently the most commonly used catalytic systems in diesel engines are selective catalyst reduction (SCR), diesel oxidation catalyst (DOC), and diesel particulate filter (DPF)

Their main function is to oxidize HC, CO and NO_X emissions through chemical reactions in the presence of oxygen thus rendering NO_X emissions ineffective and low or eliminating them altogether, or, in the case of the diesel particulate filter, clean particulate matter emissions. Figure 7 below shows how a diesel oxidation filter works in schematic diagram form.
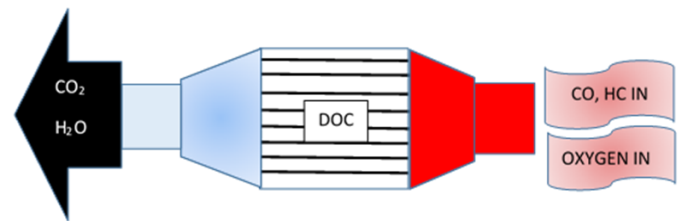

Figure 7: Schematic diagram of a diesel oxidation catalyst (DOC) and its operation in reducing emissions of CO and HC through the process of oxidation.

Exhaust Gas Recirculation (EGR)

EGR is a method of NO_X control that has increasingly become very effective and is widely used in the control and reduction of NO_X emissions in tandem with other NO_X control systems. The system works by recirculating a portion of the exhaust gases into the combustion chamber for reburning together with the fresh intake charge. Since NO_X is a temperature dependent function, EGR's main function therefore is to reduce the combustion temperatures gases for a given mass of fuel and oxygen that is burnt in the combustion chamber. However, while it is effective as a measure to control NO_X emissions, it has demerits because it tends to increase CO and PM emissions, thus limiting the extent to which it can be applied and recirculated, to about 30%.
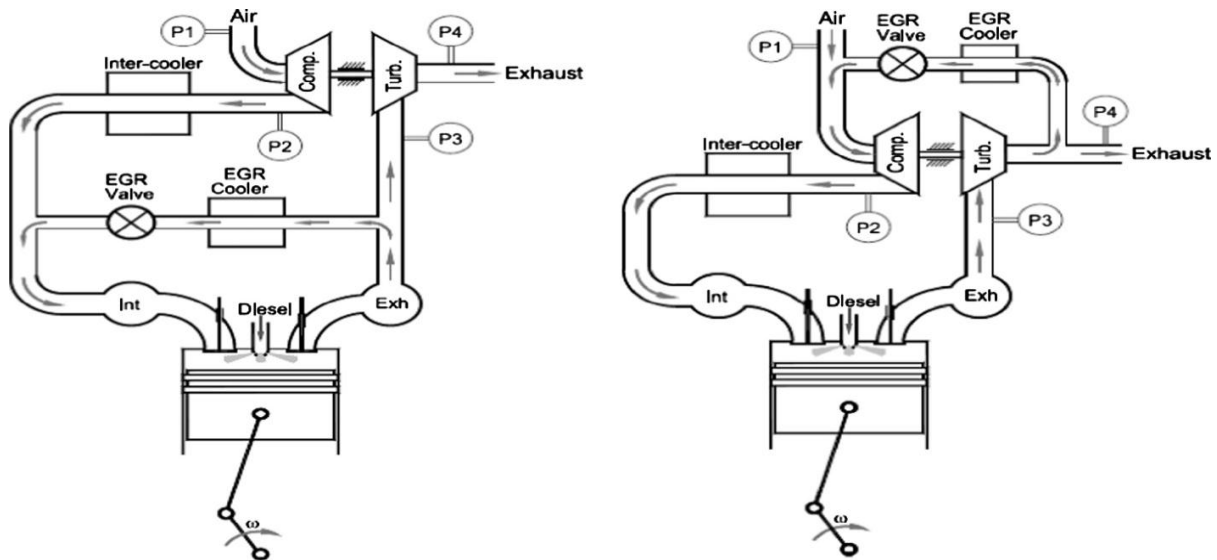
Figure 8: Two types of EGR systems in use today, where if P_3-P_2>0 the delivery arrangement pipe is shorter hence the name short part (HPL)EGR, the long part arrangement (LPL)EGR is where the exhaust gases are taken from down stream of the compressor turbine and the pressure values P_3-P_2<0 [40].

CONCLUSION

This work points out that human activities are the major source of oxides of nitrogen, especially from power generation and from power propulsion for the transport industry.

Although the effects of air pollution and environmental degradation on material, plants and animals can be measured and quantified, the effects of oxides of nitrogen emissions can only be estimated in humans from the epidemiological evidence which comes on later after exposure to high levels of NO_X concentrations.

The main significant oxides of nitrogen responsible for the pollution of the air, environmental degradation, human and animal health are nitric oxide and nitrogen dioxide.

All evidence available on the effects of NO_X emissions pollution so far provided indicate that high levels of NO_X concentrations are a threat to human and animal health, besides posing an immediate danger to the natural environment, therefore if measures are not implemented and attitudes changed, damage will continue and will increase.

The control measures discussed in the preceding sections cannot operate effectively and efficiently alone to deal with the problem of NO_X emissions but require to be included in a multifaceted approach rather than as standalone control mechanisms. Therefore, this calls for integration of all players in the transport, manufacturing, research and development, and the environmental protection agencies to harness their synergies in dealing with the problem of NO_X emission in the transport industry.

Adoption of the control measures discussed and highlighted in this work in sections 4.0 to section 4.6, will reduce and mitigate the effects of air pollution and general degradation of the natural environment.

More resources need to be allocated for research and development, so that continued studies can be conducted on those methods of NO_X control that have proved useful and efficient in dealing with the problem of emission, at the same time affording young researchers an opportunity to carry out experiments and collect data that can be useful in development of these methods and protecting the environment.

REFERENCES

[1] Geng, P., Cao, E., Tan, Q., and Wei, L., 2016, "Effects of Alternative Fuels on the Combustion Characteristics and Emission Products from Diesel Engines: A Review," Renewable and Sustainable Energy Reviews, 71, pp. 523-224.

[2] Özgür, T., Tosun, E., Özgür, C., Tüccar, G., and Aydın, K., 2017, "Performance, Emission and Efficiency Analysis of a Diesel Engine Operated with Diesel and Diesel-Ethanol (e20) Blend," MATTER: International Journal of Science and Technology, 3(3).

[3] Abdelaal, M., and Hegab, A., 2012, "Combustion and Emission Characteristics of a Natural Gas-Fueled Diesel

Engine with EGR," Energy Conversion and Management, 64, pp. 301-312.

[4] Asad, U. and Zheng, M., 2014, "Exhaust Gas Recirculation for Advanced Diesel Combustion Cycles," Applied Energy, 123, pp. 242-252.

[5] Semakula, M. and Inambao, F., 2017, "The Effects of Exhaust Gas Recirculation on the Performance and Emission Characteristics of a Diesel Engine – A Critical Review," International Journal of Applied Engineering Research, 12(23), pp. 13677-13689.

[6] Azad, A., Rasul, M., Khan, M., Sharma, S. C., and Bhuiya, M., 2016, "Recent Development of Biodiesel Combustion Strategies and Modelling for Compression Ignition Engines. Renewable and Sustainable Energy Reviews, 56, pp. 1068-1086.

[7] Qiu, L., Cheng, X., Liu, B., Dong, S., and Bao, Z., 2016, "Partially Premixed Combustion Based on Different Injection Strategies in a Light-Duty Diesel Engine," Energy, 96, pp. 155-165.

[8] Fenimore, C., 1971, "Formation of Nitric Oxide in Premixed Hydrocarbon Flames," Paper presented at the Thirteenth Symposium (International) on Combustion, The Combustion Institute, Pittsburgh.

[9] Correa, S. M., 1993, "A Review of NOx Formation under Gas-Turbine Combustion Conditions," Combustion Science and Technology, 87(1-6), pp. 329-362.

[10] Turns, S. R., 1996, An Introduction to Combustion (Vol. 287), McGraw-Hill, New York.

[11] Dangar, H., and Rathod, G. P., 2013, "Combine Effect of Exhaust Gas Recirculation (EGR) and Varying Inlet Air Pressure on Performance and Emission of Diesel Engine," IOSR Journal of Mechanical and Civil Engineering (IOSR-JMCE), 6(5), pp. 26-33.

[12] Li, L., Wang, J., Wang, Z., and Liu, H., 2015, "Combustion and Emissions of Compression Ignition in a Direct Injection Diesel Engine Fueled with Pentanol," Energy, 80, pp. 575-581.

[13] Bowman, C. T. 1992, "Control of Combustion-Generated Nitrogen Oxide Emissions: Technology Driven by Regulation," Paper presented at the Twenty Fourth Symposium (International) on Combustion, The Combustion Institute, Pittsburgh

[14] Konnov, A., Colson, G., and De Ruyck, J., 2000, "The New Route Forming NO via NNH," Combustion and flame, 121(3), pp. 548-550.

[15] Westbrook, C. K., and Dryer, F. L., 1981, "Simplified Reaction Mechanisms for the Oxidation of Hydrocarbon Fuels in Flames," Combustion science and technology, 27(1-2), pp. 31-43.

[16] Rutar, T., Lee, J. C. Y., Dagaut, P., Malte, P., and Byrne, A., 2007, "NOx Formation Pathways in Lean-Premixed-Prevapourized Combustion of Fuels with Carbon-To-Hydrogen Ratio Between 0.25 and 0.88," Proceedings of the Institution of Mechanical Engineers, Part A: Journal of Power and Energy, 221(3), pp. 387-398.

[17] Pulkrabek, W. W., 2014, Engineering Fundamentals of the Internal Combustion Engine, Pearson Prentice Hall, Upper Saddle River, NJ.

[18] Heywood, J. B., 2012, Internal Combustion Engine Fundamentals, (Vol. 930), Mcgraw-Hill, New York.

[19] Dzurenda, L., Hroncová, E., and Ladomerský, J., 2016, "Extensive Operating Experiments on the Conversion of Fuel-Bound Nitrogen into Nitrogen Oxides in the Combustion of Wood Fuel," Forests, 8(1), p. 1.

[20] Lamoureux, N., El Merhubi, H., Pillier, L., de Persis, S., and Desgroux, P., 2016, "Modeling of NO Formation in Low Pressure Premixed Flames," Combustion and Flame, 163, pp. 557-575.

[21] Harrison, R. M., 2001, Pollution: Causes, Effects and Control, Royal Society of Chemistry, Harrison, R. M., 2001, "Pollution: Causes, Effects and Control: Royal Society of Chemistry, London.

[22] Merryman, E. L., and Levy, A., 1975, "Nitrogen Oxide Formation in Flames: the Roles of NO2 and Fuel Nitrogen," Paper presented at the Symposium (international) on combustion.

[23] Lefebvre, A. H., 1998, Gas Turbine Combustion, CRC press, Boca Raton, Florida.

[24] Climate Council. 2016, "Global Heat Record Broken Again," Potts Point, Australia: Climate Council.

[25] Huang, J., Zhou, C., Lee, X., Bao, Y., Zhao, X., Fung, J., . . . Zheng, Y., 2013, "The Effects of Rapid Urbanization on the Levels in Tropospheric Nitrogen Dioxide and Ozone over East China," Atmospheric Environment, 77, pp. 558-567.

[26] Ferner, R. E., Mackenzie, A. A., and Aronson, J. K., 2014, "The Adverse Effects of Nitrous Oxide," Adverse Drug Reaction Bulletin, 285(1), pp. 1099-1102.

[27] Morris, N., Lynch, K., and Greenberg, S. A., 2015, "Severe Motor Neuropathy or Neuronopathy due to Nitrous Oxide Toxicity after Correction of Vitamin B12 Deficiency," Muscle & Nerve, 51(4), pp. 614-616.

[28] Rajagopalan, R., 2015, "Environmental Studies: from Crisis to Cure, Oxford University Press, Oxford.

[29] Sivaramanan, S., 2015, "Acid Rain, Causes, Effects And Control Strategies, DOI: 10.13140/RG.2.1.1321.4240/1.

[30] How, H., Masjuki, H., Kalam, M., and Teoh, Y., 2018, "Influence of Injection Timing and Split Injection Strategies on Performance, Emissions, and Combustion Characteristics of Diesel Engine Fueled with Biodiesel Blended Fuels," Fuel, 213, pp. 106-114.

[31] Hwang, J., Qi, D., Jung, Y., and Bae, C., 2014, "Effect of Injection Parameters on the Combustion and Emission Characteristics in a Common-Rail Direct Injection Diesel Engine Fueled with Waste Cooking Oil Biodiesel," Renewable Energy, 63, pp. 9-17.

[32] Wang, Q., Shao, C., Liu, Q., Zhang, Z., and He, Z., 2017, "Effects of Injection Rate on Combustion and Emissions of a Pilot Ignited Direct Injection Natural Gas Engine," Journal of Mechanical Science and Technology, 31(4), pp. 1969-1978.

[33] Can, Ö., Öztürk, E., and Yücesu, H. S., 2017, "Combustion and Exhaust Emissions of canola Biodiesel Blends in a Single Cylinder DI Diesel Engine," Renewable Energy, pp. 109, 73-82.

[34] Can, Ö., Öztürk, E., Solmaz, H., Aksoy, F., Çinar, C., and Yücesu, H. S., 2016, "Combined Effects of Soybean Biodiesel Fuel Addition and EGR Application on the Combustion and Exhaust Emissions in a Diesel Engine," Applied Thermal Engineering, 95, pp. 115-124.

[35] Saravanan, S., Nagarajan, G., and Sampath, S., 2013, "Combined Effect of Injection Timing, EGR and Injection Pressure in NOx Control of a Stationary Diesel Engine Fuelled with Crude Rice Bran Oil Methyl Ester," Fuel, 104, pp. 409-416.

[36] Noor, M., Wandel, A. P., and Yusaf, T., 2014, "Effect of Air-Fuel Ratio On Temperature Distribution and Pollutants for Biogas MILD Combustion," International Journal of Automotive and Mechanical Engineering, 10(1), pp. 1980-1992.

[37] Asad, U., Divekar, P., Zheng, M., and Tjong, J., 2013, "Low Temperature Combustion Strategies for Compression Ignition Engines: Operability Limits and Challenges," DOI: https://doi.org/10.4271/2013-01-0283.

[38] Kumar, N. R., Sekhar, Y., and Adinarayana, S., 2013, "Effects of Compression Ratio and EGR on Performance, Combustion and Emissions of DI Injection Diesel Engine," International Journal of Applied Science and Engineering, 11(1), pp. 41-49.

[39] Gnanamoorthi, V., and Devaradjane, G., 2015, "Effect of Compression Ratio on the Performance, Combustion and Emission of DI Diesel Engine Fueled with Ethanol–Diesel Blend," Journal of the Energy Institute, 88(1), pp. 19-26.

[40] Thangaraja, J. and Kannan, C., 2016, "Effect of Exhaust Gas Recirculation on Advanced Diesel Combustion and Alternate Fuels – A Review," Applied Energy, 180, pp. 169-184.

CHAPTER SEVEN

Influence of Exhaust Gas Recirculation and Emission Characteristics of a Diesel Engine Using Pyrolyzed Waste Plastic Biodiesel and Blends

Journal article

Influence of Exhaust Gas Recirculation and Emission Characteristics of a Diesel Engine Using Pyrolyzed Waste Plastic Biodiesel and Blends

Semakula Maroa[1]and Freddie Inambao[2]

[1, 2] *University of KwaZulu-Natal, Durban South-Africa.*
ssemakulamaroa@gmail.com; inambaof@ukzn.ac.za

Abstract

Waste plastic pyrolysis biodiesel fuels have characteristics and qualities which are identical to conventional petroleum fuels. This work studied the influence of exhaust gas recirculation (EGR) on performance and emission characteristics of a diesel engine using biodiesel from Pyrolyzed waste plastics and blends compared to conventional diesel. There are a limited number of experimental works on waste plastic pyrolysis, especially the interaction, influence and effects of EGR on diesel engines. The results show that the amount of carbon monoxide (CO) emissions seemed to decrease at low engine loads up to intermediate loads (50 %), thereafter continued to increase significantly and marginally. Among the blends WPPOB100 reported the highest BSFC with a value of 0.4751 g/kW.hr at 0 % EGR flow rate compared to 0.7235 g/kW.hr at 30 % EGR flow rate. The increase in blend ratio showed a direct decrease in brake power (BP) in a linear relationship. At 30 % engine load conventional diesel (CD), WPPOB10, WPPOB20, WPPOB30 and WPPOB40 had values of 2.125 kW, 2.15 kW, 2.05 kW, 1.98 kW, 1.86 kW and 1.75 kW respectively. Regarding exhaust gas temperature (EGT), the WPPOB10 blend at 30 % EGR flow rate had the greatest reduction in temperature compared to the other WPPO blends with a temperature value of 320 ^{0}C. For unburnt hydrocarbon (UHC) emissions, EGR flow rates of CD at 5 %, 10 %, 15 %, 20 %, 25 % and 30 %, had 43 ppm, 57 ppm, 70 ppm, 82 ppm and 85 ppm respectively, compared to WPPOB10 whose values were 23 ppm, 35 ppm, 40 ppm, 48 ppm, 50 ppm, and 52 ppm respectively. All the fuels tested indicated a drop in nitrogen oxide (NO_X) emissions with an increase in the application of EGR % flow rate, at all engine load conditions. The WPPO blends were observed to produce a continuous increase in smoke emission to almost double the values with the application of EGR flow rate. At 10 % CO emission values were 9.79 %, 10.46 %, 10.91 %, 11.25 % and 12.75 % for WPPO10, WPPO20, WPPO30, WPPO40 and WPPO100 respectively. The higher the blend ratio and the higher the increase in EGR % flow rates, the higher the carbon dioxide (CO_2) emission values and vice versa. At 30 % EGR flow rate the CO_2 emissions for CD were 10.95 % compared to WPPOB10 9.95 %, WPPOB20 9.65 %, WPPOB30 8.85 % with WPPOB100 showing the highest value of 14.35 %. Increased blend ratio and EGR % flow rate showed a steady increase in the smoke emissions within the test fuels with marginal decreases observed across all the blended fuels. At 15 % EGR flow the values were 7.53 %, 7.1 %, 6.72 %, 6.25 %, 6.0 % and 5.4 % for CD, WWPO10, WPPO20, WPPO30, WPPO40 and WPPO100 respectively.

ABBREVIATIONS

R_X	Molar Gas Ratio
n_f	Fuel Molar Quantity
Al_2O_3,	Aluminium Tri-Oxide
ASTM	American Society for Testing and Materials
BP	Brake Power
BSFC	Brake Specific Fuel Consumption
BTE	Brake Thermal Efficiency
CaO	Calcium Oxide
CD	Conventional Diesel
CO	Carbon Monoxide
CO_2	Carbon Dioxide
Cu	Copper
DEA	Department of Environmental Affairs
EGR	Exhaust Gas Recirculation
EGT	Exhaust Gas Temperature
FBP	Final Boiling Point
G-20	Group of 20 Highly Industrialized Countries
G-7	Group of 7 Developed and Industrialized Countries
GC-MS	Gas Chromatography Mass Spectrometry
GVC	Gross Calorific Value
HPDE	High-Density Polyethylene
HRR	Heat Release Rate
IBP	Indicated Brake Power
SiO_2	Silica Dioxide
kW	Kilowatt
LPG	Liquid Petroleum Gas
LTC	Low Temperature Combustion
MSW	Municipal Solid Waste
$NaAlSi_2O_6$-H_2O	Zeolite

NO$_X$	Oxides Nitrogen
PEHD	Polyethylene High-Density
PM	Particulate Matter
PVC	Poly Vinyl Chloride
UHC	Unburnt Hydrocarbons
WPPO	Waste Plastic Pyrolysis Oil
x	Exhaust Molar Gas Quantity
y	Inlet Intake Molar Gas Quantity
z	Remainder of the Intake Charge

INTRODUCTION

The importance of modern day transport systems cannot be overstated, especially the transportation of goods and services and people. The propulsion provided by internal combustion engines with diesel fuel as the primary source of energy forms the bulk of commercial use and personal transport, owing to their numerous advantages of this fuel. Diesel engines are inherently lean burn engines, and emit relatively low carbon dioxide (CO_2) emissions compared to petrol propelled internal combustion engines. Other advantages offered by diesel engines include high thermal efficiencies, durability and construction robustness [1]. These advantages mean that the use of such engines is increasing as more countries move into urbanization and industrialization and catch up with the highly industrialized countries. However, there is now a challenge to phase them out based on environmental and human health issues due to the high levels of nitrogen oxide (NO$_X$), smoke and particulate matter (PM) emissions.

There has been an increase in stringent emission regulations enacted by global industrial powers such as the United States of America, the European Union and the G-7 and G-20. Diesel engines have been identified as a major source of pollution due to their emission of NO$_X$ gases, so now alternative fuels are being sought in the interest of reducing energy consumption as well as reducing environmental degradation. The rapid expansion of the road transport industry sector is fast eroding all the technological developments and improvements thus far achieved in the war against pollution from diesel propelled engines. Issues relating to climatic change, uncontrolled or erratic energy prices, uncertainty of future fossil fuel supplies [2] and unending internal conflicts and war in major oil producing countries create a very compelling case for alternative fuels.

Due to the increase in food insecurity the production of biodiesel fuel from plant based stocks is a less viable option because of its impact on higher food prices [3]. Therefore, waste plastic from municipal solid waste management sites is increasingly being considered as an alternative source of fuel and energy due to the widespread availability of plastics and their cost of disposal and negative effect on the environment. There are two types of plastics widely used today, namely: PVC (poly-vinyl chloride) and HPDE (High-density polyethylene) also known as polyethylene high-density (PEHD) [4]. Plastic

waste wreaks havoc on the environment because plastics are petroleum based which makes them non-biodegradable [5]. Plastic waste accounts for between 8 % to 12 % of global waste with a projected increase of between 9 % to 13 % annually by the year 2025 [6] and [7]. According to a study conducted in India, nearly 5.6 million metric tonnes of plastic waste are generated every year out of which only a paltry 10 % is recirculated, while 80 % goes into landfills which causes pollution. In South Africa 24 115 402 metric tonnes of general waste is produced annually, of which 6 % (1 446 924 metric tonnes) was plastic waste with a national average waste production annual increment projection of 2 % to 3 % since 2008 [8], as shown in Figure 1. These figures support the case for using technology to degrade waste plastic mass into energy. Techniques such as pyrolysis can yield hydrocarbons similar in quality and characteristics to petroleum fuels [9] and [10].
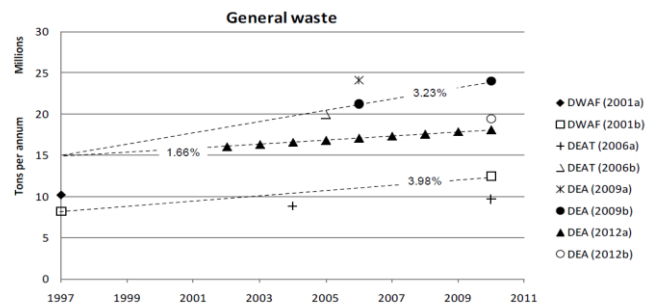
Figure 1 Analysis of available general waste data (from municipalities) in South Africa [8]

Pyrolysis is a word originally coined from two Greek words pyro "fire" and lysis "decomposition" [11]. It is a chemical decomposition process which makes fuel from plastic waste by heating and has been commended by [12] as one of the solutions to management of the menace of plastic waste. During the pyrolysis process, assorted waste plastics are introduced and fed into a reactor and subjected to high temperatures of 400 ^{0} C to 600 ^{0} C and sometimes up to 900 ^{0} C at atmospheric pressure in the absence of oxygen for 3 to 4 hours [13] to produce oil and other by-products. In order to maintain and sustain high temperatures during the pyrolysis reaction, [14] catalysts are therefore employed, including calcium oxide (CaO), silica dioxide (SiO_2), aluminium tri-oxide (Al_2O_3) and zeolite ($NaAlSi_2O_6$-H_2O) [15]. This process breaks down large molecules of waste into minute molecules resulting in hydrocarbons with a smaller molecular mass. For example, the addition of ethane enables fractional distillation to be applied and to obtain fuels, chemicals and by-products from the process. Pyrolysis as a process gives yields with a weight factor of 75 % of liquid hydrocarbons in a mixture of petrol, diesel and kerosene, 5 % to 6 % as residue coke and the remaining balance as liquefied petroleum gas (LPG) [16]. Pyrolysis as a method of producing waste plastic biodiesel is highly recommended by most researchers and commercial entities because of its cost effectiveness and its high energy conversion rate, besides the high yield when compared to any other method of plastic waste energy extraction [17].

The use of biodiesel calls for NO_X reduction techniques such as exhaust gas recirculation (EGR) due to the oxygen content inherent in most biodiesel fuels which is the single most important factor responsible for NO_X formation as it reacts with high temperature combustion mixtures thereby increasing the availability of NO_X [7]. Diesel fuels and biodiesel fuels both require fuel additives to improve engine lubricity, better ignition qualities and better mixing. Oxygenates in biodiesels are providing a promising future to reduce PM emissions since the O_2 content aids in better combustion, besides lowering exhaust emissions with a clear trade-off between PM and NO_X as suggested in the findings of [18], [19] and [20]. Most researchers suggest modifications, for example thermal barrier coating by [21], where efficiency is improved, and NOx emissions and smoke density are reduced with a minimal increase in brake thermal efficiency (BTE), although fuel economy may drop.

[22] Observed that with the application of EGR % flow rate a further reduction for both NO_X and soot emission can be achieved when n-pentanol is added. [23] observed a simultaneous reduction for both NO_X and soot emissions using a low temperature combustion (LTC) strategy, with application of EGR % flow rates coupled with late injection timing and addition of n-pentanol to the blended diesel biodiesel tested. However when [24] added n-pentanol to the diesel biodiesel the brake specific fuel consumption (BSFC) increased with no increase in BTE. This seems to confirm n-pentanol as a better fuel additive for waste plastic pyrolysis oil (WPPO) compared to n-butanol due to its high cetane number, better blend ratio stability and less hygroscopic nature as observed by [25].

Other methods that have been suggested include reduced ignition delay, which reduces combustion temperatures, thus aiding in the reduction of NO_X as its formation is temperature dependent. The use of cetane improvers is also an alternative for reducing NO_X as the poor cetane index of WPPO fuel blends leads to poor ignition quality, particularly when biodiesel fuels are used such as glycol ether which reduce PM, unburnt hydrocarbons (UHC) and CO emissions especially in common rail direct injection diesel engines. Cetane improvers also decrease cylinder pressure, ignition delay, heat release rate, and engine knock or noise [26]. The inclusion of n-pentanol in diesel biodiesel blends was observed by [27] to shorten combustion duration and increase the heat release rate (HRR), while significantly reducing the NO_X, CO and UHC emissions.

Fuel additives have also been suggested and used, with the most commonly used being diethyl ether. As an organic compound diethyl ether has a high cetane number and is capable of boosting ether compounds' cetane numbers as an improver [28]. In their study Devaraj et al. found that when used as an additive diethyl ether reduces ignition delay, cylinder peak pressure, HRR, CO, CO_2 and NO_X with a trade off in BTE which was observed to be increased. [29] on the other hand found diethyl ether to reduce the ignition delay period, UHC, and NO_X whereas BTE seemed to increased, but [14] using WPPO fuel observed and reported ignition delay and higher HRR with diethyl ether.

Diesel engines have been shown to run stably on most medium blended ratios of waste plastic oil, although they produce more NO_X, UHC and CO emissions. In order to stabilize them and the performance of higher blend ratios, injection timing has been proposed without the need for upgrading the fuel, engine modification or fuel alteration through addition of additives as observed by [30]. Injection timing was seen to affect performance from WPPO in the study by Sharma et al. [31], where Jatropa blends of 20 % tyre oil and 80 % Jatropa ester oil resulting into lower fuel consumption, CO, UHC and PM although it was observed to increase NO_X emissions. [32] Observed an increase in the BTE and NO_X emissions, thus concurring with the findings of Sharma et al. on emissions of NO_X, although on fuel consumption, CO, and UHC they noted decreased results. This work will endeavour to study the influence of EGR on the performance of a diesel engine using a biodiesel fuel derived from pyrolysis of waste plastic, and how WPPO interacts with engine performance and emission characteristics when EGR is applied.

EXPERIMENTAL

Experimental Apparatus and Equipment

Figure 1 is a schematic diagram for the experimental engine set-up and its components, which were used in the experiment. Figure 2 is ano5her schematic diagram showing the modification of the EGR loop that was adapted for the experimental engine in Figure1. Table 1 is the experimental engine specification standards of the experimental engine that was used throughout the study
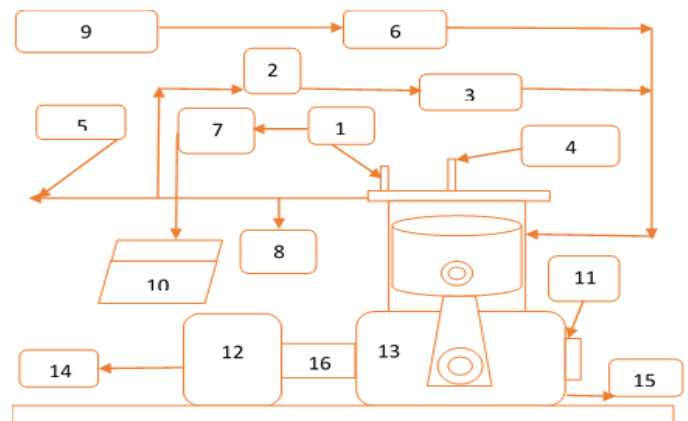
Figure 2. Experimental test engine test rig set-up diagram

Key: 1. Cylinder pressure sensor, 2. EGR control valve, 3. EGR cooler, 4. Injection Control Unit, 5. Exhaust gas exit, 6. Air box, 7. Signal amplifier, 8. Gas analyser, 9. air flow meter,10. Data acquisition system, 11. Crank position sensor, 12. Dynamometer, 13. Engine, 14. Air flow rate meter, 15. Cooling water exit to the cooling tower, 16. Dynamometer drive coupling.
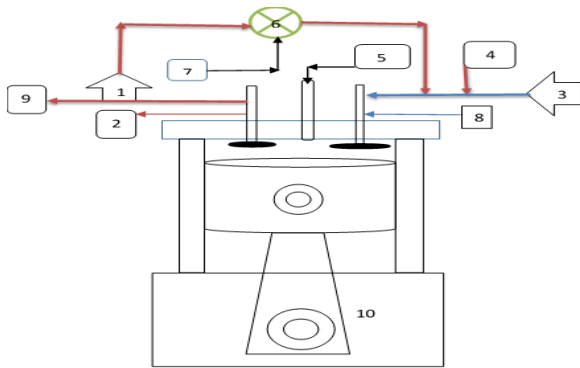
Figure 2. EGR schematic loop modification

Key; 1. The direction of EGR gases, 2. The x subscript representing the exhaust molar gas quantity, 3. The direction of inlet gases fresh charge, 4. The z subscript representing remainder of the intake charge, 5. n_f Which is the fuel molar quantity, 6. The EGR valve, 7. The R_x molar gas ratio, 8. The subscript y representing the inlet intake molar gas quantity, 9. The direction of the exhaust gases exit, 10. The engine unit

Table 1. Engine specifications, position value and type

Parameters	Position value
Ignition Type	4 (Stroke) DICI
Number of Cylinders	1
Model	TV 1
Cooling Medium	Water
Manufacturer	Kirloskar
Revolutions Per Minute	1500
Brake Power	3.5 Kw
Cylinder Bore	87.5 mm
Piston Stroke	110 mm
Compression Ratio	18.5:1
Connecting-Rod Length	234
Engine Capacity	661cc
Dynamometer Make	234
Injection Timing	23.4⊙ bTDC
Maximum Torque	28 N-M@1500
Injection Pressure	250 Bar

Waste Plastic Preparation and Conversion Process

The waste plastic materials were acquired from a municipal waste management site in Durban. The waste plastic is first sorted in a section of the pyrolysis plant. The dust and other fine waste from the sorted plastic waste materials is collected by the cyclone filter and disposed of through a vent with a particle size monitoring system within the plant. After the sorting and removal of unwanted materials and dust, the waste plastics are taken through a conveyor machine to a pressure cleaner for thorough cleaning, after which they are conveyed to a shredding machine which reduces them to the required size of 25.4 mm to 50 mm, suitable for the pyrolysis reactor. The waste material is then loaded into the pyrolysis reactor by means of an automatic feeding machine, although there is provision for manual loading in case there is a system failure. Before starting the pyrolysis, the airtight reactor door is locked. The system is started from a control panel by a machine operator with the preceding processes subsequently running automatically as indicated by the flow chart in Figure 3. The first stage is to heat up and dry the waste plastic materials and increase the reactor temperature to the required value of 400 ^{0} C to 500 ^{0} C. The heavy dense gas oil falls into the oil tank while the light oils rise up into the condenser where they are cooled and taken back into the oil tank for collection.

The liquefied gases in small quantities which cannot be converted into oil are recycled and collected by the recycling system to be burnt as fuel gas or cleaned through the after-treatment system with the smoke and flue emitted by the plant being released to the atmosphere after the removal of sulphurets and black carbon. After the pyrolysis process is over the system requires a cooling period of 4 hours to 5 hours through natural cooling, but nitrogen and carbon dioxide gases can be used as cooling agents to reduce the cooling waiting time. This enables the removal of the carbon black compound without contamination and pollution to the environment. The final operation is the removal of steel and other metals obtained in the pyrolysis reactor plant, as this requires the opening of the reactor door in preparation for the next batch of the pyrolysis process.
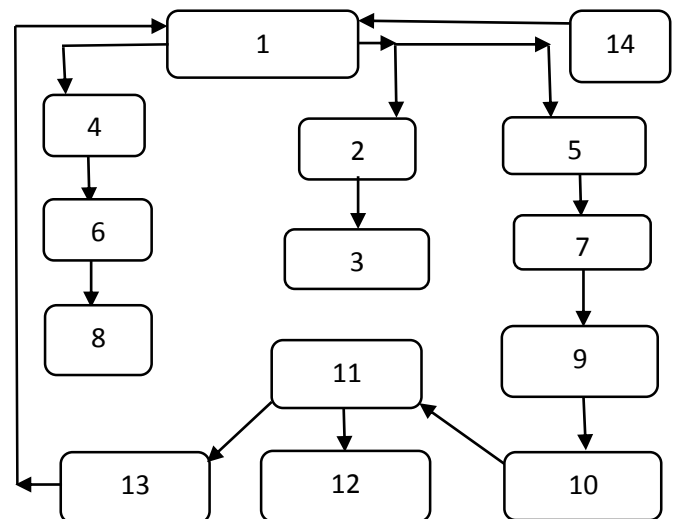
Figure 3. The waste plastic pyrolysis oil processing plant flow chart.

Key: 1. Pyrolysis reactor, 2. Carbon black discharge, 3. Carbon black deep processing, 4. Exhaust smoke discharge, 5. Gas separator, 6. Smoke scrubber to take out colour and odour, 7. Condenser, 8. Chimney, 9. Oil tank, 10. Synchronized gas purification, 11. Synchronized gas recycling system, 12. Extra gas burning, 13. Heating furnace during operation, 14. Loading of material section.

Physical Properties of Waste Plastic Pyrolysis Oil (WPPO) Sample

Table 2. The test fuel properties, their units of measurement, standard methods of testing and the values for conventional diesel in comparison to the values of waste plastic pyrolysis oil

Property	Unit	CD	WPPO	STANDARD
Appearance	-	Clear/brown	Clear/amber	Visual
Density @ 20	kg/M^3	838.8	788.9	ASTM D1298
Kinematic viscosity @ 40 ^{0} C	cSt	2.32	2.17	ASTM D445
Flash point	^{0} C	56.0	20.0	ASTM D93
Cetane index	-	46	65	ASTM D4737
Hydrogen	%	12.38	11.77	ASTM D7171
Cu corrosion	3 hrs @ 100 ^{0} C	-	1B	ASTM D130
Carbon	%	74.99	79.60	ASTM D 7662
Oxygen	%	12.45	7.83	ASTM D5622
Sulphur content	%	< 0.0124	0.15	ASTM D4294
IBP temperature	^{0} C	160	119	ASTM D86
FBP temperature	^{0} C	353.5	353.5	ASTM D86
Recovery	%		98	-
Residue and loss	%		2.0	-
Gross calorific value	kJ/kg	44.84	40.15	ASTM D4868

Table 2 shows the results of the physical properties of the WPPO obtained through the pyrolysis process of the waste plastics from municipal solid waste (MSW) management sites, at optimized conditions and compared to the properties of CD fuel oil. The appearance of the oil is yellowish in colour as shown by the photo in Figure 4 and the liquid distillate is free of visible particulate sediments with a flash point of 20 ^{0} C, and a gross calorific value (GCV) OF 40.15 KJ/kg which almost compares to the range indicated by most petroleum fuels including CD, thus making it capable of giving the same working performance results in internal combustion engines, especially diesel propelled ones.

Figure 4. The distillate samples from the waste plastic pyrolysis oil samples

The distillation report analysis shows the WPPO has an initial boiling point (IBP) of 119 ^{0} C to 353.5 ^{0} C, thus indicating some presence of other fuel oil components like kerosene,

gasoline and to some extent diesel oil in the tested samples. This leads to the observation and conclusion that it is possible for this oil to be used as a feedstock in future, if it is upgraded into a lighter compound such as diesel fuel or any other liquid fuel in the foreseeable future.

Table 3 shows the chemical composition of the WPPO from a pyrolysis plant process.

Table 3. Chemical composition of the WPPO obtained from a GC-MS laboratory analysis report

Molecular formula	Percentage composition
C_{10}	66.32
C_{10}-C_{15}	4.38
C_{15}-C_{20}	12.66
C_{20}-C_{25}	8.22
C_{25}-C_{30}	8.42

Experimental Procedure

The engine employed for this work was a Kirloskar experimental variable compression engine, four stroke single cylinder, water cooled developing 3.75 kW of power at 1500 rpm. The schematic is provided and shown in Figure 1. The technical specifications of the experimental variable compression engine are shown and indicated in Table 1. A

dynamometer was used to provide the engine with load during the experimentation, and to get measurements for the engine intake air flow an air box was fitted to the engine intake manifold system with a standard orifice mechanism. The fuel flow rate to the experimental engine was measured using a digital fuel gauge with a stop watch mounted to measure time taken for the fuel to be consumed.

The exhaust gas temperatures were measured using mounted temperature thermocouples of k-2 type, including the EGR temperature which is measured before it mixes with the intake fresh air charge and the constituents of the combustion chamber, through the same k-2 thermocouples. A cylinder pressure transducer was mounted on the engine cylinder head to monitor cylinder combustion pressure and collect data values through a system charge amplifier connected to a computer data acquisition machine. The crankshaft position or the crank angle was monitored and measured through a mounted encoder near the crankshaft pulley area. The emission gases during the experiment were monitored through a five gas exhaust gas analyser, while to measure the smoke intensity an AVL 437C smoke meter was employed.

Since the engine develops maximum power at 1500 rpm and it is a variable compression engine, all the experiments were conducted based on this nominal engine speed at part load and full load, but data could be obtained from different engine loads. Part engine load is described as 50 % of engine load and full engine load is described as the engine running at 100 % load, with a fixed compression ratio of 18.5:1. The EGR system is shown in Figure 3, modified to suit the experimental engine and enable data collection. The exhaust gases were tapped from the exhaust pipe and joined to the intake manifold air intake system via the air flow meter box through a manually controlled gate valve which made it possible for the mixing of EGR gases and the fresh air intake.

The EGR % flow rate was divided into the following modes: 0 %, 5 %. 10 %, 15 %, 20 %, 25 %, and 30 % spaced at intervals of 5 %. The waste plastic pyrolysis oil fuel blends were prepared in the following percentage order and mixed with CD fuel 10 %, 20 %, 30 %, 40 % and 100 %, where the WPPO10 blend is 90 % CD fuel and 10 % WPPO fuel in that order.

Throughout this experiment blends will be referred to in this format with digits denoting the percentage blend ratio of WPPO by volume to CD supplied. To avoid experimental fuel from being contaminated from the previous test, each test was conducted after a thorough evacuation procedure was conducted on the fuel lines and the fuel injection system mechanism of the test engine. This made it possible to conduct an experiment and collect good data and measurements with inputs from the test mode only, without fear of contamination and poor results from error.

Analysis of Error and Percentage Inaccuracies

This process was carried out for the purpose of performing and identifying the accuracy and precision of the measuring tools and instruments used in this experiment work, as errors can occur due to conditions outside of the experiment itself, such as calibration of the instruments, observational errors, manufacturing errors, errors associated with experimental set-up and planning, besides environmental conditions existing during the experiment [33]. The list of instruments used and their percentage error of analysis are provided in Table 4 together with the percentage inaccuracies of CO, CO_2, UHC, NO_X, EGT and smoke opacity.

The percentage of error analyses are derived from the following formula, the root sum square method and expressed in equation form [1] as:

$$R = \sqrt{\sum_{i=1}^{n} X_i^2} \qquad \text{Equation 1}$$

Where R is the total uncertainty percentage, X_i is the individual uncertainty of all the calculated operating parameters, n is the total number of the parameters in the experiment and i is the ith term of the computed parameters. The total percentage of the uncertainty is thus calculated based on Equation 2 as follows:

$$R = \sqrt{X_1^2 + X_2^2 + X_3^2} + \cdots X_i^2 \qquad \text{Equation 2}$$

Table 4 shows the instruments used for measurements and data collection, their measuring range, accuracies and percentages of inaccuracies, as calculated from Equation 2.

Table 4 Instruments used for measurements and data collection

Instrument	Accuracy	Measuring Range	Percentage inaccuracies
AVL 437C smoke meter Smoke intensity	± 1 %	0-100 %	± 1
AVL pressure transducer GH14D	± 0.01 bar	0-250 bar	± 0.01
AVL 365C Angle encoder	± 1^0	-	± 0.2
AVL Digas 444 (Five Gas Analyser)			
CO	± 0.03 % to ± 5 %	0-10 % by vol	± 0.3
CO_2	± 0.5 % to ± 5 % by vol	0-20 % vol	± 0.2
O_2	± 5 % by vol	0-22 % by vol	± 0.3
HC	± 0.1 % to ± 5 %	0-20000 ppm by vol	± 0.2
NOx	± 10 %	0-5000 ppm by vol	± 0.2

Instrument	Accuracy	Measuring Range	Percentage inaccuracies
K-2 Thermocouple	$\pm 1\ ^0$ C	0-1250 ^{0} C	± 0.2
Digital Stop Watch	± 0.2 s		± 0.2
Digital Fuel Gauge	± 1 mm		± 2
Burette	± 0.2 cc	1-30 cc	± 1.5

3.0 RESULTS AND DISCUSSION

3.1 Brake Specific Fuel Consumption (BSFC)

Figure 5 shows the variation of the BSFC under the effects of EGR % flow rate with different fuel blends of WPPO and CD operating at full engine load conditions.
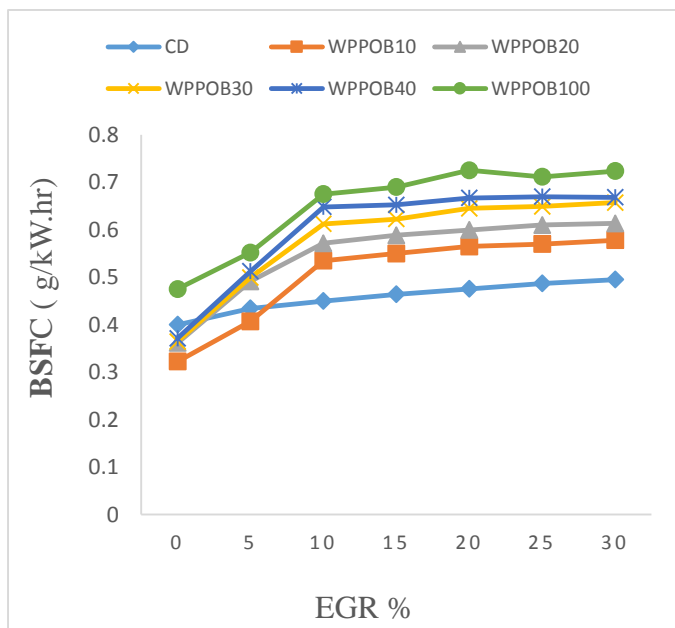
Figure 5. Brake specific fuel consumption (BSFC) versus EGR % flow rate

As can be seen from Figure 5, the lower ratio blends of WPPOB10 and WPPOB20 showed minimal reduction in BSFC at 0 % EGR flow rate compared to the values of CD and WPPOB100 which showed significantly higher values of BSFC at that mode. At 0 % EGR flow rate CD had a BSFC value of 0.4 g/kW.hr compared to WPPOB100 with a value of 0.4751 g/kW.hr, indicating that the fuel blend WPPOB100 had a higher BFSC than CD and the other blends of WPPO at 0.3225 g/kW.hr, 0.3615 g/kW.hr, 0.3645 g/kW.hr and 0.3715 g/kW.hr, for WPPOB10, WPPOB20, WPPOB30 and WPPOB40 respectively.

A similar trend was noted under the influence of EGR % flow rate where for example at 20 % to 25 % EGR flow rate, the BSFC showed increased tendencies. These findings concur with the findings of [34]. This phenomenon can be explained due to the effects of dilution of the fresh air intake as it mixes with exhaust gases that are being recirculated through the EGR system which leads to incomplete combustion of the inducted mixture, thus leading to a drop in power and engine torque as

observed by the findings of [35]. This scenario forces the engine to increase its fuel consumption in order to maintain constant speed and its increased load hence the increase in BSFC.

The WPPO biodiesel blends with EGR % flow rate applications showed a better fuel economy, especially the lower blend ratios of WPPOB10 and WPPOB20, compared to conventional diesel test fuels. However, as the EGR % flow rate increased there was a noticeable increase in the BSFC across all the test fuels used. At 0 % EGR CD was 0.4 g/kW.hr compared to 30 % EGR flow rate which was 0.495 g/kW.hr. For the WPPO biodiesel WPPOB10 blend the value was 0.3225 g/kW.hr compared to 0.5780 g/kW.hr at 30 % EGR flow rate. From Figure 5 it is evident that the test fuel that showed the highest BSFC among the blends of diesel and the CD test fuel was WPPOB100 which at 0 % EGR flow rate had a value of 0.4751 g/kW.hr compared to 0.7235 g/kW.hr at 30 % EGR % flow rate.

An interesting observation during experimentation was that after the 10 % EGR flow rate the values for the BSFC across all the test fuel seemed to show and pick a lineal increment trend as can be shown in Figure 5 by the flattening of the graph curves and the close value trends.

Brake Thermal Efficiency (BTE)

BTE studies specifically help us to know the ability of the combustion system to accept the fuel provided and how efficient it is in converting that fuel and turning it into a mechanical output, as observed by [28] and [27].

Figure 6 shows the BTE % variations, under different blends of WPPO and conventional diesel fuel, with the application of EGR % flow rate.
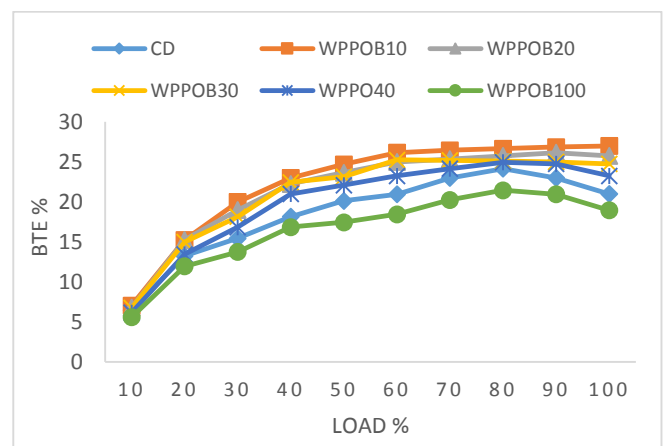
Figure 6 brake thermal efficiency (BTE) versus engine load %

Figure 7 shows the variation of BTE % with the application of EGR % flow rate using different blends of WPPO and CD.
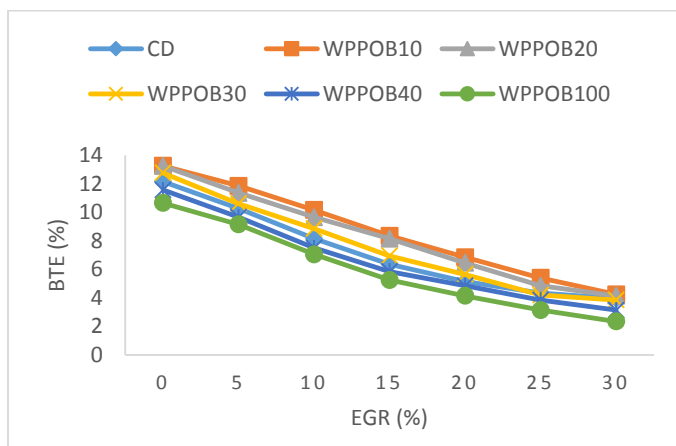
Figure 7. Brake thermal efficiency (BTE) % versus EGR % flow rate

From Figure 7 it is evident that there was a noticeable decrease in the BTE especially with all high ratio fuel blends of WPPOB40 and WPPOB100 compared to CD. In comparison to other WPPO blends WPPOB100 obtained the lowest decrease of BTE with a value of 7.05 % at 10 % EGR flow rate and the least value of 2.35 % at 30 % EGR flow rate.

Although there was a reduction in BTE due to the application of EGR % flow rate as shown in Figure 7, the trends of decreased BTE continued to be observed. For example, at 0 % EGR flow rate, the value of BTE for CD was 12.15 % compared to WPPOB10 and WPPOB20 with values of 13.25 % and 13.05 %. The WPPOB100 blend had the lowest value for BTE for all EGR rate flow modes than any other test fuel.

Brake Power (BP)

Figure 8 shows engine brake power (BP) variations with EGR % flow rate application with CD and different WPPO blends at full engine load conditions.
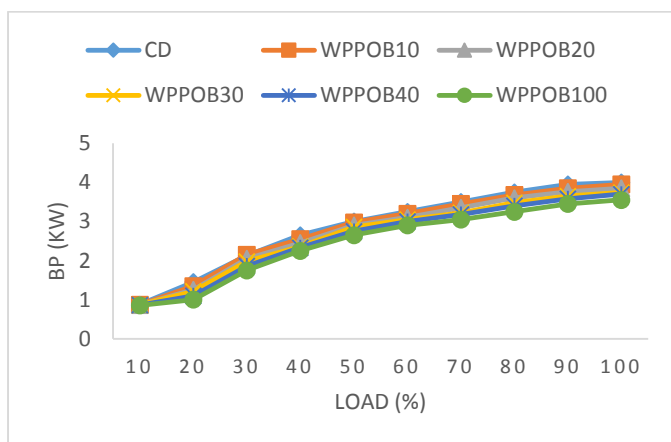
Figure 8. Engine brake power (BP) versus varying engine load %

The results in Figure 8 show that there was a lineal increase in BP for all the test fuels with an increase in the engine load. CD had the highest increase in BP values compared to the blended fuels of WPPO. At 20 % engine load, the BP value for CD was 1.45 kW while WPPOB10 had a value of 1.350 kW representing a difference of 6.8 % in BTE when the two fuels are compared.

The blended fuels in Figure 8 also show very close increments in BP with an increase in engine load conditions and a decrease in BP with an increase in the blend ratio for all the blended fuels tested. The increase in blend ratio showed a direct decrease in BP in a linearly incremental relationship. For example, at 30 % engine load CD, WPPOB10, WPPOB20, WPPOB30 and WPPOB40 had values of 2.125 kW, 2.15 kW, 2.05 kW, 1.98 kW, 1.86 kW and 1.75 kW respectively, showing a decrease in the value of the BP throughout the experimentation period. The WPPOB100 blend showed the lowest values for the BP compared to the blends of WPPOB10, WPPOB20, WPPOB30 and WPPOB40 used in this study. These findings concur with the findings by [19] in relation to WPPO blends.

The application of EGR % flow rate was observed to cause no significant change in BP. However, there was a negligible drop in the engine brake power with the influence of EGR flow rate except for the blend WPPOB10 which had almost identical value to CD as the curve of the two fuels indicate in Figure 8. This leads to the conclusion that the blends of WPPO have identical BP values with CD.

Exhaust Gas Temperature (EGT)

Figure 9 shows the variation of exhaust gas temperature under different types of WPPO blend and CD with application of EGR % flow rate.
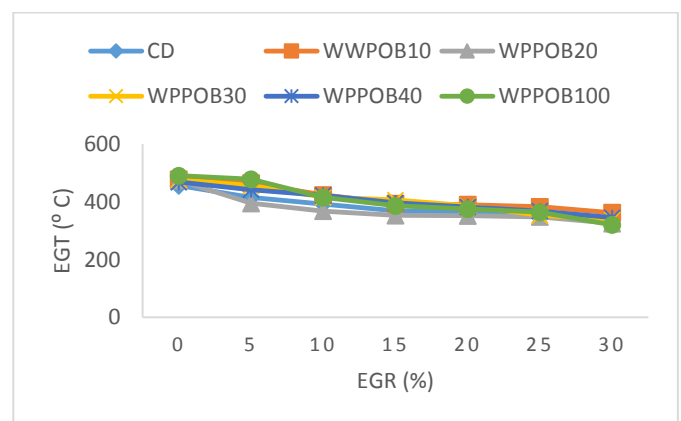
Figure 9. Exhaust gas temperature (EGT ^{0} C) versus EGR % flow rate

Temperature is one of the key factors in determining the formation of engine exhaust emissions, besides providing or helping in the analysis and study of combustion processes in relation to fuel as observed by [36].

It is evident from the results in Figure 9 that there was a variation in EGT of WPPO and CD with the application of EGR

% flow rate. The results indicate that EGT decreased with different blends of WPPO compared to CD. The temperature difference between them was that WPPO blends had higher temperature increases in all the test conditions compared to CD. However, it should be mentioned that as the blend ratio increased with EGR % flow rate application, the EGT reduced significantly and marginally especially for WPPOB30 and WPPOB40. The highest temperature value obtained for CD was 456 ^{0} C at 0 % EGR flow rate, whereas the highest temperature value for WPPO blend was 490 ^{0} C obtained from WPPOB100 at 0 % EGR flow rate, although at 30 % EGR flow rate this blend had the most reduction in temperature compared to the other WPPO blends with a temperature value of 320 ^{0} C.

The application of EGR % flow rate in increasing modes brought further reduction in EGT with the highest value for CD obtained being 440 ^{0} C with an EGR % flow rate of 5 % while the minimum or lowest value of 340 ^{0} C was obtained at 30 % EGR flow rate. The WPPO blends showed a similar trend with decreasing temperatures with the application of EGR % flow rate with WPPOB10 showing the highest value of 467 ^{0} C and lowest of 362 ^{0} C at 5 % and 30 % EGR rate flow respectively, while WPPOB40 showed a highest value of 472 ^{0} C and a lowest of 330 ^{0} C at 5 % and 30 % EGR flow rate respectively.

The cause of the reduction in EGT can be attributed to several factors. The reduction in EGT among the different blends of WPPO is a result of low calorific value of the blends and the low exhaust loss, which concurs with the findings of [37]and [38]. The WPPO has a calorific value of 40.15 kJ/kg compared to the calorific value of CD at 44.84 kJ/kg as shown in Table 2. Other causes are directly linked to the effects of EGR rate flow, the dilution effect, chemical effects and thermal effects [39] and [40].

Unburnt Hydrocarbon (UHC) Emissions

Figure 10 shows the variation of UHC emissions in parts per million under full engine load with the application of various EGR % flow rates, and different blends of WPPO and CD. The UHC emissions were significantly higher across all the blended test fuels of WPPO, especially with higher engine load conditions as indicated by the values shown in Figure 10. However, CD produced more and higher values of UHC emissions compared to all the blends of WPPO across all the engine loading conditions and operating modes.

Figure 10 shows UHC emissions (ppm) values under engine load with different fuel blends of WPPO and CD under the effects of EGR % flow rate application.
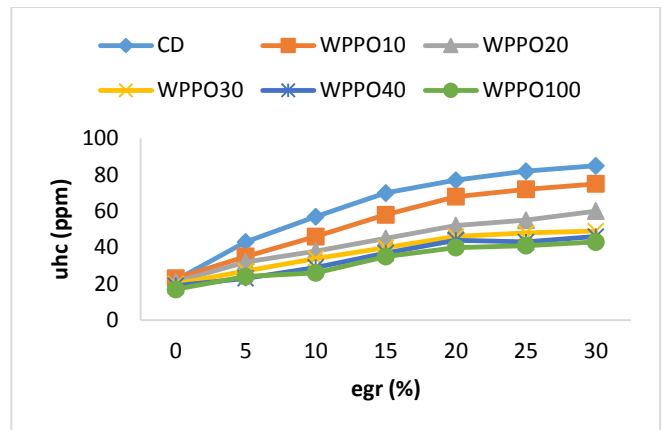
Figure 10. Unburnt hydrocarbons (UHC) emissions versus EGR % flow rate

As can be seen from Figure 10, when the EGR % flow rate application was 0 %, there was no application effect. Figure 10 shows that there were less UHC emissions for all the test fuels applied in this experiment, reporting values of 22 ppm, 23 ppm, 21 ppm, 20 ppm, 19 ppm and 17 ppm for WPPOB10, WPPOB20, WPPOB30, WPPOB40 and WPPOB100 respectively, compared to 20 % EGR percentage flow rates with 77 ppm, 68 ppm, 52 ppm, 46 ppm, 44 ppm and 40 ppm respectively.

Although the application of EGR % flow rate reduces the amount of UHC emissions remitted by the applied test fuels across the board, CD fuel produced more UHC emissions from the test engine compared to all the WPPO blends tested. Figure 10 shows that at EGR flow rates of 5 %, 10 %, 15 %, 20 %, 25 % and 30 %, CD UHC emissions were 43 ppm, 57 ppm, 70 ppm, 82 ppm and 85 ppm respectively, compared to WPPOB10 whose values were 23 ppm, 35 ppm, 40 ppm, 48 ppm, 50 ppm, and 52 ppm respectively.

Therefore, the application of EGR % flow rate increased UHC emissions as observed from the results and values presented and obtained in Figure 10, with CD fuel producing the highest UHC emission values compared to all the test fuel blends of WPPOB10, WPPOB20, WPPOB30, WPPOB40 and WPPOB100.

Nitrogen Oxide (NO$_X$) Emissions

Figure 11 shows variations of NO$_X$ emissions (ppm) and engine loads with different blends of WPPO and CD fuel with EGR % flow rate application.
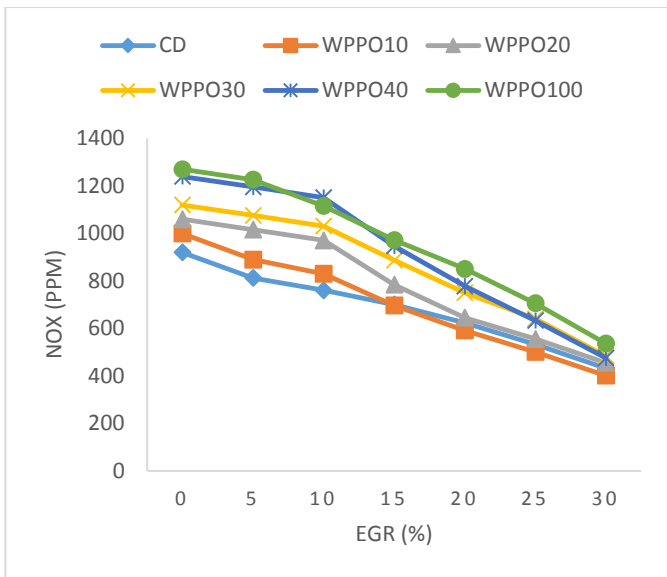
Figure 11. Variations of NO$_X$ emissions (ppm) versus EGR % flow rate

NO$_X$ emission formation is highly dependent on in-cylinder temperature, the concentration of oxygen, and the residence time the fuel-air mixture spends in the combustion chamber during the pre-mixing phase [41]. All the fuels tested indicated a drop in the NO$_X$ emissions with an increase in the application of EGR % flow rate, at all engine load conditions. Figure 11 shows this was due to the rise in the total heat capacity of the working gases that increased with increasing EGR % flow rate, thus concurring with the studies and findings of [42], [43] and [44].

The NO$_X$ emissions value for the CD in Figure 11 at full load was 920 ppm with application of EGR % flow rate, while WPPOB100 was 1270 ppm, compared to the reduced values with application of EGR % flow rate of 30 % in Figure 11, where CD NO$_X$ emissions decreased to 432 ppm compared to 536 ppm before application of EGR % flow rate.

Figure 12 shows variations of NO$_X$ emissions (ppm) under varying engine load with different blends of WPPO and CD test fuel without EGR % flow rate application.
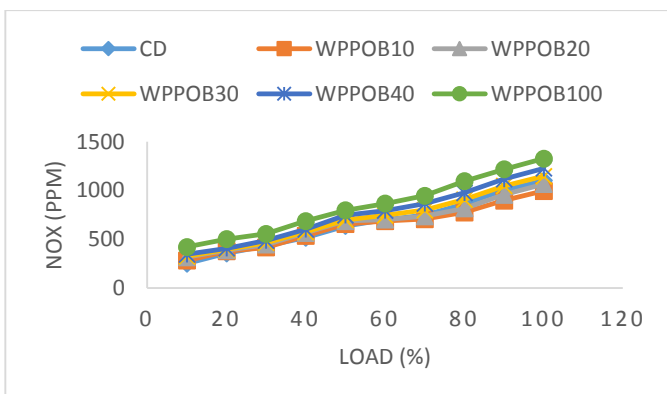
Figure 12. Variations of NO$_X$ emissions (ppm) versus varying engine load % without application of EGR flow rate

During study it was observed that at engine part load, as shown in Figure 12, the values for NO$_X$ emissions for all the fuels were lower compared to the values at full load engine conditions. The NO$_X$ emissions for CD at engine part load (50 %) was 635 ppm compared to full load at 1100 ppm, whereas the value for WPPOB100 at engine part load (50 %) was 850 ppm compared to 1250 ppm at full engine load. This seems to indicate a concurrence that at part engine load (50 %) the values of NO$_X$ emissions emitted by all the blends of WPPO except WPPO100 were lower compared to the values at full engine load conditions.

Carbon Monoxide (CO) Emission

Figure 13 shows CO emissions % variations versus varying engine load with different fuel blends of WPPO and CD test fuel with EGR % flow rate application.
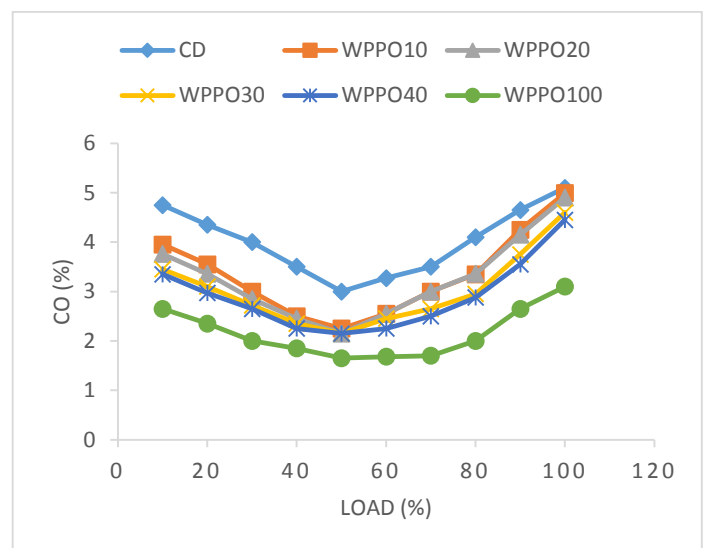
Figure 13. Carbon monoxide (CO) emissions % versus varying engine load

CO is a toxic gas that requires substantial control to acceptable levels. It is caused by poor combustion of hydrocarbon fuels as a result of dependency on the air-fuel ratio relative to the stoichiometric proportions [42].

For all the test fuels the amount of CO emissions seemed to decrease at lower engine loads up to part load percentages or intermediate loads of (50 %), after which the CO emissions continued to increase significantly and marginally as in Figure 13. At 0 % engine load the value of conventional diesel was 0.051 % compared to 50 % engine load when the value was reduced to 0.03 % by volume. However, as the engine load increased from 50 % there was a significant continuous and marginal increase in the percentage of carbon emissions by volume across all the test fuels irrespective of the EGR % flow rate. For example, at 80 % engine load the value for WPPOB100 was 0.02 % up from 0.0165 % by volume. The other WPPO biodiesel blends also showed a similar trend and concurrency. WPPOB20 and WPPO30 test fuels at 50 % engine load condition had values of 2.25 % and 2.15 %

compared to 3.36 % and 2.95 % respectively at 80 % engine load.

Figure 14 shows the variation of CO emissions with EGR % flow rate application under different blends of WPPO and CD.
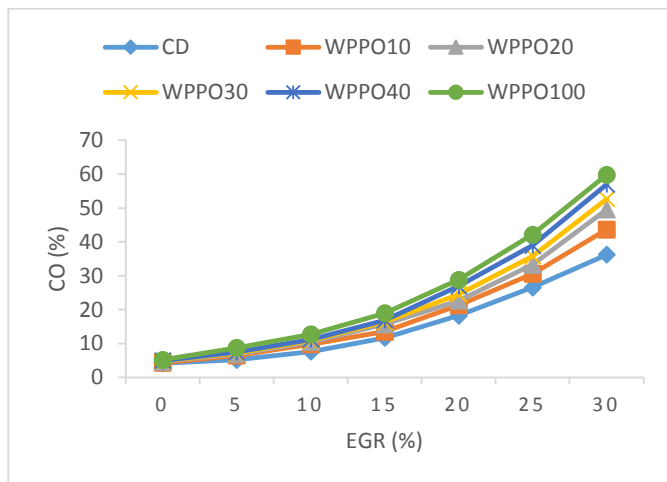
Figure 14. Carbon monoxide (CO) versus EGR % flow rate application

As shown in Figure 14, the WPPO blends are observed to produce a continuous increase in smoke emissions to almost double the values with the application of EGR % flow rate as in Figure 14. For example, at 10 % EGR flow rate, CO emission values were 9.79 %, 10.46 %, 10.91 %, 11.25 % and 12.75 % for WPPO10, WPPO20, WPPO30, WPPO40 and WPPO100 respectively. CD reported the lowest carbon emissions with the application of EGR % flow rate with a value of 7.65 %.

There was also a correlation between the blend ratio and EGR % flow rate on the amount of CO emissions produced. During experimentation it was observed that as the blend ratio increased the CO emissions increased as the EGR % flow rate increased as seen in Figure 10. At 20 % EGR flow rate CO emission values were 18.25 %, 21.35 %, 22.65 %, 24.55 %, 26.95 % and 28.85 % respectively for CD, WPPO10, WPPO20, WPPO30, WPPO40 and WPPO100. However, WPPO30 reported values of 4.85 %, 7.28 %, 10.91 %, 16.37 %, 35.75 % and 52.69 % as the EGR flow rate increased from 0 % to 30 % respectively. This may be due to the effects of EGR % flow rate application and for dilution, thermal and chemical reasons some of the oxygen in the inlet charge was replaced with recirculated exhaust gas which caused incomplete combustion.

Carbon Dioxide (CO_2) Emissions

Figure 15 shows the CO_2 % variations under varying engine load with different blends of WPPO and CD test fuels.
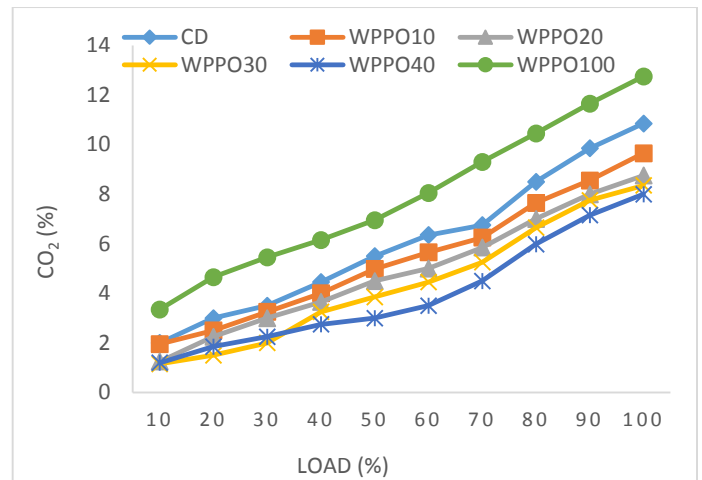
Figure 15. Variation of carbon dioxide (CO_2) % emissions versus engine Load %, with different types of fuel blends of WPPO and CD

CO_2 is the principal composition of EGR gases, and is a core indicator of the quality of combustion and the temperature [6] of combustion within the combustion chamber. CO_2 gas has a higher heat capacity which makes it act like a thermal heat sink especially during the combustion process, making it possible to reduce peak cylinder temperatures, hence is of particular importance in the process leading to the reduction in NO_X emissions.

Without EGR % flow rate and at lower engine loads, the value of CO_2 was considerably high for all the test fuels used. For example, at 20 % engine load WPPOB100 had the highest CO_2 emission value of 4.65 % compared to the other test fuels used, namely CD, WPPO10, WPPO20, WPPO30 and WPPO40 with 3 %, 2.50 %, 1.5 %, 1.85 % respectively, as shown in Figure 15.

However, it can also be observed from Figure 15 that the amount of CO_2 increased with an increase in the engine load. As the engine load increased to 40 % the value of WPPOB40 was 2.75 % compared to WPPOB30 at 3.25 %, while at 70 % engine load the values 4.5 % and 5.25 % respectively. This leads us to the observation that as the engine load is increased with an increase in the blend ratios, lower ratio blends are observed to emit more CO_2 compared to higher ratio blends except blend WPPOB100 which released more CO_2 than any test fuel as mentioned earlier. At full engine load the value of CO_2 emissions were at their highest values across all the test fuels. The values were 12.75 %, 10.85 %, 9.65 %, 8.75 %, 8.35 % and 8 % for WPPOB100, CD, WPPOB10, WPPOB20, WPPOB30 and WPPOB40 respectively.

Figure 16 shows CO_2 % variations with different blends of WPPO and conventional diesel test fuel under engine load, with application of EGR % flow rate.
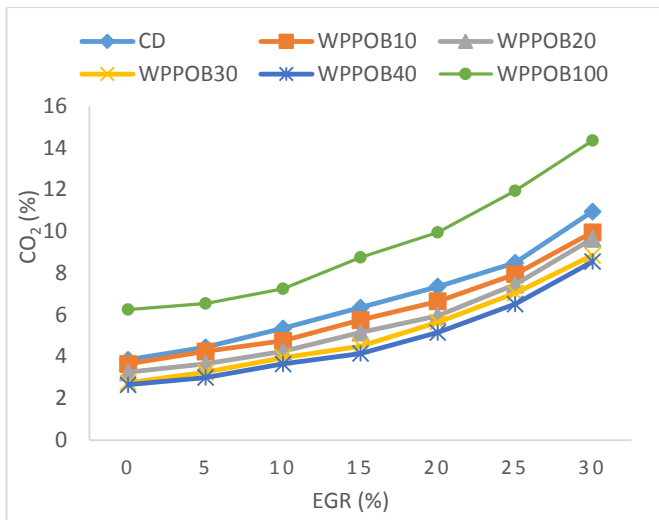
Figure 16. Variations of carbon dioxide (CO_2) % versus EGR % flow rate, with different types of WPPO fuel blends and CD

The application of EGR % flow rate increased the CO_2 emissions exponentially by almost doubling the values as can be seen in Figure 16. For example, at 10 % EGR flow rate the value of CD was 5.35 % compared to WPPOB100 at 7.25 %, WPPOB10 was at 4.75 %, WPPOB20 at 4.25 %, WPPOB30 at 3.95 %, and WPPOB40 at 3.65 % respectively. These results reinforce the observation that CO_2 emissions with the application of EGR % flow rate have a correlation with blending i.e., the lower the blend ratio, the higher the emission values and vice versa. The values for 30 % EGR flow rate for all the test fuels contained high emissions for CO_2, for example CD was 10.95 %, WPPOB10 9.95 %, WPPOB20 9.65 %, WPPOB30 8.85 %, and WPPOB100 had the highest value of 14.35 %.

Smoke Emissions (Opacity)

This can be defined as the solid hydrocarbon soot particles that are found in exhaust system gases [45] and are directly linked to smoke emissions formation. For all the blends of WPPO there was a noted increase in the level of smoke emissions, although the levels and values were considerably lower compared to CD.

Figure 17 shows smoke emissions or opacity % variations at full engine load, with different blends of WPPO and CD under the effect of EGR % flow rate application.
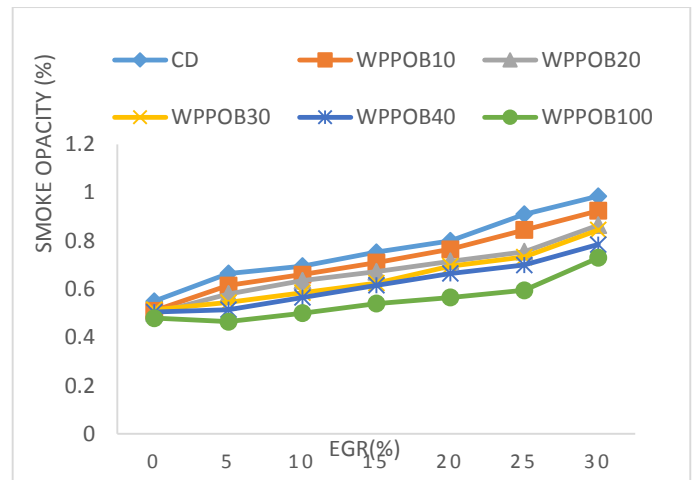
Figure 17. Variation of smoke emissions or opacity % versus EGR % flow rate, with different WPPO blends and CD

The steady increase in smoke emissions can be explained by the fact that WPPO blends of fuel have a high kinematic of viscosity compared to CD fuel, and they have low volatility values. Other possible explanations for this phenomenon are the poor injection and spray characteristics observed for WPPO blends of fuels compared to those of CD fuel which has better spray qualities. Another likely cause is associated with the high aromatic compounds found in most WPPO blends of fuel compared to CD fuel.

The application of EGR % flow rate showed that there was a significant increase in the values of smoke emissions and particulate matter emissions across all the test fuels. Smoke emissions with WPPOB10 blend were 7.2 % lower compared to CD at 0 % EGR flow rate, with CD being 11.5 % higher than WPPOB100 blend fuel at 30 % EGR flow rate. This result seems to concur with the study findings of [46].

The WPPOB10 blend used in this study emitted the highest levels of smoke emissions of the blended fuels followed by WPPOB100. However, it should be mentioned here that as the blend ratio and the EGR % flow rate increased there was a steady increase in the smoke emissions across all the test fuels compared to when the EGR % flow rate was at 0 %.

CONCLUSION

- As the percentage of the blends of WPPO increased there was a marked decrease in the engine BP of the blended fuels compared to CD. This is true considering that the energy content (Table 2) for the WPPO test fuel was lower compared to the CD test fuel.
- Peak power produced using WPPO biodiesel blends failed to match the peak power produced by CD, being in the region of 5% to 8% less compared to the peak power produced from the CD test fuel.
- Data presented in this work provides more reasons to support the widespread use of WPPO as an alternative fuel for all types of compression ignition engines with

or without modifications to the engines, especially when blends of WPPOB10 and WPPOB20 are used because in this study their peak BP and BSFC values were identical to CD.

- Results (Figure 12) indicate that less NO_X emissions occurred during part and intermediate engine load for the WPPO test fuels and CD test fuel compared to full engine load.

- As the percentage ratio of the biodiesel WPPO increased there was a significant increase in the BSFC (Figure 5) for the blends of WPPO compared to the BSFC values of CD.

- An interesting observation during this experiment was that as the blends ratio increased there was a reduction in the percentage amount of CO emissions released by the test engine (Figure 13). This can be attributed to a higher oxygen content in WPPO blended fuels compared to CD, aiding in complete combustion.

- The values of CO emission by WPPOB10 and WPPOB20 were observed to be close with minimal differences in terms of their volume percentage emissions of CO produced by the test engine (Figure 13).

- For all the test fuels, it was observed that at low engine loads from 10 % to 40 % there was a decrease in the amount of CO_2 emissions (Figure 14). However, there was a significant continuous and marginal increase in the percentage of CO_2 emissions by volume as the load increased to 50 % across all the test fuels irrespective of the EGR % flow rate.

- There was a steady increase in smoke emissions for all the blends of WPPO with or without EGR % flow rate application, with test fuel blend WPPOB10 producing the highest values of smoke emissions followed by the WPPOB100 test fuel blend (Figure 16).

- There was a steady increase in smoke emissions due to the WPPO blends of fuel having a high kinematic of viscosity compared to the CD test fuel, in addition to having the low volatility. Other possible explanations for this phenomenon could be the poor injection and spray characteristics observed with WPPO blends of fuels compared to CD which offers better spray qualities. Another likely cause is the high level of aromatic compounds found in most WPPO blends of fuel compared to CD.

- The NO_X emission for CD at engine part load (50 %) was 635 ppm compared to full load at 1100 ppm, whereas the value for WPPOB100 at engine part load (50 %) was 850 ppm compared to 1250 ppm at full engine load. This seems to indicate a concurrence that at part engine load (50 %) the values of NO_X emissions emitted by all the blends of WPPO except WPPO100 were lower compared to the values at full engine load conditions.

ACKNOWLEDGEMENT

REFERENCES

[1]   V. K. Kaimal and P. Vijayabalan, "A detailed study of combustion characteristics of a DI diesel engine using waste plastic oil and its blends," *Energy conversion and Management,* vol. 105, pp. 951-956, 2015.

[2]   İ. A. Reşitoğlu, K. Altinişik, and A. Keskin, "The pollutant emissions from diesel-engine vehicles and exhaust aftertreatment systems," *Clean Technologies and Environmental Policy,* vol. 17, pp. 15-27, 2015.

[3]   B. R. Kumar and S. Saravanan, "Use of higher alcohol biofuels in diesel engines: A review," *Renewable and Sustainable Energy Reviews,* vol. 60, pp. 84-115, 2016.

[4]   S. Kumar, R. Prakash, S. Murugan, and R. Singh, "Performance and emission analysis of blends of waste plastic oil obtained by catalytic pyrolysis of waste HDPE with diesel in a CI engine," *Energy conversion and management,* vol. 74, pp. 323-331, 2013.

[5]   D. Damodharan, A. P. Sathiyagnanam, B. R. Kumar, and K. C. Ganesh, "Cleaner emissions from a DI diesel engine fueled with waste plastic oil derived from municipal solid waste under the influence of n-pentanol addition, cold EGR, and injection timing," *Environmental Science and Pollution Research,* pp. 1-15, 2018.

[6]   K. Muralidharan, D. Vasudevan, and K. Sheeba, "Performance, emission and combustion characteristics of biodiesel fuelled variable compression ratio engine," *Energy,* vol. 36, pp. 5385-5393, 2011.

[7]   H. Yamada, K. Misawa, D. Suzuki, K. Tanaka, J. Matsumoto, M. Fujii*, et al.*, "Detailed analysis of diesel vehicle exhaust emissions: Nitrogen oxides, hydrocarbons and particulate size distributions," *Proceedings of the Combustion Institute,* vol. 33, pp. 2895-2902, 2011.

[8]   Department of Enviromental Affairs, "National Waste Management Strategy," *Department of Enviromental Affairs, Pretoria,* 2012.

[9]   A. Azad, M. Rasul, M. Khan, S. C. Sharma, and M. Bhuiya, "Recent development of biodiesel combustion strategies and modelling for compression ignition engines," *Renewable and Sustainable Energy Reviews,* vol. 56, pp. 1068-1086, 2016.

[10]   C. T. Bowman, "Control of combustion-generated nitrogen oxide emissions: technology driven by

regulation," in *Symposium (International) on Combustion*, 1992, pp. 859-878.

[11] V. Mangesh and C. Thamotharan, "Evaluation of Engine Performance, Emissions, of a Twin Cylinder Diesel Engine Fuelled with Waste Plastic Pyrolysis Oil, Ethanol and Diesel Blends with Cetane Additive AC2010A," 2015.

[12] R. Geyer, J. R. Jambeck, and K. L. Law, "Production, use, and fate of all plastics ever made," *Science advances,* vol. 3, p. e1700782, 2017.

[13] S. Kumar, A. K. Panda, and R. Singh, "A review on tertiary recycling of high-density polyethylene to fuel," *Resources, Conservation and Recycling,* vol. 55, pp. 893-910, 2011.

[14] I. Kalargaris, G. Tian, and S. Gu, "Combustion, performance and emission analysis of a DI diesel engine using plastic pyrolysis oil," *Fuel Processing Technology,* vol. 157, pp. 108-115, 2017.

[15] C. Wongkhorsub and N. Chindaprasert, "A comparison of the use of pyrolysis oils in diesel engine," *Energy and Power Engineering,* vol. 5, p. 350, 2013.

[16] D. Kim, S. Shin, S. Sohn, J. Choi, and B. Ban, "Waste plastics as supplemental fuel in the blast furnace process: improving combustion efficiencies," *Journal of hazardous materials,* vol. 94, pp. 213-222, 2002.

[17] S. D. A. Sharuddin, F. Abnisa, W. M. A. W. Daud, and M. K. Aroua, "A review on pyrolysis of plastic wastes," *Energy conversion and management,* vol. 115, pp. 308-326, 2016.

[18] C. Güngör, H. Serin, M. Özcanlı, S. Serin, and K. Aydın, "Engine performance and emission characteristics of plastic oil produced from waste polyethylene and its blends with diesel fuel," *International journal of green energy,* vol. 12, pp. 98-105, 2015.

[19] J. Pratoomyod and K. Laohalidanond, "Performance and emission evaluation of blends of diesel fuel with waste plastic oil in a diesel engine," *Carbon,* vol. 79, pp. 75-99, 2013.

[20] M. Mani, G. Nagarajan, and S. Sampath, "Characterisation and effect of using waste plastic oil and diesel fuel blends in compression ignition engine," *Energy,* vol. 36, pp. 212-219, 2011.

[21] V. Guruprakash, N. Harivignesh, G. Karthick, and N. Bose, "Thermal barrier coating on IC engine cylinder liner," *Archives of Materials Science,* vol. 38, p. 38, 2016.

[22] S. Saravanan, "Effect of exhaust gas recirculation (EGR) on performance and emissions of a constant speed DI diesel engine fueled with pentanol/diesel blends," *Fuel,* vol. 160, pp. 217-226, 2015.

[23] B. R. Kumar and S. Saravanan, "Effects of iso-butanol/diesel and n-pentanol/diesel blends on performance and emissions of a DI diesel engine under premixed LTC (low temperature combustion) mode," *Fuel,* vol. 170, pp. 49-59, 2016.

[24] L. Wei, C. Cheung, and Z. Huang, "Effect of n-pentanol addition on the combustion, performance and emission characteristics of a direct-injection diesel engine," *Energy,* vol. 70, pp. 172-180, 2014.

[25] J. Calder, M. M. Roy, and W. Wang, "Performance and Emissions of a Diesel Engine Fueled by Biodiesel-Diesel Blends with Recycled Expanded Polystyrene and Fuel Stabilizing Additive," *Energy,* 2018.

[26] S. Gnanasekaran, N. Saravanan, and M. Ilangkumaran, "Influence of injection timing on performance, emission and combustion characteristics of a DI diesel engine running on fish oil biodiesel," *Energy,* vol. 116, pp. 1218-1229, 2016.

[27] L. Li, J. Wang, Z. Wang, and J. Xiao, "Combustion and emission characteristics of diesel engine fueled with diesel/biodiesel/pentanol fuel blends," *Fuel,* vol. 156, pp. 211-218, 2015.

[28] J. Devaraj, Y. Robinson, and P. Ganapathi, "Experimental investigation of performance, emission and combustion characteristics of waste plastic pyrolysis oil blended with diethyl ether used as fuel for diesel engine," *Energy,* vol. 85, pp. 304-309, 2015.

[29] S. Hariharan, S. Murugan, and G. Nagarajan, "Effect of diethyl ether on Tyre pyrolysis oil fueled diesel engine," *Fuel,* vol. 104, pp. 109-115, 2013.

[30] I. Kalargaris, G. Tian, and S. Gu, "The utilisation of oils produced from plastic waste at different pyrolysis temperatures in a DI diesel engine," *Energy,* vol. 131, pp. 179-185, 2017.

[31] A. Sharma and S. Murugan, "Combustion, performance and emission characteristics of a DI diesel engine fuelled with non-petroleum fuel: a study on the role of fuel injection timing," *Journal of the Energy Institute,* vol. 88, pp. 364-375, 2015.

[32] A. K. Wamankar and S. Murugan, "Effect of injection timing on a DI diesel engine fuelled with a synthetic fuel blend," *Journal of the Energy Institute,* vol. 88, pp. 406-413, 2015.

[33] P. Senthilkumar and G. Sankaranarayanan, "Production of waste polyethylene bags in to oil and studies performance, emission and combustion characteristics in di diesel engine," *International journal of humanities, arts, medicine and science,* vol. 3, pp. 149-158, 2015.

[34] M. Hawi, R. Kiplimo, and H. Ndiritu, "Effect of exhaust gas recirculation on performance and emission characteristics of a diesel-piloted biogas

engine," *Smart Grid and Renewable Energy,* vol. 6, p. 49, 2015.

[35] M. Paul Daniel, K. V. Kumar, B. Durga Prasad, and R. K. Puli, "Performance and emission characteristics of diesel engine operated on plastic pyrolysis oil with exhaust gas recirculation," *International Journal of Ambient Energy,* vol. 38, pp. 295-299, 2017.

[36] D. Jagadish, P. R. Kumar, and K. Madhu Murthy, "Performance characteristics of a diesel engine operated on biodiesel with exhaust gas recirculation," *International Journal of Advanced Engineering Technolog,* vol. 2, pp. 202-208, 2011.

[37] M. H. M. Yasin, R. Mamat, A. F. Yusop, D. M. N. D. Idris, T. Yusaf, M. Rasul, *et al.*, "Study of a diesel engine performance with exhaust gas recirculation (EGR) system fuelled with palm biodiesel," *Energy Procedia,* vol. 110, pp. 26-31, 2017.

[38] P. N. Krishnan and D. Vasudevan, "Performance, combustion and emission characteristics of variable compression ratio engine fuelled with biodiesel," *International Journal of ChemTech Research,* vol. 7, pp. 234-245, 2015.

[39] S. Maroa, Samwel   and F. Inambao, "The Effects of Exhaust Gas Recirculation on the Performance and Emission Characteristics of a Diesel Engine–A Critical Review," *International Journal of Applied Engineering Research,* vol. 12, pp. 13677-13689, 2017.

[40] A. Sharma and S. Murugan, "Potential for using a tyre pyrolysis oil-biodiesel blend in a diesel engine at different compression ratios," *Energy Conversion and Management,* vol. 93, pp. 289-297, 2015.

[41] J. B. Heywood, "Internal combustion engine fundamentals," 2012.

[42] M. Mani, G. Nagarajan, and S. Sampath, "An experimental investigation on a DI diesel engine using waste plastic oil with exhaust gas recirculation," *Fuel,* vol. 89, pp. 1826-1832, 2010.

[43] M. Ghazikhani, M. E. Feyz, and A. Joharchi, "Experimental investigation of the exhaust gas recirculation effects on irreversibility and brake specific fuel consumption of indirect injection diesel engines," *Applied Thermal Engineering,* vol. 30, pp. 1711-1718, 2010.

[44] K. I. Abaas, "Effect of Exhaust Gas Recirculation (EGR) on the Performance Characteristics of a Direct Injection Multi Cylinders Diesel Engine," *Tikrit Journal of Engineering Science (TJES),* vol. 23, pp. 32-39, 2016.

[45] H. Venkatesan, S. Sivamani, K. Bhutoria, and H. H. Vora, "Assessment of waste plastic oil blends on performance, combustion and emission parameters in direct injection compression ignition engine,"

International Journal of Ambient Energy, pp. 1-9, 2017.

[46] P. Bridjesh, P. Periyasamy, A. V. K. Chaitanya, and N. K. Geetha, "MEA and DEE as additives on diesel engine using waste plastic oil diesel blends," *Sustainable Environment Research,* 2018.

CHAPTER EIGHT

THE EXPERIMENTAL SET-UP AND EQUIPMENT

8.1 Introduction

As discussed in section 2.1 in the literature review, one of the grey areas is the paucity of literature related to plastic pyrolysis oil biodiesel. This work is motivated by the lack of experimental work on waste plastic pyrolysis oil biodiesel in relation to EGR. Considering this trend and the level of experimental work thus far achieved, it is important that an experimental work be attempted to increase and deepen understanding in this area. Using a mathematical model and an experimental approach was deemed to be the best way to achieve the study aims and objectives as set forth to investigate the effects of exhaust gas recirculation (EGR) on the performance parameters of a diesel engine.

8.2 Experimental Apparatus and Equipment

The engine experimental set up is shown on Figure 8.1 followed by its position names.
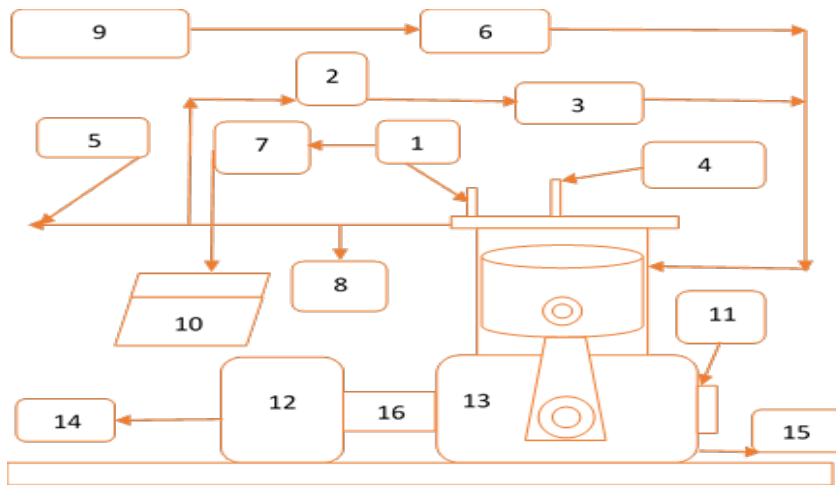
Figure 8.1: Experimental test engine schematic set-up diagram

Figure 8.1 shows the schematic diagram of the experimental engine test rig set up and its nomenclature. 1. Cylinder pressure sensor, 2. EGR control valve, 3. EGR cooler, 4. Injection Control Unit, 5. Exhaust gas exit, 6. Air box, 7. Signal amplifier, 8. Gas analyzer, 9. air flow meter,10. Data acquisition system, 11. Crank position sensor, 12. Dynamometer, 13. Engine, 14. Air flow rate meter, 15. Cooling water exit to the cooling tower, 16. Dynamometer drive coupling.
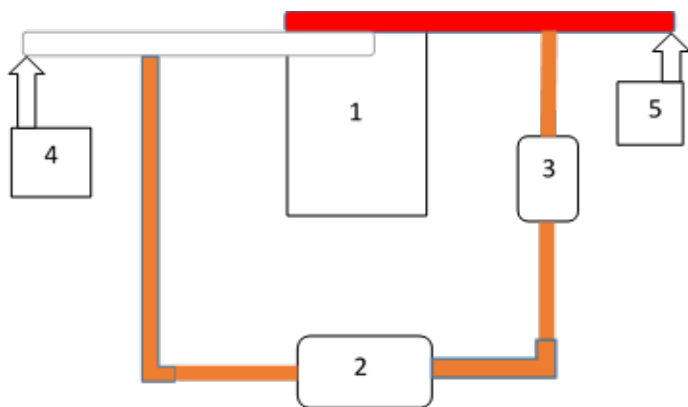
Figure 8.2: schematic of the lab set-up of the fabricated and modified exhaust recirculation mechanism to conform to the engine experimental set-up in Figure 8.1

Figure 8.2 nomenclature. 1. Engine, 2. EGR cooler system, 3. EGR control valve, 4. Inlet intake manifold, 5. Exhaust manifold.

Table 8.1: The engine specifications, position value and their type

Parameter	Position value
Ignition Type	4 (Stroke)
Number of Cylinders	DICI 1
Model	TV 1
Cooling Medium	Water
Manufacturer	Kirloskar 1500
Revolutions per Minute	3.5 Kw
Brake Power	87.5 mm
Cylinder Bore	110 mm
Piston Stroke	18.5:1
Compression Ratio	234
Connecting-Rod Length	661cc
Engine Capacity	234
Dynamometer Make	23.4 bTDC 28º
Injection Timing	N-M@1500
Maximum Torque	250 Bar
Injection Pressure	

8.3 Waste Plastic Preparation and the Conversion Process

a. The waste plastic materials were acquired from a municipal waste management site and offloaded into a waste plastic sorting section of the pyrolysis plant. The dust and other fine wastes collected from the sorted plastic waste materials were collected by the cyclone filter and disposed of through a vent with a particle size monitoring system within the plant.

b. After the sorting and removal of unwanted materials and dust, the waste plastics were taken through a conveyor machine to a pressure cleaner for thorough cleaning, as they were being conveyed to the shredding machine which reduced them to the required size of 25.4 mm to 50 mm for the pyrolysis reactor.

c. The waste material was then loaded into the pyrolysis reactor through an automatic feeding machine, although there was provision for manual loading in case there is system failure. Thereafter the reactor door was air tight locked ready to begin the pyrolysis process.

d. The system was started from a control panel by a machine operator, with the preceding processes subsequently running automatically as indicated by the flow chart in Figure 8.3.

e. The first stage was to heat up and dry the waste plastic materials and increase the reactors temperature to the required value of 400 ºC to 500 ºC. The heavy dense gas oil fell into the oil tank while the light oils rose up into the condenser where they were cooled and taken back into the oil tank for collection.

f. The small quantity of liquefied gases which could not be converted into oil were recycled by the recycling system to be burned as fuel gas or cleaned through the after-treatment system with smoke and flue emitted by the plant released to the atmosphere after the removal of sulphurets and black carbon.

g. After the pyrolysis process was over the system required a cooling period of 4 hours to 5 hours through natural cooling, but faster cooling to reduce cooling waiting time can be done using nitrogen and carbon dioxide gases as cooling agents. This enables the removal of the carbon black compound without contamination and pollution to the environment.

h. The final operation was the removal of steel and other metals obtained in the pyrolysis reactor plant, as this required the opening of the reactor door in preparation for the next batch of the pyrolysis process.

Figure 8.3 illustrates the waste plastic pyrolysis oil processing plant flow chart.
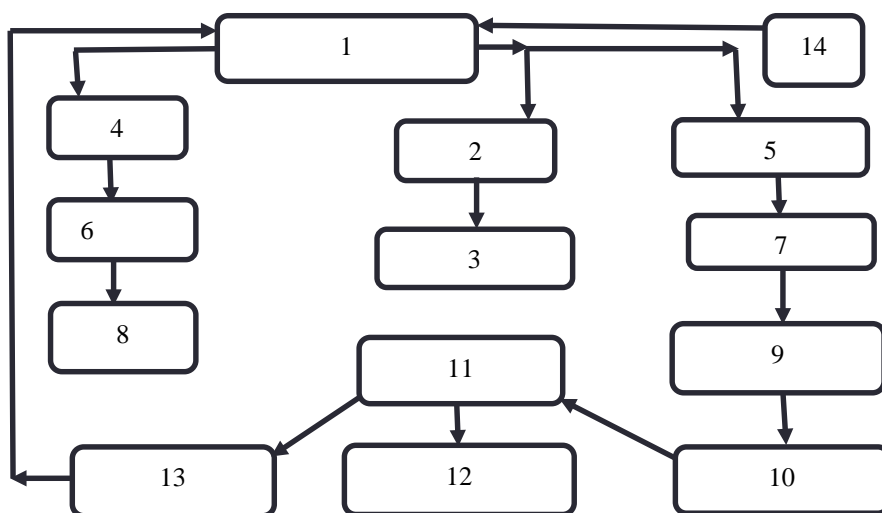
Figure 8.3: Pyrolysis flow chart

The nomenclature of the pyrolysis plant flow chart illustrated in Figure 7.3 is as follows: 1. Pyrolysis reactor, 2. Carbon black discharge, 3. Carbon black deep processing, 4. Exhaust smoke discharge, 5. Gas separator, 6. Smoke scrubber to take out color and odor, 7. Condenser, 8. Chimney, 9. Oil tank, 10. Synchronized gas purification, 11. Synchronized gas recycling system, 12. Extra gas burning, 13. Heating furnace during operation, 14. Loading of material.

8.4 Physical Properties of Waste Plastic Pyrolysis Oil (WPPO) Sample

Table 8.2 shows the results of the physical properties of the waste plastic pyrolysis oil obtained through the pyrolysis process of the waste plastics from municipal solid waste (MSW) management sites, at optimized conditions and compared to the properties of conventional diesel fuel oil.

The appearance of the oil was yellowish in color as shown by photograph in Figure 8.4. The liquid distillate is free of visible particulate sediments with a flash point of 20 ⁰C, and a gross calorific value (GCV) of 40.15 KJ/kg which almost compares to the range indicated by most petroleum fuels including conventional diesel, thus making it capable of giving the same working performance in internal combustion engines, especially diesel propelled ones.

Table 8.2: The test fuel properties, their units of measurement, standard methods of testing and the values for conventional diesel in comparison to the values of waste plastic pyrolysis oil

Property	Unit	CD	WPPO	ASTM Standard
Appearance	-	Clear/brown	Clear/amber	Visual
Density @20	kg/M^3	838.8	788.9	ASTM D1298
Kinematic viscosity @40°C	cSt	2.32	2.17	ASTM D445
Flash point	°C	56.0	20.0	ASTM D93
Cetane index	-	46	65	ASTM D4737
Hydrogen	%	12.38	11.77	ASTM D7171
Cu corrosion	3hrs@100°C	-	1B	ASTM D130
Carbon	%	74.99	79.60	ASTM D 7662
Oxygen	%	12.45	7.83	ASTM D5622
Sulphur content	%	<0.0124	0.15	ASTM D4294
IBP temperature	°C	160	119	ASTM D86
FBP temperature	°C	353.5	353.5	ASTM D86
Recovery	%		98	-
Residue and loss	%		2.0	-
Gross calorific value	kJ/kg	44.84	40.15	ASTM D4868

Figure 8.4: The distillate samples from the waste plastic pyrolysis oil samples

The distillation report analysis (Table 8.3) shows that the WPPO had an initial boiling point (IBP) of 119 °C to 353.5 °C, thus indicating some presence of other fuel oil components like kerosene, gasoline and to some extent diesel oil in the tested samples. This leads to the observation and conclusion that it is possible for this oil to be used as feedstock in future if it is upgraded into a lighter compound such as diesel fuel or any liquid.

153

Table 8.3: The chemical composition of the waste plastic oil from a pyrolysis plant process: the carbon chains and percentage compositions in the test fuel, obtained from a GC-MS laboratory analysis report

Molecular formula	Percentage composition
C_{10}	66.32
C_{10}-C_{15}	4.38
C_{15}-C_{20}	12.66
C_{20}-C_{25}	8.22
C_{25}-C_{30}	8.42

8.5 Experimental Procedure

a. The engine that was employed for this work was a Kirloskar experimental variable compression engine, four stroke single cylinder, water cooled developing 3.725 kW of power at 1500 rpm. The schematic of the experimental set-up being as in Figure 8.1.

b. The technical specifications of the experimental variable compression engine are shown and indicated in Table 8.1. A dynamometer was used to provide the engine with load during the experimentation. To get measurements for the EGR system and engine intake air flow, an air box was fitted to the engine intake manifold system with a standard orifice mechanism, and a fabricated EGR valve and cooler exchanger as provided for in Figure 8.3 and by the equations on orifice systems as presented in Chapter 3 sub-sections 3.4 to 3.53.

c. The fuel flow rate to the experimental engine was measured using a digital fuel gauge with a stop watch mounted to measure time taken for the fuel to be consumed. The calculations were as per the equations in Chapter 3 sub-section 3.3.5 and 3.3.7.

d. The EGR % flow rate was calculated according to the equation on air fraction provided in Chapter 3 subsection 3.4.3.

e. The BTE from the experimental engine was calculated according to the equations in Chapter 3 subsection 3.3.5.

f. The BP in this experiment was given as per the equation in Chapter 3 subsection 3.3.6.

g. The EGTs were measured using mounted temperature thermocouples of k-2 type, including the EGR temperature which was measured before it mixed with the intake air fresh charge and the constituents of the combustion chamber, through the same k-2 thermocouples.

h. A cylinder pressure transducer was mounted on the engine cylinder head to monitor cylinder combustion pressure and collect data values through a system charge amplifier connected to a computer data acquisition machine.

i. The crankshaft position or the crank angle was monitored and measured through a mounted encoder near the crankshaft pulley area and data transferred to the data processor.

j. The emission gases during the experiment were monitored through a five gas exhaust gas analyzer, and the smoke intensity was measured by means of an AVL 437C smoke meter.

k. Since the engine developed maximum power at 1500 rpm and was a variable compression engine, all the experiments were conducted based on this nominal engine speed at part load and full load, but data could be obtained from different engine loads. Part engine load is described as 50 % of engine load and engine full load is described as engine running at 100 % load, with a fixed CR of 18.5:1.

l. The EGR system was modified to suit the experimental engine and to enable the study to be conducted, with exhaust gases being tapped from the exhaust pipe and joined to the intake manifold air intake system via the air flow meter box through a manually controlled gate valve which made it possible for the mixing of EGR gases and the fresh air intake.

m. The EGR % flow rate was divided into the following modes 0 %, 5 %. 10 %, 15 %, 20 %, 25 %, and 30 % spaced at intervals of 5 %.

n. The WPPO fuel blends were prepared in the following percentages order and mixed with diesel fuel in 10 %, 20 %, 30 %, 40 % and 100 %, where a 10 % blend was 90 % conventional diesel fuel and 10 % WPPO fuel in that order, referred to as WPPOB10 with 10 denoting the percentage blend of WPPO by volume supplied.

o. To avoid contamination of the experimental fuel, each test was conducted after a thorough evacuation procedure was conducted on the previous preceding experiment on the fuel lines and the fuel injection system mechanism of the test engine. This made it possible to conduct an experiment and collect good data and measurements with inputs from the test mode only, without fear of contamination and poor results from error.

8.6 Performance Measurements

The following are the tables for the various performance parameters and the values obtained during the experiment and study of the interactions between test fuels (conventional diesel and

blends of WPPO diesel), EGR application percentages, engine load percentages and EGT values in relation to BSFC, BTE and BP.

Table 8.4: BSFC values in relation to engine load and various test fuel blends of WPPO and conventional diesel (CD)

LOAD %	CD	WPPOB10	WPPOB20	WPPOB30	WPPOB40	WPPOB100
10	0,612	0,575	0,585	0,595	0,605	0,675
20	0,560	0,515	0,535	0,545	0,560	0,595
30	0,525	0,465	0,485	0,540	0,550	0,565
40	0,465	0,375	0,425	0,535	0,542	0,555
50	0,375	0,300	0,325	0,475	0,440	0,550
60	0,355	0,275	0,315	0,450	0,540	0,548
70	0,350	0,300	0,325	0,400	0,440	0,540
80	0,356	0,325	0,330	0,385	0,420	0,520
90	0,360	0,315	0,335	0,380	0,415	0,510
100	0,380	0,310	0,338	0,375	0,410	0,500

Table 8.5: BSFC kg/kW. hr. values under the effects of EGR % flow rate, full engine load with different fuel blends of WPPO and conventional diesel (CD)

EGR %	CD	WPPOB10	WPPOB20	WPPOB30	WPPOB40	WPPOB100
0	0,4000	0,3225	0,3615	0,3645	0,3715	0,4751
5	0,4345	0,4070	0,4915	0,4995	0,5125	0,5522
10	0,450	0,5350	0,5715	0,6125	0,6483	0,6751
15	0,464	0,5500	0,5885	0,6225	0,6525	0,6862
20	0,4755	0,5650	0,5995	0,6452	0,6671	0,6695
25	0,487	0,5700	0,6100	0,6491	0,6697	0,7116
30	0,495	0,5780	0,6135	0,6573	0,6682	0,7235

Table 8.6: BTE % values, at full engine load with blends of WPPO and conventional diesel (CD)

LOAD %	CD	WPPOB10	WPPOB20	WPPOB30	WPPOB40	WPPOB100
10	6,5	7,05	6,8	6,75	6,15	5,6
20	13,25	15,25	15,25	15	13,45	11,95
30	15,45	20	19	18,15	16,85	13,75
40	18,15	23	22,25	22,45	21	16,85
50	20,25	24,7	23,65	23,15	22,1	17,45
60	20,95	26,15	25	25,25	23,25	18,45
70	23	26,45	25,35	25,2	24,15	20,25
80	24,15	26,65	25,75	25,1	24,95	21,45
90	23	26,85	26,15	25	24,75	20,96
100	21	27	25,75	24,75	23,25	18,95

Table 8.7: BTE % values, under load with EGR % flow rate application with blends of WPPO and conventional diesel (CD)

EGR %	CD	WPPOB10	WPPOB20	WPPOB30	WPPOB40	WPPOB100
0	12,15	13,25	13,05	12,75	11,55	10,65
5	10,25	11,85	11,35	10,6	9,65	9,15
10	8,15	10,15	9,65	8,85	7,5	7,05
15	6,35	8,35	8,15	6,95	5,85	5,25
20	5,15	6,85	6,45	5,65	4,85	4,15
25	4,35	5,4	4,85	4,2	3,85	3,15
30	3,95	4,25	4,15	3,85	3,15	2,35

Table 8.8: BP values under engine load with blends of WPPO and conventional diesel (CD)

LOAD %	CD	WPPOB10	WPPOB20	WPPOB30	WPPOB40	WPPOB100
10	0,875	0,87	0,868	0,865	0,862	0,855
20	1,45	1,35	1,255	1,215	1,1	1
30	2,125	2,15	2,05	1,98	1,86	1,75
40	2,65	2,55	2,45	2,36	2,33	2,25
50	3	2,98	2,9	2,86	2,75	2,65
60	3,25	3,2	3,1	3,05	3	2,9
70	3,5	3,45	3,35	3,22	3,18	3,05
80	3,75	3,68	3,6	3,48	3,4	3,25
90	3,95	3,85	3,76	3,65	3,58	3,45
100	4	3,95	3,85	3,74	3,7	3,55

Table 8.9: Temperature values for exhaust gas under different WPPO blends and conventional diesel (CD) with the application of EGR % flow rate at full engine load

EGR %	CD	WWPOB10	WPPOB20	WPPOB30	WPPOB40	WPPOB100
0	456	478	478	476	468	490
5	440	464	395	456	460	478
10	392	424	378	416	422	415
15	369	394	370	406	410	386
20	365	390	360	386	382	375
25	363	383	358	353	368	364
30	340	362	345	338	331	320

8.7 Emission Measurements

This section deals with emission measurements and the data obtained from emissions of NO_X, CO_2, CO, O_2 and UHC and smoke opacity. The emissions for these gases were measured by the five gas analyzer while the smoke emissions or smoke opacity were measured with a smoke meter as mentioned in section 8.5 on experimental procedure. The data obtained is tabulated in Tables 8.10 to 8.17.

Table 8.10: NO_X emissions (ppm) values versus engine load with different WPPO blended fuels and conventional diesel (CD) under the influence of EGR % flow rate application

EGR %	CD	WPPO10	WPPO20	WPPO30	WPPO40	WPPO100
0	920	1000	1060	1120	1240	1270
5	812	890	1016	1076	1196	1226
10	760	830	971	1031	1151	1116
15	700	696	784	887	947	972
20	623	591	645	750	778	851
25	533	501	555	640	633	706
30	432	401	455	483	475	536

Table 8.11: NOₓ emissions (ppm) values versus full engine load with different blends of WPPO and conventional diesel (CD)

LOAD %	CD	WPPOB10	WPPOB20	WPPOB30	WPPOB40	WPPOB100
10	250	280	315	325	345	420
20	355	375	385	395	405	500
30	432	415	445	465	485	555
40	515	535	565	575	600	685
50	635	655	686	698	745	795
60	700	685	700	745	792	865
70	745	705	735	798	865	945
80	860	775	815	905	975	1095
90	1000	895	955	1045	1115	1215
100	1100	995	1065	1145	1225	1325

Table 8.12: UHC emissions (ppm) values under engine load with different fuel blends of WPPO and conventional diesel (CD) under the effects of EGR % flow rate application

EGR %	CD	WPPOB10	WPPOB20	WPPOB30	WPPOB40	WPPOB100
0	22	23	21	20	19	17
5	43	35	32	27	23	24
10	57	46	38	34	29	26
15	70	58	45	40	37	35
20	77	68	52	46	44	40
25	82	72	55	48	43	41
30	85	75	60	49	46	43

Table 8.13: CO emissions % values versus engine load with the different fuel blends of WPPO and conventional diesel CD)

LOAD %	CD	WPPO10	WPPO20	WPPO30	WPPO40	WPPO100
10	4,75	3,95	3,76	3,45	3,35	2,65
20	4,35	3,55	3,36	3,1	2,97	2,35
30	4,0	3,	2,85	2,72	2,65	2,
40	3,5	2,5	2,45	2,35	2,25	1,85
50	3,	2,25	2,15	2,15	2,15	1,65
60	3,27	2,55	2,55	2,45	2,25	1,68
70	35	3,	3,	2,65	2,5	1,7
80	4,1	3,35	3,36	2,95	2,88	2,
90	4,65	4,25	4,15	3,75	3,55	2,65
100	5,1	4,99	4,9	4,6	4,45	3,1

Table 8.14: CO emissions % values versus EGR % flow rate with different fuel blends of WPPO and conventional diesel (CD)

EGR %	CD	WPPO10	WPPO20	WPPO30	WPPO40	WPPO100
0	4,2	4,35	4,65	4,85	5	5,25
5	5,25	6,52	6,98	7,28	7,5	8,75
10	7,65	9,79	10,46	10,91	11,25	12,75
15	11,68	13,55	15,7	16,37	16,88	18,95
20	18,25	21,35	22,65	24,55	26,95	28,85
25	26,56	30,56	33,25	35,75	38,94	42,15
30	36,25	43,65	49,58	52,69	56,95	59,79

Table 8.15: CO_2 emissions % values for various blends of WPPO and conventional diesel (CD) under engine load

LOAD %	CD	WPPO10	WPPO20	WPPO30	WPPO40	WPPO100
10	2	1,95	1,25	1,15	1,2	3,35
20	3	2,5	2,25	1,5	1,85	4,65
30	3,5	3,25	3	2	2,25	5,45
40	4,45	4	3,65	3,25	2,75	6,15
50	5,5	4,98	4,5	3,85	3	6,95
60	6,35	5,65	5	4,45	3,5	8,05
70	6,75	6,25	5,85	5,25	4,5	9,3
80	8,5	7,65	7	6,65	5,98	10,45
90	9,85	8,55	8	7,75	7,15	11,65
100	10,85	9,65	8,75	8,35	8	12,75

Table 8.16: CO_2 % values for various blends of WPPO and conventional diesel fuel under engine load with the application of EGR % flow rate

EGR %	CD	WPPOB10	WPPOB20	WPPOB30	WPPOB40	WPPOB100
0	3,85	3,65	3,25	2,75	2,65	6,25
5	4,45	4,25	3,65	3,25	3	6,55
10	5,35	4,75	4,25	3,95	3,65	7,25
15	6,35	5,75	5,15	4,5	4,15	8,75
20	7,35	6,65	5,95	5,65	5,15	9,95
25	8,5	7,95	7,45	7,05	6,52	11,95
30	10,95	9,95	9,65	8,85	8,55	14,35

Table 8.17: Smoke emissions or opacity % values at full engine load, with different blends of WPPO and conventional diesel (CD) under the effects of EGR % flow rate application

EGR %	CD	WPPOB10	WPPOB20	WPPOB30	WPPOB40	WPPOB100
0	5,5	5,1	5	5,15	5,05	4,8
5	6,65	6,15	5,8	5,45	5,15	4,65
10	6,95	6,6	6,25	5,85	5,55	5
15	7,53	7,1	6,72	6,25	6	5,4
20	8	7,65	7,15	6,95	6,55	5,65
25	9,1	8,45	7,75	7,33	6,9	5,95
30	9,85	9,25	8,65	8,45	7,85	7,15

8.8 Analysis of Error and Percentage Uncertainties

This process is carried out for the purpose of performing and identifying the accuracy and precision of the measuring tools and instruments used in this experiment work, as errors can occur due to other conditions outside of the experiment itself [1], such as calibration of the instruments, observational errors [2], manufacturing errors, errors associated with experimental set-up and planning, as well as environmental conditions existing during the experiment [3]. The list of instruments used and their percentage error of analysis are provided in Table 8.18 together with the uncertainties of CO, CO_2, UHC, NO_X, EGT and smoke opacity.

This percentages of error analysis is derived from the following formula, the root sum square method and expressed in equation form [4] as:

$$R = \sqrt{\sum_{i=1}^{n} X_i^2}$$ Equation 1

Where R is the total uncertainty percentage, X_i is the individual uncertainty of all the calculated operating parameters, n is the total number of the parameters in the experiment and i is the ith term of the computed parameters. The total percentage of the uncertainty is thus calculated based on Equation 2 as follows [5].

$$R = \sqrt{X_1^2 + X_2^2 + X_3^2} + \cdots X_i^2$$ Equation 2

Table 8.18: Instruments used for measurements and data collection, their measuring range, accuracies and percentages of inaccuracies, as calculated from Equation 2

| Instrument	Accuracy	Measuring Range	Percentage inaccuracies
AVL 437C (smoke meter) Smoke intensity	±1%	0-100%	±1
AVL pressure transducer GH14D	±0.01 bar	0-250 bar	±0.01
VL 365C Angle encoder	±1°		±0.2
AVL digas 444 (five gas analyzer)			
CO	±0.03% to ±5%	0-10% by vol	±0.3
CO_2	±0.5% to ±5% by vol	0-20% vol	±0.2
O_2	±5% by vol	0-22% by vol	±0.3
HC	±0.1% to ±5%	0-20000ppm by vol	±0.2
NOx	±10%	0-5000 ppm by vol	±0.2
K-2 thermocouple	±1°C	0-1250°C	±0.2
Digital stop watch	±0.2s		±0.2
U-tube Manometer	±1mm		±2
Burette	±0.2cc	1-30cc	±1.5

References

[1]   M. Kanoğlu, "Cryogenic turbine efficiencies," *Exergy, An International Journal,* vol. 1, pp. 202-208, 2001.

[2]   K. Krisnangkura, "A simple method for estimation of cetane index of vegetable oil methyl esters," *Journal of the American Oil Chemists Society,* vol. 63, pp. 552-553, 1986.

[3]   P. Senthilkumar and G. Sankaranarayanan, "Production of waste polyethylene bags in to oil and studies performance, emission and combustion characteristics in di diesel engine," *International journal of humanities, arts, medicine and science,* vol. 3, pp. 149-158, 2015.

[4]   V. K. Kaimal and P. Vijayabalan, "A detailed study of combustion characteristics of a DI diesel engine using waste plastic oil and its blends," *Energy conversion and Management,* vol. 105, pp. 951-956, 2015.

[5]   D. Damodharan, A. P. Sathiyagnanam, B. R. Kumar, and K. C. Ganesh, "Cleaner emissions from a DI diesel engine fueled with waste plastic oil derived from municipal solid waste under the influence of n-pentanol addition, cold EGR, and injection timing," *Environmental Science and Pollution Research,* pp. 1-15, 2018.

RESULTS AND DISCUSSION

9.1 Brake Specific Fuel Consumption (BSFC)

Figure 9.1 shows the variation of the BSFC under the effects of EGR % flow rate with different fuel blends of WPPO and conventional diesel operating at full engine load conditions.
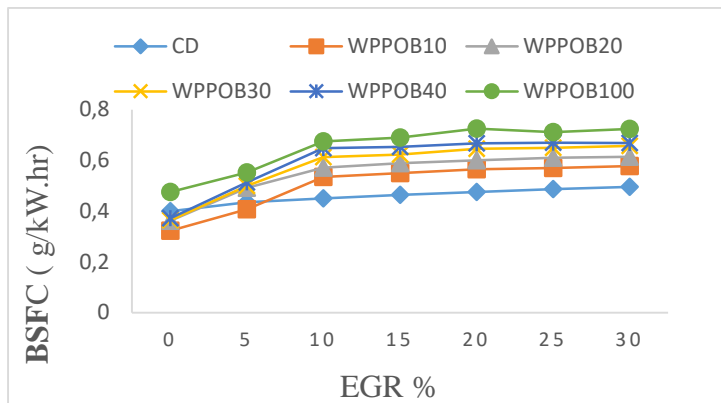
Figure 9.1: BSFC versus EGR % rate flow under full engine load conditions

As can be seen from Figure 9.1, The lower ratio blends of WPPOB10 and WPPOB20 show low and reduced values of BSFC at 0 % EGR flow rate as in Figure 9.1 and Table 8.5 in Chapter 8 compared to the values of conventional diesel. However, WPPOB100 shows a significant high value of 0.4751 g/kW.hr for BSFC at 0 % EGR flow rate compared to all other test fuels even with application of any percentage rate of EGR flow. This is an indication that WPPOB100 has a higher BSFC than diesel and the other blends of WPPO which have values of 0.3225 g/kW.hr, 0.3615 g/kW.hr, 0.3645 g/kW.hr and 0.3715 g/kW.hr, for WPPOB10, WPPOB20, WPPOB30, WPPOB40 and conventional diesel with 0.4 g/kW.hr respectively. From the graph in Figure 8.1, it can be seen that as the EGR % flow rate increases from 0 % to 10 % all the test fuels report an increased BSFC except for the conventional diesel test fuel, which continues to have lower values of BSFC irrespective of the EGR flow rate applied. For example, at 10 % its value is 0.45 g/kw.hr compared to 0.5715 g/kW.hr, 0.5885 g/kW.hr, 0.6483 g/kW.hr, 0.6483 g/kW.hr and 0.6751 g/kW.hr respectively for WPPO10, WPPO20, WPPO30, WPPO40 and WPPO100.

At 10 % EGR flow rate the values for the BSFC across all the test fuel except conventional diesel seem to show and pick up a sharp increasing curve below the 10 % EGR flow rate, as in

Figure 8.1 but as the EGR flow rate increases from 10 % there is a flattening of the graph curves and close value trends observed.

The WPPO biodiesel blends with EGR % flow rate application showed better fuel economy especially the lower blend ratios of WPPOB10 and WPPOB20 as compared to high ratio blended test fuels. However, as the EGR % flow rate is increased there is a noticeable increase in the BSFC across all the test fuels used. At 0 % EGR conventional diesel is 0.4 g/kW.hr compared to 30 % EGR flow rate at 0.495 g/kW.hr, while for the WPPO biodiesel blends WPPOB10 is 0.3225 g/kW. as compared to 0.5780 g/kW.hr at 30 % EGR. From Figure 9.1 it is evident that the test fuel that showed the highest BSFC value among the blends of diesel and conventional diesel test fuel is WPPOB100 which at 0 % EGR % flow rate had a value of 0.4751 g/kW.hr compared to 0.7235 g/kW.hr at 30 % EGR % flow rate.

A similar trend is noted regarding the influence of EGR % flow rate where, for example at between 20 % to 25 % EGR flow rate, the BSFC continued to show increasing tendencies. This finding concurs with the findings of [1]. This phenomenon can be explained due to the effects of dilution of the fresh air intake as it mixes with exhaust gases that are being recirculated through the EGR system which leads to incomplete combustion of the inducted mixture, thus leading to a drop in power and engine torque as reported by the findings of [2]. This scenario forces the engine to increase its fuel consumption in order to maintain momentum and constant speed, these changes lead to increased load hence the increase in BSFC.

9.2 Brake Thermal Efficiency (BTE)

BTE studies specifically help us to know the ability of the combustion system to accept the fuel provided as a comparable means of assessing how efficiently fuel conversion was carried in turning that fuel into a mechanical output able to do work, as observed by [3, 4].

Figure 9.2 shows the BTE % variations under engine load with different blends of WPPO and conventional diesel test fuels.
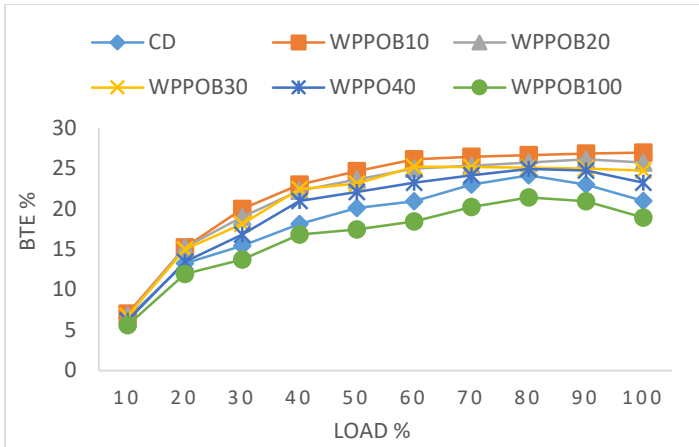
Figure 9.2: Variation of BTE versus engine load %

Figure 9.3 shows the BTE % variations under engine loads with different blends of WPPO and conventional diesel fuel, with application of EGR % flow rate.
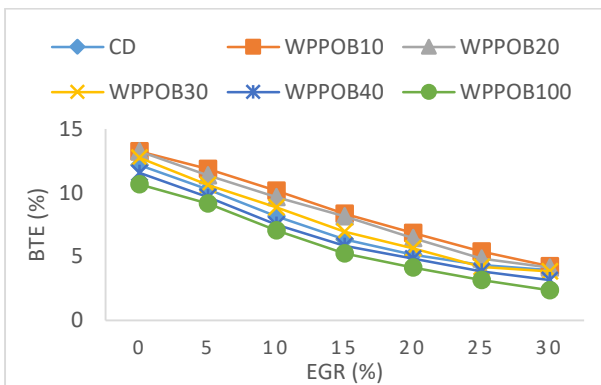
Figure 8.3: BTE % versus EGR % flow rate

The BTE is as provided in Tables 8.6 and 8.7 in Chapter 8 and as provided for in Chapter 3 sub-section 3.3.5. Figure 9.2 is the variation of the brake thermal efficiency under load with different blends of WPPO. There is a noticeable increase in the BTE especially with all low ratio fuel blends of WPPOB10 and WPPOB20 as compared to conventional diesel fuel. However, in comparison to other WPPO blends WPPOB100 obtained the lowest increment of BTE with a value of 5.6 % at 10 % engine load and a maximum increment of 18.95 % at 100 % engine load. The other blends of WPPO as aforementioned exhibited higher BTE values, especially for the low ratio blends compared to the high ratio blends. For example, at 10 % engine load the value of the BTE for WPPOB10 is 7.05 % while WPPOB30 and WPPO40 have values of 6.75 % and 6.15 % respectively. The other blends of WPPO continued to show

this same trend because at 100 % engine load the value for WPPOB10 and WPPO20 is observed to be 27.0 % and 25.75 % as compared to WPPOB30 and WPPOB40 which have values of 24.75 % and 23.35 % respectively.

The high BTE values observed for WPPO blends in Figure 8.2 may be due to the high viscosity of the WPPO blends as compared to conventional diesel during the combustion pre-mixing phase. It is observed that at high engine load the brake thermal efficiency for conventional diesel is 21.0 % but to the values for the WPPO blends are 27 %. 25.75 %, 24.75 %, 23. 25 and 18.95 for WPPOB10, WPPOB20, WPPOB30, WPPOB40 and WPPOB100 respectively.

Although there is a reduction in BTE due to the application of EGR % flow rate as in Figure 8.3 here and in Table 8.7 in Chapter 8, the trends of decreased BTE continue to be observed, despite showing higher values than conventional diesel except for WPPO100. For example, at 5 % EGR flow rate, the value of BTE for conventional diesel is 10.25 % compared to WPPOB10 and WPPOB20 with values of 11.85 % and 11.35 %. The WPPOB100 blend has the lowest value for BTE of all EGR flow rate modes out of all test fuels. At an EGR flow rate of 0 % WPPOB100 has a maximum value of 10.65 % compared to 2.35 % at 30 % EGR flow rate which was the minimum value obtained.

There is a correlation between the blend ratio and the rate of EGR flow that is observed. As the blend ratio increases there is a general decrease in the BTE across and within all the blended test fuels, with an increase in EGR flow rate. For example, all the blends of WPPO at 10 % EGR flow rate report values of 10.15 kW.hr, 9.65 kW.hr 8.85 kW.hr, 7.5 kW.hr and 7.05 kW.hr. However, WPPO20 reports decreasing values of 13.05 kW.hr, 11.35 kW.hr, 9.65 kW.hr, 8.15 kW.hr, 6.45 kW.hr, 4.85 kW.hr and 4.15 kW.hr as the rate of EGR % flow is increasing from 0 % to 30 % respectively.

9.3 Brake Power (BP)

Figure 9.4 shows engine BP variations with exhaust gas recirculation (EGR) % flow rate application with conventional diesel fuel and different blends of WPPO at full engine load conditions.
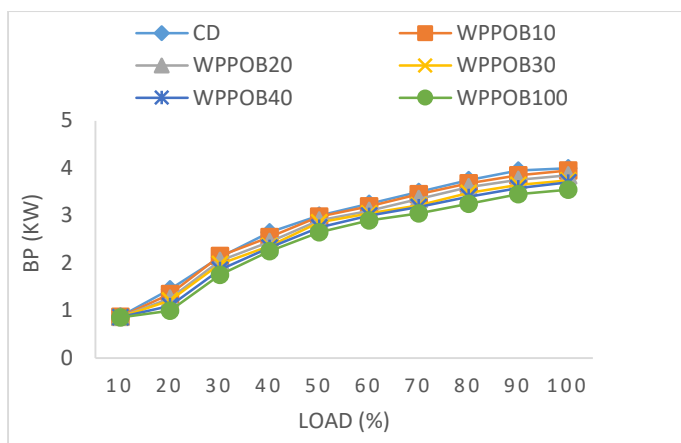
Figure 9.4: Variation of engine brake power versus varying engine load %

As can be seen from Figure 9.4 there is a lineal increase in the BP for all the test fuels applied with an increase in the engine load. Conventional diesel fuel has the highest increase in BP values compared to the blended fuels of WPPO. At 20 % engine load WPPOB10 has a value of 1.350 kW compared to conventional diesel at 1.45 kW, representing a difference of 6.8 % when the two fuels are compared.

The blended fuels in Figure 9.4 also show very close increments with increase in engine load conditions and a decrease in BP with an increase in the blend ratio for all the blended fuels tested when compared to conventional diesel fuel. The increase in the blend ratio showed a direct decrease in BP in a linear incremental relationship across the blends. For example, at 60 % engine load WPPOB10, WPPOB20, WPPOB30 WPPOB40 and WPPO100 have values of 3.2 kW, 3.1kW, 3.05 kW, 3 kW and 2.9 kW respectively showing a decrease in the value of the engine BP as the load increased across the blends throughout the experimentation period. These findings concur with the findings by another researcher in relation to WPPO blends [5].

WPPOB100 blend showed the lowest values for the engine BP compared to the blends of WPPOB10, WPPOB20, WPPOB30 and WPPOB40. At 30 % engine load WPPOB100 has a value of 1.75 kW compared to WPPOB10 at 2.15 kW, WPPOB20 at 2.05 kW, WPPOB30 at 1.98 kW and WPPOB40 at 1.86 kW respectively. From this result, it can be established that all the blends of WPPO produce less engine power compared to the power produced by the conventional diesel test fuel. This result is attributed to their differences in GCV as outlined in Table 8.2 in Chapter 8.

The application of EGR % flow rate is observed to cause no significant change in BP. However, there was a negligible drop in the engine BP with the influence of EGR % flow rate except for the blend WPPOB10 which had almost identical values to conventional diesel as the curve of the two fuels indicate in Figure 9.4 and Table 8.8 in Chapter 8.

9.4 Exhaust Gas Temperature (EGT)

Temperature is one of the key factors in determining the formation of engine exhaust emissions, besides providing or helping in the analysis and study of combustion processes in relation to fuel as observed by [6].

Figure 9. 5 shows the variation of EGT under different types of WPPO blends and conventional diesel test fuel with application of EGR % flow rate.
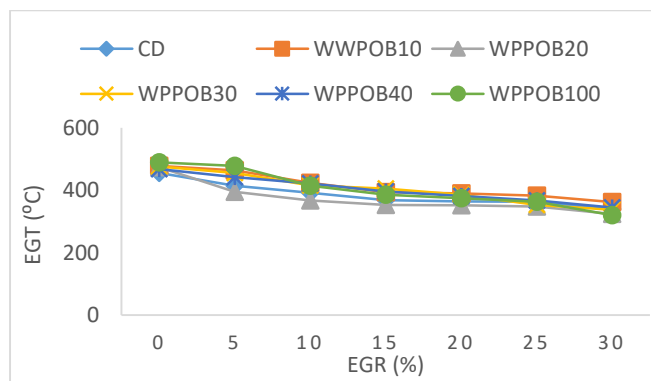
Figure 9.5: Variation of EGT ⁰C versus EGR % flow rate

The graph in Figure 9.5 and Table 8.9 in Chapter 8 show a variation in EGT with different fuel blends and conventional diesel with the application of EGR % flow rate. The result indicates that EGT decreases with different blends of WPPO compared to conventional diesel, although the temperature difference between them is that WPPO blends have higher temperature increases in all the test conditions compared to conventional diesel fuel. However, it should be mentioned that as the blend ratio increases with increase in application of the EGR % flow rate, the EGT reduced significantly and marginally especially for WPPOB30 and WPPOB40. For example, at 10 % EGR flow rate the values are 416 ⁰C and 422 ⁰C. However, when the rate of EGR flow is increased to 20 % the values drop to 386 ⁰C and 382 ⁰C respectively. The highest temperature obtained for conventional diesel is 456 ⁰C at 0 % EGR flow rate, whereas the highest temperature value for a WPPO blend is 490 ⁰C obtained from WPPOB100 at 0 % EGR flow rate, although at 30 % EGR flow rate this blend was most reduced in temperature

169

compared to the other WPPO blends with a temperature value of 320 ºC, while WWPO10, WPPO20, WPPO30 and WPPO40 had values of 362 ºC, 345 ºC, 338 ºC and 331 ºC respectively.

The application of EGR % flow rate in increasing modes brings further reduction in EGT with the highest value for conventional diesel test fuel obtained being 440 ºC when EGR % flow rate was at 5 %, while the lowest value of 340 ºC was obtained at 30 % EGR flow rate. The WPPO blends show a similar trend with decreasing temperatures with the increasing application of EGR % flow rate. WPPOB10 reports the highest values to be 467 ºC and the lowest to be 362 ºC at 5 % and 30 % EGR flow rates respectively, while WPPOB40 shows its highest value to be 472 ºC and the lowest to be 330 ºC at 5 % and 30 % EGR flow rates respectively. This concludes that all the WPPO blends report low EGT values compared to the conventional diesel test fuel.

It is imperative to note here that a decrease in EGT is noticed irrespective of the continuous increase in EGR % flow rate even after the 15 % point EGR flow rate is reached. The main cause for reduction in the EGT can be attributed to several factors: The reduction in EGT among the different blends of WPPO could result from low CV of the blends and low exhaust loss which concurs with the findings of [7, 8].The WPPO has a CV of 40.15 kJ/kg compared to the CV of conventional diesel at 44.84 kJ/kg as seen in Table 8.2.The third cause is directly linked to the effects of exhaust gas recirculation percentage flow rate, the dilution effect, chemical effects and thermal effects [9, 10] which are extensively discussed in Chapter 2.

9.5 NOX Emissions

Figure 8.6 shows the variations of NOX emissions (ppm) and engine load with different blends of WPPO and conventional diesel fuel with EGR % flow rate application.
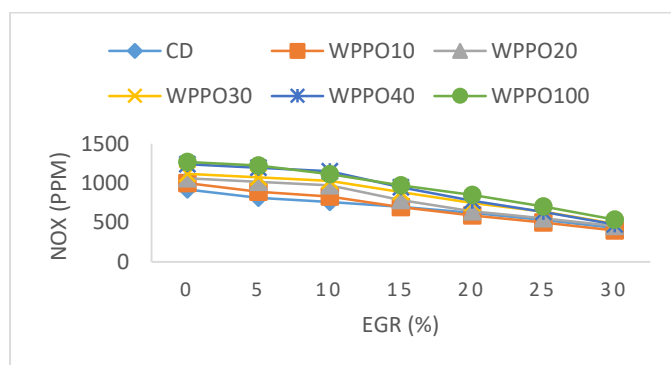

Figure 9.6: Variations of NOX emissions (ppm) versus EGR % flow rate

NO$_X$ emissions formation is highly dependent on in-cylinder temperature, the concentration of oxygen and the residence time the fuel-air mixture spends in the combustion chamber during the pre-mixing phase [11]. All the fuels tested indicated a drop in NO$_X$ emissions with an increase in the application of EGR % flow rate, at all engine load conditions. Table 8.10 in Chapter 8 and Figure 9.6 shows that this could be due to the rise in the total heat capacity of the working gases that are increasing with increasing EGR % flow rate thus concurring with the studies and findings of [12, 13].

The NO$_X$ emissions values for conventional diesel in Figure 9.6 and Table 8.10 is 920 ppm for conventional diesel test fuel, while for WPPOB100 it is 1325 ppm at full engine load of 100 %, compared to the reduced values with application of EGR flow rate of 30 % as in Figure 9.7 and Table 8.11, where conventional diesel decreases its NO$_X$ emissions to 432 ppm compared to 1100 ppm at full load of 100 % before application of EGR % flow rate.

As the blend ratio increases with increased EGR % flow rate there is an increase in NO$_X$ emissions across CD and the WPPO blends but with reduced NO$_X$ emissions within the blends and within the CD test fuel as in Figure 9.6 and Table 8.10. For example, at 20 % EGR flow rate, blends WPPO10, WPPO2O, WPPO30, WPPO40 and WPPO100 had 591 ppm, 645 ppm, 750 ppm, 778 ppm and 851 ppm respectively. However, WPPO20 has reduced values of 1060 ppm, 1016 ppm, 971 ppm, 784 ppm, 645 ppm, 555 ppm and 455 ppm as the rate of EGR flow increases from 0 % to 30 %.

Figure 9.7 shows variations of NO$_X$ emissions (ppm) under engine load with different blends of WPPO and conventional diesel test fuel.
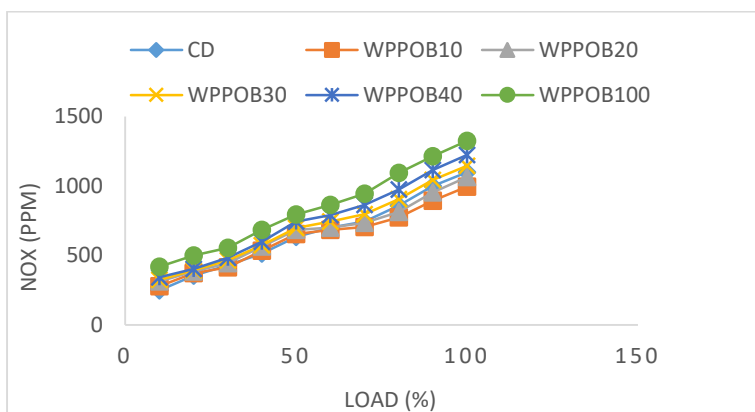

Figure 9.7: Variations of NO$_X$ emissions (ppm) versus varying engine load %

During experimentation it was observed that at part engine load as in Table 8.11 in Chapter 8 and Figure 9.7 the values for NO$_X$ emissions for the same fuels were lower compared to the full load engine conditions. The NO$_X$ emission for conventional diesel at engine part load (50 %) is 635 ppm compared to full load at 1100 ppm, whereas the value for WPPOB100 at engine part load (50 %) is 795 ppm compared to 1325 ppm at full engine load. This seems to indicate a concurrence that at part engine load (50 %) the values of NO$_X$ emissions emitted by all the blends of WPPO except WPPO100 are lower as compared to the values reported at full engine load conditions.

9.6 Hydrocarbon (HC) Emissions

Figure 9.8 shows the variation of HC emissions in parts per million under full engine load with the application of various EGR % flow rates, different blends of WPPO and conventional diesel. The HC emissions were significantly higher across all the blended test fuels of WPPO, especially with higher engine load conditions as indicated by the values shown in Figure 9.8 and Table 8.12 in Chapter 8. However conventional diesel still produced higher values of HC emissions compared to all blends of WPPO across all the engine loading conditions and operating modes.

Figure 9.8 shows UHC emission (ppm) values under engine loads with different fuel blends of WPPO and conventional diesel under the effects of EGR % flow rate application.
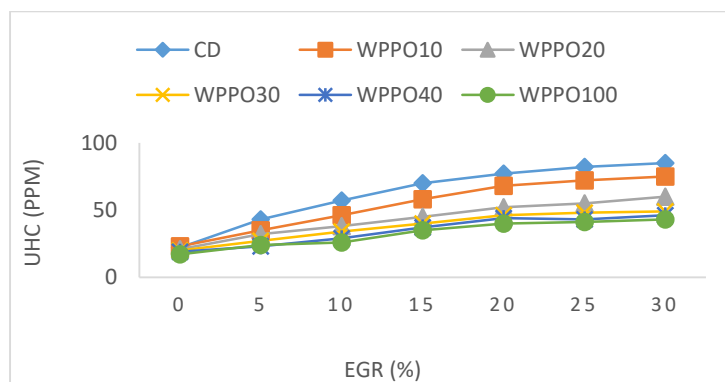
Figure 9.8: Unburnt hydrocarbons emissions versus EGR % flow rate

When the EGR % flow rate application is 0 % there is no application effect. Figure 9.8 shows that there are less HC emissions for all the test fuels applied in this experiment, compared to

20 % or 30 % EGR percentage flow rates. The value for the conventional diesel test fuel was 22 ppm at 0 % EGR flow rate and for the blends of WPPO the values were 23 ppm, 21 ppm, 20 ppm, and 17 ppm for WPPOB10, WPPOB20, WPPOB30, WPPOB40 and WPPOB100 respectively. However, with EGR flow rate of 10 % was applied the values are 57 ppm for conventional diesel and the blends of WPPO 46 ppm, 38 ppm, 34 ppm, 29 ppm and 26 ppm respectively.

Although the application of EGR % flow rate reduces the amount of HC emissions from the applied test fuels across the board, conventional diesel fuel still produced more HC emissions from the test engine compared to all the WPPO blends tested. Figure 8.8 shows that at EGR flows rate of 5 %, 10 %, 15 %, 20 %, 25 % and 30 %, conventional diesel had 43 ppm, 57 ppm, 70 ppm, 82 ppm and 85 ppm respectively, as compared to WPPOB10 whose values are 23 ppm, 35 ppm, 40 ppm, 48 ppm, 50 ppm, and 52 ppm respectively.

Therefore, the application of EGR % flow rate increased HC emissions as observed and indicated from the results and values presented in Figure 9.8 and Table 8.12 in chapter 8, with conventional diesel fuel producing the highest HC emission values as compared to all the test fuel blends of WPPOB10, WPPOB20, WPPOB30, WPPOB40 and WPPOB100.

There was a correlation established between blend ratio, EGR flow rate and the amount of UHC emissions. As the EGR flow rate increases there is an increase in total UHC emissions produced within a blend and vice versa for all test fuel. However, there is a decrease in UHC as the blend ratio increased with different blends of WPPO as the EGR flow rate increased and vice versa. For example, the values of WPPO10 are 23 ppm, 35 ppm, 46 ppm, 58 ppm, 68 ppm, 72 ppm and 75 ppm for EGR flow rates of 0 %, 5 %, 10 %, 15 %, 20 %, 25 % and 30 % respectively, while the values for conventional diesel and the other blends of WPPO at 10 % EGR flow rate are 57 ppm, 46 ppm, 38 ppm, 34 ppm, 29 ppm and 26 ppm.

9.7 Carbon Monoxide (CO) Emission

Figure 9.9 shows the variations of CO emission % with load under the effects of EGR % rate flow application, with different fuel blends of WPPO and conventional diesel fuel. CO is a toxic gas that requires substantial control to maintain acceptable levels. It is caused by poor combustion of hydrocarbon fuels as a result of dependency on the AFR relative to the stoichiometric proportions [12, 14].

Figure 9.9 shows CO emission % variations versus varying engine load with different fuel blends of WPPO and conventional diesel test fuel.
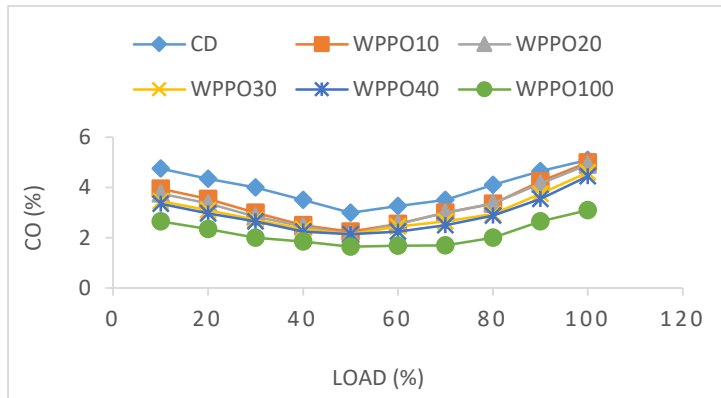
Figure 9.9: CO emission % versus varying engine load

For all the test fuels the amount of CO emissions seemed to decrease at lower engine loads up to part load percentages or intermediate loads of (50 %), thereafter the CO emissions continued to increase significantly and marginally as in Table 8.13 in Chapter 8and Figure 9.9. At 10 % engine load the value of conventional diesel is 4.75 % compared to 50 % engine load when the value is reduced to 3.0 % by volume. However, as the engine load is increased from 50 % upwards there is a significant continuous and marginal increase in the percentage of CO emissions by volume as the load is increased across all the test fuels. For example, at 80 % engine load the value for WPPOB100 is 2.0 % up from 1.65 % by volume, at 50 % part engine load the value of conventional diesel is 4.1 % compared to 2.95 % for WPPOB100 by volume at 50 % part engine load. The other WPPO biodiesel blends also show a similar trend and concurrency. WPPOB20 test fuel at 50 % part engine load condition has a value of 2.15 % by volume as compared to 3.36 % by volume at 80 % engine load.

Figure 9.10 shows the variation of CO emissions with EGR % flow rate application under different blends of WPPO and conventional diesel.
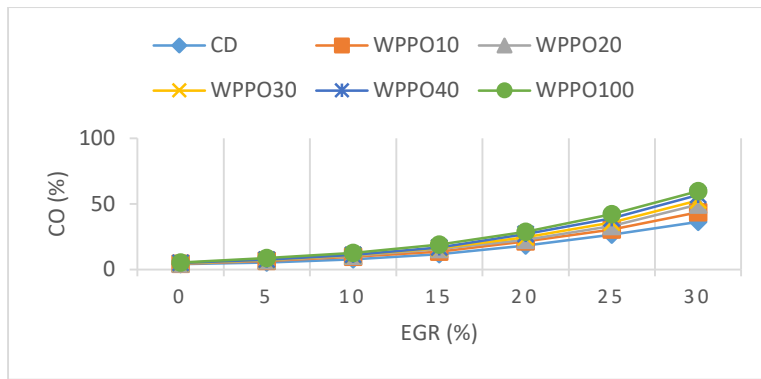
Figure 9.10: Variation of CO VS EGR % flow rate application

As can be seen from Figure 9.10, the WPPO blends are observed to produce a continuous increase in the smoke emissions almost to double the values with the application of EGR % flow rate as in Figure 9.10 and Table 8.14 in Chapter 8. For example, at 10 % EGR flow rate, CO emission values are 9.79 %, 10.46 %, 10.91 %, 11.25 % and 12.75 % for WPPO10, WPPO20, WPPO30, WPPO40 and WPPO100 respectively. Conventional diesel test fuel reported the lowest CO emissions with the application of EGR % flow rate with a value of 7.65 %.

There is also a correlation between the blend ratio and EGR % flow rate and the amount of CO emissions produced. During experimentation it was observed that as the blend ratio increases the CO emissions increase within the blend as the EGR % flow rate increases as in Figure 9.10 and Table 8.14 in chapter 8. At 20 % EGR flow rate CO emission values are 18.25 %, 21.35 %, 22.65 %, 24.55 %, 26.95 % and 28.85 % respectively for conventional diesel, WPPO10, WPPO20, WPPO30, WPPO40 and WPPO100. However, WPPO30 reports values of 4.85 %, 7.28 %, 10.91 %, 16.37 %, 24.55 %, 35.75 % and 52.69 % as the EGR flow rate increases from 0 % to 30 %. This may be due to the effects of EGR % flow rate in terms of dilution, and thermal and chemical effects as a result of some of the oxygen in the inlet charge being replaced with recirculated exhaust gas causing incomplete combustion.

## 9.8 Carbon Dioxide (CO_2) Emissions

CO_2 is the principal gas composition of the recirculating exhaust gas; however it is a core indicator of the quality of combustion and the existing in-cylinder temperatures [15] of combustion within the combustion chamber. CO_2 gas with a higher heat capacity makes it act like a thermal heat sink especially during the combustion process, leading to a possible

reduction of peak cylinder temperatures and of particular importance is the reduction in the NO_X emissions.

Without EGR % flow rate and at lower engine loads, the value of CO_2 is considerably high for all the test fuels used. For example, at 20 % engine load WPPOB100 has the highest CO_2 emissions compared to all the other test fuels used. CO_2 emission values for conventional diesel fuel is 3.0 % by volume compared to WPPOB100 which is 4.6 % by volume as seen in Figure 9.11 and Table 8.15 in Chapter 8.

However, it can also be observed from Figure 9.11 and Table 8.15 in Chapter 8 that the amount of CO_2 increases with increase in engine load. As the engine load increases to 40 % the value of WPPOB40 is 2.75 % compared to 60 % when the value is 3.5 %. The test blend WPPOB30 at 40 % is 3.25 % by volume compared to 4.5 % and 5.25 % for WPPOB40 and for WPPOB30 respectively at 70 % engine load. This leads to the observation that as the engine load increases and the blend ratios increase, lower blends ratios are observed to emit more CO_2 emissions compared to those blends with high ratios except for blend WPPOB100 which released more carbon emissions than any of the WPPO blended test fuels. At full engine load the value of CO_2 emissions is at its highest values as seen in Figure 9.11 and Table 8.15 in Chapter 8 across all the test fuels. The value for conventional diesel is 10.85 % compared to the blend WPPOB100 at 12.75 %, WPPOB10 at 9.65 %, WPPOB20 at 8.75 %, WPPOB30 at 8.35 % and WPPOB40 at 8.0 %.

Figure 9.11 shows CO_2 % variation under engine loads with different blends of WPPO and conventional diesel test fuel.
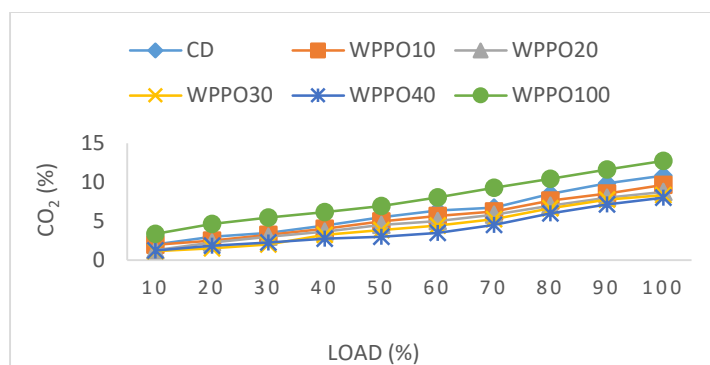
Figure 9.11: Variation of CO₂ % emissions versus engine load %, with different types of fuel blends of WPPO and conventional diesel

Figure 9.12 shows CO_2 % variations with different blends of WPPO and conventional diesel test fuel under varying engine loads, with application of EGR % flow rate.
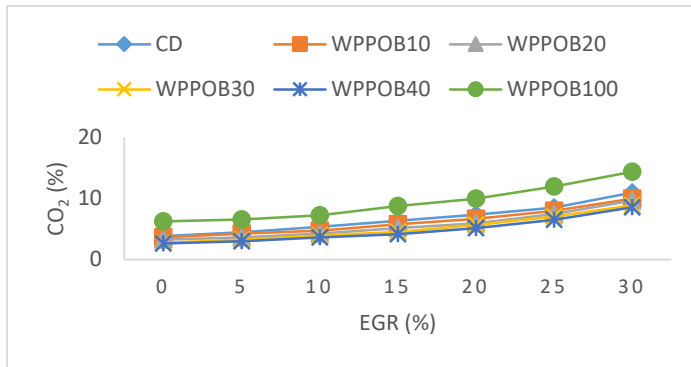
Figure 9.12: Variations of CO_2 % versus EGR % flow rate

The results in Figure 9.12 and Table 8.16 in Chapter 8 reinforce the observation that under EGR % flow rate CO_2 emissions increase with increase in the blend ratio and EGR % flow rate. The higher the blend ratio and the higher the increases in EGR % flow rates the higher the CO_2 emission values and vice versa. The values for 30 % EGR flow rate for all the test fuels contain high emissions CO2, for example conventional diesel is 10.95 %, WPPOB10 9.95 %, WPPOB20 9.65 %, WPPOB30 8.85 % and with WPPOB100 showing the highest value of 14.35 % for carbon dioxide emissions.

9.9 Smoke Emissions (Opacity)

This can be defined as the solid hydrocarbon soot particles that are found in the exhaust gas system [16] and directly linked to smoke emissions formation. For all the blends of WPPO there is a noted increase in the level of smoke emissions, although compared to conventional diesel the levels and values are considerably lower.

The application of EGR % flow rate as seen in Figure 9.13 and Table 8.17 in Chapter 8 shows that there is a significant increase in the values of smoke emissions and particulate matter emissions across all the test fuels employed. Smoke emissions with WPPOB10 blend are seen to be 5.1 % lower compared to conventional diesel at 0 % EGR flow rate with 5.5 %. On the other hand, conventional diesel is higher than WPPOB100 blend of fuel at 30 % EGR flow rate with a value 9.85 % compared to WPPO100 with a value of 7.3 %. This result seems to concur with the findings and study of [17].

The WPPOB10 blend during experimentation is seen to emit the highest levels of smoke emissions for the blended fuels compared to the other WPPO blends. However, it should be mentioned here that as the blend ratio and the EGR % flow rate increased there is consistent increase in the smoke emissions within the test fuels with marginal decreases observed across all the blended fuel with values at 15 % EGR flow rate reporting 7.53 %, 7.1 %, 6.72 %, 6.25 %, 6.0 % and 5.4 % for conventional diesel, WWPO10, WPPO20, WPPO30, WPPO40 and WPPO100 respectively in decreasing marginal values, compared to increasing values within the blend of WPPO20 with values of 5.0 %, 5.8 %, 6.35 %, 6.72 %, 7.15 %, 7.55 % and 8.65 %, for increasing EGR flow rates of 0 % to 30 %.

Figure 9.13 shows smoke emissions or opacity % variations at full engine load, with different blends of WPPO and conventional diesel under the effects of EGR % flow rate application.
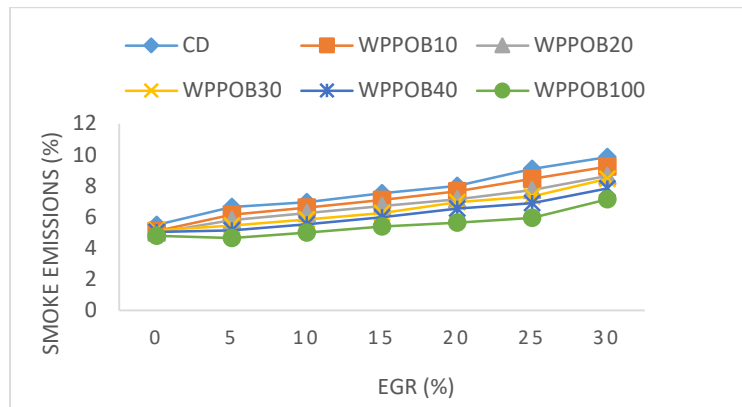
Figure 9.13: Variation of smoke emissions or opacity % versus EGR % flow rate

The constant increase in smoke emissions can be explained by the fact that WPPO blends of fuel have a high kinematic of viscosity compared to conventional diesel test fuel. Besides the low volatility values of the WPPO tested blends, this affects their spray characteristics, mixing qualities and combustion patterns. Other possible explanations for this phenomenon is the poor injection and spray characteristics observed with most WPPO blends of fuels compared to the spray and injection characteristics of conventional diesel fuel, which has better spray and mixing qualities. Another likely cause associated with this phenomenon is the high aromatic compounds found in most WPPO blends of fuel compared to conventional diesel test fuel.

References

[1] M. Hawi, R. Kiplimo, and H. Ndiritu, "Effect of exhaust gas recirculation on performance and emission characteristics of a diesel-piloted biogas engine," *Smart Grid and Renewable Energy,* vol. 6, p. 49, 2015.

[2] M. Paul Daniel, K. V. Kumar, B. Durga Prasad, and R. K. Puli, "Performance and emission characteristics of diesel engine operated on plastic pyrolysis oil with exhaust gas recirculation," *International Journal of Ambient Energy,* vol. 38, pp. 295-299, 2017.

[3] L. Li, J. Wang, Z. Wang, and J. Xiao, "Combustion and emission characteristics of diesel engine fueled with diesel/biodiesel/pentanol fuel blends," *Fuel,* vol. 156, pp. 211-218, 2015.

[4] J. Devaraj, Y. Robinson, and P. Ganapathi, "Experimental investigation of performance, emission and combustion characteristics of waste plastic pyrolysis oil blended with diethyl ether used as fuel for diesel engine," *Energy,* vol. 85, pp. 304-309, 2015.

[5] J. Pratoomyod and K. Laohalidanond, "Performance and emission evaluation of blends of diesel fuel with waste plastic oil in a diesel engine," *Carbon,* vol. 79, pp. 75-99, 2013.

[6] D. Jagadish, P. R. Kumar, and K. Madhu Murthy, "Performance characteristics of a diesel engine operated on biodiesel with exhaust gas recirculation," *International Journal of Advanced Engineering Technolog,* vol. 2, pp. 202-208, 2011.

[7] P. N. Krishnan and D. Vasudevan, "Performance, combustion and emission characteristics of variable compression ratio engine fuelled with biodiesel," *International Journal of ChemTech Research,* vol. 7, pp. 234-245, 2015.

[8] M. H. M. Yasin, R. Mamat, A. F. Yusop, D. M. N. D. Idris, T. Yusaf, M. Rasul*, et al.*, "Study of a diesel engine performance with exhaust gas recirculation (EGR) system fuelled with palm biodiesel," *Energy Procedia,* vol. 110, pp. 26-31, 2017.

[9] A. Sharma and S. Murugan, "Potential for using a tyre pyrolysis oil-biodiesel blend in a diesel engine at different compression ratios," *Energy Conversion and Management,* vol. 93, pp. 289-297, 2015.

[10] S. Maroa, Samwel and F. Inambao, "The Effects of Exhaust Gas Recirculation on the Performance and Emission Characteristics of a Diesel Engine–A Critical Review," *International Journal of Applied Engineering Research,* vol. 12, pp. 13677-13689, 2017.

[11] J. B. Heywood, "Internal combustion engine fundamentals," 2012.

[12] M. Mani, G. Nagarajan, and S. Sampath, "An experimental investigation on a DI diesel engine using waste plastic oil with exhaust gas recirculation," *Fuel,* vol. 89, pp. 1826-1832, 2010.

[13] K. I. Abaas, "Effect of Exhaust Gas Recirculation (EGR) on the Performance Characteristics of a Direct Injection Multi Cylinders Diesel Engine," *Tikrit Journal of Engineering Science (TJES),* vol. 23, pp. 32-39, 2016.

[14] C. Ilkilic, "The emission characteristics of a CI engine fueled with a biofuel blend," *Energy Sources, Part A: Recovery, Utilization, and Environmental Effects,* vol. 34, pp. 1901-1912, 2012.

[15] K. Muralidharan, D. Vasudevan, and K. Sheeba, "Performance, emission and combustion characteristics of biodiesel fuelled variable compression ratio engine," *Energy,* vol. 36, pp. 5385-5393, 2011.

[16]   H. Venkatesan, S. Sivamani, K. Bhutoria, and H. H. Vora, "Assessment of waste plastic oil blends on performance, combustion and emission parameters in direct injection compression ignition engine," *International Journal of Ambient Energy,* pp. 1-9, 2017.

[17]   P. Bridjesh, P. Periyasamy, A. V. K. Chaitanya, and N. K. Geetha, "MEA and DEE as additives on diesel engine using waste plastic oil diesel blends," *Sustainable Environment Research,* 2018.

CHAPTER TEN

CONCLUSION AND RECOMMENDATIONS

10.1 Conclusion

- As the percentage of the blends of WPPO increased there was a marked decrease in the engine BP from the blended fuels of WPPO compared to conventional diesel. This makes sense considering that the energy content (as seen in the table of properties of the WPPO test fuel) is lower compared to the energy content of conventional diesel.

- Peak power produced using WPPO biodiesel blends failed to match the peak power produced by conventional diesel test fuel. The difference in peak power ranged between 5 % to 8 % less compared to the peak power produced from conventional diesel test fuel.

- Data presented in this work provides more reasons to support the widespread use of WPPO as an alternative fuel for all types of compression ignition engines with or without modifications to the engine, especially when blends of WPPOB10 and WPPOB20 are used because their peak BP and BSFC values have identical values to conventional diesel fuel.

- As the percentage of the blend ratio of the biodiesel WPPO increased there was a significant increase in the BSFC as in Figure 9.1 for the blends of WPPO compared to the brake specific fuel consumption (BSFC) values of conventional diesel test fuel.

- During experimentation it was noted that after the 10 % EGR flow rate the values for the BSFC across all the test fuel except conventional diesel seem to show and pick a sharp increasing curve below the 10 % EGR flow rate, as in Figure 9.1 and Table 8.5 in Chapter 8, but as the EGR flow rate increases from 10 % there is a flattening of the graph curves leading to close value trends.

- After the 10 % EGR flow rate the values for the BSFC across all the test fuel seem to show and pick a lineal increment trend as can be shown in Figure 9.1 by flattening of the graph and close value trends.

- Another observation reported during this experiment is that as the blends ratio is increased with increasing load there is a reduction in the percentage amount of CO emissions released by the test engine as seen in Table 8.13 in Chapter 8 and Figure 9.9

181

in Chapter 8. This can be attributed to a high oxygen content in WPPO blended fuels compared to conventional diesel, which aided in complete combustion.

- The results values of CO emissions by two blends of WPPOB10 and WPPOB20 are observed to be close with minimal differences in terms of their volume percentage emissions of CO produced by the test engine as seen in Figure 9.9 in Chapter 9.

- There is a correlation between the blend ratio and EGR % flow rate on the amount of CO emissions produced. During experimentation it was observed that as the blend ratio increases the CO emissions increase within the blend as the EGR % flow rate increased as evident in Figure 9.10 in Chapter 9 and Table 8.14 in Chapter 8.

- Figure 9.11 in Chapter 9 and Table 8.15 in chapter 8 show that the amount of CO_2 increases with the increase in the engine load; as the engine load increases to 40 % the value of WPPOB40 is 2.75 % compared to 60 % where the value is 3.5 %.

- Under the influence of EGR % flow rate, CO_2 emissions increase with increases in the blend ratio and EGR % flow rate. The higher the blend ratio and the higher the increases in EGR % flow rates the higher the CO_2 emission values and vice versa.

- There was an observed constant increase in smoke emissions during experimentation for all the blends of WPPO with or without EGR % flow rate application, with test fuel blend WPPOB10 producing the highest values of smoke emissions followed by the WPPOB 100 test fuel blend.

- The EGTs during experimentation were seen to constantly decrease with application of EGR % flow rate. It is imperative to note here that decrease in EGT is noticed irrespective of the continuous increase in EGR % flow rate even when the EGR % flow rate went above the 15 % point.

- There was a concurrence that at part engine load (50 %) the values of NO_X emissions emitted by all the blends of WPPO except WPPO100 were lower compared to the values at full engine load conditions.

- During part load and intermediate engine load it was observed that the engine operating under different blends of WPPO and conventional diesel fuel emitted less NO_X emissions compared to the full load mode condition as demonstrated in the results shown in Figure 9.7 in Chapter 9 and Table 8.11 in Chapter 8.

- The application of EGR % flow rate increased HC emissions as observed from the results and values presented and obtained in Figure 9.8 in Chapter 9 and Table 8.12 in Chapter 8, with conventional diesel fuel producing the highest HC emission values compared to all the test fuel blends of WPPOB10, WPPOB20, WPPOB30, WPPOB40 and WPPOB100.

- There was a correlation established between blend ratio, EGR flow rate and the amount of UHC emissions. As the blend ratio increased there was a reduction in total UHC emissions produced across all blends. For example, at 10 % EGR flow rate the values of WPPO10, WPPO20, WWPO30, WPPO40 and WPPO100 were 46 ppm, 38 ppm, 34 ppm, 29 ppm and 26 ppm respectively.

10.2 Future Recommendations

- EGR as a method of controlling emissions, although seeming to contribute to other emission problems, thus making the use of compression ignition engines undesirable, is an effective technique in the control of NO_X emissions in diesel engine emissions. This technique in combination with other NO_X emission control systems is one of the most efficient technique in combustion control strategies in not only controlling compression ignition engines harmful emissions but also in reducing emissions to acceptable standards.

- It can be safely concluded that EGR can be used as a technique for controlling emissions of NO_X, CO, CO_2, HC and SOF in conjunction with other techniques. However, more needs to be done to bridge the gap between research and industry, for example increase the use of EGR cooling particularly in stationery engine systems and in marine applications and spread to a wider area in industrial production where carbon emissions are more pronounced. In this regard, the use of high boost pressure coupled with EGR application should be encouraged.

- EGR cooling will allow us to retain the benefits of low NO_X emissions without compromising engine efficiency. EGR cooling is necessary as it reduces soot and SOF emissions, for example when used with other techniques like variable gas turbine technology, which recirculates all exhaust gases together with the inlet intake mixture, thus increasing the mixture heat capacity leading to lowered in-cylinder combustion temperatures and consequently a reduction in NO_X emissions.

- During the review it was observed that the preheating of the inlet air reduced CO emissions. However, the introduction of EGR % flow rate into the system is observed to increase CO emissions linearly as the EGR % flow rate was being increased, which calls for the question of harmonization of the two systems to achieve low carbon emissions without compromising engine performance and emission control.

- From the combustion control strategies that were discussed, what implementation strategies can we employ to harness improving the combustion characteristics of the alternative fuels available, especially their chemical and physical properties? The chemical and physical properties of biodiesels lack proper testing and analysis facilities because this is still a grey area in terms of industrial commercial development, as industry regulators impose stringent control on the use of alternative fuels.

- More work needs to be done to develop high quality alternative biodiesel fuels suitable for future combustion engines and systems, especially projects involving waste to energy alternatives such as using waste plastic to generate propulsion fuel. This will address two issues – finding an answer to an alternative fuel and reducing pollution to natural environment from municipal solid waste management landfill sites.

- Although EGR mitigates formation of the NO_X gases, it promotes smoke emissions especially during higher engine loads, i.e. it requires to be used in combination with other emissions control techniques and combustion control strategies like LPL EGR, HPL, selective catalytic reduction (SCR), diesel particulate filter (DPF), diesel oxidation catalyst (DOC) and retarded timing. Another area that needs new studies and research is the development of accurate measurement of different rates of EGR in transient engine conditions for implementation and control of the exhaust gases when hot EGR or cold EGR is used.

- The personal modern day transport system is a major contributor to traffic related pollution, followed by the mass transport vehicles, buses, the rail and air transport. These systems impact negatively on the health of the world population. More work needs to be done to improve air pollution control strategies to include control of additional key pollutants. There is a need to do improve measuring technology, increase observatory sites and increase satellite information recovery and retrieval time beside the development of more advanced simulation models.

184

- During the literature review it became evident that more information is needed regarding the toxicity of some of the toxic gases emitted by diesel engines. The real impact of exhaust gas emissions is still limited according to the studies that have been conducted so far. Therefore, more impact assessment studies need to be conducted.

- Although tremendous progress has been made in reducing air pollution and thus improving public health, there is still a need for more isolation of the individual pollutants species and source categorization to increase specific understanding on the effects produced on human health, making it possible institute control actions on different sources and better prioritization of mitigation measures.

- The differences in the disciplinary backgrounds of most air pollution research groups has to be bridged. The current pollution problem requires a multi-disciplinary and inter-disciplinary approach to increase interaction between the disciplines of science and engineering technology going forward, to better incorporate new findings, capabilities, limitations, and research priorities as team work instead of individual fields with individual discipline solutions.

- Funding of new and young researchers, better educational opportunities for young researchers and encouragement of the inter-disciplinary conferences and meetings to break barriers of traditional disciplinary boundaries should be encouraged. This is necessary considering the importance and urgency of the air pollution problem globally.